UNIVERSITAT POLITÈCNICA DE CATALUNYA BARCELONATECH

Nanoengineering approaches for guiding cellular behavior

Dencho Gugutkov

NANOENGINEERING APPROACHES FOR GUIDING CELLULAR BEHAVIOR

Doctoral Thesis

Dencho Gugutkov

Molecular Dynamics at Cell-Biomaterial Interface Group
Institute for Bioengineering of Catalonia (IBEC)

Biomedical Engineering Doctoral Program
Universitat Politècnica de Catalunya · BarcelonaTech (UPC)

Director
Prof. Dr. George Altankov

Tutor
Prof. Dr. Maria Pau Ginebra Molins

Barcelona (Spain) 2017

На дъщеря ми Лорея!

На съпругата ми Оляна!

На майка ми, баща ми и брат ми!

На дядо ми Денчо!

“Една борба,

Една любов,

Един отбор в света -

Има свята истина една:

САМО, САМО ЦСКА!”

Песен на привържениците на ЦСКА (София**)**

CSKA (Sofia) supporters’ song

“Walk on through the wind,

Walk on through the rain,

Though your dreams be tossed and blown,

Walk on, walk on, with hope in your heart,

And you’ll never walk alone,

You’ll never walk alone.”

Liverpool FC supporters’ song

“It is not our part to master all the tides of the world, but to do what is in us for the succor of those years wherein we are set, uprooting the evil in the fields that we know, so that those who live after may have clean earth to till. What weather they shall have is not ours to rule.”

Gandalf

J.R.R. Tolkien, *The Last Debate, The Return of the King*

“The important thing is not to stop questioning. Curiosity has its own reason for existence. One cannot help but be in awe when he contemplates the mysteries of eternity, of life, of the marvelous structure of reality. It is enough if one tries merely to comprehend a little of this mystery each day.”

Albert Einstein

"Old Man's Advice to Youth: 'Never Lose a Holy Curiosity.'" *LIFE Magazine, 1955*

“You know nothing, Jon Snow.”

Ygritte

George R.R. Martin, *A Game of Thrones*

ACKNOWLEDGEMENTS

Inspiration, motivation and friendly support have always played a key role in the success of any undertaking and this dissertation does not make an exception.

Above all, I would like to express my deepest gratitude to my supervisor Prof. Dr. George Altankov. For your excellent guidance, your caring, for your patience, for your knowledge and wisdom, for your endless support, for your understanding and true friendship – thank you, George!

I would like to thank my tutor, Prof. Maria Pau Ginebra Molins, for her valuable counselling during the accomplishing and the submission of my dissertation. Thank you, Pau, for always keeping the door of your office open for me.

I would like to extend my acknowledgments to those who offered collegial guidance and support during the years:

My sincerest sense of thankfulness to Prof. Manuel Salmeron-Sanchez and his group, who provided with an excellent scientific support and priceless assistance in making this work come true.

Words fail me to express my gratefulness to all my colleagues from “Molecular Dynamics” group of the Institute for Bioengineering of Catalonia (IBEC). I am immensely obliged to Dr. Johan Gustavsson, Georgi Toromanov and Dr. Salima Nedjari for their encouraging guidance and, mostly, for being good friends of mine.

Deep gratitude also to Dr. Ricardo Pérez-Tomás , Dr. Soledad Alcantara and all their co- workers for the invaluable help and for the always friendly atmosphere in our lab.

To all my friends, thank you for the countenance given, for the irreplaceable understanding, for believing and inspiring me in this journey.

I would like to give my heartfelt thankfulness to my mother and my father, who paved the path before me and upon whom shoulders I stand. Thanks God I have you, I know, I am what I am because of you.

Last, but actually first, I feel to say that my family - my wife Olyana and my daughter Loreya, was the most important factor behind me in this work. Thank you for giving me strength and courage when I need it most, for being next to me in good times and bad, for making my life worthwhile. You are my Everything.

TABLE OF CONTENTS

PREFACE TO THESIS

Tissue engineering aims to replace restore or help regeneration of injured tissue or organ with scaffolds that mimic the natural extracellular matrix (ECM). However, the design of such scaffolds requires deeper understanding of the factors that determine the cellular behavior. This Thesis is focused on the cell-biomaterials interaction, but it strives to go beyond the classical material science, looking for new options to obtain control over the cell behavior.

Cellular interaction with artificial substrata is a well-described paradigm usually attributed to the adsorption of adhesive proteins from the surrounding medium. The recognition of these proteins triggers an order of specific signaling events, reminiscent of the natural cell-ECM interactions, which affect the behavior of adhering cells. One important aspect of such an interaction, however, is the organization of the matrix proteins - a hallmark for the ordinary ECM.

Recent studies in our group showed that even *in-vitro* the cells tend to create organization. They remodel the adsorbed matrix proteins (mostly in a fibril-like pattern) as an attempt to make their own provisional ECM. Though this phenomenon is described and settled basically to fibronectin (FN), it appears to involve also other matrix proteins, for example fibrinogen (FBG), and even collagen IV and vitronectin, which, being non fibrillar proteins by their nature, also undergo linear reorganization. Thus, cells somehow “prefer” fibrillar protein assemblies trying to imprint such patterns in their closest environment. Other types of protein arrangements, however, for example network-like assemblies, which are also typical for the ECM, are still insufficiently studied and this is an essential part of this PhD work.

In the first part of the thesis particular attention was devoted on the peculiar behavior of adsorbed FN and FBG in the nanoscale that was recently observed by atomic force microscopy (AFM). Joint work with the group of Prof Salmeron-Sanches from the Polytechnic University in Valencia (currently in The University of Glasgow) revealed that apart from the classical view for a rather stochastic adsorption of matrix proteins, the lateral protein-protein interactions may prevail on some surfaces giving rise to self-assembly in a network-like structure, which has significant consequences on the protein behavior. The thesis is focused particularly on the biological activity of these networks, while the phenomenon of networks assembly itself and its nano-engineering aspects are a matter of separate investigations. The studies performed in this thesis clearly suggested that the modulation of the network formation (using model surfaces with varying density of -OH groups) has strong impact on the cellular behavior – a fact, confirmed with two different cell systems: fibroblasts and endothelial cells.

Another line of research that was followed lies on the fact that in solution matrix proteins can sequestrate from the surrounding liquid phase to form structures of various shapes, including fibers with a diameter of only few nanometers and lengths up to centimeters, thus resembling the natural

ECM components. A fascinating possibility to mimic similar structures is to engineer nanofibers based on matrix proteins via electrospinning technology - an approach that was extensively explored in the second part of the thesis. It was evidently shown that the cells attach faster to such fibrils and readily recognize them – a phenomenon that even not entirely understood was confirmed in series of studies. Thus, one can anticipate that mimicking the fibrillar organization of ECM will help to understand how cells respond to such an environment, an issue that is fundamental for biology. Besides, this approach represents an additional tool for controlling the cell behavior as proposed in this thesis. Therefore nanofibers based on natural matrix proteins (e.g., fibrinogen, fibronectin) and synthetic polymers (e.g. poly(lactic acid), (PLA); poly(ethylacrilate), (PEA)) were elaborated and their implication as a model system revealed that varying with the composition, the organization and the mechanical properties of these fibers may be obtained a tight control over the cellular response.

The Thesis is based on 5 original publications separated in 5 Chapters (2 to 6) ordered in a logic and hierarchic way and carrying homonymous titles. A comprehensive Introduction (Chapter 1) and short Prefaces to each chapter describes the rationale of the published work and its place within the whole topic of the Thesis, formulated in the Aim and Specific Objectives paragraph.

RESUMEN DEL THESIS

La ingeniería de tejidos tiene el objetivo de reemplazar, restaurar o estimular la regeneración de tejidos dañados con matrices (“scaffolds”) que mimetizan la matriz extracelular natural (MEC). El diseño de dichas matrices, no obstante, requiere un profundo conocimiento de los factores que gobiernan el comportamiento celular. Esta tesis se centra en las interacciones entre células y biomateriales, pero pretende ir más allá de los límites de la ciencia de materiales con el fin de contribuir al desarrollo de nuevos métodos para controlar el comportamiento celular.

Las interacciones de las células con sustratos artificiales se han descrito dentro de un paradigma bien caracterizado, atribuido a la adsorción de proteínas adhesivas del medio circundante. El reconocimiento de dichas proteínas desencadena una serie de eventos de señalización celular reminiscentes de las interacciones célula-MEC que se dan in vivo y que afectan al comportamiento de las células adherentes.

Un aspecto importante de dicha interacción es la organización de las proteínas de la matriz, que caracteriza la MEC. Estudios recientes de nuestro grupo han demostrado que incluso in vitro las células tienden a crear organización, remodelando las proteínas de matriz adsorbidas (en un patrón fibrilar) a fin de generar su propia MEC provisional. Aunque este fenómeno depende básicamente de la fibronectina (FN), otras proteínas como el fibrinógeno (FBG), el colágeno IV y la vitronectina, también participan, experimentando una reorganización fibrilar a pesar de últimos ser proteínas no fibrilares por naturaleza. Por lo tanto, las células aparentemente “prefieren” una disposición “fibrilar” de las proteínas a su alrededor y tratan de crear estos patrones en su entorno. Otros tipos de disposición típicos en la MEC, por ejemplo, en forma de red, han sido sin embargo poco estudiados, y serán el eje esencial de este trabajo doctoral.

En la primera parte de esta tesis, se presta especial atención al peculiar comportamiento en la nanoescala de la FN y la FBG adsorbidas, recientemente observado mediante microscopía de fuerza atómica (MFA). Nuestro trabajo conjunto con el Prof. Salmerón-Sanches de la Universidad Politécnica de Valencia (ahora en Glasgow), reveló que aparte de la visión clásica de la adsorción de proteínas como un proceso estocástico, las interacciones laterales proteína-proteína pueden prevalecer en algunas superficies dando lugar al auto-ensamblaje en estructuras de red, con efectos significativos en su comportamiento. Esta tesis se centra especialmente en la actividad biológica de estas redes, mientras que los fenómenos de formación de estructuras reticulares y sus aspectos de bioingeniería son objeto de investigaciones aparte. Los estudios realizados en esta tesis claramente sugieren que la modulación de la reticulación (usando superficies modelo con densidad variable de grupos hidroxilo) tiene un fuerte impacto en el comportamiento celular, confirmado mediante dos sistemas modelo muy diferentes (fibroblastos y células endoteliales).

Otra línea de investigación se ha centrado en el hecho de que las proteínas de la matriz en solución pueden secuestrar de la fase líquida circundante, formando estructuras de formas diversas, incluyendo fibras con un diámetro de tan solo unos pocos nanómetros, pero una longitud hasta varios centímetros, similares a los componentes naturales de la MEC. La ingeniería de nanofibras basada en las proteínas de la matriz, mediante tecnología de "*electrospinning*", ofrece posibilidades fascinantes para mimetizar estas estructuras. Esta aproximación se explora en la segunda parte de esta tesis, en la que se demuestra que las células se anclan más rápido y reconocen más fácilmente estas fibrillas, un fenómeno que aunque no es muy bien comprendido se ha confirmado en diversos estudios. Por lo tanto, puede anticiparse que mimetizar la organización fibrilar de la MEC puede contribuir a comprender como las células responden a su entorno, un fenómeno esencial para la biología.

Aparte, este método representa una herramienta adicional para controlar el comportamiento celular como se propone en esta tesis. Por lo tanto, utilizamos nanofibras basadas en las proteínas naturales de la matriz (por ejemplo, FBG o FN) así como polímeros sintéticos (como el ácido poliláctico, (PLA), o el poli (acrilato de etilo), (PEA)) y estudiamos sus propiedades como sistemas modelo. Nuestro trabajo revela que variando la composición, organización y propiedades mecánicas de estas fibras puede obtenerse un estrecho control sobre las respuestas celulares. Esta tesis se basa en cinco publicaciones originales separadas en 5 capítulos (2 a 6) de título homónimo y ordenados de forma lógica y jerárquica. Una detallada introducción (capítulo 1) y cortos prefacios en cada capítulo describen la base de cada uno de los trabajos publicados y su lugar en el tema general de esta tesis, formulado en el párrafo en que se detallan los objetivos globales y específicos.

УВОД КЪМ ДИСЕРТАЦИЯТА

Тъканното инженерство цели възстановяване или регениране на увредени тъкани или органи посредством матрици (“scaffolds”), които имитират естествения екстрацелуларен матрикс (ЕЦМ). Разработването на такива подложки обаче изисква дълбоко познаване на факторите, определящи клетъчното поведение. Тази дисертация се фокусира върху взаимодействието клетка-биоматериал като се стреми да надникне отвъд класическото материалознание, тъсейки нови подходи за осъществяване на контрол върху поведението на клетката.

Клетъчното взаимодействие с изкуствени субстрати е добре описан парадигъм, който обикновено се свързва с адсорбцията на адхезивни протеини от заобикалящата среда. Разпознаването на тези протеини запуска редица сигнални механизми, наподобяващи естественото взаимодействие на клетките с екстрацелуларния матрикс, и повлиява поведението на адхериралите клетки. Важен аспект на едно такова взаимодействие е организацията на адхезивните матриксни протеини – знакова характеристика за нативния екстрацелуларен матрикс.

Предишни изследвания в нашата група показаха, че дори *in-vitro* клетките са склонни да създават организация. Те ремоделират адсорбираните матриксни протеини (най- често във фибриларна форма) в опит да създадат собствен, кратковременен екстрацелуларен матрикс. Въпреки, че този феномен е установен и описан предимно за фибронектина (ФН), се оказва, че той включва и други матриксни протеини, например фибриноген (ФБГ), и дори колаген тип IV и витронектин (ВН), които, макар и нефибриларни по своята природа, също претърпяват линейна реорганизация. Следователно, клетките по някакъв начин „предпочитат“ фибриларната организация на протеините и се опитват да „отпечатат“ подобни структури в най-непосредствено си обкръжение. Други типове организация, обаче, като например мрежовидната, също типична за ЕЦМ, са недосатъчно изследвани и това съставлява съществена част от настоящата дисертация.

Първата част на този тезис обръща особено внимание на специфичното поведение на адсорбирани ФН и ФБГ в наноразмерната област, което може да бъде наблюдавано посредством атомно-силова микроскопия (АФМ). Съвместната работа с групата на проф. Салмерон-Санчес от Политехническия университет на Валенсия (в момента в Университета на Глазгоу (Шотландия)), показа, че отделно от класическото разбиране за стохастична адсорбция на матриксните протеини, върху някои повърности може да пробладава латералното взаимодействие между техните молекули, водещо до самоорганизирането им в мрежоподобни структури, имащи значителни последствия както върху поведението на протеина, така и върху неговата биоактивност. Настоящият труд е фокусиран именно върху

биологичната активност на тези супрамолекулни структури, докато феноменът на образуването им сам по себе си, както и неговите наноинженерни аспекти, са обект на отделни изследвания. Проучванията, проведени в обхвата на тази дисертация ясно доказаха, че чрез промяна в повърхностната плътност на –OH групи може силно да се повлияе способността за мрежовидна самоорганизация на някои белтъци, а от там и клетъчното поведение – факт, потвърден при две отделни клетъчни системи: фибробласти и ендотелни клетки.

Друга линия на изследвания се основава на факта, че, в разтвор, белтъците могат да секвестират от заобикалящата ги течна фаза и да формират различни структурни форми, включително фибри с диаметър от само няколко нанометра и дължина до сантиметри, наподобяващи естествената организация на ЕЦМ. Интригуваща възможност за имитиране на подобни структури е разработването на нановлакна, базиращи се на матриксни протеини, посредством технологията на електроовлакняване (електроспининг) – подход, който е широко застъпен във втората част на дисертацията. Там безспорно е показано, че клетките се прикрепят по- добре към такива нановлакна и явно ги разпознават – феномен, който макар и не напълно разбран, бе потвърден в редица изследвания. Следователно, имитирането на фибриларната организация на ЕЦМ би спомогнала да разберем как клетките реагират на подобна среда – въпрос, който е фундаментален за клетъчната биология. Наред с това, подобен подход представлява и допълнителен инструмент за контрол на клетъчното поведение, въпрос които подробно е застъпен в настоящия тезис. И така, базирайки се на естествени матриксни протеини, какъвто е фибриногенът, и на синтетични полимери, каквито са полимлечната киселина (PLA) и полиетилакрилатът (PEA), бяха разработени нов тип хибридни нановлакна и тяхното използване като модална система разкри, че варирайки с тяхната композиция, организация и механични свойства би могло да се осъществи прецизен контрол върху клетъчния отговор. Настоящата дисертация се базира на пет оригинални публикации, организирани в пет отделни глави (Глава 2 до Глава 6), подредени в логична и йереархична последователност, и носещи едноименни със съответната публикация заглавия. Подробното Въведение (Глава 1) и кратките уводни бележки към всяка глава отразяват същественото в публикуваната работа и негйното положение спрямо цялостната тематика на дисертацията, формулирана ясно в раздела “Цел и задачи”.

AIM OF THESIS AND SPECIFIC OBJECTIVES

Aim of thesis

To develop systems for guiding cellular behavior based on the phenomenon of ***substratum-driven protein assembly*** and the application of ***bioinspired electrospun nanofibers*** as positional cues that mimic the ECM organization.

Specific objectives

- To explore the novel phenomenon of material substratum-driven protein assembly as platform to engineer positional ques for the adhering cells, involving:
    - Studies on the effect of substratum properties that can modulate the lateral assembly of the matrix proteins fibronectin and fibrinogen
    - Biological characterization of the assembled protein networks
    - Developing of system that utilize substratum driven protein assembly of fibronectin and fibrinogen for guiding the cellular behavior

- Elaboration of bioinspired electrospun nanofibers and their use as positional cues for the adhering cells, involving:
    - Design of appropriate equipment and technology for the production of fibrinogen based nanofibers.
    - Production of fibrinogen-based nanofiber samples and elaboration of technique for their alignment
    - Application of nanofibers at dorsal and ventral surfaces of living cells. Observation via time-laps microscopy and evaluation of the impact on the cell behavior.
    - Studies on the initial cellular interaction with differently structured nanofibers - random and aligned, including morphological and functional response of endothelial cells in 2D and 3D environment
    - Exploring fibrinogen-based nanofibers for vascular tissue engineering purposes

CHAPTER 1

INTRODUCTION

Extracellular matrix

The tissues of a multicellular organism contain two main components: the cells themselves, the “living” matter, and the material that lies between the cells - the **extra- cellular matrix (ECM)**. The ratio of volumes occupied by ECM to that occupied by cells in tissues can vary from less than 1:10 (e.g. in muscles) to more than 10:1 (e.g. in tendons, cartilage and bone). ECM is composed of polymeric networks of several types of macromolecules in which smaller molecules, ions and water are bound. The major types of macromolecules are **polymer-forming proteins**, such as collagens, elastin, fibrillins, fibronectin, laminins etc. and hydrophilic **hetero-polysaccharides**, such as glycosaminoglycan hyaluronan and proteoglycans. It is the combination of protein polymers and hydrated proteoglycans that give extracellular matrices their resistance to tensile and compressive mechanical forces, (Hubbell 2007).

Over the years, the understanding of ECM function has evolved from the early concept of a static “connective tissue” that ties everything together to one that considers ECM as a dynamic structure that provides strength and elasticity, interacts with cell-surface receptors, and controls the availability of growth factors. It is clear now that the ECM is a complex system that is able to control the cell behavior. The main functions of ECM along with the structural one are: **(1)** to provide a barrier that isolates tissues from each other, **(2)** to provide navigational cues for migratory cells, **(3)** to provide signals that alter cell be`havior, and **(4)** to sequester biologically active compounds such as growth factors.

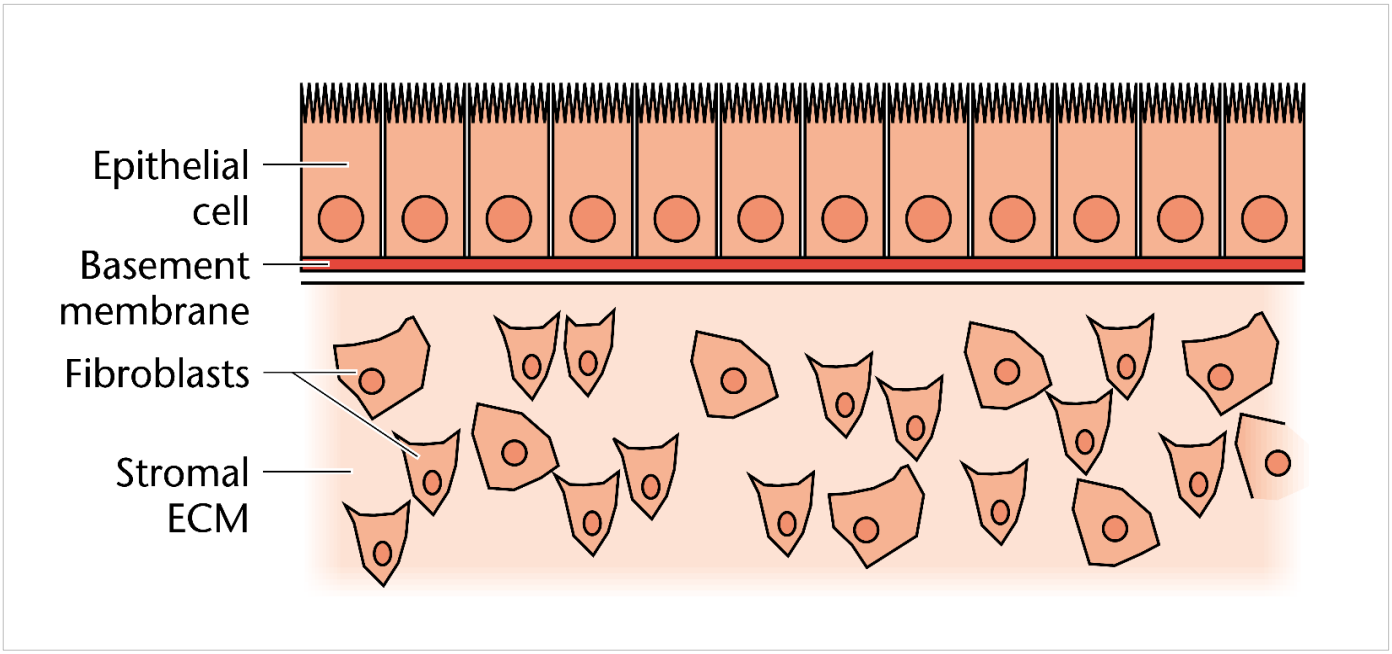

Figure 1. *Main types of ECM: a basement membrane underlying the epithelial cells of the tissue and a stromal ECM surrounding the cells of the mesenchymal part of the tissue. Adapted from* ***(Davies 2001).***

Being in different forms the ECM is a feature of all multicellular organisms, in plants it appears mainly as cell walls, while in animal tissues it appears in two main forms: **basement membranes (BM)** and **interstitial ECM**, often termed **rough ECM** or **stromal ECM,** (Figure1)**.**

Basement membranes are thin layers of ECM that underlie epithelial or endothelial cell sheets effectively separating them from the underlying stromal tissues. Stromal matrix is associated with connective tissues and is frequently fibrous, particularly in load-bearing tissues such as artery walls, tendons, cartilage and skin. The stromal ECM can also be mineralized producing the hard structure of bone.

The ECM is a mixture of many different molecular components that varies between organisms and between tissues within one organism, and sometimes varies with developmental age. The internal structure of the ECM is **highly organized,** resulting partly from the biological properties of the ECM's molecules and partly from the activities of the cells that produce ECM. Cells contact ECM through specialized **receptor molecules.** They use their receptors not only to adhere to the matrix components but also to signal for the presence of particular components. ECM receptors transmit this signal to the internal cell machinery allowing dynamic control on the overall cell behavior. Moreover, ECM is not a static structure, but it constantly undergoes remodeling by the cells involving opposing processes of synthesis and controlled destruction, as well as continuous rearrangement, (Davies 2001).

Structural components of ECM

Animal ECM is composed mainly of **glycoproteins** and **proteoglycans**, but many of them bind other ECM glycoproteins resulting in highly **complex structures**. Therefore, the ECM might be considered as a highly cross-linked gel consisting of approximately 100 known ECM components, and they are more if one counts the bioactive molecules (for example growth factors) that are not structural part of the matrix but bind to it. Generally, ECM components are glycoproteins and proteoglycans, however in some cases the more abundant proteins such as collagens might be described separately due to their unique mechanical properties. Proteoglycans contain long, charged glycosaminoglycan (GAG) chains covalently attached to serine or threonine of the core protein. Some GAG chains are also found unconnected to a protein, such as the hyaluronan, (Mecham 2011).

The main structural components of the ECM are the **matrix proteins** that show high structural and functional variability. Despite their structural and functional diversity however, they have also common features: Many proteins of the ECM have very large molecules being often extensively glycosylated or, in the case of proteoglycans - containing covalently attached GAG chains. Molar masses of 100–1,000 kDa are most frequent. In general, ECM proteins are highly asymmetric in shape because they are multidomain proteins, in which different or equal structural domains are specifically arranged. Domains are defined as homologous units with homology following from

amino acid sequence similarity. Individual domains may have distinct functions even after fragmentation from the intact protein. The combination of different domains leads to a multi-functionality of essentially all ECM proteins. The multifunctionality and the expanded shapes provide the potential for lateral interactions, favoring the formation of fibers and other supramolecular assemblies of ECM proteins, (Mecham 2011).

ECM proteins

As noted above, ECM is composed mainly of glycoproteins and proteoglycans. ECM proteins might be further classified, depending on their function, in three major subtypes: structural, adhesive and multifunctional.

Structural ECM proteins

Collagens

Collagens are the most abundant proteins of the ECM. There are 28 different types of collagen that assemble into a variety of supramolecular structures including fibrils, micro- fibrils, and network-like structures. Their numeration from I to XXVIII is based on the chronological order of discovery.

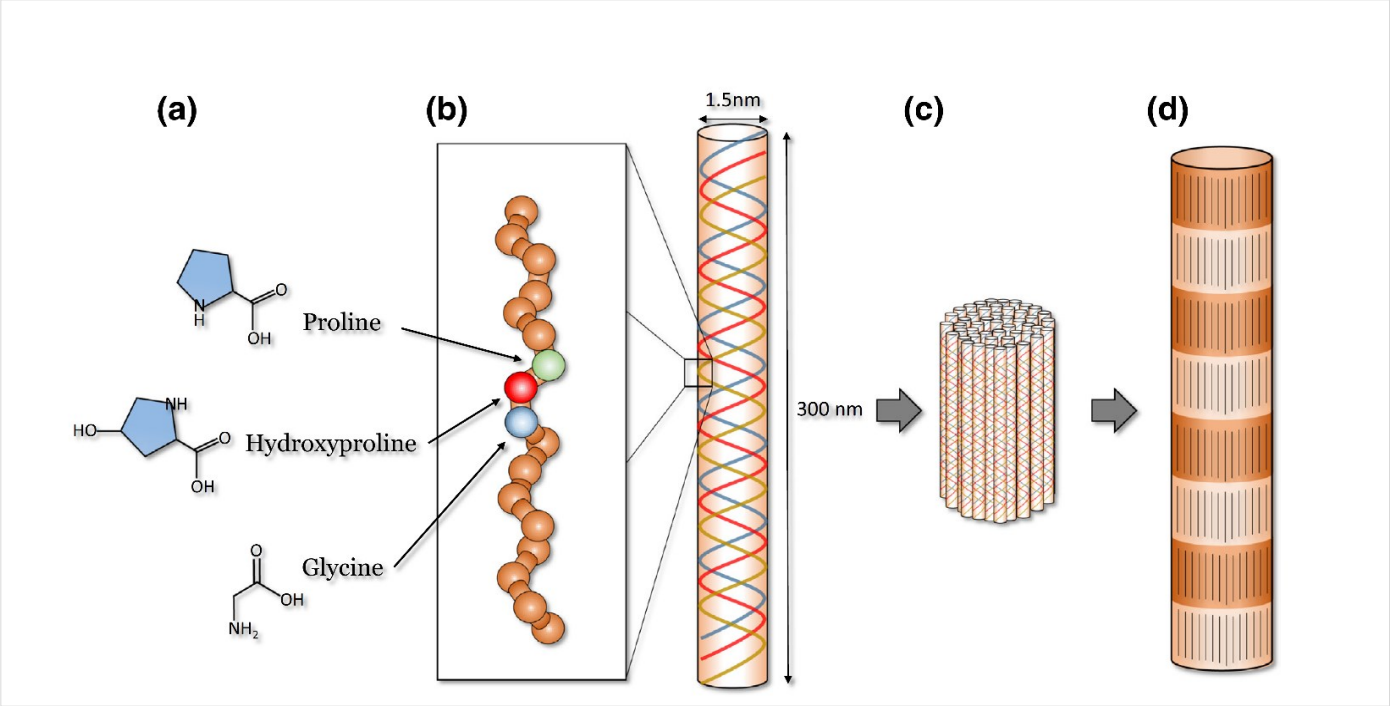

Figure 2. *Scheme of the assembly of collagen I.* ***(a)*** *Individual collagen polypeptide chains. The polypeptides consist of the repeating sequence Gly-X-Y, where X is often proline and Y is often hydroxyproline;* ***(b)*** *collagen is made up of three polypeptide strands which are all left-handed helixes and twist together to form a right-handed coiled coil. The polypeptide strands are synthesized as precursor chains with propeptides (globular extensions) on the C and N ends. The propeptides are cleaved into short nonhelical telopeptides;* ***(c)*** *collagen molecules self-assemble into collagen fibrils;* ***(d)*** *collagen fibers are formed by end-to-end and lateral assembly of collagen fibrils, resulting in a regular banding pattern that is characteristic of collagen. Adapted from* ***(Sicari et al. 2014)****.*

At least 45 different collagen genes exists that code for collagen polypeptides, called **alpha chains**. Majority of collagens are homotrimeric molecules being composed of three identical alpha chains,

but some collagens can be also heterotrimeric, for example α1(I)2α2(I) for collagen type I or α3(IV), α5(IV) and α6(IV) for one of the isoforms of collagen type IV. In addition, a single collagen type can have multiple chain compositions like α1(V)2α2(V), α1(V)α2(V)α3(V), or α1(V)3 for collagen type V.

All collagens have structure called **triple helix**, a tight right-handed helix of three individual collagen α-chains, each individual chain having the structure of a left-handed helix. The amino acid sequence of the collagen chain involved in the triple helix is unusual - all have glycine residues in every third amino acid and about a fifth of the other amino acids consist of proline and hydroxyproline, forming hydrogen bonds that stabilize the helical structure. Collagens are synthesized by the normal secretory pathway, but are modified in the endoplasmic reticulum and Golgi apparatus so that many prolines are hydroxylated to become hydroxyproline. The collagen chains are further stabilized by disulfide bond formation, and complex carbohydrates are added to the non-triple helix regions of the molecules. Cells do not secrete collagens directly, but rather secrete large precursors called procollagens that have 'extra' domains at each end of the molecule. These domains are cleaved outside the cell by specific proteinases, and once free of them most collagen chains associate with each other to form fibrils, which line up with one another to form larger fibres, (Figure 2), (Sicari, Londono, and Badylak 2014). The collagens are normally assembled into **suprastructures**, such as **fibrils, micro- fibrils, filaments,** and **networks**. These

Classification	Collagen types	Supramolecular structure
Fibril-forming collagens	I, II, III	Striated fibrils
Regulatory fibril-forming collagens	V, XI,	Striated fibrils, retain regulatory, noncollagenous N-terminal domains
	XXIV, XXVII	Unknown
FACIT[a] collagens	IX, XII, XIV	Associated with fibrils, other interactions
FACIT-like collagens	XVI, XIX, XXI, XXII	Interfacial regions, basement membrane zones
Basement membrane collagen	IV	Chicken-wire network with lateral association
Beaded filament-forming collagen	VI	Beaded filaments, networks
Anchoring fibrils	VII	Laterally associated anti-parallel dimers
Network-forming collagens	VIII, X	Hexagonal lattices
Transmembrane collagens	XIII, XVII, XXIII, XXV Gliomedins, ectodysplasin	Transmembrane and shed soluble ecto-domains
Multiplexin collagens (endostatin-XV and -XVIII)	XV, XVIII	Basement membrane proteoglycans, cleaved C-terminal domains influence angiogenesis
Other molecules with collagenous domains	XXVI, XXVIII C1q, collectins, acetylcholinesterase, adiponectin, surfactant protein, and others	Collagenous domains in primarily noncollagenous molecules

[a]Fibril-associated collagens with interupted triple helices

Figure 3. *Suprastructural organization of collagens. Adapted from* ***(Mecham 2011).***

suprastructures further assemble into higher organized tissue structures. For example, fibrils form fibers and lamellae. Beaded filaments combine to form broad-banded structures. Networks assemble into basement membranes, anchoring fibrils, and lattices. The diversity of extracellular matrix suprastructures is dependent on the collagen type and further diversity is achieved by copolymerization of several types of collagen and noncollagenous macromolecules. The components of the suprastructure can differ in their identities, (Figure 3). Collagen types I, II and III account for about 90% of all collagen in the body, and form strong fibrils. Practically however, most individual fibrils are composed of a mixture of these collagens and may also include small amounts of the other fibrillar collagens (e.g. V and XI), (Davies 2001).

While most fibrillar collagens are common in connective tissue, the basement membranes usually contain a quite different type collagen, *collagen IV*, which forms three-dimensional network rather than fibrils. This collagen will be described in more details below, as BM component. Here we will only mention that type IV collagen has ligand affinity for endothelial cells and is present within the BMs of most vascular structures. On the other hand, Type VII collagen is also present within the BM of the epidermis and facilitates fibril anchoring to protect overlying keratinocytes from the mechanical stress, (Yurchenco and O'Rear 1994).

Many of the collagen types provide tissue-specific physical and mechanical characteristics and allow for tissue-specific cell–ECM interactions. An example is the less rigid type III collagen that is present in the submucosal layers of tissues that require increased flexibility and compliance such as the urinary bladder, (Barnard and Gathercole 1991; Sicari et al. 2014).

Basement membrane proteins

Laminin

Laminins (LN) are present in worms and flies and are among the first extracellular matrix proteins produced during embryogenesis. Laminin is cell adhesive proteins, a major component of the basement membrane, (Yurchenco and Wadsworth 2004). Compared with fibronectin, which is found only in chordates, laminins are evolutionarily ancient and conserved, (Tzu and Marinkovich 2008). Laminins bind cell surface receptors and thereby connect basement membrane with adjacent cell layers. Laminins are large (400–900 kDa) heterotrimeric glycoproteins of three different polypeptide chains: α, β, and γ, (Figure 4). Unlike fibronectin, which is encoded by a single gene and generates variants through alternative splicing, multiple genes encode each of the three laminin subunits, which results in different combinations of laminin variants. Laminins undergo self-polymerization and form filaments and layered sheets, which initiate basement membrane assembly. Interestingly, laminin sheets are generally mixtures of multiple laminins instead of separate networks of each laminin, (Schéele et al. 2007). When laminin polymerization is inhibited, basement membrane assembly seems to be disrupted even in the presence of other major constituents such as entactin,

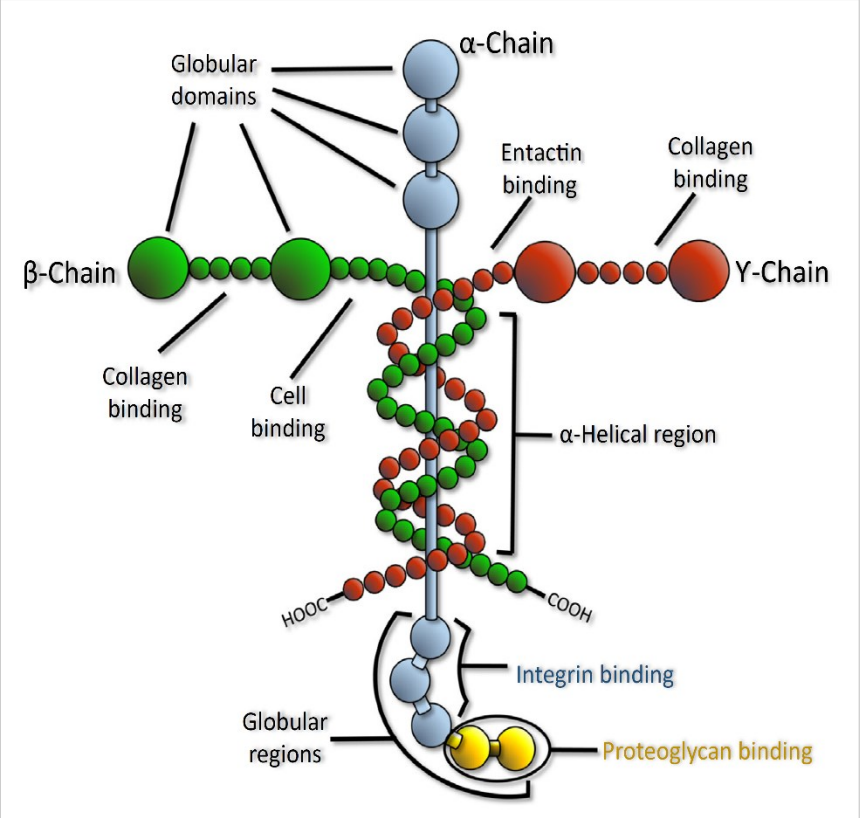

Figure 4. *Laminin strucrure: Laminin is composed of three polypeptide chains (α, β1, and β2) organized into the shape of a cross. Laminin has binding domains for heparin, collagen IV, heparin sulfate, and cells. Adapted from* ***(Sicari et al. 2014).***

type IV collagen, and perlecan, (Li et al. 2002). Laminin binds cell surface receptors like integrins and α-dystroglycan, which make laminin the central adhesive protein of basement membranes. Laminins interact with other laminins via their N-terminal globular LN domains to self-polymerize and initiate basement membrane assembly. There are also many protein-binding sites on laminins for ECM proteins, such as entactin (or nidogen), and for cells surface receptors, such as syndecans and integrins. Interestingly, most of the non-cellular ECM protein-binding sites are in the short arms of the three chains, whereas most of the cell surface receptor-binding sites are in the N- and C-terminus of laminin α chains, especially in the globular domain called LG-domain, (Timpl et al. 2000). A major class of laminin receptors for linking cells is the integrins. Laminin–integrin interaction activates variety of intracellular signaling pathways involving focal adhesion kinases (FAK), small Rho-GTPases, mitogen-activated protein kinases (MAPK), phosphatases and cytoskeleton components, and therefore mediates cell adhesion, migration, proliferation, differentiation, and survival, (Belkin and Stepp 2000; Givant-Horwitz, Davidson, and Reich 2005; Schéele et al. 2007; Watt 2002).

Type IV Collagen

Here up on Collagen IV (Col IV) is described separately as main structural component of the basement membrane. Col IV is not fibrillary protein, but it produces a unique network within the BM, which polymerize independently from laminin and play pivotal role on BM physiology.

As most members of the Collagen superfamily in vertebrates, Col IV is presented in at least 27 different isoforms, (Myllyharju et al., 2004). Col IV however is unique, because it occurs only in the BM. Collagen IV is heterotrimeric molecule, consisting of three alpha-chains, (Yurchenco and Furthmayr 1984). Each molecule is a combination of three out of six genetically distinct α-chains designated α1(IV) to α6(IV). Out of many potential combinations, these chains interact and assemble with a remarkable specificity to form only three distinct heterotrimers of α1α1α2, α3α4α5, and α5α5α6. The α1 and α2 chains, which were discovered first, and therefore called “classical” chains are present in the BM of all tissues, whereas the other four α-chains are spatially and temporally regulated in their tissue distribution during development, (Figure 5), (Khoshnoodi, Pedchenko, &

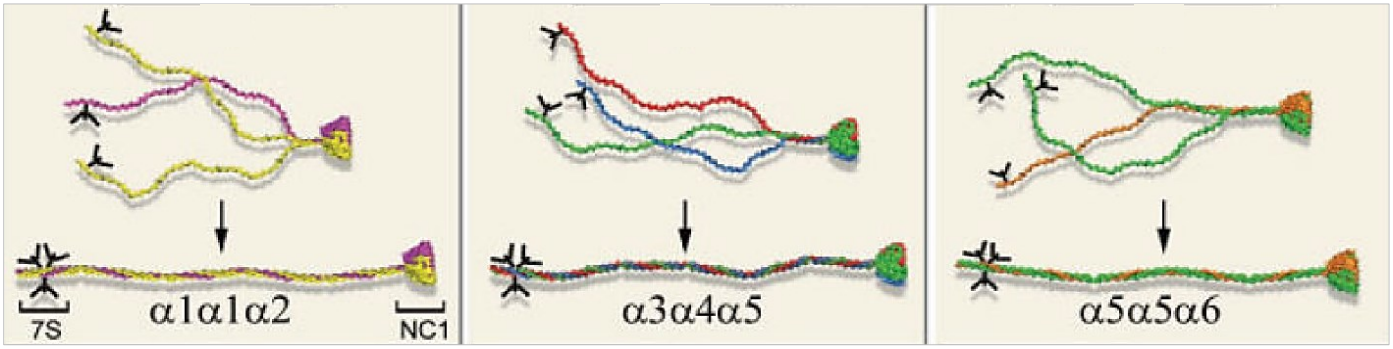

Figure 5. *Schematic view of assembly of collagen IV: Each heterotrimer is with characteristic stoichiometry of chains. The assembly initiates by chain-specific recognition of NC1 domains, formation of NC1-trimers followed by supercoiling of the triple-helical collagenous domains which proceeds toward the N-terminal 7S domains. Out of 56 potential heterotrimers, only three specific combinations: α1α1α2, α3α4α5, and α5α5α6, have been found in vivo. Adapted from* ***(Khoshnoodi, Pedchenko and Hudson 2008)****.*

Hudson, 2008). Each α-chain contains three structurally distinct domains: **(1)** a long collagenous domain of ~1400 residues, interrupted by about 20 short non collagenous sequences, which is flanked by **(2)** short N-NC sequence of 25 residues rich in cysteine and lysine, called 7S-domain, and **(3)** a globular non-collagenous carboxy-terminal domain (C-NC domain) of 230 residues, (Hudson et al. 2003). The presence of cysteine- and lysine-rich residues at the amino terminus is essential for intrachain crosslinking of four triple-helical molecules through disulfide bonds and lysine- hydroxylysine crosslinks. A characteristic feature of Col IV is the presence of 21 to 26 (depending on the type of the chain) interruptions in the collagenous Gly-X-Y triple repeats. This interruptions provide molecular flexibility for network formation and some of them also serve as cell-binding sites and inter-chain crosslinking, (Vandenberg et al. 1991). The NC1 domains are the sites for molecular recognition through which the stoichiometry of chains and the specificity in the assembly is directed. Khoshnoodi and co-workers have shown that a complex interaction of NC1 domains provides a high degree of specificity and serves as “folding matrix” for triple-helical assembly of Col IV molecule, (Figure 6), (Khoshnoodi et al. 2006). Once secreted into the ECM, the triple-helical molecules self-associate to form distinct networks providing a molecular scaffold onto which other ECM components such as laminins, perlecans, and proteoglycans interact. Yurchenco

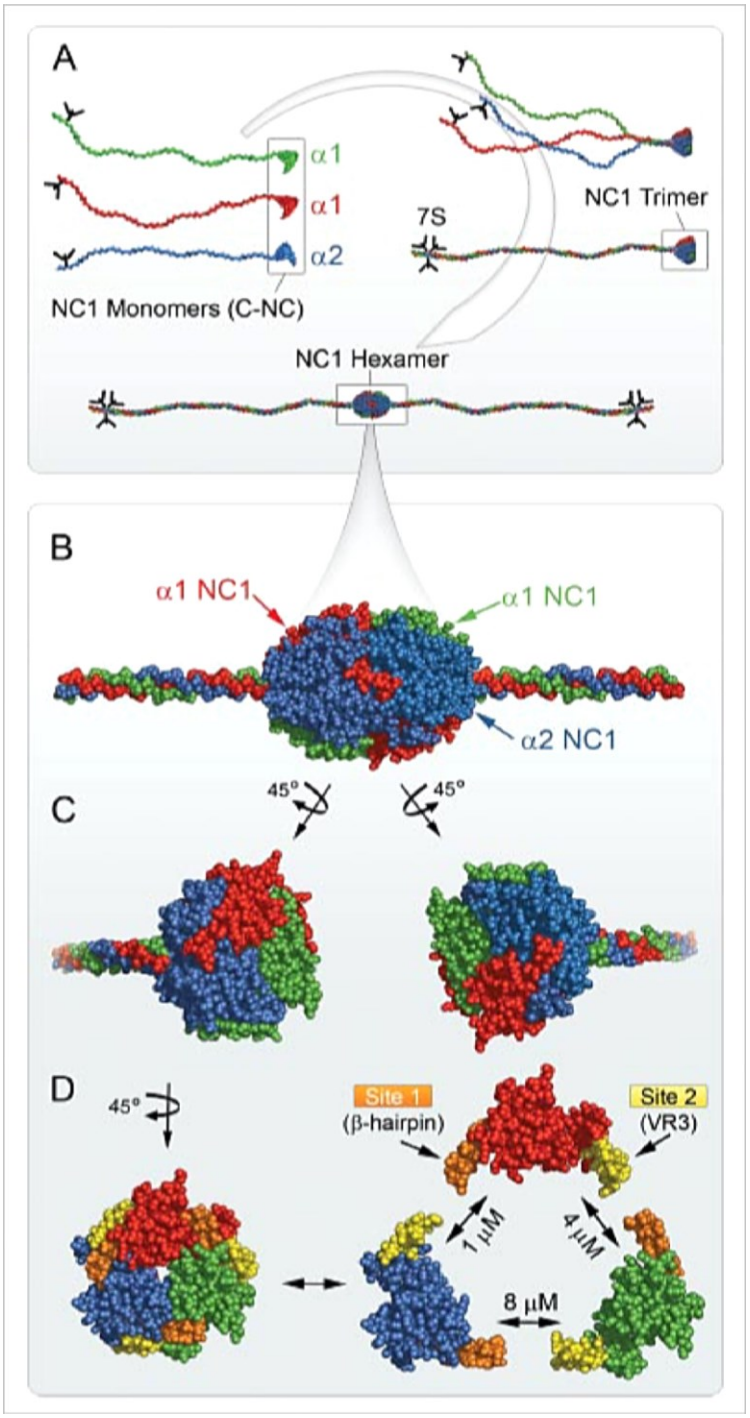

Figure 6. *Protomer assembly of collagen IV. Assembly is initiated by specific interactions of the C-NC domains **(A)**, after which folding of the triple helical domain proceeds toward the amino terminus, forming a heterotrimeric protomer. Dimerization of protomers occurs via the equatorial faces **(A and B)** of the NC trimers, yielding NC hexamers. Within each NC trimer, the monomers recognize one another through a domain-swapping mechanism in which an α -hairpin motif (Site 1) of one monomer is swapped into a docking site (Site 2) of its swapping partner **(C and D)**. Dimers also oligomerize at their N termini forming network suprastructures. Adapted from **(Khoshnoodi et al. 2006)**.*

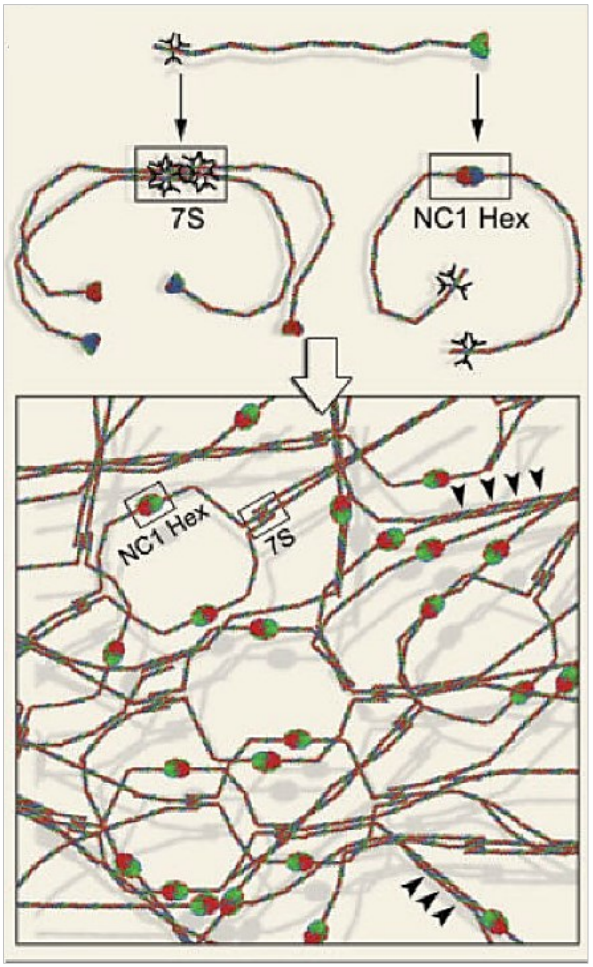

Figure 7. *Heterotrimeric collagen IV molecule interacts through its N-terminal 7S domains to form a tetramer (left) or through its NC1 domains to form a dimer (right). Through complex interactions, these molecules can further interact to form higher order of supramolecular organization and three-dimensional networks. Adapted from **(Khoshnoodi, Pedchenko and Hudson 2008)**.*

and Ruben investigated the supramolecular structure of collagen IV network in situ and showed that collagen molecules assemble into irregular polygonal networks held together by lateral interactions along the triple-helical domain, as well as the N-terminal and C-terminal end-domains, (Figure 7), (Yurchenco and Ruben 1987). Despite of providing a scaffold for assembly and mechanical stability of the BM, Col IV is an important cells interaction component. This interaction is crucial for many important biological processes as cell adhesion and growth, migration and differentiation. Cell attachment to Col IV is mediated by multiple binding sites within both triple-helical and NC1 domains and involves both integrin receptors (α1β1, α2β1, α10β1 etc.) and

nonintegrin receptors (for example, cell-surface heparin sulfate proteoglycans, chondroitin sulfate proteoglycan, CD44, mannose receptor family, etc, (Leitinger and Hohenester 2007).

Entactins (Nidogens)

Entactins, also known as nidogens, are basement membrane glycoproteins playing important role in integrating the laminin and Col IV networks together. Two entactins expressed by distinct genes have been identified in vertebrates, named *entactin-1* (~150 kDa) and *entactin-2* (~20 0 kDa) (or nidogen-1 and nidogen-2), (Kohfeldt et al. 1998). Each isoform contains three globular domains - two in the N-terminus (G1 and G2) and another one in the C-terminus (G3). A rod-like connecting domain composed of cysteine-rich epidermal growth factor-like repeats, which include the Arg-Gly-Asp (RGD) integrin-binding sequence and a thyroglobulin-like repeat, connects the N- and C-terminal globules. Entacin-1 binds strongly to both the laminin γ1 chain through globular domain G3 and to collagen IV through G2, (Fox et al. 1991; Pöschl et al. 1996; Reinhardt et al. 1993). Except as a linker between self-assembled laminin and collagen IV it acts to stabilize basement membrane, (Timpl and Brown 1996), but also integrates other ECM proteins. Entactin-1 binds fibronectin, perlecan, and fibulins through its G2 and G3 domains, (Kvansakul et al. 2001; Mecham 2011; Reinhardt et al. 1993).

Adhesive ECM proteins

Cells adhere to the extracellular matrix through interaction with the cell **adhesive ECM proteins**, including fibronectin, vitronectin, thrombospondins, tenascins, fibrinogen, and others. The structural BM proteins can also be described as adhesive proteins as they are recognized by integrins and induce cell adhesion, but they have other main function. Most adhesive glycoproteins bind cells through surface integrin receptors often in conjunction with other receptors, such as dystroglycans and syndecans. They also interact with each other or with other extracellular matrix components to form a rich ECM network. Interactions between cells and the ECM may mediate plethora of cellular responses, such as cell migration, growth, differentiation, cell survival etc. Cells receive and respond to signals from surrounding extracellular matrix, and in turn, modulate surrounding extracellular matrix through control of matrix assembly.

Fibronectin

As studies with fibronectin (FN) represent a significant part of this Thesis, it will be considered with more details.

FN was first discovered in 1948 as a contaminant of plasma fibrinogen showing insolubility at low temperature and therefore termed “cold-insoluble globulin”, (Morrison, Edsall, and Miller 1948; Mosesson and Umfleet 1970). FN is a high molecular weight dimeric glycoprotein (~450 kDa per dimer) widely expressed by a variety of cells in embryos and adult tissues, (Clark 1989; R. O. Hynes

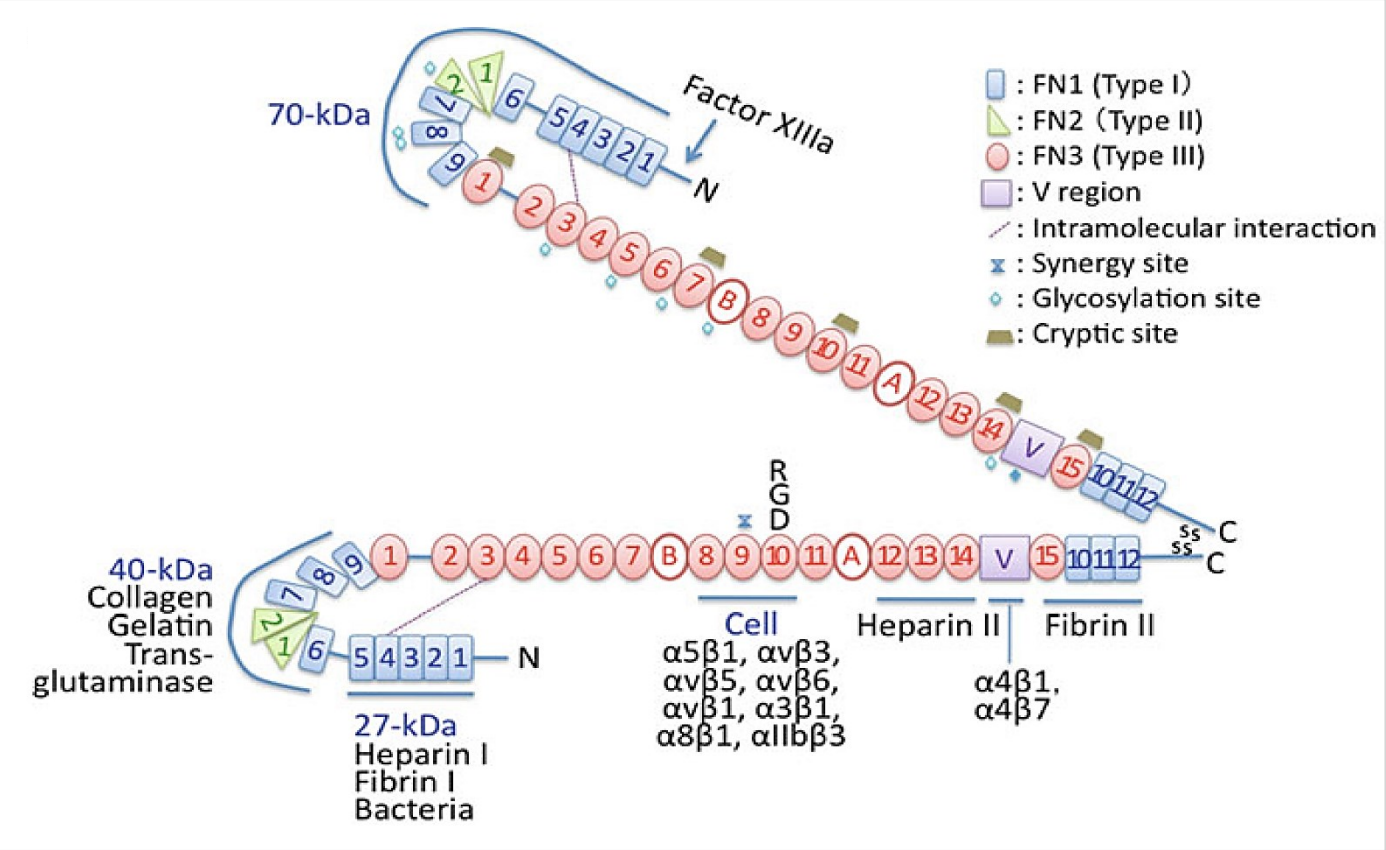

Figure 8. *Modular structure of fibronectin. (a) Each fibronectin dimer is composed of two monomers linked at the C-terminus by a pair of disulfide bonds. 12 type I modules (blue rectangles) termed FN1, 2 type II modules (green triangles) termed FN2, and 15–17 type III modules (rose ovals) termed FN3. Proteolytic 27, 40 and 70 kDa N-fragments and the protein-binding sites on fibronectin are underlined with receptors listed. Adapted from* ***(Mecham 2011)****.*

1990). Plasma fibronectin is synthesized in the liver by hepatocytes and present in a soluble form in blood plasma at a concentration of around 300-400 mg/mL. Cellular fibronectin is secreted by fibroblasts and multiple other cell types and is organized into fibrils contributing to the insoluble extracellular matrix. The name “fibronectin” is derived from the Latin word *fibra*, meaning “fiber”, and *nectere*, meaning “to bind”.

- *Basic structure of fibronectin*

Fibronectin mainly exists as a dimeric glycoprotein, with two similar ~240-kDa subunits covalently linked through a pair of disulfide bonds near the C-terminus. There are three types of repeating modules in each fibronectin subunit: 12 type I (termed FN1), 2 type II (termed FN2), and 15–17 type III repeats (termed FN3), (Figure 8), accounting for 90% of the sequence. The remaining sequences include a connector between modules $FN1^5$ and $FN1^6$, a short connector between $FN3^1$ and $FN3^2$, and a variable (V) sequence that is not homologous to other parts of fibronectin.

It has been noted that the N-terminal subdomain of the Von Willebrand factor (VWF) type C module of α2 procollagen are structurally similar to fibronectin FN1 module (O’Leary et al. 2004)suggesting that the VWF type C module may be the precursor of the fibronectin FN1 module.

FN2 modules are rare and are similar to some cringle domains, which are present in organisms evolutionary lower to vertebrates, (Ozhogina et al. 2001). Each FN2 module is approximately 60

residues long with two inter-chain disulfide bonds in each repeat. NMR studies identified an interaction between $FN1^{6}$ and $FN2^{2}$, (Pickford et al. 2001), and thus the FN2 modules are thought to be involved in a “head-to-tail” arrangement of FN modules, (Figure 8). FN2 modules are observed also in the structure of matrix metalloproteinases, (Collier et al. 1988).

The FN3 module is found in multiple copies in many other extracellular matrix proteins, cell surface receptors, and cytoskeletal proteins of vertebrates and non- vertebrates, (Bork and Doolittle 1992). Each FN3 has is about 90 residues and lacks disulfide bonds. It consists of two antiparallel b-sheets formed from seven b-strands that are connected by flexible loops. The main integrin-binding motif RGD is in one of the flexible loops connecting two b-strands, (Dickinson et al. 1994). One large single gene (~50 kb for human fibronectin) encodes this protein in most species (Hirano et al. 1983). Alternative splicing and various posttranslational modifications give a heterogeneity of FN, with up to 20 variants in human fibronectin, (Kosmehl, Berndt, and Katenkamp 1996). There are two alternatively spliced segments in fibronectin due to alternative exon usage*: extra domain A* (EDA) located between the $FN3^{11}$ and $FN3^{12}$ modules, and *extra domain B* (EDB) between $FN3^{7}$ and $FN3^{8}$ modules, (Figure 8). The Alternative splicing of fibronectin is regulated by the cell type, developmental stage, and aging, (Kornblihtt et al. 1996). Fibronectin isolated from plasma tends to have a lower molecular weight than one isolated from cell culture, which leads to the distinguishing of two types of FN, **plasma fibronectin** and **cellular fibronectin**. Studies showed that plasma FN generally lacks EDA and EDB sequences. Cellular fibronectin is more heterogeneous and is represented by splice variants with variable presence of EDA, EDB. Certain isoforms of FN, especially those containing EDA and EDB modules, are upregulated in malignant cells, (Ffrench-Constant 1995).

The EDA module of FN mediates cell differentiation, (Jarnagin et al. 1994). FN containing the EDA module is much better at promoting cell adhesion and spreading than FN lacking the EDA module. The presence of EDA enhances fibronectin-α5β1 integrin interaction and promotes cell adhesion, (Manabe et al. 1997). Genetically manipulated mice that lacked EDA developed normally, but with a shorter life span, abnormal wound healing, and edematous granulation tissue, (Muro et al. 2003), suggesting that EDA is not required for embryonic development but is important for a normal life span and emphasizing the role of FN in organization of the granulation tissue and in wound healing. On the other hand, EDB knockout mice developed normally as well, but with reduced fibronectin matrix assembly, (Fukuda et al. 2002). EDB-containing fibronectins are concentrated in tumors and are found at low levels in plasma, (Menrad and Menssen 2005). For this reason, tumor therapy research has focused on developing antibodies specific to the FN’s EDB module for diagnostic and prognostic purposes.

- *Posttranslational Modifications*

In addition to alternative pre-mRNA splicing, various posttranslational modifications that occur intracellularly in the endoplasmic reticulum and Golgi contribute to the heterogeneity of FN. Fibronectin can be glycosylated, phosphorylated, and sulfated, (Paul and Hynes 1984). The intrachain and intramodule disulfide bonds of FN1 and FN2 modules are often formed in this step. Generally, FN contains about 5% carbohydrate although higher levels of glycosylation occurs in some tissues. Nonglycosylated. FN is more sensitive to proteolysis than glycosylated fibronectin and has an altered binding affinity to proteins such as collagen, suggesting that carbohydrates stabilize FN against degradation and regulate its affinity to some substrates

FN is crucial for vertebrate development, presumably by mediating a variety of adhesive and migratory events. FN not only binds to cells through the cell surface receptors (integrins) but specifically interacts with other proteins, including collagen, fibrin, and heparin/heparan sulfate, (Pankov 2002).

- *Integrin binding domains*

Two main sites of fibronectin that mediate the cell adhesion are named cell-binding domains. They are located respectively in $FN3^{9}$–$FN3^{10}$ modules and in the alternatively spliced V-region. FN interacts with many integrins including α3β1, α5β1, α8β1, αvβ1, αIIbβ3, αVβ3, αVβ5, and αVβ6 that recognize its Arg-Gly-Asp (RGD) sequence in the central cell-binding domain. Integrins α4β1 and α4β7 however recognize also the Leu-Asp-Val (LDV) sequence in the V-region, (Humphries, Byron, and Humphries 2006; Leiss et al. 2008). The integrin binding motifs all contain a critical residue aspartate (Asp (D)), which interacts with a metal in the metal-ion dependent adhesion site (MIDAS) of integrins. Other Integrin-binding sites are also presented in the EDA module, which binds α4β1or α9β1 integrins, (Liao et al. 2002), in the $FN3^{14}$ module, which binds α4β1 integrin through the IDAPS sequence, (Pankov 2002), as well as in $FN3^{5}$, which binds activated α4β1or α4β7 integrin through the KLDAPT sequence, (Moyano et al. 1997).

- *Collagen binding domain*

The collagen-binding domain of fibronectin is identified as $FN1^{6}$–$FN1^{9}$ including also the first two FN2 modules. Fibronectin binds denatured collagen (gelatin) more effectively than native collagen. Fibronectin–collagen interaction may mediate cell adhesion to denatured collagen, form noncovalent crosslinking of fibronectin and collagen in migratory pathways, and regulate the removal of denatured collagenous materials from blood and tissue, (Pankov 2002).

- *Fibrin binding domain*

There are three fibrin binding sites in the fibronectin molecule. The first and the most important is located in the N-terminal $FN1^{4}$ –$FN1^{5}$ (Williams et al. 1994)The second binding site is $FN1^{10}$ – $FN1^{12}$, close to the C-terminus. The third binding site appears following chymotrypsin digestion of

fibronectin, and is immediately adjacent to the collagen binding domain (Clark 1989) At physiological temperatures, the fibronectin–fibrin interaction is weak. Covalent crosslinking of fibrin and FN however might be mediated by Factor XIII transglutaminase at a Gln-residue close to the N-terminus and stabilizes this interaction. In such a way fibronectin is incorporated into the fibrin clot, stimulates platelets, fibrin conversion and modulates cell adhesion or migration into the clots during wound healing, (Cho and Mosher 2006).

- *Heparin binding domains*

Fibronectin molecule contains at least two heparin-binding domains that interact mainly with heparan sulfate proteoglycans. The first domain localizes at $FN3^{12}$ – $FN3^{14}$ modules in the C-terminus. (Sharma et al. 1999) while second site is in the N-terminal: $1FN^{1}$ – $FN1^{5}$ modules. Heparin binding domains cooperate with cell binding domain of FN and potentiate cell adhesion, spreading, and formation of actin filaments.

- *Bacteria binding domain*

Besides heparin and fibrin, the N-terminal $FN1^{1}$–$FN1^{5}$ can bind several types of bacteria, such as Staphylococus aureus or Streptococcus pyogenes, (Clark 1989). Much attention has been paid recently to the bacterial ***fibronectin-binding proteins*** (FnBPs) that mediate cell adhesion and induce entry of bacteria into non-phagocytic host cells via fibronectin, (Schwarz-Linek, Höök, and Potts 2004). FnBPs are disordered in unbound state and upon interactions with fibronectin become ordered through an unusual and distinctive tandem b-zipper mechanism, (Bingham et al. 2008).

- *Fibronectin matrix assembly*

Functionally, FN is organized into a fibrillar network on the cell surface. Through interaction with the cell receptors it regulates various cell functions, such as cell adhesion, migration, growth, and differentiation, (Clark 1989; R. O. Hynes 1990). The majority of biological activities of FN require its assembly into fibrils, which are one of the earliest formed components of the ECM, and provide scaffolding for deposition of the fibronectin-interacting proteins such as collagen and heparan sulfate proteoglycans etc., (Hynes 2009). Inhibition of FN fibril formation causes delay in embryonic development, (Darribère et al. 1990). Unlike assembly of collagen or laminin, fibronectin fibrillogenesis does not occur spontaneously in natural physiological conditions. It requires the presence of cells. Soluble compact FN is assembled to its fibrillar form in a cell-mediated, stepwise manner. The process initiated by binding of soluble fibronectin to cell surface receptors that induce conformational changes to expose cryptic binding sites. These changes facilitate fibronectin–fibronectin interactions, forming fibronectin fibrils elongation through cell-generated tension (actually generated by integrins) and the formation of an insoluble fibrillar network, (Figure 9). One hypothesis is that fibronectin assembly begins by interactions of the fibronectin cell- binding domain (RGD motif

in FN3[10]) with cell surface integrins, (Mao and Schwarzbauer 2005; Mecham 2011). On the other hand, the dimeric fibronectin (i.e. the soluble FN) induces **integrin clustering** upon binding two integrins with its two cell-binding domains. Clustered integrins become activated that provokes actin filament rearrangement, facilitates the extension of fibronectin and exposes cryptic binding sites, as stated above. It enables interactions of the N-terminal 70K region FN1[1] – FN1[9], termed 70K fragment, with other parts of fibronectin, and causes irreversible association of fibronectin to a fibrillar matrix. Another hypothesis suggests that FN assembly is initiated by interaction between the N-terminal 70-kDa region and its cell surface receptors. Accordingly, binding of the 70K region to cell surface receptors unfolds FN, which exposes the integrin binding site RGD to interact with cell surface integrins causing elongation of bound FN, and exposing cryptic fibronectin–fibronectin binding sites form FN fibrils, (Tomasini-Johansson, Annis, and Mosher 2006)

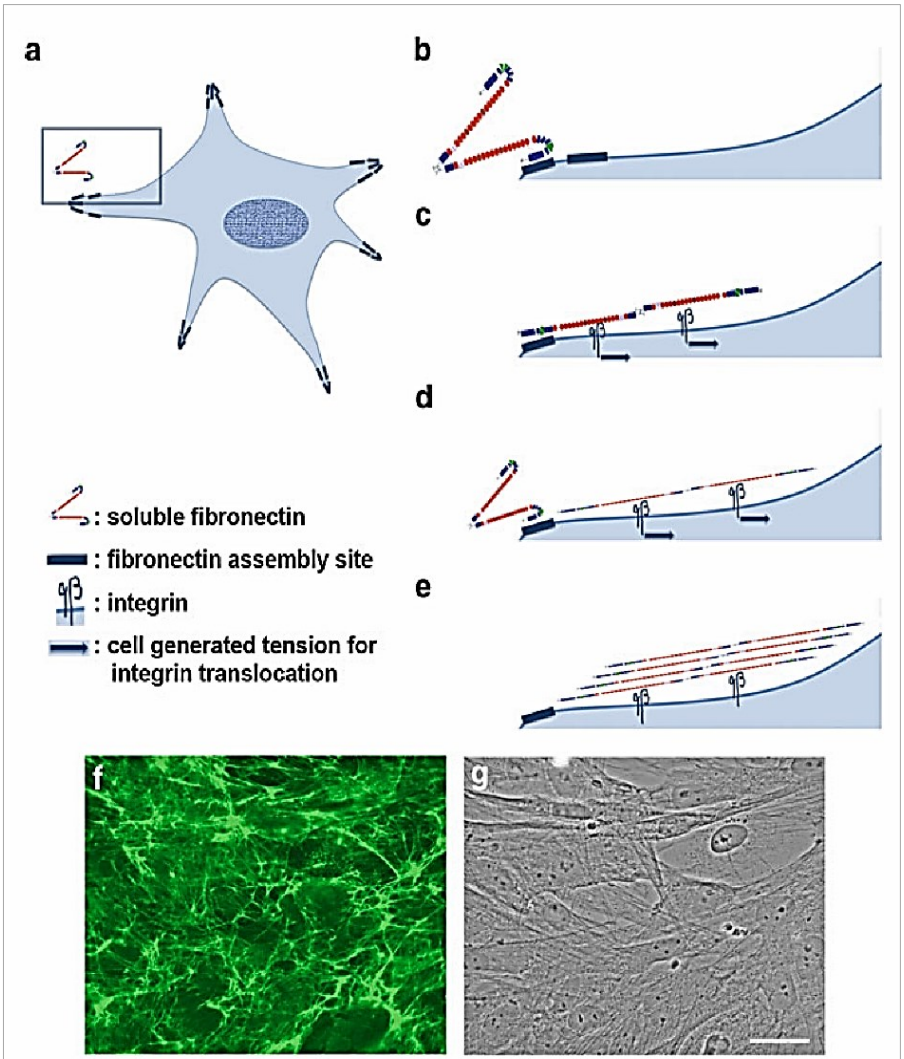

Figure 9. *Hypothetical model of fibronectin assembly.* ***(a)*** *FN assembly sites on the cell surface is controlled by the adherent substrates to which cells are attached;* ***(b)*** *Soluble fibronectin dimer binds to linearly arrayed fibronectin assembly sites through the N-terminal 70-kDa region of fibronectin;* ***(c)*** *The binding of 70 K to the cell surface fibronectin assembly receptors induces unfolding of fibronectin, which exposes the RGD sequence in FN3[10];.****(d)*** *The RGD- integrin interaction leads to stretching FN through tension generated from integrins and cytoskeleton contractility;* ***(e)*** *Elongation of fibronectin exposes more cryptic fibronectin– fibronectin interacting sites, leading to the formation of insoluble fibronectin fibrils through fibronectin–fibronectin interactions.* ***(f)*** *Immunofluorescence staining of fibronectin matrix.* ***(g)*** *Cells shown by phase contrast microscopy. Adapted from* ***(Xu et al. 2009)****.*

Vitronectin

Vitronectin (VN) is a 75-kDa glycoprotein present in blood plasma at a concentration of 200–400 mg/ml (2.5–5.0 mM). This adhesive protein is present also in other body fluids such as amniotic fluid and urine, and in the ECM of most tissues, (Preissner 1991; Tomasini and Mosher 1991). VN was independently studied under the names “serum spreading factor”, “epibolin,” and “S protein (site-specific protein)” in the late 1970s and early 1980s, until it was realized that all studies relate to the

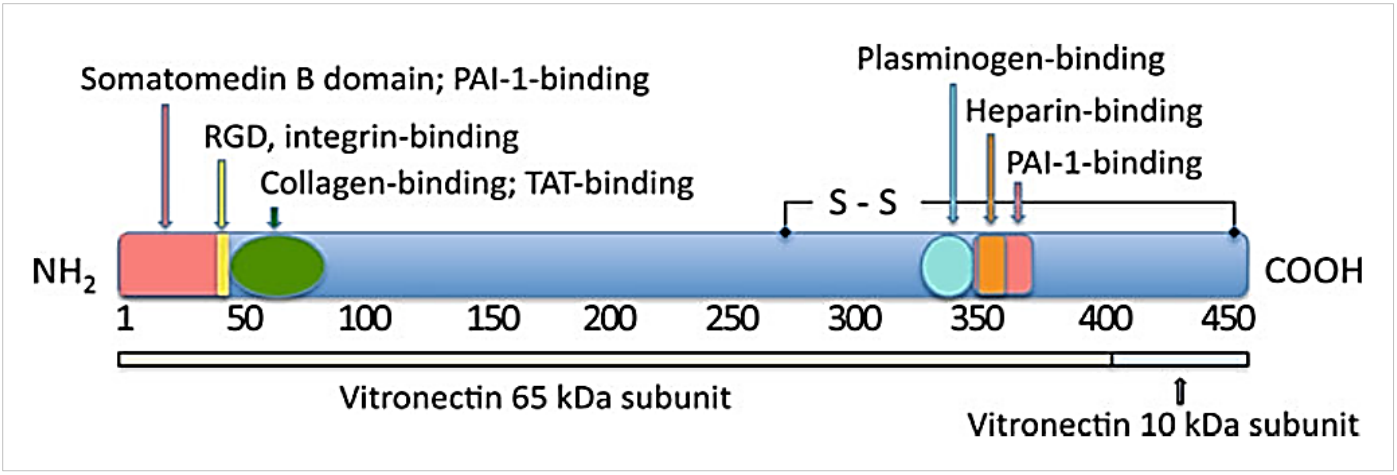

Figure 10. *Protein-binding domains of vitronectin. Vitronectin's major ligand-binding sites are indicated. The major integrin-binding site RGD locates in residues 45–47. A disulfide bond connects the 65 kDa and the 10 kDa subunits of the cleaved form of vitronectin. PAI-1:Pplasminogen activatorr inhibitor-1, TAT: thrombin-antithrombin. Adapted from* ***(Mecham 2011)****.*

same protein - **vitronectin**, given the name for its ability to bind glass ("vitrus", Latin). Human VN is a protein of 459 amino acids, mainly synthesized in the liver, (Seiffert et al. 1994). In human blood, it exists in two forms: one is a single chain 75-kDa form, and the other is a two-chain form of 65 and 10-kDa chains connected by a disulfide bridge, Schvartz, Seger, and Shaltiel 1999). Vitronectin has many important protein-binding domains, (Figure 10). A somatomedin B domain is located at the N-terminus and binds plasminogen activator inhibitor-1 (PAI-1),(Zhou et al. 2003), and interacts with the urokinase receptor, (Wei et al. 1994). Immediately adjacent to the somatomedin B domain is an RGD cell adhesion sequence, which is the major integrin binding site in the protein. Close to the RGD are the binding domains for thrombin–antithrombin complex and collagen, Schvartz, Seger, and Shaltiel 1999). At the C terminus, there are also a plasminogen-binding site, two heparin-binding sites and another (PAI-1) binding site, (Kost et al. 1992). Vitronectin interacts with the extracellular matrix through its collagen- and heparin binding domains, and with cells through its RGD integrin binding sequence. Integrins αIIbβ3, αVβ1, αVβ3, αVβ5, αVβ8, and α8β1 are those recognizing the RGD motif of VN, (Marshall et al. 1995; Nishimura, Sheppard, and Pytela 1994) Vitronectin–integrin interaction activates important intracellular signaling pathways, induces protein phosphorylation, activates MAP kinase pathways, and thereby plays an important role in processes like cell adhesion, spreading, migration, cell growth, differentiation, proliferation, and apoptosis Schvartz, Seger, and Shaltiel 1999). VN functions in wound healing, viral infection and tumor growth and metastasis are also well recognized, (Felding-Habermann and Cheresh 1993; Schvartz, Seger, and Shaltiel 1999).

Curiously, VN knockout mice developed normally with no major defects, (Zheng et al. 1995), suggesting either vitronectin is dispensable or other molecule might play a rescue role in the absence of vitronectin.

Multifunctional matrix components

This group includes multiple ECM proteins. Except in cell adhesion those proteins are involved also in various specific functionalities

Von Willebrand factor

Von Willebrand factor is another adhesion protein that is primarily involved in the adhesion of vascular cells (McGrath et al. 2010; Sadler 1998). It is synthesized by the megakaryocyte (the platelet-generating cells of the bone marrow) and is stored in the α-granules of circulating platelets. Activation of platelets leads to the release of von Willebrand factor. It is also synthesized and stored by endothelial cell. A multimeric form of the protein, with tens of copies linked together into insoluble form, is present in the sub-endothelium, where it is involved in blood platelet adhesion in cases of vascular injury,(Hubbell 2007; Springer 2011).

Thrombospondins

Thrombospondins are a family of structurally related multifunctional, multimodular calcium-binding ECM glycoproteins encoded by separate genes. Five thrombospondins have been identified so far and can be divided into two groups: group A with thrombospondin-1 and -2 forming homotrimers, and group B with thrombospondin-3, -4, and -5 (also known as *cartilage oligomeric matrix protein*) forming homopentamers, (Lawler 2000). Thrombospondins are shown to bind to cells, platelets, calcium, and various substances such as heparin, integrins, fibronectin, collagen, laminin, fibrinogen, plasminogen, osteonectin, and TGF-β; and are important for cell adhesion and spreading, platelet aggregation, angiogenesis, neurite growth and apoptosis, (Esemuede et al. 2004; Mosher 1990) For example, thrombospondin-1 can inhibit endothelial cell proliferation and migration, inhibit neovascularization, but promote growth and migration of smooth muscle cells and fibroblasts, (Bagavandoss and Wilks 1990; Esemuede et al. 2004; Vogel et al. 1993). Generally, the medical focus of thrombospondin is on its role in angiogenesis and tumor therapy.

Fibrinogen

Studies with fibrinogen constitute a considerable part of this thesis, therefore it will be reviewed in more details.

Fibrinogen (FBG) is a fibrous protein that was first discovered together with keratin, myosin, and epidermin and separated of them based on its X-ray diffraction patterns, (Bailey, Astbury, and Rundall 1943). Later on it was found to be associated with an α-helical coiled-coil structure. FBG is a glycoprotein normally present in human blood plasma at concentration of about 2.5 g/L. This plasma protein is essential for hemostasis, wound healing, inflammation, angiogenesis and other

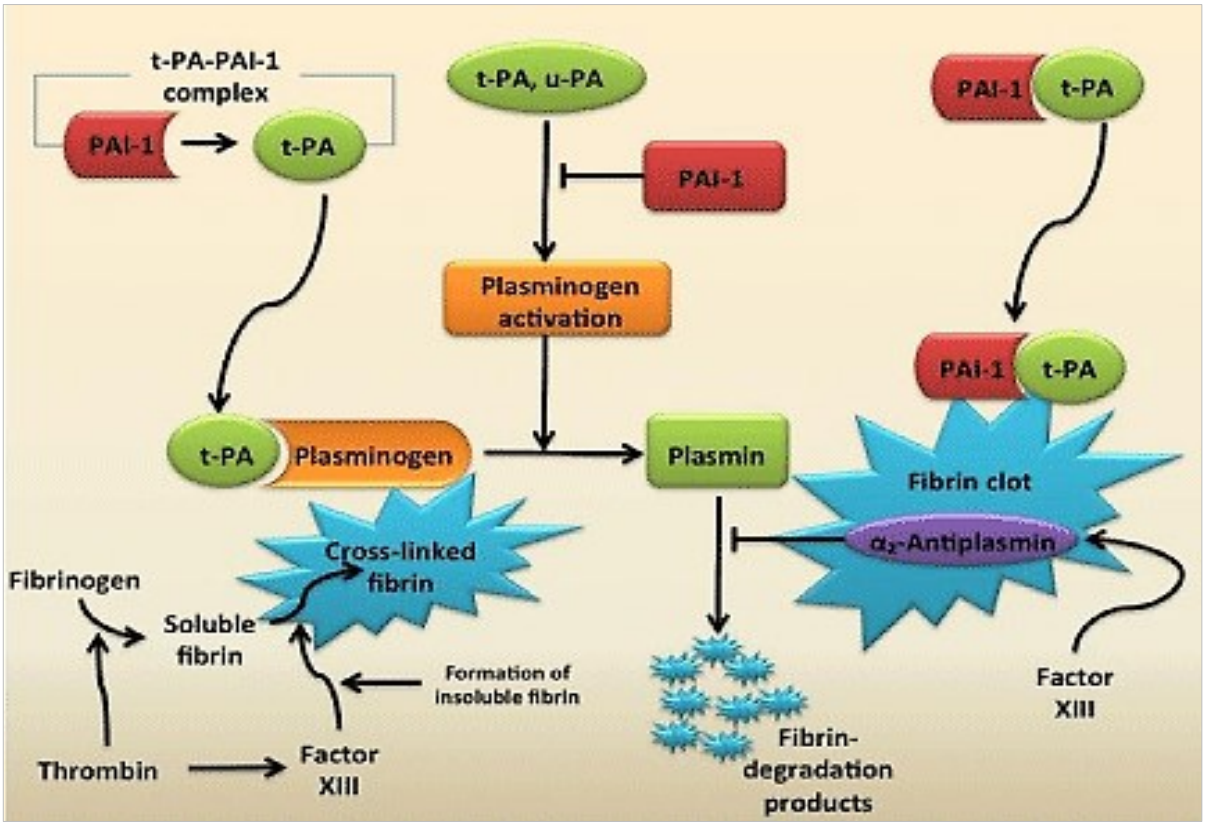

Figure 11. *Fibrinolytic system: Tissue plasminogen activator (t-PA) circulates in plasma as a complex with plasminogen-activator inhibitor type 1 (PAI-1). On the surface of the clot. t-PA or urokinase-type plasminogen activator (u-PA) activates plasminogen. The complex of plasminogen, t-PA, and fibrin promotes the formation of plasmin. Plasmin causes lysis of the cross-linked fibrin into fibrin degradation products. PAI-1 also binds to fibrin and is able to retain inhibition against t-PA. α2-antiplasmin inhibits plasmin from creating fibrin degradation products. Factor XIII activates α2-antiplasmin as well as cause soluble fibrin to become cross-linked fibrin. Figure adapted from* ***(Del Rosario and Tsai 2015)****.*

biological functions. FBG is a soluble macromolecule, but it forms a clot, or insoluble gel, upon conversion to fibrin by the action of the serine proteolytic enzyme **thrombin**, (Figure 11), which itself is activated by a cascade of enzymatic reactions triggered by injury or upon contact with foreign surface. Fibrinogen is also necessary for the aggregation of blood platelets, an initial step in hemostasis. Each end of a fibrinogen molecule can bind with high affinity to the integrin receptor on activated platelets, αIIbβ3, so the bi-functional fibrinogen molecules act as bridges to link platelets. In its various functions as a clotting and adhesive protein, the fibrinogen molecule is involved in many intermolecular interactions and has specific binding sites for several proteins and cells. **Fibrin** clots are dissolved by another series of enzymatic reactions termed the fibrinolytic system, (Figure 11). In this system the proenzyme plasminogen is activated to plasmin by a specific proteolytic enzyme, typically tissue-type plasminogen activator or urokinase-type plasminogen activator. Plasmin then cleaves fibrin at certain unique locations to dissolve the clot. The activation of the fibrinolytic system is greatly enhanced on the surface of fibrin, thus, the fibrinolysis highly specific for cleavage of the insoluble fibrin clot, rather than circulating fibrinogen, (Weisel 2005). Fibrinogen is a large glycoprotein with three pairs of polypeptide chains linked together by disulfide bonds. FBG molecules are elongated 45 nm structures that consist of two outer D domains, each connected by a coiled-coil segment to its central E domain (Figure 12, A). The molecule is comprised of two sets of three polypeptide chains designated Aα,Bβ, γ with molecular masses of 66.5, 52 and 46.5 kDa,

respectively. Posttranslational addition of carbohydrates to the Bβ and γ chains brings the total molecular mass to about 340 kDa. The nomenclature for fibrinogen, $(A\alpha,B\beta, \gamma)_2$, arises from the designation of the small peptides that are cleaved from fibrinogen by thrombin to yield fibrin as **fibrinopeptides A** and **B** (FpA and FpB) and the parent chains, without fibrinopeptides α and β. No peptides are cleaved from the γ chains by thrombin. The entire amino acid sequence of all polypeptide chains of human fibrinogen has been determined from the nucleotide sequences of the cDNA coding for the polypeptide chains, (Doolittle 1984; Henschen and Mcdonagh 1986). There are respectively 610, 461, and 411 amino acids in each of the human Aα, Bβ, and γ chains. The amino acid sequences of the three chains are homologous, but also differences exist, determining specific functions for certain molecular domains. All six chains are held together by disulfide bonds in the

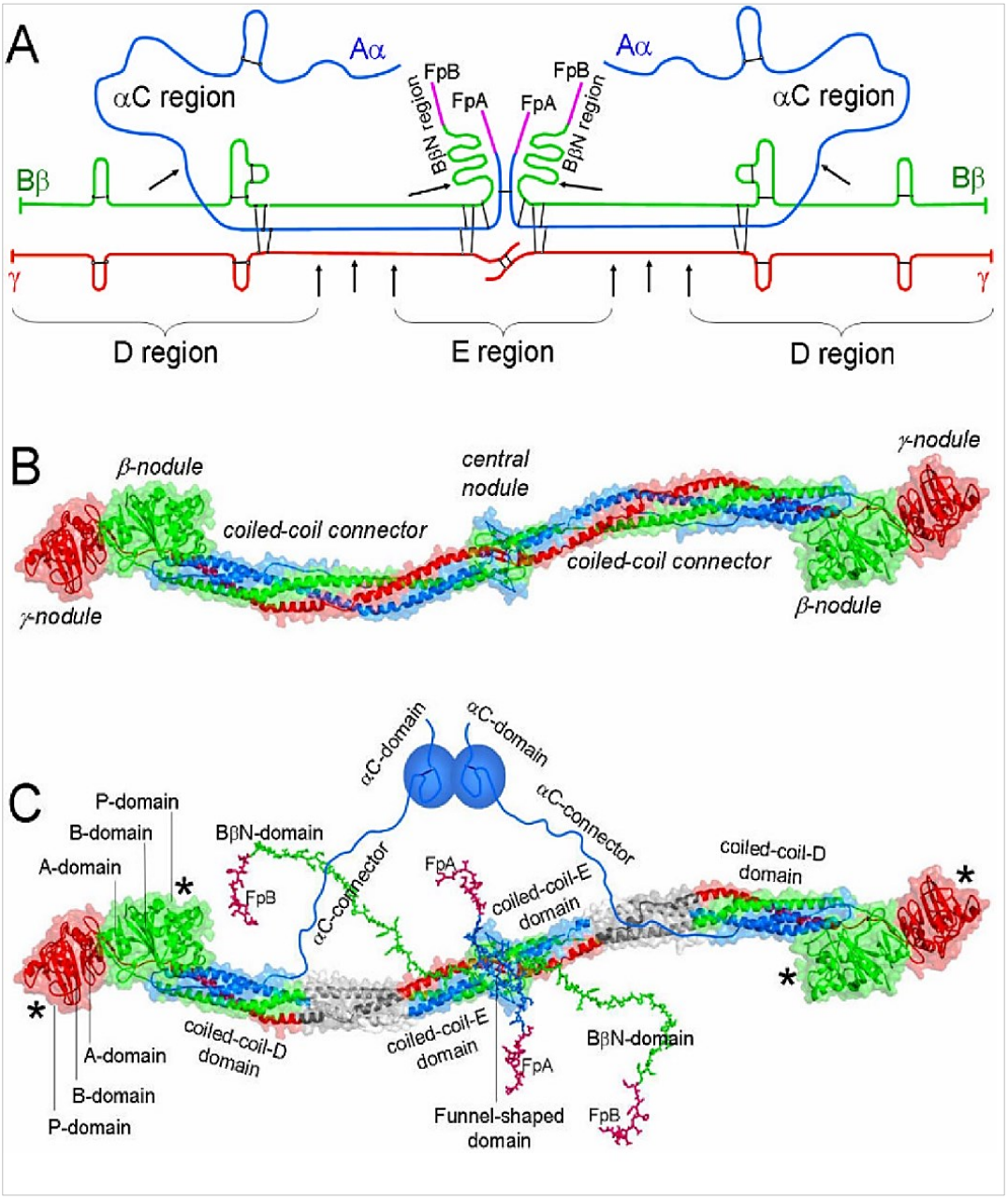

Figure 12. *Fibrinogen structure.* ***(A)*** *Polypeptide chain composition of fibrinogen. The individual chains, Aα, Bβ and γ, are blue, green and red, respectively; fibrinopeptides A and B (FpA and FpB) are magenta; the disulfide bonds are indicated as black bars; triple arrows show proteolytic cleavage sites between the D and E regions in the removal of the αC and BβN regions.* ***(B)*** *Crystal structure of fibrinogen* ***(C)*** *Domain structure of FBG. The individual domains of the D regions, A-domain, B-domain, and P-domain, are indicated only in one subunit of the molecule. Color indications from* ***(A)*** *are preserved. Adapted from* ***(Medved and Weisel 2009)***.

central domain, (Henschen and Mcdonagh 1986). Three interchain disulfide bonds link the two halves of the molecule together, one between the two Aα chains and two between the two γ chains. The A and B fibrinopeptides are located at the N-terminal ends of the α and β chains, respectively, (Doolittle 1984; Weisel 2005)

- *Domain structure of FBG*

The shape of fibrinogen and its organization into domains have been defined by a variety of physicochemical and structural techniques. Fibrinogen was one of the first biological macromolecules visualized by electron microscopy, (Hall and Slayter 1959). It was recognized as elongated molecule about 45 nm in length with nodular regions at both ends connected by rod-like strands. The central region contains the two pairs of A and B fibrinopeptides and binds thrombin. The distal end nodule is the **C-terminal γ chain** (γC nodule) is made up of three domains, and the proximal end nodule is the **C-terminal Bβ chain** (βC nodule), also made up of three domains, (Medved et al. 1990; Rao et al. 1991; J. W. Weisel et al. 1985). The C-terminal portions of the two Aα chains (**αC domains**) extend from the molecular ends and interact with each other and with the **central domains** in fibrinogen, (Figure 11, B), (Gorkun et al. 1994). It was found that each terminal part of the fibrinogen molecule is made up of six cooperative domains, with three domains formed by the C-terminal part of the β-chain and three other domains formed by the C-terminal part of the γ-chain, (Medved et al. 1990; Privalov and Medved 1982). Several proteolytic fragments of fibrinogen has been used as a basis for defining its domain structure and identifying functional sites, (Hantgan et al. 2000). The fibrinolytic enzyme **plasmin** cleaves fibrinogen at distinct locations. Initial digestion removes the C-terminal Aα chains and Bβ 1-42, creating fragment X. Cleavages in all three chains then yield two D fragments and one E fragment, (Figure 11, C).

Tenascin

Tenascins are a group of ECM-glycoproteins including **tenascin-C, tenascin-R, tenascin-W, tenascin-X,** and **tenascin-Y,** (Jones and Jones 2000). Tenascin-C was the first tenascin identified and is predominantly synthesized by the nervous system and connective tissues. Tenascin-R is also found in the nervous system. Tenascin-X and tenascin-Y are presented primarily in muscle connective tissues. Tenascin-W is found in kidney and developing bone with a KGD sequence that interacts with integrins (Meloty-Kapella et al. 2008). The basic structure of tenascins contains numbers of epidermal growth factor-like repeats followed by alternatively spliced fibronectin type III modules and a fibrinogen-like globular C- terminal domain. Like thrombospondin-1, tenascin-C contains an RGD motif and is recognized by diverse integrins, yet classified as a rather antiadhesive or adhesion-modulatory protein (Orend and Chiquet-Ehrismann 2000). Human umbilical vein endothelial cells (HUVEC) adhere to tenascin-C by α2β1and αvβ3 integrins and partially spread, but generally, adhesion to tenascins is weak, with adherent cells being elongated instead of flattened.

In most cases adhesion does not result in rearrangement of actin cytoskeleton, (Sriramarao, Mendler, and Bourdon 1993). Tenascin-C provokes cells adherent to fibronectin to detach through direct interaction of tenascin-C with the 13 FN3 module of FN (Midwood and Schwarzbauer 2002). The metalloprotease meprin cleaves human tenascin-C at the seventh fibronectin type III repeats and destroys the antiadhesive ability of tenascin-C by removing the C-terminal anti-adhesion domain, (Ambort et al. 2010).

Nephronectin

Nephronectin is an ECM - glycoprotein found as a ligand for α8β1 integrin, an interaction that is essential for kidney development, (Brandenberger et al. 2001). Nephronectin has 70–90 kDa molecule with five epidermal growth factor like-repeats, an RGD-containing linker domain and a C-terminal domain named the MAM domain. It is widely expressed in kidney, lung, brain, uterus, placenta, thyroid gland, and blood vessels - a distribution similar to that of α8β1 integrins, (Brandenberger et al. 2001; Huang and Lee 2005; Manabe et al. 2008). To date, a8b1 integrin is the only identified receptor for nephronectin and interaction is through its RGD sequence in the linker domain and a synergetic sequence on the C-terminal side of the RGD motif, (Sato et al. 2009).The high affinity of nephronectin to α8β1 integrin explains why other ligands with lower affinities to that integrin such as fibronectin, vitronectin, or tenascin-C are not able to compensate the deficiency of nephronectin in kidney development.

Elastin

Elastin is ECM protein able to interact with neighboring cells and critical for the mechanical properties of ECM. It springs back tissues into their initial shape after deformation, tissues in which this ability is particularly vital, including arteries, tendons and skin. (Davies 2001). The tissue elasticity is normally achieved by a random network of elastic fibers embedded within and supporting the ECM. These fibers contain high amount of elastin on which depend their mechanical properties. Elastin is synthesized and secreted as a soluble precursor, tropoelastin, which forms elastic fibers in association with other ECM components, mainly fibrillins 1and 2. The fibers are stabilized by an enzymatically stabilized by lysyl oxidase, which deaminates specific lysine amino acids in the elastin molecule and allows the covalent crosslinking of fibers. The balance of elastic fibers of elastin and the relatively inelastic fibers of collagen, which varies between different ECMs, is thought to be a key regulator of their mechanical properties, (Davies 2001).

Fibrillins

Fibrillin 1 and 2 are large cysteine-rich glycoproteins that serve two key physiological functions: as supporting scaffold on which elastin is laid down to make elastic fibers maintaining the tissue integrity and as regulators of signaling events that instruct cell performance. The structural role of

fibrillins is connected with providing temporal and hierarchical assembly of microfibrils and elastic fibers, whereas the instructive role includes their ability to sequester transforming growth factor β (TGF-β) and bone morphogenetic protein (BMP) complexes in the ECM, (Ramirez and Sakai 2010).

Proteoglycans

Proteoglycans are also important component of the ECM. They are present in a diverse set of molecules characterized by having very large and complex carbohydrates attached to a protein core. The complex carbohydrates are often referred as **glycosaminoglycans** (GAGs), (Figure 13). GAGs possess a variety of biologic activities including the ability to bind growth factors and cytokines and promote water retention, (Bülow and Hobert 2006). There are several types of protein core, and many types of GAGs classified into distinct families (e.g. heparin, heparan sulfate, chondroitin sulfate A and B, hyaluronic acid (HA) or hyaluronan, dermatan sulfate, keratan sulfate etc., (Iozzo and Schaefer 2015). Within each of these families there is variation in the precise sequences of sugars. Each protein core of proteoglycans can carry a variety of GAGs, and different cores may bear the same type of GAG. The protein cores are synthesized by the normal secretory pathway in the endoplasmic reticulum and then pass to the Golgi apparatus, where certain of their serine residues are linked via xylose to long GAG chains that are synthesized in situ. In most proteoglycans, these chains are then sulfated by sulfotransferases, thus obtaining sulfate groups giving the GAGs a net negative charge. Proteoglycans have a variety of functions. Many can be bound by receptors on cells, promoting cell–ECM adhesion, and also by ECM molecules such as

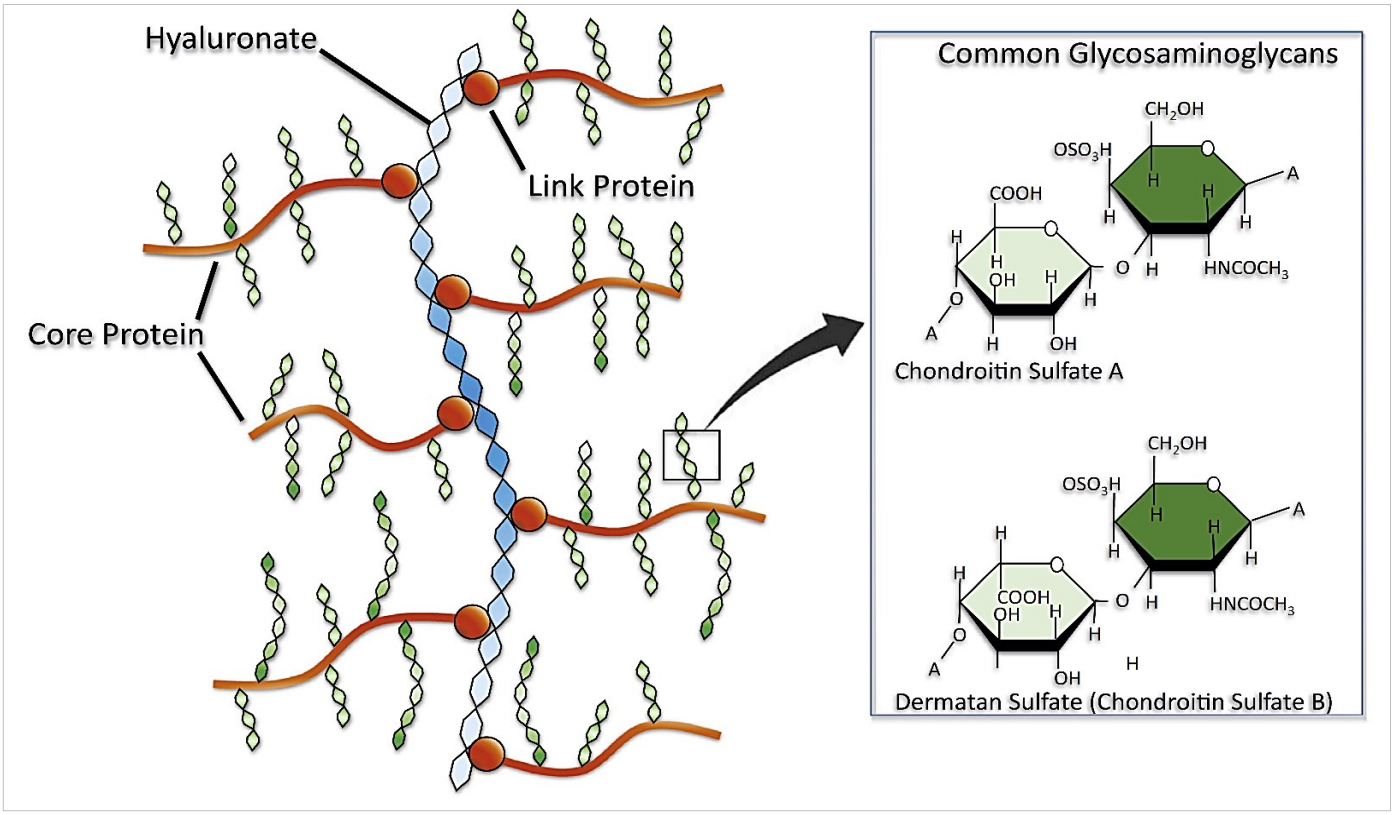

Figure 13. *Structure of Proteoglycans. GAGs are long unbranched polysaccharides that are composed of a repeating disaccharide unit. The disaccharide unit is composed of one of either N-acetylgalactosamine or N-acetylglucosamine. Adapted from (Sicari et al. 2014).*

fibronectin. Most of them can take up water to form hydrated gels to fill space in the ECM, and some, like heparan sulfate, bind to a variety of growth factors, concentrating them in the ECM and preventing their diffusion, (Davies 2001). Examples of matrix proteoglycans include aggrecan, which accounts for 10 % of the weight of cartilage and forms a hydrated gel into which collagen fibers are embedded; lumican, which forms a gel that aids the transparency of the cornea; neurocan, which appears to guide developing nerves to their targets when the nervous system wires itself up in embryonic life; fibromodulin, which appears to inhibit collagen fibril assembly; and perlecan, which forms a filter-like gel in basement membranes. HA retains significant biological activity and directly promotes cell proliferation, migration, and differentiation. The concentration of HA within ECM is highest in fetal and newborn tissues and is therefore associated with enhanced healing properties, (Hodde et al. 1996; Sicari et al. 2014).

Structural dynamic of ECM

The micro-environmental conditions that cells find are key regulators of the normal tissue function and disease appearance. Cells continuously adapt to their environment by modifying their behavior but also by remodeling their microenvironment ,(Cox and Erler 2011)). Hence, understanding the complex processes accompanying ECM production, modification and remodeling, and how these processes change the physiological, biochemical and biomechanical properties of the ECM, are key to understand the cells behavior at biomaterials interface.

Except synthesis, ECM undergoes continuous organization and remodeling based on mechanical reorganization or enzymatic degradation (Altankov et al. 2010; Coelho et al. 2016). Observed *in vivo* or *in vitro*, these processes play a critical role in adaptation of cells to their microenvironment and reveal the importance of the reciprocal cell-ECM interactions for the normal tissue homeostasis and function.

ECM remodeling

Within tissues, cells build and reshape the ECM by **synthetizing, degrading or reassembling** it. Remodeling rates are particularly high during development, regeneration of tissues and wound repair, but when miss-regulated, they can contribute to diseases such as atherosclerosis, fibrosis, ischemic injury and cancer, (Curino et al. 2005; Reisenauer et al. 2007; Yu, Mouw, and Weaver 2011).

Mechanical reorganization of ECM proteins

Although the processes involved in the organization of ECM are poorly understood, there are evidences for distinct hierarchical steps in matrix assembly starting with the recognition of ECM components followed by an order of complex inter-ECM interactions. For example, the integrin-mediated arrangement of fibronectin into fibrils is dependent on integrins but is also connected with

the tethering of other ECM proteins, including thrombospondin 1 and type I collagen to the cell surface, (Sottile and Hocking 2002). The basement membrane assembly is also initiated by recognition of laminins by the cells; in fact, they self-assemble into heterotrimers only at the cell surface interacting with cell surface receptors - mainly integrins, (Daley, Peters, and Larsen 2008; Li et al. 2003)Type IV collagen also assembly only in contact with cells, but is further internally stabilized by Met-Lys crosslinks in the basement membrane, (Than et al. 2002). Kurban et al. showed that a small protein named von Hippel-Lindau tumor-suppressor protein is required for this assembly. Other proteins also play role in basement membrane structuring: an example is the nidogen, which interacts with specific domains of laminin and also links collagen IV within the basement membrane, (Kurban et al. 2008).

The ability of cells to **rearrange adsorbed matrix proteins** in a **fibril-like pattern** is well described in literature phenomenon, (Christopher, Kowalczyk, and McKeown-Longo 1997; Sottile and Hocking 2002; Velling 2002). Several cell types (including fibroblasts and endothelial cells) tend to rearrange adsorbed matrix proteins, such as fibronectin, fibrinogen, and even collagen IV in a fibril-like pattern seeking to mimic the natural organization of these proteins in ECM, (Altankov and Groth 1994; Coelho et al. 2011, 2013, 2016; Tzoneva et al. 2002), or creating appropriate microenvironment for secretion of own matrix. Such a cellular activity are strongly dependent on the surface properties of materials like hydrophility, surface chemistry, electrical charges, stiffness etc. (Altankov and Groth 1994; Gustavsson et al. 2008; Rhee and Grinnell 2007) and have their importance for the biocompatibility of the materials. It is postulated that biocompatibility of materials is connected with the allowance of cells to remodel surface associated proteins, presumably as an attempt to form their own matrix (G. Altankov & Groth, 1994; Georgi Altankov, Grinnell, & Groth, 1996; Nuno Coelho et al 2011, 2013, 2016, Tzoneva et al 2002). For example, the cells trigger Integrin-mediated organization of substrate adsorbed fibronectin into specific fibrillar structures, very similar to fibronectin matrix fibrils that occur during the physiological fibronectin fibrillogenesis (Altankov&Groth 1994; Altankov, Grinnell, and Groth 1996; Altankov et al 2010). Moreover, there are observations that organized fibronectin may recruit other matrix proteins to the cell surface, and therefore is required for their organization. For example, Tzoneva et al showed that fibronectin fibrillogenesis is required for rearrangement of substratum associated fibrinogen; endothelial cells were able to reorganize both adsorbed and soluble fibrinogen in specific fibrillar structures that follow the fibrillar organization of the fibronectin (Tzoneva et al. 2002). Even collagen IV, which is a non-fibrillar protein in its nature, can undergo fibril-like linear rearrangement by fibroblasts along fibronectin fibrils, (Coelho et al. 2013, 2016; Maneva-Radicheva et al. 2008).

Relatively little is known about the fate of the already arranged matrix proteins. Recent data indicate that organized ECM proteins have distinct properties from non-polymerized (protomeric) ones not only in respect to the stability of ECM, but also according the regulation of its composition,

integrity and adhesive behavior, (Mosher et al. 1992; Sottile and Hocking 2002). What is clearly known is that they may undergo proteolytic remodeling.

Enzymatic (proteolytic) remodeling of ECM

In general, ECM remodeling is a dynamic process that consists of two opposite events: assembly and degradation of matrix. Enzymatic degradation (also proteolytic or proteolysis) is a mechanism for the removal of the excess ECM and is usually approximated with remodeling (Salmeron-Sanchez, Altankov, and Eberli 2010). Normally it is active during development and regeneration, but when miss-regulated, these processes can have serious pathological consequences, such as fibrosis, arthritis, reduced angiogenesis, and developmental abnormalities, (Wagenaar-Miller et al. 2007). The invasive behavior of cancer cells is also due to the up-regulation of matrix remodeling, (Curino et al. 2005).

The proteolytic cleavage of ECM components is the main mechanism for ECM degradation and removal, (Koblinski, Ahram, and Sloane 2000; Mohamed and Sloane 2006). Several families of proteases operate at the ECM level, including **matrix metalloproteinases, cysteine proteases** and **serine proteases**. Proteolysis regulates the ECM assembly, removing the excess ECM components. During enzymatic remodeling of ECM structures, bioactive fragments and growth factors can be transformed from their inactive stage to an active form allowing accomplishing their functions.

The major enzymes that degrade ECM and the cell surface associated proteins are **matrix metalloproteinases (MMPs)**. MMPs form a large family (24 members) of proteolytic enzymes, which together with adamalysin-related membrane proteinases that contain disintegrin and metalloproteinase domains (ADAMs or MDCs), such as thrombin, t-PA, u-PA and plasmin, are involved in the degradation of ECM, (Page-McCaw, Ewald, and Werb 2007). All MMPs require metal ions (zinc and calcium) for its activity, and each of them lyses various ECM proteins (each MMP cleaves a different range of ECM components). Secreted MMPs are all produced and secreted from cells in an inactive proenzyme form, which are activated when they are cleaved themselves by other proteases. Instead of being secreted, MMP-11 is embedded in the plasma membrane; this membrane-bound MMP is believed to be activated by signaling pathways inside a cell, and to be capable of activating other MMPs in the ECM outside. The actions of MMPs directed at destroying ECM are antagonized and regulated by tissue inhibitors of metalloproteinases (TIMPs), (Davies 2001). The overall rate of matrix destruction is determined largely by the balance between the TIMPs and MMPs embedded within ECM.

Matrix remodeling is subject of extensive biomedical research during last decade, but the question how it relates to the ***biocompatibility*** of materials remains unanswered. Upon implantation, foreign materials often trigger an uncontrolled and undesired deposition of fibrous matrix, despite difficult to predict, compromises the biocompatibility of the implant. The complex 3D organization of ECM in

vivo is difficult to recreate on biomaterial interface. Thus, identifying factors and mechanisms that control the matrix secretion and organization on the materials interface is a critical step the development of materials reliable for application in the field of biomedical engineering.

Cellular receptors

Interactions between cells and ECM are mediated by cell-surface receptors, which are glycoproteins and proteoglycan by their nature. They may be systematized in two classes of adhesion receptors: **1)** involved mainly in **cell-cell adhesion** (briefly mentioned in this work) and **2)** receptors accomplishing **cell-ECM interactions**. Some receptors from the second class might be involved in both cell-cells and cell-matrix adhesion.

Cell-cell receptors

Cadherins

Cadherins are a family of cell-surface receptors involved in homophilic binding (i.e., the binding of a cadherin on one cell with an identical cadherin on another cell), (Leckband and Prakasam 2006; Leckband and Sivasankar 2012).These molecules make possible that a cell of one type recognizes and adheres to other cells of same type, an interactions that normally require the presence of extracellular Ca^{2+}. Cadherins are not directly involved in cell-ECM interaction but may be involved indirectly by organizing tissues in conjunction with other receptors and interactions, (Figure 14, (b)).

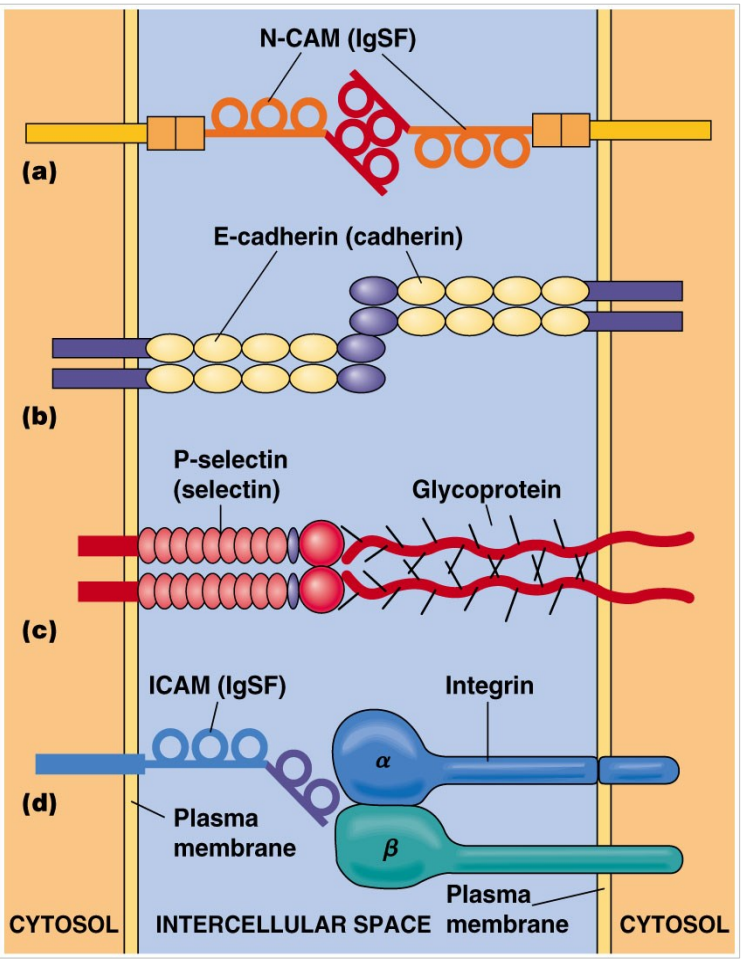

Figure 14.. *Cellular receptors mediating cell to cell interactions: (**a**) and (**d**) CAMS; (**b**) Cadherins; (**c**) Selectins.*
Figure copyright of **Pearson Education Inc.** *Adapted from* www.mun.ca/biology/desmid/brian/BIOL2060/CBhome.html.

Selectins

Selectins are receptors family that accomplishes the heterophilic binding between cells (for example blood cells and endothelial cells) also in a Ca^{2+} dependent manner. These proteins show lectin-like properties and recognize as their ligands branched oligosaccharides. Selectins receptor - ligand interactions are involved mainly in cell-cell adhesion, with particular importance in the inflammatory processes, (Rosen and Bertozzi 1994; Vestweber and Blanks 1999), (Figure 14, (c)).

Cell adhesion molecules (CAMs)

This class of receptors belongs to the immunoglobulin superfamily of cell adhesion molecules and is denoted as **Ig-CAMs, ICAMs** or simply **CAMs**. These proteins bind their protein ligands both homophilically and heterophilically, but independently of extracellular Ca^{2+}. CAMs bind to different cell-surface proteins realizing primarily cell-cell interactions. One class ligands for these receptors includes several members of the integrin receptors family, (Walsh and Doherty 1997), (Figure 14, (a), (d)).

Cell-ECM receptors

Integrin receptors

The integrin receptor family is involved in both cell-cell and cell-ECM binding. Integrins are heterodimers of non-covalently associated α- and β-subunit. The α and β subunits are constructed from several domains with flexible linkers between them. The size varies but typically the α-subunit contains around 1000 and the β- around 750 amino acids. Each subunit has a single membrane-spanning helix and a short, usually unstructured cytoplasmic tail, (Hubbell 2007).

In vertebrates, there are 18 α and 8 β subunits that can assemble into 24 different receptors with different binding properties and different tissue distribution, (Barczyk, 2010; Hynes, 2002). Some of the α- β combinations are conditionally combined in β1, β2, β3 and β4 subclasses as shown in **Table 1**, which are in fact the most commonly expressed integrins (Hubbell 2007). The β2 integrins are involved primarily in cell-cell recognition; for example, the integrin αLβ2 binds to ICAM-1 and ICAM-

Integrin heterodimer	Ligands
α1β1	Collagen, laminin
α2β1	Collagen, laminin
α3β1	Collagen, fibronectin, laminin, thrombospondin-1
α4β1	Fibronectin, osteopontin, vascular cell adhesion molecule-1
α5β1	RGD, fibronectin, L1
α6β1	Laminin
α7β1	Laminin
α8β1	RGD, fibronectin, tenascin
α9β1	Collagen, laminin, osteopontin, tenascin, vascular cell adhesion molecule-1
α10β1	Collagen
α11β1	Collagen
αvβ1	RGD, collagen, fibrinogen, fibronectin, vitronectin, von Willebrand factor
αXβ2	Complement protein C3bi, fibrinogen
αMβ2	Complement protein C3bi, fibrinogen, intercellular adhesion molecule-1, vascular cell adhesion molecule-1
αLβ2	Intercellular adhesion molecule-1 - intercellular adhesion molecule-5
αDβ2	Intercellular adhesion molecule-3, vascular cell adhesion molecule-1
αvβ3	RGD, bone sialoprotein, fibrinogen, fibronectin, thrombospondin, vitronectin, von Willebrand factor
αIIbβ3	Fibrinogen, fibronectin, thrombospondin, vitronectin, von Willebrand factor
α6β4	Laminin, hemidesmosomes

Table 1. *Some of the members of the integrin receptor family and their corresponding ligands. Adapted from Adapted from* ***(Hubbell 2007).***

2, both members of the immunoglobulin superfamily of cell adhesion molecules described above. By contrast, the β1, β3 and β4 integrins are primarily involved in ECM interaction. On the other hand, the β1, β2 and αV-containing integrins are the largest groups in this classification. The α and β subunits show no homology to each other, but the α subunits have similarities among themselves (Barczyk et al. 2010).

Integrin α-subunits

The α-chain consists of four or five extracellular domains: a seven-bladed *β-propeller*, a *thigh*, and two *calf* domains. Nine of the 18 integrin α chains have an α-I domain of around 200 amino-acids, inserted within the β- propeller, (Larson et al. 1989). The α-I domain, a copy of which also appears in the β-chain (respectively β-I domain), has five β-sheets surrounded by seven α helices similar to those of the von Willebrand factor A-domains. The β- propeller contain domains that bind Ca^{2+} that has been shown to influence ligand binding, (Humphries, Symonds, and Mould 2003; Oxvig and Springer 1998). The *thigh* and *calf* domains have similar, immunoglobulin-like, β-sandwich folds, (Xiong et al. 2002), and 140–170 residues with more β-strands than typical Ig-like domains (~100 residues). Two main regions are responsible for the intradomain flexibility: one is the linker between the β-propeller and the *thigh*; the other is between the *thigh* and the *calf*-1 domain. The α-I domain in αxβ2 heterodimer is also inserted in the β-*propeller* domain with flexible linkers (Figure 15). Unlike

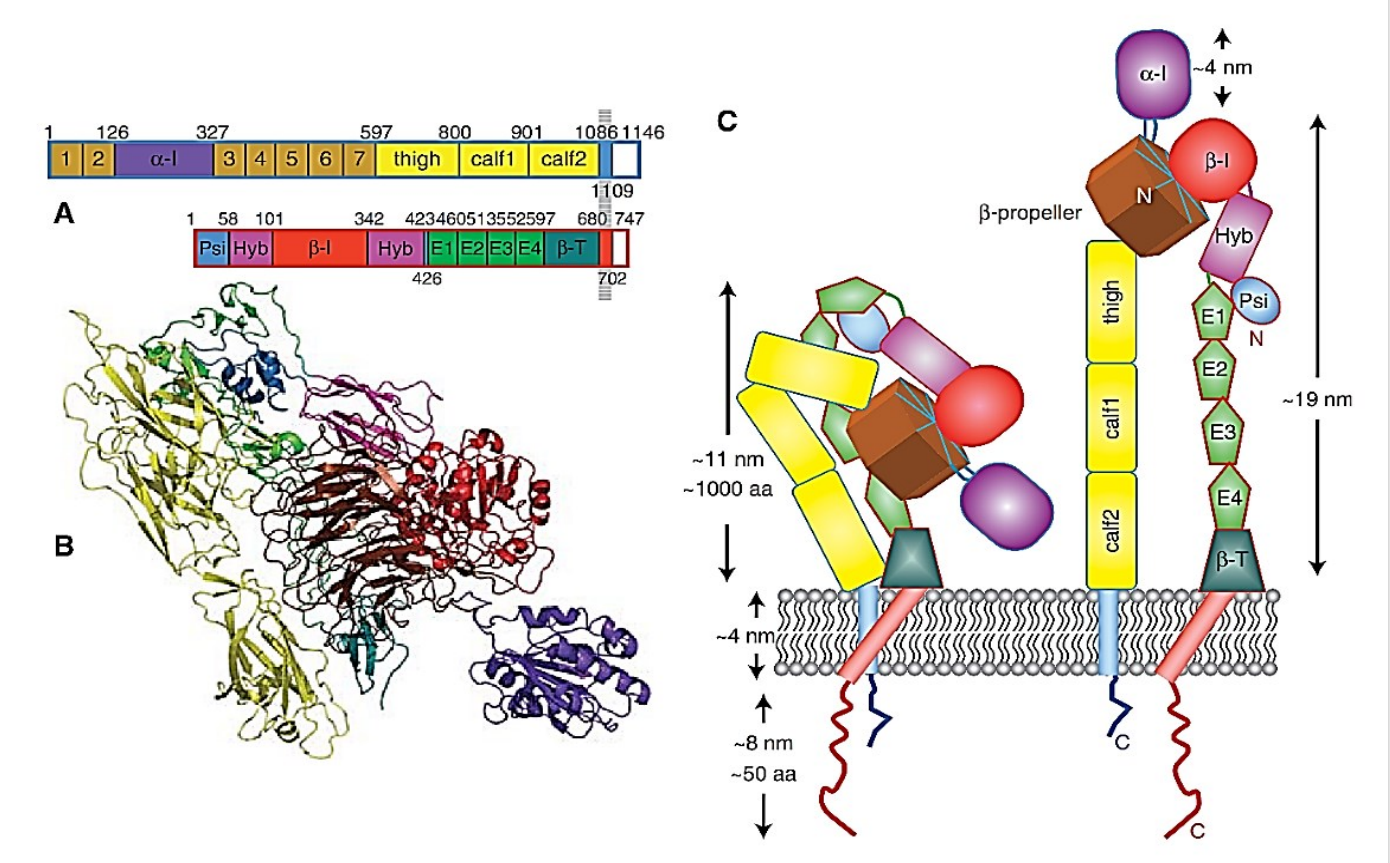

Figure 15. *Integrin structure.* ***(A)*** *Domain structure of αxβ2 (Xie et al. 2009);* ***(B)*** *structure of αxβ2 repeating the color code afrom (A).* ***(C)*** *Schematic representation of bent and upright conformations. Adapted from* ***(Campbell and Humphries 2011)****.*

the other four α-domains, which have relatively rigid structures, I domains show conformational changes that are important for the regulation of the binding affinity (Campbell and Humphries 2011).

Integrin β-subunits

The β subunit contains a plexin-semaphorin-integrin (PSI) domain, a β-I domain, (Lee et al. 1995), and four cysteine-rich EGF repeats. As shown in Figure 16, the β-I domain contains an Mg2+ coordinating the metal-ion-dependent adhesion site (MIDAS) and a site adjacent to MIDAS (ADMIDAS) binding an inhibitory Ca2+ ion. This ADMIDAS site binds the Mn2+ ion leading to a conformational change resulting in an active form of the integrin, (Humphries et al. 2003). There is also a second Ca^{2+} binding site called the **synergistic metal ion binding site** (SyMBS), (Zhu et al. 2008).

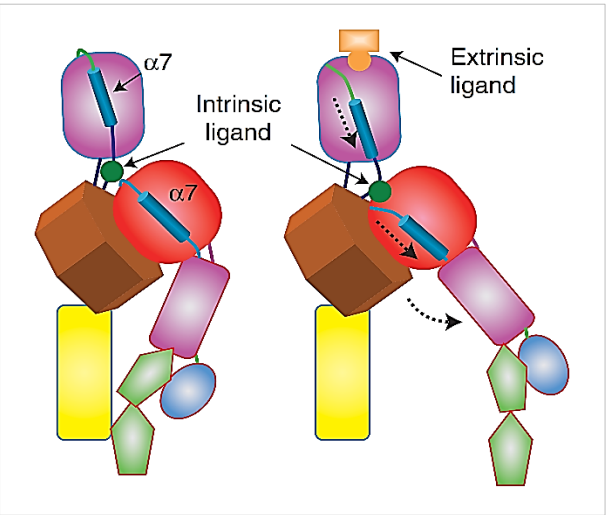

Figure 16. *Illustration of the movement of a7 helix in the β-I domain of intedrins and the swing of the hybrid domain (the domains are defined in **Figure 15**. Adapted from **(Campbell and Humphries 2011)**.*

The β-leg has seven domains with flexible and complex interconnections. A β-I domain is inserted in a hybrid domain, which is, in turn, inserted in a plexin-semaphorin-integrin (PSI) domain. These domains are followed by four cysteine-rich epidermal growth factor (EGF) modules and a β-tail domain. The hybrid domain in the upper β-leg has a β-sandwich construction, (Barczyk et al. 2010) There is evidence for important conformational changes occurring in the β-I/hybrid region. A transition from a “closed” (Figure 16, left) to an “open” conformation (Figure 16, right) of the β-I domain has been observed when an a7-helix in the β-I moves toward the hybrid domain, (Xiao et al. 2004),and via a rod-like motion the a7-helix causes the hybrid domain to swing-out by around 60° resulting in alterations of their activity, (Campbell and Humphries 2011).

Conformational changes in integrins upon ligand binding

Crystallization studies have shown that integrins can exist in a compact bent conformation, (Xiong et al. 2002) mostly associated with their inactive state. Locking the integrins in this state through disulphide bonds abolishes ligand binding. Electron microscopy under conditions in which ligand binding was low, e.g. in low Ca^{2+} containing buffers, showed also predominantly bent structures, (Nishida et al. 2006; Takagi et al. 2002). In bent conformation, the ligand-binding pocket is oriented toward the plasma membrane, thereby “protecting” ligand engagement, but flexibility at the membrane domain could enable the conversion of bent to extended integrin conformation, (Beglova et al. 2002). More recently, mechanical tension has been demonstrated to stabilize the active

conformation and thereby increasing affinity, (Askari et al. 2009; Astrof et al. 2006). For example, in integrin α5β1 the mechanical tension induces α5β1 engagement with the synergy site in fibronectin, in turn leading to FAK activation, (Friedland, Lee, and Boettiger 2009).

Early studies reported activation-dependent changes in monoclonal antibodies (mAb) binding to integrins that were attributed to conformational changes of the molecule, (McEver and Martin 1984), and revealed several epitopes, involved in ligand binding. The acronym LIBS (ligand-induced binding sites) was proposed to describe these epitopes and usually the activating mAbs appear to function by increasing the affinity of ligand binding. Most LIBS mAbs have epitopes that are regulated by divalent cations, and because cations also regulate ligand binding, it appears that many cation-responsive, or activating mAbs, actually recognize naturally occurring conformers of integrins. These mAbs may therefore shift the conformational equilibrium leading to high affinity binding state for given integrin. Some other activating mAb epitopes however are unaffected by either ligand or cation binding and here the most likely mechanism of action is through inducing the activated conformation of the integrin, (Chen 1999). In addition to the affinity modulation, integrin clustering by multivalent ligands or changes in membrane fluidity, may cause remarkable changes in integrin binding activity, (Carman and Springer 2003).

Thus, the conformational changes in the head are the key determinant of ligand-binding activity. The conformation of the β-I domain however might be determined by the position of a *hybrid* domain, which swinging-out away from the α-subunit may pulls downward the β-I domain and favors the upward movement of the α1-helix, (Xiao et al. 2004). Such motions shifts the β-I domain from a low-affinity into a high-affinity conformation by backbone movements of loops that contain cation-coordinating residues. Not accidentally mutations that favor a downward shift of the β-I domain also result in a high-affinity state, (Campbell and Humphries 2011; Cheng et al. 2007; Hato et al. 2006).

Ligand binding specificity

A characteristic feature of most integrin receptors is their ability to bind a wide variety of ligands. Conversely, many ECM and cell surface adhesion proteins bind to multiple integrin receptors, (van der Flier and Sonnenberg 2001; Humphries 2000; Plow et al. 2000). One molecular explanation for this low specificity is the evolutionary selection of common acidic peptide motifs in ECM proteins that mediate integrin binding via coordination to a divalent cation-containing binding pocket. Integrin-ligand combinations can be classified into at least four groups, based on the nature of the molecular interaction, (Figure 17). All five αV integrins, two β1 integrins (α5, α8), and αIIbβ3 recognize ligands containing an RGD tripeptide active site. Indeed the reported crystal structures of αVβ3 and αIIbβ3 complexed with RGD ligands reveal an identical interaction model, (Xiao et al. 2004; Xiong et al. 2002). RGD binds at an interface between the α- and β-subunits fitting to a cleft in a β-*propeller* module of the α-subunit. RGD-binding integrins bind to a large number of ECM and soluble vascular ligands, but with different affinities mainly determined by conformational correspondence. Although

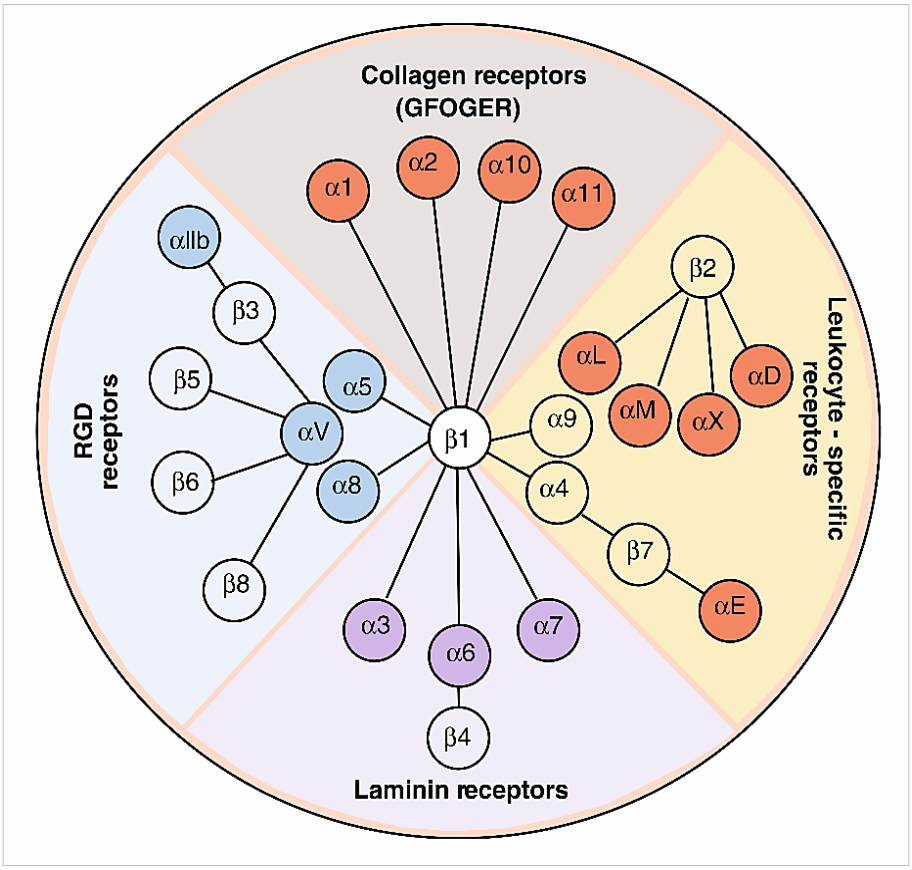

Figure 17. *Representation of the integrin family. In vertebrates, the integrin family contains 24 heterodimers.Adapted from* ***(Barczyk et al. 2010).***

RGD is an essential element of the ligand binding process, ligands can contain other binding sites. An example is a synergy sequence in fibronectin that also binds the α5 β-*propeller,* (Mould et al. 2003). Conversely, the α4β1, α4β7, α9β1, the four members of the β2 subfamily, and αEβ7 recognize related sequences in their ligands. The first group (α4β1, α4β7 and α9β1) bind to an acidic motif, termed LDV that is functionally related to RGD. Fibronectin for example (a typical RGD protein) contains the prototype LDV ligand in its type III repeat region, but other ligands (such as VCAM-1 and MAdCAM-1) also employ related sequences. Though the crystal structures of this integrin subfamily is not known, it is likely that LDV peptides bind similarly to RGD. On the other hand, the subunits containing α-I-domain (α1, α2, α10, and α11) combine with β1 to form the **laminin-collagen binding** subfamily. A crystal structure of a complex between the α2 I-domain and the α subunits of the triple-helical collagenous peptide has revealed the Gly-Phe-Hyp-Gly-Glu-Arg (GFOGER) motif providing the key cation-coordinating residue, (Emsley et al. 2000). The mechanism of laminin binding is less understood, although a recent study has suggested that the extreme carboxyl terminus of the γ-chain and an undefined site in laminin G-domains together constitute an integrin-binding site, (Ido et al. 2007).

In addition to physiological ligands, integrin ligands generated by proteolysis are receiving increasing recognition. Integrins can also bind snake toxins called **disintegrins,** (Calvete et al. 2005; Swenson, Ramu, and Markland 2007), certain viruses, (Stewart and Nemerow 2007), and bacteria, (Hauck et al. 2006; Palumbo and Wang 2006). Some of these interactions occur outside the regular

ligand-binding sites in the integrins and display different binding characteristics compared with the binding of physiological ligands, (Barczyk et al. 2010).

Activation of intergrins

Adhesion is highly dynamic process, with cells continuously changing their pericellular environment and responding by rapid alterations their position and state of differentiation, and therefore a highly responsive receptor activation mechanism is required. As integrins don't have enzymatic activity, intensive signaling is instead induced by the assembly of signaling complexes on the internal face of the plasma membrane. The activation of these complexes is achieved in two manners; first, by **receptor clustering**, which increases the amount of molecular interactions thereby increasing the rate of binding of effector molecules ("**outside-in signaling**"), and second, by **induction of conformational changes** in receptors that creates or exposes effector binding sites. For example, in leukocytes or blood platelets, intracellular signals can release a self-inhibitory function of **talin**, which consequently binds to the cytoplasmic tails of inactive integrins. This leads to conformational change, transmitted through the cell membrane to the extracellular integrin domains, which become activated and able to bind their ECM-ligands ("**inside-out signaling**"),

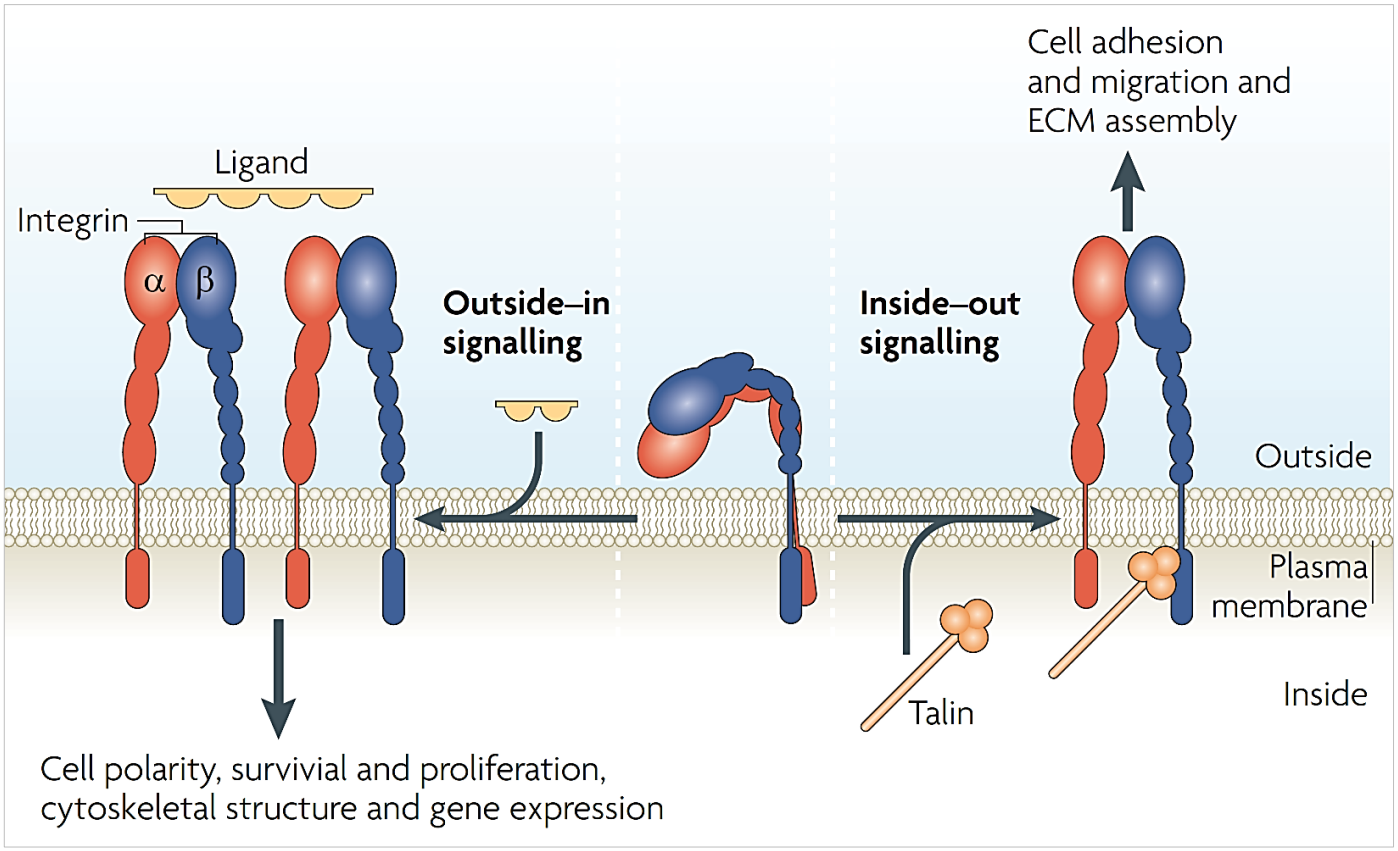

Figure 18. *Diagram of bidirectional activation of integrins. During 'inside–out' signaling, an intracellular activator, such as talin, binds to the β-integrin tail, leading to conformational changes that result in activation and increased affinity for extracellular ligands (right). Integrins can also transmit information into cells by 'outside–in' signaling. Binding of integrins to their extracellular ligands changes the conformation of the integrin leading to integrin clustering and subsequent activation. Adapted from* ***(Shattil et al. 2010).***

(Figure 18), (Shattil, Kim, and Ginsberg 2010). Current evidence suggests that conformational regulation is the primary mode of affinity regulation of integrins, (Campbell and Humphries 2011).

Functions of integrins

It is clearly noted by Hynes that integrins form supramolecular complexes with their extracellular and cytosolic partners, (Figure 19), (Hynes et al. 2002). These networks are highly ordered and perform their distinct functions. Thus, the first function is to establish links between the ECM and the cytoskeleton. For a majority of integrins, the linkage is to the actin cytoskeleton, (Geiger, Spatz, and Bershadsky 2009), but there are also exceptions – for example, integrin α6β4 connects to the intermediate filament system, (Nievers, Schaapveld, and Sonnenberg 1999). Recently, the intermediate filament protein ***vimentin*** has been shown to be dependent on β3 integrins for its recruitment to the cell surface indicating that an intimate relationship exists between the various cytoskeletal networks and integrins, (Bhattacharya et al. 2009). Some of the components in this mechanical linkage, such as talin, play a dual role activating integrins via an inside-out signaling mechanism, (Tadokoro et al. 2003).

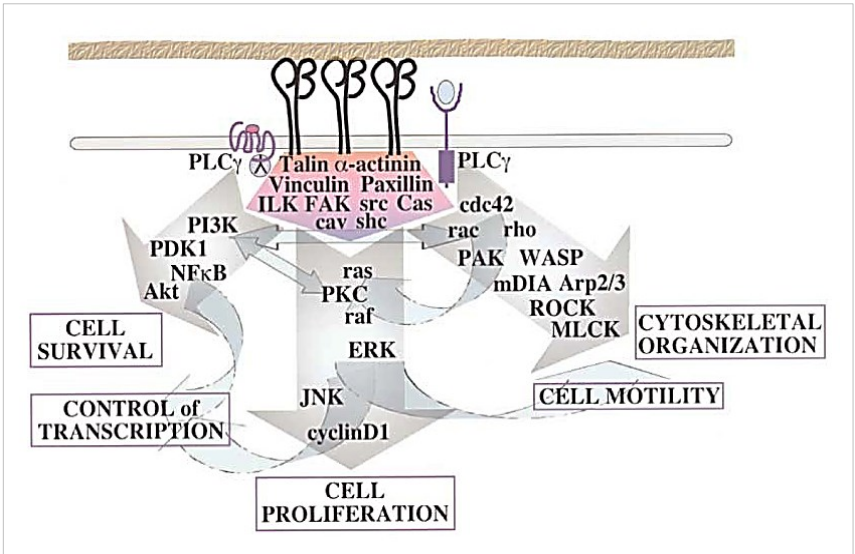

Figure 19. *Integrin signaling. The major signal transduction pathways and many of the key players in them are shown together with the major effects on cell behavior mediated by integrins. Adapted from* ***(Hynes et al. 2002)***

Integrins are responsible not only for cell adhesion to ECM, but also for the **transmission of mechanical forces** across the cell, thus playing a central role in **mechanotransduction**, i.e., the process by which mechanical stimuli are converted into chemical signals within the cell, (Ross et al. 2013). A new dimension in understanding of integrins function has come with the realization that integrins can act as **mechanosensors** and generate signals that affect cell physiology via complex intracellular signaling mechanisms including autocrine and paracrine mechanisms, (Chen and O'Connor 2005; Linton, Martin, and Reichardt 2007; Zhu et al. 2007)

It is clear now that integrin-containing matrix adhesions are assembly platforms for a multitude of signaling pathways that control cell growth, differentiation, and death (Zaidel-Bar, Itzkovitz, et al. 2007).These adhesion structures mediate the synergy between growth factor- and integrin-dependent signaling, which is responsible for the anchorage-dependent growth of most normal cells (Reddig and Juliano 2005). All this determines other important function of Integrins: namely the fact that integrins are **bi-directional receptors** involved in both outside-in and inside-out signaling. The

inside-out signaling mainly acts to bring the integrin in to the active conformation. **Talins, kindlins, filamins, migfilin, FAK,** and **ILKs.** are only part of the proteins that are involved in the regulation of integrin activation, (Honda et al. 2009).

Cell-ECM interactions in-vivo

As stated above, upon ligand binding, integrins undergo conformation changes leading to the classical outside-in signaling. This activates signaling events that are complex and cell-specific, depending on what other signaling receptors and signaling systems are available in the cell. The ligation of integrins triggers a large variety of signal transduction events that serve to modulate many aspects of cell behavior including proliferation, survival/apoptosis, shape, polarity, motility, gene expression, and differentiation. These signal transduction pathways are as complex as those emanating from receptors for soluble factors (e.g., G protein-coupled and kinase receptors). Indeed,

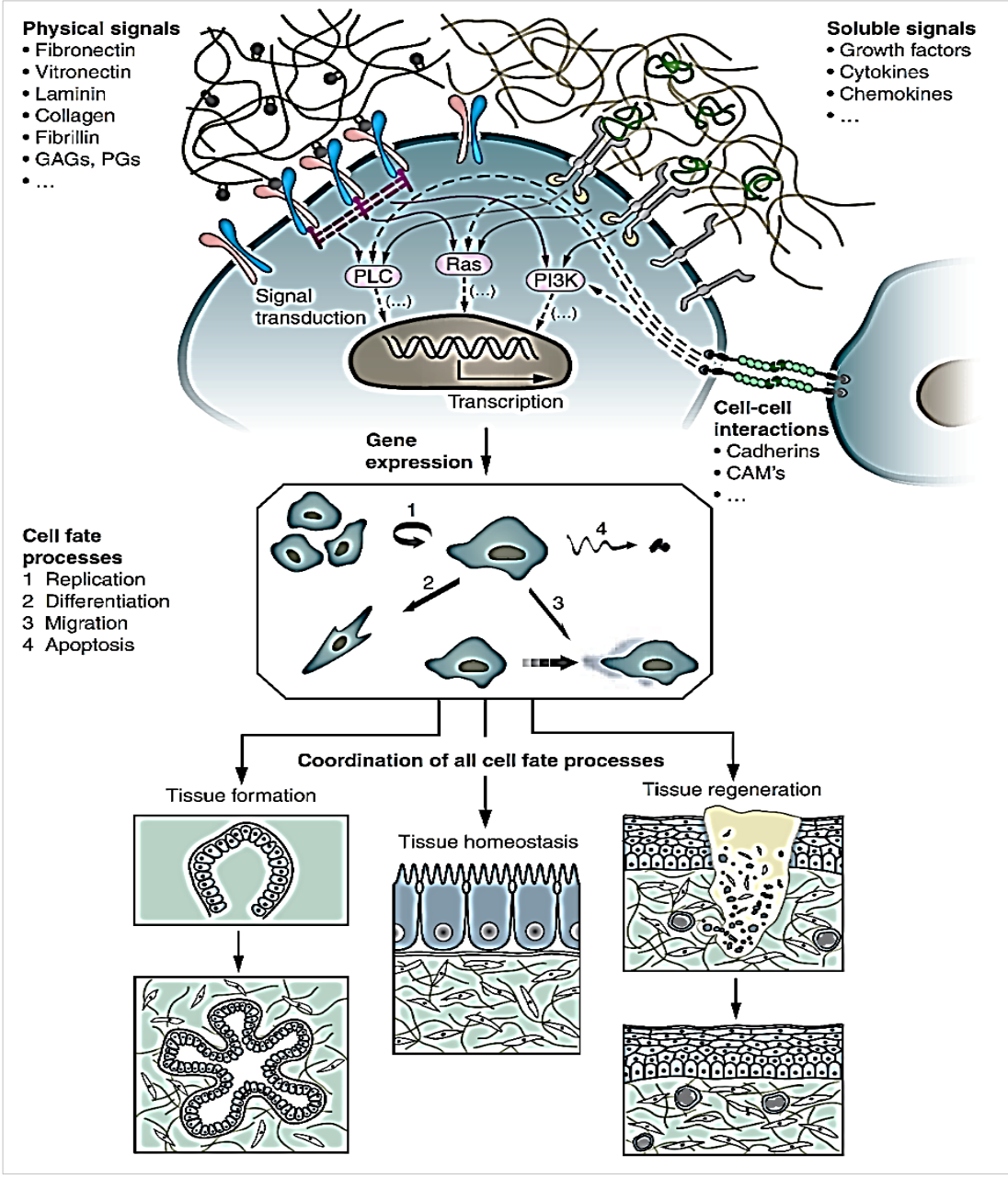

Figure 20. *The behavior of individual cells and the dynamic state of multicellular tissues is regulated by intricate reciprocal molecular interactions between cells and their surroundings. Adapted from* ***(Lutolf and Hubbell 2005)****.*

many integrin-dependent pathways are very similar to those triggered by growth factor receptors and are intimately coupled with them (Figure 20).

Tissue dynamics, in its formation, development, function, regeneration after damage or pathological appearance, is result of an intricate temporal and spatial coordination of numerous crucial cell fate processes, each of which is induced and controlled by a multitude of signals from the extracellular microenvironment, (Kleinman, Philp, and Hoffman 2003). This dynamic composite of biophysical and biochemical cues is transmitted from the outside of a cell by its surface receptors, then is integrated by intracellular signaling pathways to regulate gene expression and, ultimately, establishes cell behavior and phenotype. The extracellular microenvironment, as mentioned before, integrates three main groups of effectors: **a)** insoluble hydrated macromolecules (fibrillary proteins such as collagens, fibronectin, laminin, elastin, hydrophilic proteoglycans etc.; **b)** soluble macromolecules (growth factors, chemokines and cytokines); and **c)** surfaces proteins of adjacent cells. Thus, the determination of a cell to proliferate, migrate, differentiate, trigger apoptosis or perform other specific functions is a strictly coordinated response to molecular interactions with these ECM effectors. Noteworthy, apart from the other signaling pathways the flow of information between cells and their ECM is highly bidirectional, and precisely regulated as observed in processes like ECM degradation and remodeling, (Lutolf and Hubbell 2005).

Cell-biomaterial interactions

Cell-matrix interactions at biomaterial interface

Understanding the cellular events that take place upon contact with biomaterials interface is powerful approach for not only determining the phenomenon of biocompatibility of materials, but also for further spreading of our knowledge over the fundamental processes of dynamic interaction between cells and their microenvironment. The initial cell-biomaterial interaction mimics to a certain extent the natural interplay between cells and ECM, (Williams 2008), and some of the ECM proteins (called adhesive proteins) are considered to play a main role in mediating such an interactions. It is a paradigm that cells cannot interact directly with the foreign material surfaces, as they cannot recognize them. However they possess a machinery to recognize and interact with adsorbed proteins or other bioactive molecules, containing adhesive sequences (e.g., RGD). Generally, cell-biomaterials interaction can be divided into **early** and **late events**. Early events involve recognition of signals, incorporated in the material or coming from the adsorbed adhesive proteins and transition of these biological signals to cell interior, (Altankov et al. 2010; Grinnell 1986). Late events cover the proliferation of the cells under continuous exchange of biological signals with the biomaterial, which establishes distinct cellular behavior, (Place, Evans, and Stevens 2009; Sipe 2002). In fact, many cellular responses to soluble growth factors, such as EGF, PDGF, LPA, thrombin, etc., are dependent on the cell's being adherent to a substrate via integrins. That is the essence of **anchorage dependence** of cell survival and proliferation and integrin-dependent cell adhesion lie at the basis of this phenomenon, (Assoian 1997; Schwartz and Assoian 2001).

Adsorption of proteins at biomaterials interface

Real cell-biomaterials interaction depends primarily on the adsorption of proteins. The adsorption of larger biomolecules, such as proteins, is of high physiological relevance. However, it should be considered that they adsorb with different mechanisms than their analogs at molecular or atomic level. By definition **adsorption** (not to be mistaken for absorption) is the accumulation and adhesion of molecules, atoms, ions, or larger particles to a surface, without occurring of surface penetration, (Boyle 2005). Proteins are molecules composed of amino acid subunits. Each amino acid has a side chain that gains or loses charge depending on the pH of the surrounding environment, as well as its own individual polar/nonpolar qualities. Usually the protein adsorption is considered as positive event because ordinarily supports cellular interactions with foreign material, otherwise biologically unrecognizable. Such are principally the biomedical implants. However, in some cases, protein adsorption to biomaterials can be an extremely unfavorable event. For example the adhesion of clotting factors may induce thrombosis.

Some of the major driving forces behind protein adsorption include: surface energy, intermolecular forces, hydrophobicity/hydrophobicity balance, and ionic or electrostatic interaction. Knowing how these factors affect protein adsorption, they could be manipulated by different engineering techniques for most optimal performance in biomedical or physiological environment.

Protein adsorption on surfaces is a process driven by energetic interactions between the molecular groups on the substrate and on the protein (i.e., hydrogen bonding, electrostatic, van der Waals interactions), Moreover, it is dependent on the **entropic changes** resulting from the protein **unfolding** and the concomitant release of bound water, (García 2006; Werner, Pompe, and Salchert 2006). Thus, the amount of adsorbed protein and its conformation depend on the chemical nature of the substrate and the molecular structure of the protein itself, which determine the balance between energetic and entropic interactions. The adsorption of ECM proteins has been extensively investigated utilizing different model substrata such as mica, glass or self-assembled monolayers. Particularly well described is the behavior of FN, laminin, collagens, FBG and several other “popular” proteins, exploring the capacity of different techniques and approaches, such as the classical SDS-electrophoresis, spectroscopy and various fluorescence probes and ongoing with the ellipsometry, quartz crystal microbalance, FTIR, electron microscopy and atomic force microscopy (AFM), (Keselowsky, Collard, and García 2004; Lord et al. 2006; Michael et al. 2003; Noh and Vogler 2006; Prime and Whitesides 1991; Sousa et al. 2007; Steiner et al. 2007; Tsapikouni and Missirlis 2007). These studies clarify that in addition to the differences in the amount of adsorbed protein, many proteins undergo conformational changes upon adsorption on biomaterial substrates, and these structural changes actually determiner their biological activity. Due to their secondary and tertiary structure the proteins represent more or less defined folding of their molecules, as well as specific distribution of hydrophobic, hydrophilic or differently charged moieties, which has a major impact on their adsorption profile. And it becomes even more complex considering that the properties of the proteins can vary in different environmental conditions, depending for example on pH, ionic strength, or temperature. In the fluid phase the proteins normally move to the surface interface by diffusion; small proteins diffuse faster than larger ones and therefore are predominant in the early adsorption phase. Depending on the relative strength of the initial attachment, protein molecules can stay adsorbed or may be displaced by other molecules with higher affinity for the surface, called **Vroman effect,** (Noh and Vogler 2007).

Whereas in solution proteins rotate freely, on a surface each protein adapt a certain orientation depending on which part of the molecule interacts and which part is exposed to the solution. Obviously, this is an important issue when adsorbed proteins have specific bioactivity connected with a certain part of the molecule. The active sides can become either available or hidden after the adsorption. For example, on hydrophilic interfaces proteins will predominantly expose to the surface those parts of the molecule that are rich of hydrophilic residues and on hydrophobic surfaces proteins will direct their hydrophobic patches to the surface. Analogously, proteins adsorbing at

positively or negatively charged interfaces will tend to expose oppositely charged regions to the surface. Therefore, a protein has a favorable conformational state on a given surface, which often differs from the native conformational state in solution. Thermodynamically, this is because the free energy minimum of the protein in solution typically differs from the free energy minimum after contact with the surface, (Santore and Wertz 2005; Sethuraman and Belfort 2005). Initially proteins approach the surface in their native state and bind through some initial contact sites to the surface. Then structural reorganizations start driven by favorable protein-surface interactions and increase in entropy due to a loss of ordered secondary structure. This leads to release of water molecules or different ions from the surface.

When protein molecules not only interact with the sorbent surface, but also between each other, **lateral interactions** can be expected to occur. Often proteins bear a charge of equal sign that causes intermolecular repulsions. For example, at pH values below and above the isoelectric point (pI) the density of protein layers is usually smaller than at pH equal to pI, (Demanèche et al. 2009). Such a repulsive interactions lead to higher desorption rates along time. However, lateral interaction can be also in favor of adsorption rates and causing some cooperative effects. It was shown by Ball and Ramsden that the cumulative electrostatic field in the periphery of adsorbed proteins induces an electrostatic self-assembly which enhances the protein uptake rates. This positive cooperative effect is explained by a mechanism through which proteins are at the same time attracted toward the surface in vertical direction and repelled from the neighboring protein in horizontal direction. Characteristic feature of such an adsorption kinetics is the almost linear increase before the saturation levels are reached, (Ball and Ramsden 1997, 2000).

An important aspect of protein adsorption is the formation of clusters or larger aggregates of proteins or protein monomers upon contact with a substrate. These processes can highly alter the protein adsorption at solid interfaces and influence the adsorption kinetics as well as the resulting layer structure. The mechanisms of protein clustering may include either the diffusion of surface bound molecules towards precursor aggregates or direct adsorption of free protein molecules tending to form protein aggregates in advance – both mechanism implying that clusters increase their size directly on the surface mediated by stronger protein–protein interactions, (Minton 2001). Another mechanism that can lead to development of clusters consist of the formation of larger protein assemblies in the solution which later deposit onto the surface where they spread and flatten, (Rabe et al. 2009). The growth of protein clusters in such a mechanism is not so restricted to the surface but could also proceed into third dimension, (Ishiguro et al. 2005).

Relevant to our studies is important to note that clustering in most cases is a surface driven process. Protein clusters could appear as stable, ordered or amorphous aggregates that grow in a protein solution and their appearance ranges from fibril-like features to spheres or beads with diameters of up to a several hundred nanometers, (Zhang and Liu 2003). These structural arrangements however, are of particular interest when affect the fate of ECM proteins at the

biomaterials interfaces, which might be considered as still insufficiently studied issue. A special attention deserves the characteristic nanoscale behavior of adsorbed matrix proteins such as fibronectin, collagen, laminin, fibrinogen, etc., observed by AFM,(Coelho et al. 2010; Gugutkov et al. 2009, 2010, 2011; Llopis-Hernández et al. 2013; Salmeron-Sanchez et al. 2010). Apart from the "classical view" for a rather stochastic adsorption of proteins, these studies showed that on some surfaces the lateral protein-protein forces may prevail over the protein-substratum interactions giving rise to the formation of a network-like structure. For example, Salmeron Sanchez and co-workers, via exploring an amphiphilic system based on copolymers of poly(ethylacrylate) (PEA) and hydroxyl poly(ethylacrylate) (PHEA), (Salmeron-Sanchez et al. 2010), have shown that the amount of expressed —OH groups strongly affects the probability for lateral assembly of adsorbed proteins. However, this co-polymer system affects not only the lateral assembly of adsorbed proteins, but also their biological activity, which constitute considerable part of the current Thesis. In fact using this system, named **material driven protein assembly,** we demonstrated that it can be used to obtain **control over the cell behavior**, particularly shown by us for fibronectin and fibrinogen, (D. Gugutkov et al. 2011; D Gugutkov et al. 2010; Rico et al. 2009), while other authors from our group extended it validity to the behavior of collagen IV (Coelho et al. 2010), and vitronectin (Toromanov et al. 2010).

Cell adhesion

According to the classical **ligand receptor theory,** (Grinnell 1986), the initial interaction of cells with foreign substratum might be approximated with **cell adhesion,** a multi-step process initiated by the adsorption of proteins from the surrounding medium, followed by cell adhesion, spreading and polarization (Altankov et al., 2010; Grinnell, 1986). The continuous cell spreading is accompanied by organization of actin into microfilament bundles. The initial adhesive

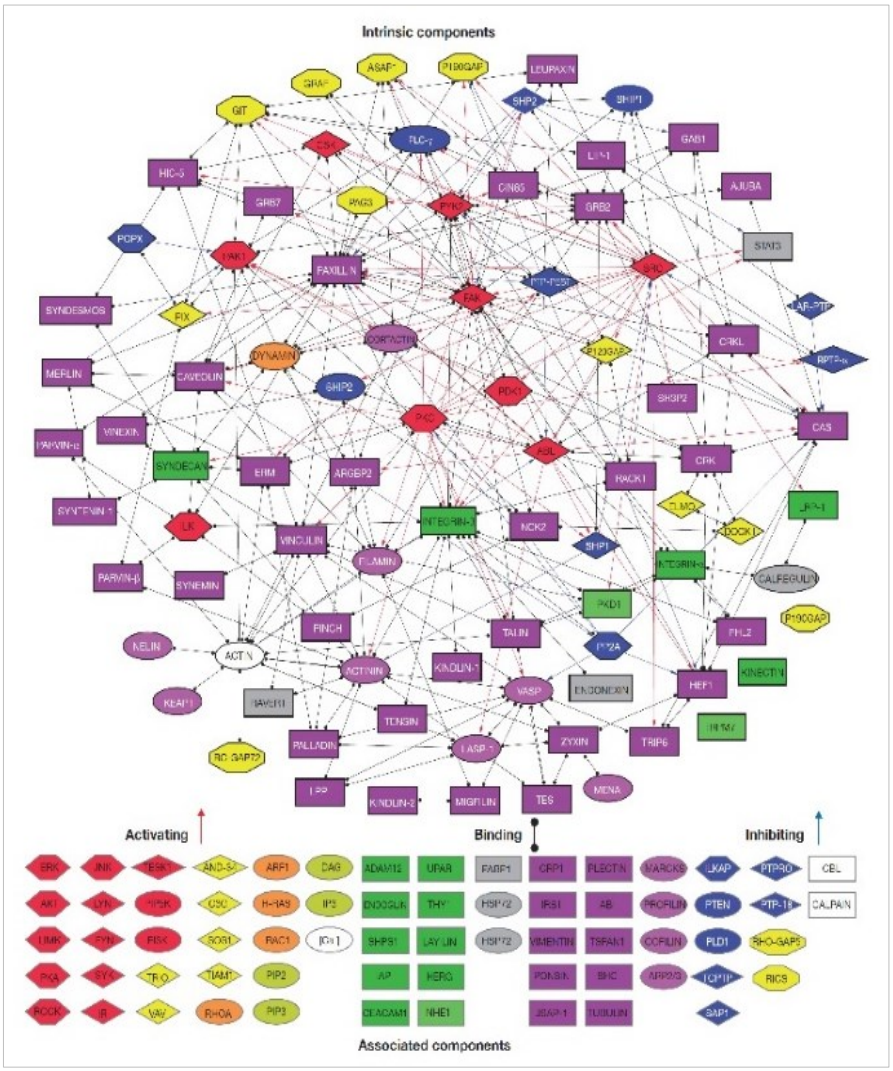

Figure 21. *The adhesome and its complicity. Interactions between all intrinsic components. Adapted from* ***(Zaidel-Bar, Itzkovitz, et al. 2007)****.*

interaction is driven, in most cases, by the integrins. Cell attachment require formation of receptor-ligand bonds that quickly enhance in number, thus increasing the total attachment strength and allowing cells to bound its actin cytoskeleton resulting in a morphological changes usually approximated with cell spreading, (Khalili and Ahmad 2015).Thus, the primary interaction of cells with a biomaterial is the adhesive contact. Cell adhesion is a well described paradigm in the literature, but it should be also considered that it is a process that realizes bidirectional interaction between cells and foreign material. The cells recognize adsorbed protein but also can remodel them as will be stated below. It provides an interactive interface between the extracellular microenvironment (often termed scaffold) and the internal cellular signaling machinery. The dynamic regulation of these intracellular processes and their coupling to the substratum events is mainly integrin-dependent, but involves many other components comprising all together the **adhesome**, (Figure 21). The adhesome is the entire collective of molecules associated with the adhesion structures participating in both the physical/structural and sensing/signaling activities of these structures, (Zaidel-Bar, Itzkovitz, et al. 2007). Integrin-triggered adhesions possess an ability to form morphologically different adhesion structures. Distinct types of cell adhesions are:

- **Dot-like nascent adhesions**, often called **focal adhesion complexes,** are the earliest integrin-containing structures. Approximately 100 nm in diameter these short living adhesions are positioned at the interface between the cell lamellipodium and the matrix. Focal complexes contain a few hundred protein molecules, including integrins, talin, and paxillin and can easily evolve in classical focal adhesions,(Figure 22), (Alexandrova et al. 2008; C. K. Choi et al. 2008).
- **Classical focal adhesions** are typically generated when cells interact with flat and rigid surfaces. These adhesions are usually several square micrometers in size and are located at the ends of actin stress fibers. Actin filaments at these sites often co-align with extracellular fibronectin fibrils. The transformation of focal complexes at the cell edge into stress fiber-bound focal adhesions normally occurs at the boundary between the lamellipodium and the lamella. The process is

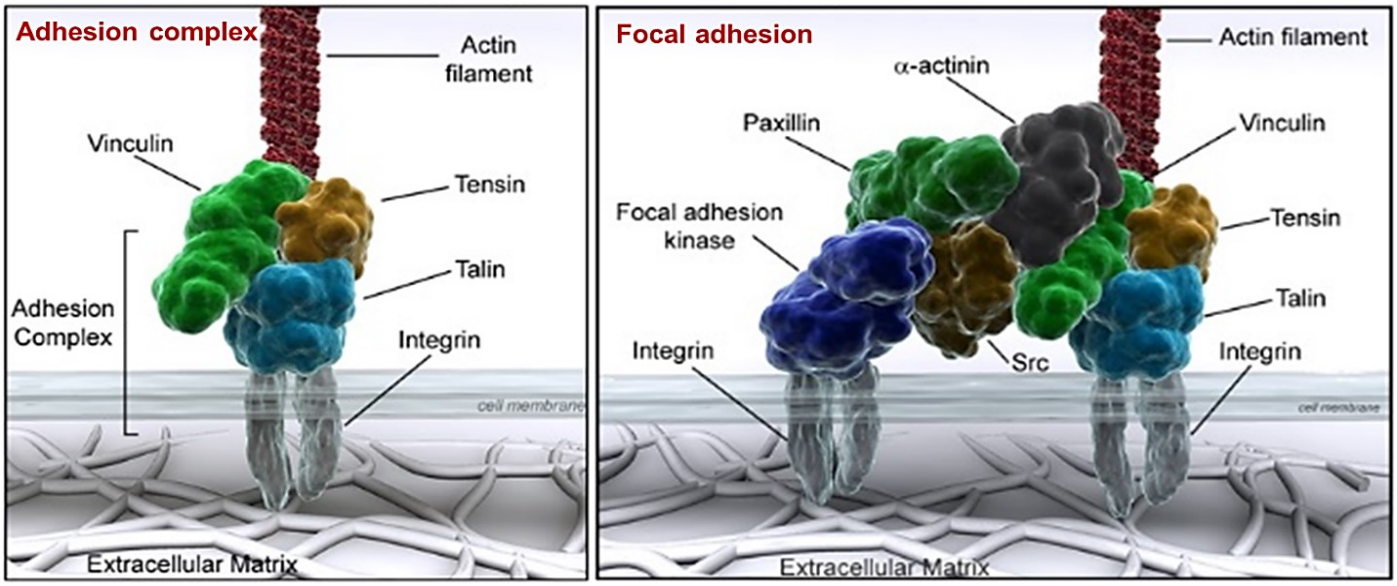

Figure 22. *Adhesion complex (left) and focal adhesion (right). Adapted from www.reading.ac.uk .*

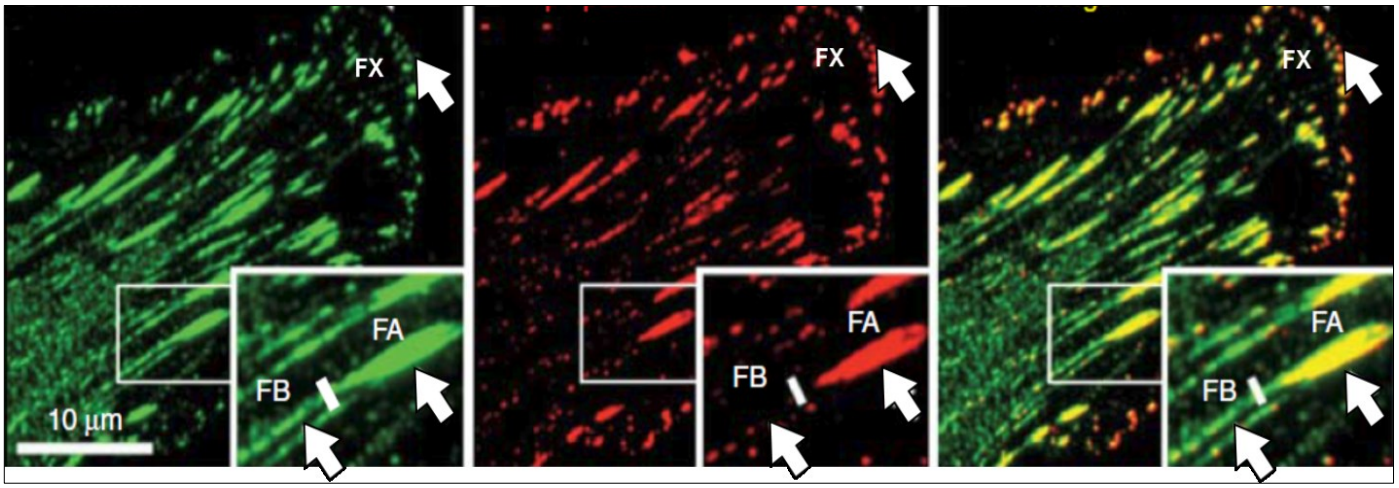

Figure 23. *Main forms of integrin-mediated adhesions adhesions. Endothelial cells cell labeled for paxillin (green) and tyrosine-phosphorylated paxillin (pY-paxillin, red.In these images, three major forms of integrin adhesions are detected: dotlike focal complexes* ***(FX),*** *"classical" focal adhesions* ***(FA)****, and fibrillar adhesions* ***(FB)****. Adapted from* ***(Geiger and Yamada 2011)****.*

associated with recruitment of additional proteins, which undergo a common tyrosine phosphorylation which triggers all subsequent cellular pathways, (Zaidel-Bar, Milo, et al. 2007), (Figure 22, Figure 23). In general, the signaling cascades initiated or modulated by integrins triggers distinct signal transduction pathways including focal adhesion kinase (FAK), various Src family kinases, MAP kinases, PKCs and phosphatidylinositol lipids turnover. as well as leads to the recruitment of the cytoskeletal components a-actinin, tensin, paxillin, talin and vinculin, (Harburger and Calderwood 2009; Zaidel-Bar and Geiger 2010).

- **Fibrillar adhesions** are recently described and are rather connected with the formation of FN matrix. They are prominent in the central areas of cells and forms mainly along FN matrix fibrils (Pankov et al. 2000; Zamir et al. 1999), (Figure 23).
- **Podosomes** and **invadopodia** are small, cylindrical adhesions formed around an actin bundle or thin membranous protrusions, respectively. They are associated with the actin-contraction and cell movement, (Poincloux, Lizarraga, and Chavrier 2009), and are prominent in different mesenchymal cells derivatives (osteoclasts, macrophages, dendritic cells). Invadopodia are typically involved in the matrix invasion characteristic for cancer cells, (Gimona et al. 2008), while

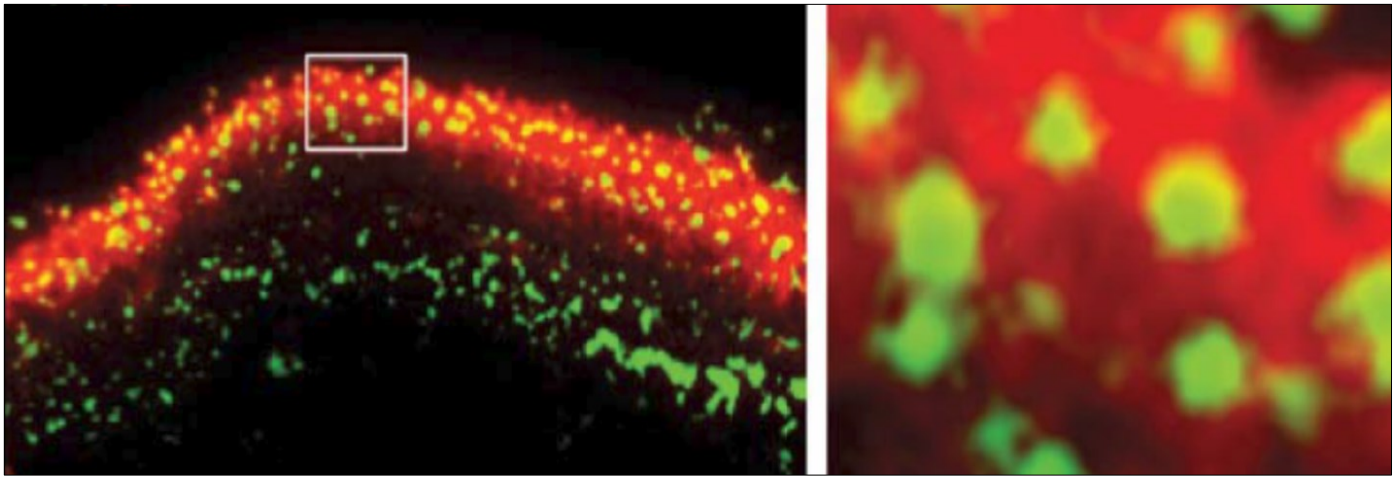

Figure 24. *Podosomes formed by osteoclasts Green is actin and red is paxillin. Adapted from* ***(Geiger and Yamada 2011)****.*

podosomes appear to diverse vinculin distribution and their primary purpose is connected to **cellular motility** and **invasion**. Therefore, they often serve as both sites of attachment and degradation along the ECM. Many different specialized cells exhibit both types of these dynamic structures such as invasive cancer cells, osteoclasts, (Figure 24), vascular smooth muscle cells, endothelial cells, and certain immune cells like macrophages and dendritic cells, (Artym et al. 2011).

Though cell adhesion is a phenomenon generally attributed to the behavior of cells *in vitro,* it naturally comes from the mechanism that cells utilize for the interaction with ECM, e.g. in 3D environment. Therefore such structures are called also 3D matrix adhesions, (Cukierman et al. 2001). For example, the dense plaques of smooth muscle form firm, integrin-based adhesions linking the actin cytoskeleton to the ECM, (Wang, Stromer, and Huiatt 1998). Another example are endothelial cells that form structures similar to focal adhesions at sites of high hydrodynamic stress in blood vessels, (Davies, Robotewskyj, and Griem 1994). Prolonged, narrow focal and fibrillar adhesions appear also in decellularized matrices, as well as in the loose matrix in which embryonic cells migrate *in vivo* ,(Cukierman et al. 2001).

These issues are particularly important for the understanding of cellular behavior in 3D scaffolds where the formation of 3D matrix adhesion induces important alterations on cell behavior. Cells cultured on 3D matrices showed increased proliferation, faster migration and altered morphology when compared with cells cultured on 2D surfaces, (Cukierman et al. 2001). Whether cells sense the artificial materials prepared for example for implantation as a real 3D environment is difficult to answer. However, the existence of different signal transduction pathways in 3D versus 2D environment, together with the specific morphological characteristics of 3D matrix adhesions, clearly suggest that there exist principal differences between these microenvironments and further investigations are needed in this field. They will provide a tool for better understanding the role three-dimensionality and will allow precise characterization of diverse artificial scaffolds prepared for use in regenerative medicine, (Pankov & Momchilova, 2010).

Tissue engineering

One important implication of our knowledge about cell-ECM interaction is in the field of **Tissue engineering (TE)**: an advanced, multidisciplinary and rapidly developing research topic that is expected to have great impact on human health and life span in near future.

Definition of tissue engineering

Tissue engineering is an interdisciplinary research field that applies biological and engineering principles to develop biological substitutes that restore, maintain, or improve tissue function, (Dvir et al. 2011; Ma 2008). The term 'Tissue engineering' was officially accepted at a National Science Foundation workshop in 1988 and was defined as **"*The application of principles and methods of engineering and life sciences toward the fundamental understanding of structure-function relationships in normal and pathological mammalian tissues and the development of biological substitutes to restore, maintain or improve tissue function*"**. Nevertheless the idea of replacing damaged tissue with other, healthy one is not new and it was first publish back in the 16th century by Gasparo Tagliacozzi (1597) in his work *"De Custorum Chirurigia per Insitionem" (The Surgery of Defects by Implantation)*, where he describes replacement of a nose with part of forearm tissue. Nowadays the field of tissue engineering is modern, highly multidisciplinary trend that recruits efforts from clinical medicine, materials science, genetics, engineering and life sciences to fulfill its challenging goals.

Scaffolds

Tissue engineering usually requires the use of porous 3D supporting matrices, or **scaffolds** to provide an appropriate environment for the regeneration of tissues and organs. These scaffolds act as a template for tissue formation and are normally populated with cells, occasionally with growth factors, or subjected to biophysical stimuli in a bioreactor; a device which applies different types of mechanical or chemical stimuli to cells, (Martin et al. 2004). The cell-seeded scaffolds can be either

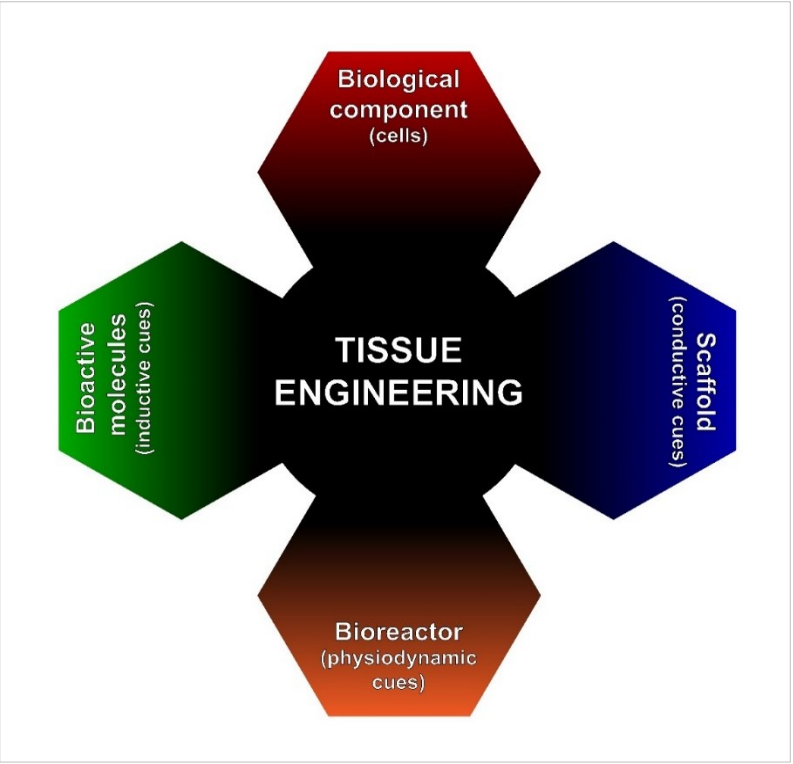

Figure 25. *Tissue engineering quadrat.*

cultured in-vitro to synthesize tissues, which can then be implanted into an injured site, or directly implanted into the damaged site and use the body's own capacity for regeneration of tissues or organs in-vivo. The combination of **cellular component, bioactive molecules** (inductive cues), **scaffolds** (conductive cues) and **bioreactors** (physio-chemo-dynamic cues) is often referred to as a **tissue engineering quadrat,** (Figure 25).

Requirements to scaffolds

Several key properties of the scaffolds should be considered as important when designing or determining their suitability for use in tissue engineering, (O'Brien 2011):

- **Biocompatibility**: cells must adhere, function normally, and migrate onto the surface and eventually through the scaffold and begin to proliferate before laying down new matrix. After implantation, the scaffold or tissue engineered construct must elicit a negligible immune reaction.
- **Biodegradability**: Scaffolds are not intended as permanent implants. The objective of tissue engineering is to allow the body's own cells, over time, to eventually replace the implanted scaffold or tissue engineered construct. They must be therefore biodegradable, by meaning to allow cells to produce their own extracellular matrix. Moreover, the products of the scaffold degradation should also be non-toxic and able to exit the body without interference with other organs. In addition, in order to allow degradation to occur parallel with tissue formation, often an inflammatory response combined with controlled infusion of cells such as macrophages is demanded.
- **Mechanical properties**: Ideal scaffold should have mechanical properties consistent with the tissue that is to be replaced and, from a practical point of view; it must be strong enough to allow handling during production and implantation.
- **Scaffold architecture**: The architecture of scaffolds used for tissue engineering is of critical importance. Scaffolds should have an interconnected porous structure and desired controllable porosity in order to ensure, first, cellular penetration and second, an adequate internal diffusion of nutrients. Furthermore, a porous interconnected structure is required to allow diffusion of waste and degradation products out of scaffold. The issue of core degradation, arising from lack of vascularization and waste removal from the center of tissue engineered constructs, is another major concern in tissue engineering, (Phelps et al. 2010).
- **Material consideration**: The material (or biomaterial) from which the scaffold is fabricated is one of the most important parameter for scaffolds with application in tissue engineering. This criterion is one of which all of the desired scaffold properties listed above are dependent on.
- **Other** important properties of the scaffold are connected with its **surface topography** (important for cell adhesion, orientation and tissue integration), **surface chemistry** (presence of chemical groups and functionalizations) and **biological activity** (involvement of bioactive components like ligand binding motifs, growth factors, enzymes etc.)

Biomaterials

First definition for biomaterial comes from the Consensus Conference of the European Society for Biomaterials (ESB) in 1976, and says: **"*A nonviable material used in a medical device, intended to interact with biological systems*"**. Current definition of ESB however is enriched as: ***"A material intended to interface with biological systems to evaluate, treat, augment or replace any tissue, organ or function of the body"***, (O'Brien 2011). This refined definition is demonstration of how the concept of biomaterials has evolved. Biomaterials have turned from *low recognizable* ("stelt" materials) or *merely interacting* with the body to **actively influencing biological processes** toward the goal of proper tissue regeneration. Based on their nature, three individual groups of biomaterials might be distinguished in respect to fabrication of scaffolds for tissue engineering: **(i) ceramics, (ii) synthetic polymers and (iii) natural polymers**. Each of these groups has its specificity, advantages and, respectively, disadvantages, leading recently to consideration for development and use of *composite scaffolds* that combine materials from different groups in order to improve their desirable properties.

The usage of **ceramic scaffolds**, such as hydroxyapatite (HA), (Figure 26, (b)), and tri-calcium phosphate (TCP) is widespread when we talk for bone regeneration applications. Ceramic scaffolds are characterized by high mechanical stiffness (Young's modulus), low elasticity, and brittleness, but they exhibit excellent biocompatibility due to their chemical and structural similarity to the mineral phase of native bone. The interactions of osteogenic cells with ceramics are important for bone regeneration as ceramics are known to enhance osteoblast differentiation and proliferation, (Ambrosio et al. 2001). Various ceramics have been used in dental and orthopedic surgery as bone defects fillers or as integration improving coatings for metallic implants. Ceramic's clinical applications however have some limitations, because of their brittleness, difficulty of shaping, and because new bone tissue formed in a porous HA network cannot sustain the mechanical loading needed for remodeling, (Wang 2003). In addition, it is difficult to control the degradation rate of the bone grafts, (Tancred, McCormack, and Carr 1998).

Numerous **synthetic polymers** have been widely used to produce scaffolds, including for example polystyrene, poly(L-lactic acid) (PLLA), poly(glycolic acid) (PGA) and poly-dl-lactic-co-glycolic acid (PLGA). While these materials have shown themselves as successful in fabrication and tailoring

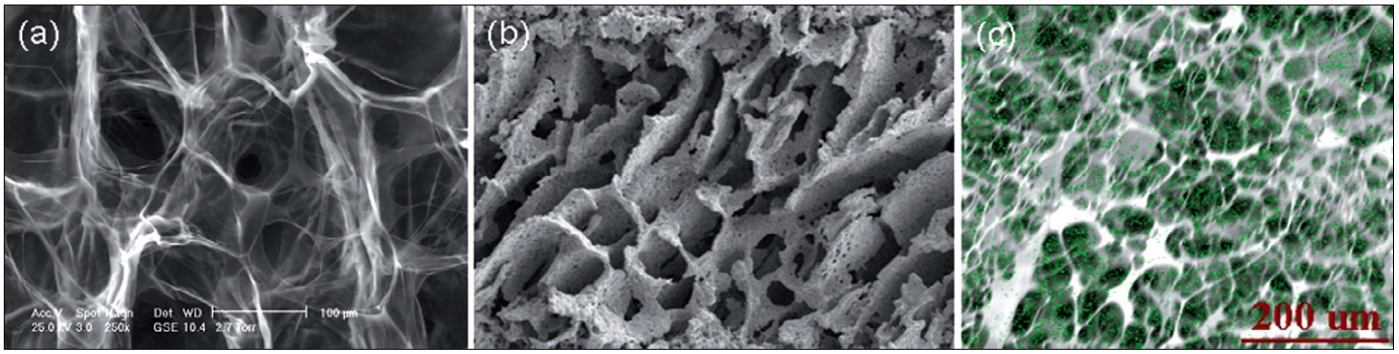

Figure 26. *Different types of scaffolds: comparative SEM images of* ***(a)*** *collagen-GAG scaffold;* ***(b)*** *hydroxyapatite; and* ***(c)*** *composite collagen-hydroxyapatite scaffold. Adapted from* ***(O'Brien 2011)***

architecture, and their degradation characteristics can be controlled by modifying the polymer chemistry and composition, (Rowlands et al. 2007), they have drawbacks mainly related with their reduced bioactivity, slow degradation (as some of them degrade only by hydrolysis), or body rejection, (Liu, Slamovich, and Webster 2006).

The third commonly used approach is the use of **biological materials** as scaffold biomaterials, (Figure 26, (a)). Biological materials such as collagen, fibrinogen, various proteoglycans, alginate-based substrates and chitosan have all been used in the production of scaffolds for tissue engineering. Unlike synthetic polymer-based scaffolds, natural polymers are biologically active and typically promote excellent cell adhesion and growth. Furthermore, they are also biodegradable and so facilitate host cells to produce their own extracellular matrix and rebuild, with the time, the degraded scaffold. Main drawbacks here are connected with the fabricating of scaffolds with a homogeneous and reproducible structure. Other important drawbacks relate to their poor mechanical properties and immunogenicity, which narrows their direct use in tissue engineering.
The limitations, described above for each of the groups have resulted in considerable efforts for development of **composite scaffolds** at present comprising the nature of a number of biomaterials, for example introducing GAG into native collagen sponge, (Figure 26, (c)), ceramics into polymer-based scaffolds, (Huang et al. 2008), or combination of synthetic polymers with natural ones in order to enhance either their biological activity or mechanical properties, (Friess and Schlapp 2006; Gugutkov et al. 2016). However, although composite scaffolds have shown some promises, they consists of at least one phase which is not found naturally at this place in the body and thus they all have associated problems with biocompatibility, biodegradability or immunogenicity, (O'Brien 2011).

Recreating the extracellular microenvironment

With understanding the importance of proper interactions between cells and their microenvironment, an exceptional attention was recently directed to development of scaffolds that can **imitate the structural aspects of extracellular matrix** and are expected to facilitate cell adhesion, proliferation, differentiation and neo tissue genesis.

Until recently, it was believed that the macroporous features of scaffolds only needs to mimic the dimension scale of the extracellular matrix (ECM), and the matrix itself (natural or artificial) is only to serve as a support for the cells. The stress was set on critical engineering of the material properties, such as pore size, mass transfer, biocompatibility, biodegradability and mechanical characteristics that suits certain tissue. However, now, when the field evolved, more and more attention is focused on the biological aspects of scaffolds design, and how they affect various cell types behaviors, (Lutolf and Hubbell 2005). Tissue engineers had realized that some of the widely used scaffolds do not correctly recapitulate the cell microenvironment, because ECM is a complex, dynamic and hierarchically organized nanocomposite structure that is able to regulates most essential cellular functions such as adhesion, proliferation, directional migration, differentiation and

morphogenesis, (Tsang et al. 2010),(Figure 27). As a consequence, existing and newly developed nanotechnological tools were used to design advanced nanocomposite scaffolds that can better mimic the ECM and eventually assemble into more complex, functional tissues. This requires effective organization of cells into tissues with architecture and physiological features matching those in the nature. Unfortunately, this is a difficult task, because the signaling factors that drive tissue assembly have not yet been fully understood. In general, the morphogenesis in a three-

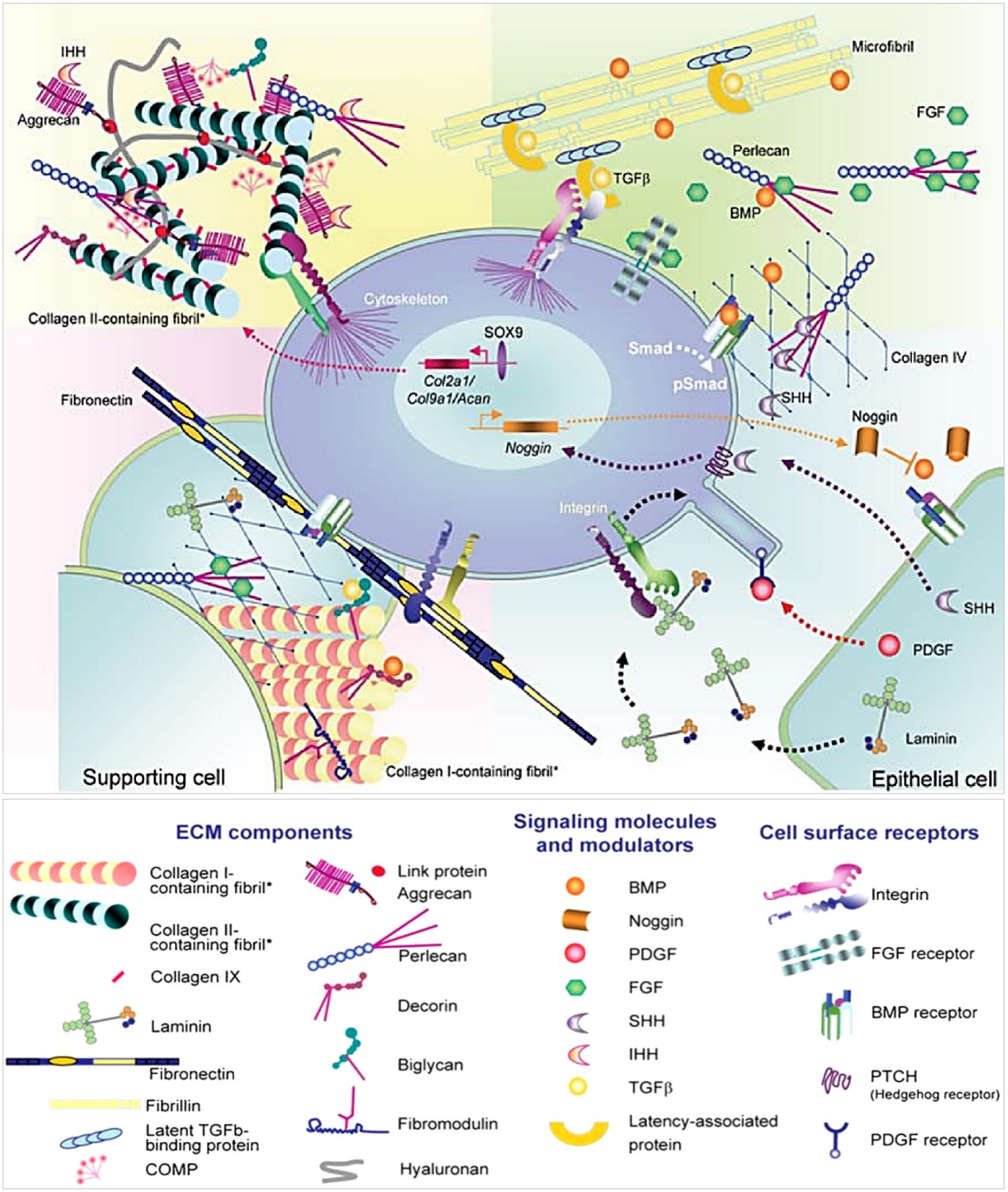

Figure 27. *Prototypic cell - extracellular matrix interactions and their complicity. Adapted from* ***(Tsang et al. 2010).***

dimensional (3D) scaffold should resemble the processes of natural tissue development. It is known that cells are able to organize upon interaction with the ECM on the basis of topography, (Bauer, Jackson, and Jiang 2009), mechanical properties, (Levental et al. 2009), concentration gradients of the immobilized growth factors or distinct ECM molecules, (Rozario and Desimone 2011). Ott et al. reported a study emphasizing the importance of the ECM structure in guiding the cells and promoting morphogenesis. In this study hearts from rats were decellularized with preserving the underlying ECM and then repopulated with cardiac and endothelial cells. The cells migrated and self-organized in their natural location within eight days. Moreover, under physiological load and electrical stimulation, the constructs were able to generate pump function, (Ott et al. 2008). All this comes to show the significance of the unique microenvironment that ECM creates to foster tissue organization, but still, it does not reveal what is the essence of its important cues and their particular nature.

Organizational cues within ECM that may control cell behavior

Morphologically ECM is composed of intricate interweaving fibrillar compounds, ranging from 10 to several hundreds of nanometers which presumably are those providing cells with a wealth of informational cues. In vivo cells encounter and interact with differently organized topographical features ranging from folded protein to banded collagen fibrils. They also align and orient on them: a phenomenon known as contact guidance, (Flemming et al. 1999). Topographical cues imprinted within the structural organization of the ECM may have significant effects on the whole cellular behavior. Great number of studies have shown that the topography of substrates has immediate effects on the ability of cells to orient, to produce organized cytoskeletal arrangements and to migrate. One approach to study these effect is to recreate some of the structural parameters of the native ECM by micro- or nanopatterning utilizing different geometries (such as grooves, nanoposts and nanopits), or alternatively by production of nanofibrous structures. In respect to the patterning, though it is only applied on 2D surfaces, this technique reveals aspects of cell behavior and reaction to topographical cues that could be relevant also in 3D environment.

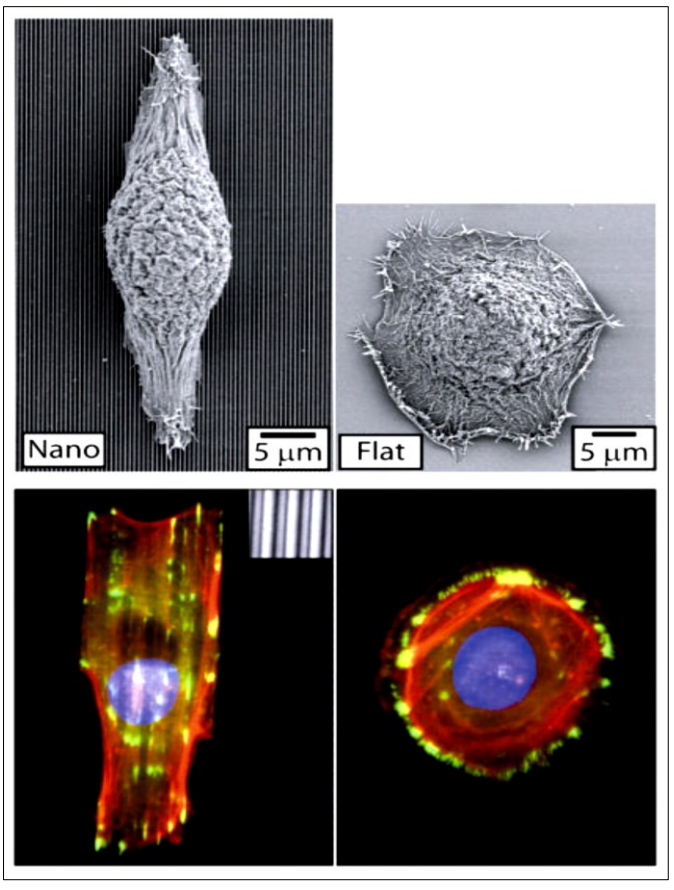

Figure 28. *Epithelial cells respond to nanopaterning through alignment and elongation. Adapted from* ***(Bettinger, Langer, and Borenstein 2009)***

The topography of substrates influences a variety of cellular processes, including adhesion, overall morphology, migration and differentiation, (Bettinger, Langer, and Borenstein 2009). For example, epithelial cells respond to patterns of grooves and ridges with elongation and alignment only if dimensions are as small as 70 nm, whereas on smooth substrates, cells spread in rounded shape (Figure 28), (Teixeira et al. 2003). Effect on human mesenchymal stem cell (MSC) differentiation using nanoscale symmetry and disorder was reported by Dalby et al., where ordered topographies resulted in low to negligible cell adhesion and osteoblastic differentiation, whereas nanoscale topographic disorder stimulated MSCs to produce bone mineral, (Dalby et al. 2007). In the studies, included in this Thesis, was shown that endothelial cells cultured on aligned and randomly deposited fibrinogen nanofibers not only attach and grow in a different orientation, but also express altered nitric oxide secretion (higher on random and lower on aligned fibers), i.e. different functionality, (Gugutkov, Gustavsson, Ginebra, & Altankov, 2013). The precise mechanism responsible for such a different cellular behavior on diverse nanotopographies is still not fully understood, although the involvement of cell adhesion machinery (integrins and actin cytoskeleton) and the activation of distinct signaling cascades has no doubt.

Implication of nanofibers

Structurally, natural ECM consists of various interwoven fibrillary components (mostly proteins) with diameters ranging from tens to hundreds of nanometers. Their nanoscale structure offers a natural network to support cells and to present an instructive environment to guide cell behavior, (Wang, Ding, and Li 2013). Thus, obtaining scaffolds that imitate the architecture of tissues at the nanoscale is one of the major challenges in the field of tissue engineering. Indeed, recent developments in nanofibers production techniques have improved the perspectives for fabrication of such scaffolds.

The preparation of scaffolds that can imitate the complex architecture of natural tissues at nanoscale is one of the major tasks. It has led to the development of various techniques for production of nanofibers. Among them, the electrospinning has gained significant recognition because of its ability to generate fibers similar to those of native ECM. Moreover this fabrication technique allows implementation of a wide range of biomaterials and provides tools for control over the geometrical organization of the scaffolds, (Wang et al. 2013). In the studies presented here the electrospinning technique was mostly used to produce nanofibers, though other techniques for generating nanofibers such as self-assembly and phase separation also take place in tissue engineering of today.

Self-assembly

Self-assembly is a process of spontaneous organization of individual components into an ordered and stable structure with non-covalent bonds. It is also a natural process involved in essential biological functions like nucleic acids and protein synthesis. However, self-assembly is a complex

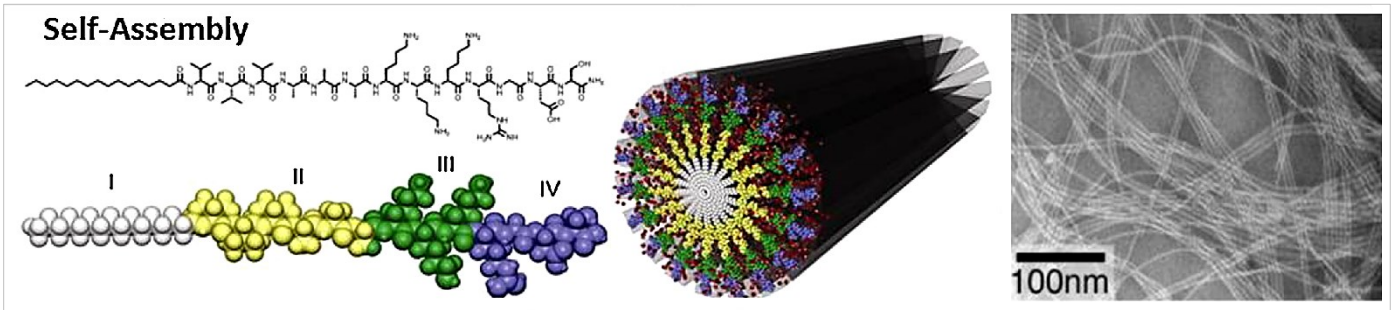

Figure 29. *Schematic of self-assembly technique used to fabricate fibrillar synthetic scaffolds. Adapted from* ***(Wang et al. 2013).***

laboratory procedure that is limited to only a few polymer configurations (diblock copolymers, triblock copolymers, triblocks from peptide-amphiphile, and dendrimers, (Mosher et al. 1992). The most common of these are the peptide-amphiphiles (PA) – molecules with some specific structural features, namely a hydrophilic head, a long alkyl tail for hydrophobicity, cysteine residues to create disulfide bonds for polymerization, and a linker region of glycine residues to provide flexibility to the

group, (Hartgerink, Beniash, and Stupp 2001, 2002; Zhang 2003). When placed in water, the hydrophobic alkyl tail groups assemble together to form a cylindrical micelle that exposes the hydrophilic head groups to the water phase, (Figure 29). This technique is capable to create nanofibers even 5– 8 nm in diameter and 1μm in length, but the complexity of the procedure and the low productivity of the method limit it as a large-scale tissue engineering option Another limitation of this technique is the difficulty to obtain control on the nanofibers organization, (Ma et al. 2005).

Phase separation

Phase separation has been widely used as a technique to create porous polymer membranes. It is a thermodynamic separation of a polymer solution into a polymer-rich component and a polymer-poor/solvent-rich component. In general the polymer is dissolved in solution and the driving force

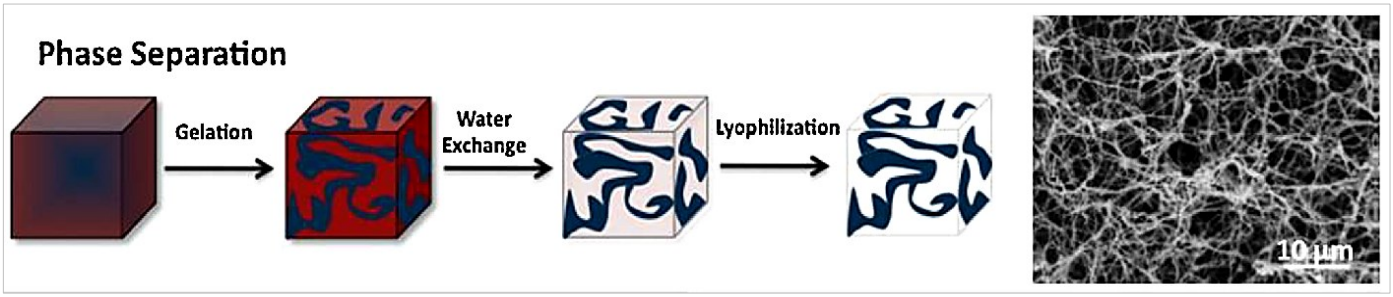

Figure 30. *Schematic of phase separation technique used to obtain fibrillar synthetic scaffolds. Adapted from* ***(Wang et al. 2013).***

for the phase separation is the thermal treatment (most common), or the addition of a nonsolvent component to the polymer solution which creates a gel. Water is then used to extract the solvent from the gel; the gel is lyophilized to produce a nanofibrous scaffold, (Figure 30), (Jayaraman et al. 2004; Ma et al. 2005; Smith and Ma 2004). Ma and Zhang applied this technique to produce nanofibrous, three-dimensional scaffolds whit porosity as high as 98.5%. A variety of biodegradable aliphatic polyesters can be used for preparation of these scaffolds, composed of fibers with diameters that range from 50 to 500 nm (similar to natural collagen in the ECM), (Chen and Ma 2004; Ma and Zhang 1999). Unlike self-assembly, the phase separation is a simple technique that does not require specialized equipment. The desired mechanical properties and architecture of the scaffold is easily achieved by varying component concentrations. However, this method is limited by only a selected number of polymers and is strictly a laboratory scale technique, (Jayaraman et al. 2004).

Electrospinning

The electrospinning process has attracted significant attention because of its ability to generate fibers similar to the native ECM and to process a wide range of materials. Other advantages are the straightforward nature of the process and its cost-effectiveness. The large surface area of electrospun nanofibers as well as their porous structure favors cell adhesion, proliferation, migration,

and differentiation, (Bhattarai et al. 2004; Shi et al. 2010). If necessary, the nanofibers can be further functionalized via incorporation with bioactive species (e.g. enzymes, DNAs, and growth factors) to better control the proliferation and differentiation of cells, (Mosher et al. 1992). These attributes make electrospun nanofibers one of the best candidates for scaffolds applicable in the field of tissue engineering, (Wang et al. 2013).

Due to the fact that electrospining is one of the core techniques used in this work, it will be summarized in more details

Short history of electrospinning

Electrospinning, also known as electrostatic spinning, is considered as a variant of the electrostatic spraying process which was first described by Bose in early 1745, (Greiner and Wendorff 2007). The first devices however to spray liquids through the application of an electrical charge were patented by Cooley and Morton at the beginning of the 20th century, (Cooley 1899; Morton 1900). In 1914 Zeleny reported that the fine fiber-like liquid jets could be emitted from a charged liquid droplet in the presence of an electrical potential, which is considered to be the origin of principle for the modern needle electrospinning, (Zeleny 1914). In 1934, a crucial patent, revealing the experimental apparatus for the production of artificial filaments using electrical field, (Figure 31), was published for the first time by Formhals, (Formhals 1934).

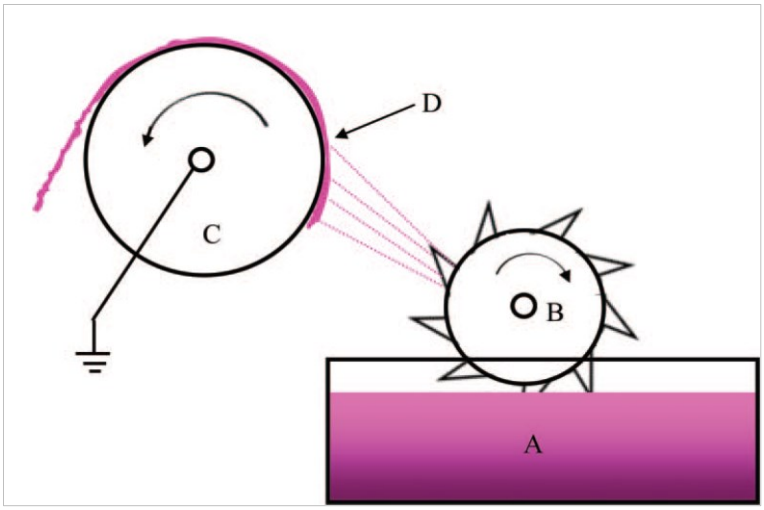

Figure 31. *Formhals' experimental apparatus for producing filaments via electrospinning: (A) spinning solutions are passed through electrical field between two electrodes- a slender rotating serrated wheel in a pool (B) and a collector wheel (C). The electrospun filaments are indicated as (D). Adapted from* ***(Lin et al. 2012)****.*

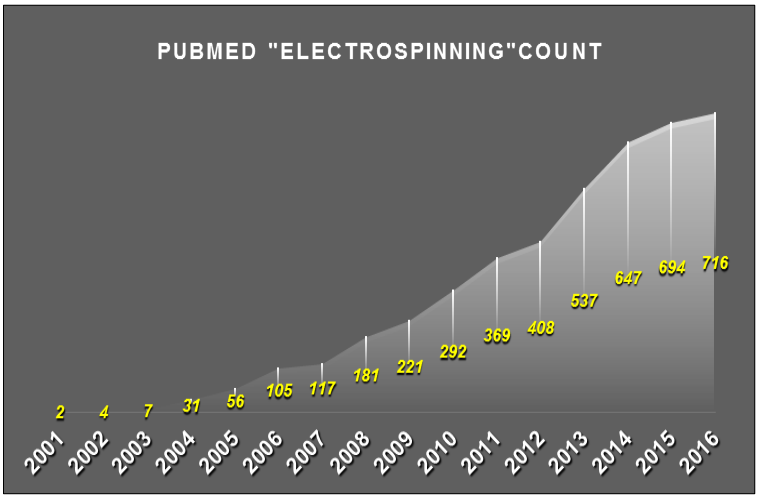

Figure 32. *Number of published papers containing the concept of the "electrospinning" process searched for on* ***PUBMED****.*

Firstly, electrospinning did not obtain substantial attention in the scientific community due to incapacity to observe the obtained nanofibers. However, with the booming of nanotechnology in 1990s several research groups, especially the Reneker's one, rediscovered this

technique by fabrication of ultra-thin fibers from various polymers, (Doshi and Reneker 1995; Reneker et al. 1996). Since then the popularity of electrospinning has increased exponentially if one looks on the number of publications describing the usage of this method, (Figure 32).

The electrospinning process

The basic setup for electrospinning consists of three main components: a high voltage supply, a polymer source, connected with spinneret (normally bunt metallic needle) and grounded collector, (Figure 33). The spinneret is connected with container (syringe) hosting polymer solution (or melt). With the help of syringe pump or by simple gravity forces the polymer is fed to the spinneret in a constant flow rate. In the same time high voltage is applied between the spinneret and the grounded collector charging the polymer droplet. Two types of electrostatic forces – electrostatic repulsion between the charges and Coulomb force caused by the electrical field, are acting in this moment and convert the drop in conic structure named **Taylor cone,** (Figure 34, (A)). When electrostatic forces overcome the surface tension of the polymer solution an electrified jet is generated that is further stretched by the electromagnetic field forming very thin continuous fiber. By simultaneously but demanded evaporation of the solvent the diameter of the jet significantly reduce and before it reaches the grounded collector a nanometric fiber is formed, (Haider, Haider, and Kang 2015).

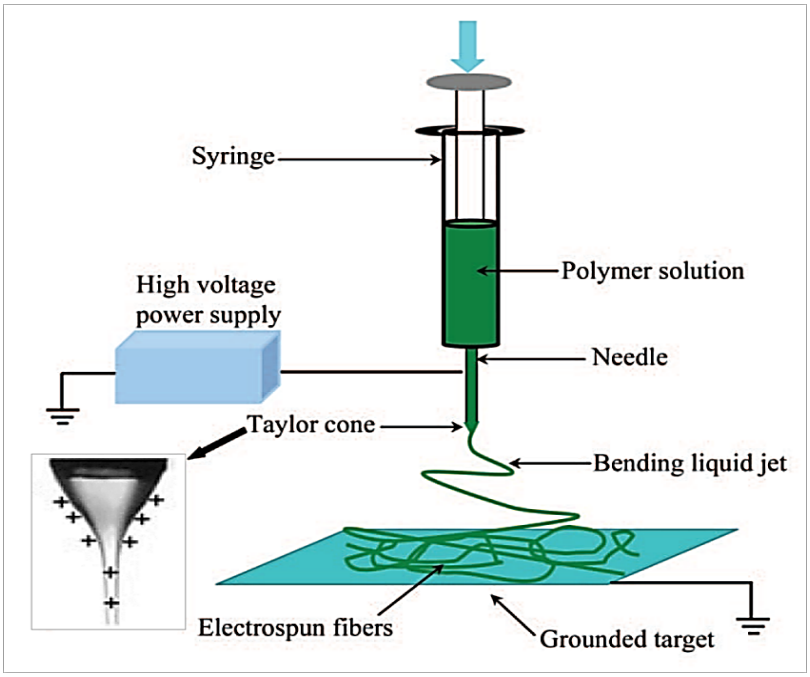

Figure 33. *Schematic illustration of electrospinning set-up. Adapted from* ***(Lin et al. 2012)****.*

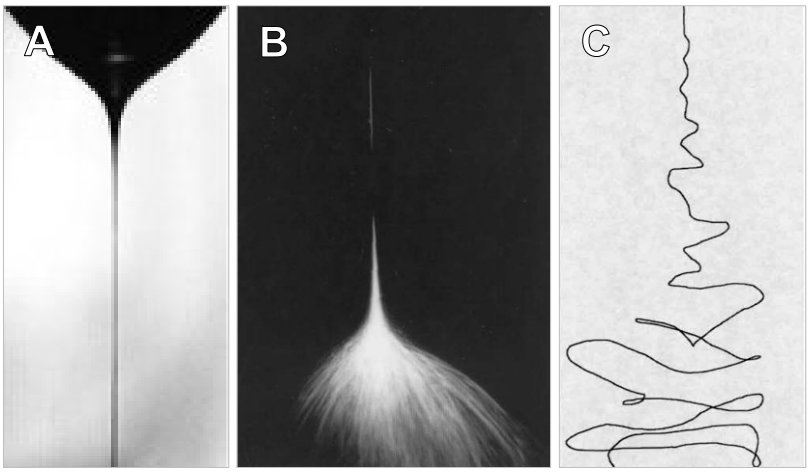

Figure 34. *Taylor cone,* ***(A)****; Instability of the jet during electrospinning,* ***(B)*** *and* ***(C)****. Photographic images taken with different exposure times. Adapted from* ***(B. D. Li and Xia 2004)****.*

Before 1999, most of researches believe that the repulsion between the charges is the reason of splitting and splaying of the polymer solution. Recent studies however showed that the bending

instability is what causes thinning of the jet during electrospinning as shown on Figure 34, (B) and(C), (Li and Xia 2004; Reneker et al. 1996).

Parameters affecting electrospinning process

Variety of factors has influence on the electrospinning process. They may be generally classified in three groups: electrospinning parameters, polymer-solution parameters and environment parameters, (Haider et al. 2015):

- ***The electrospinning parameters*** include the applied voltage, the distance between the needle and collector, the diameter of needle and the flow rate.
- ***Polymer-solution parameters*** include, the nature of solvent, the polymer concentration, the viscosity and the conductivity of the solution.
- ***Environmental parameters*** are the humidity and temperature.

All of these parameters play role in the formation of the electrospun fibers and have direct influence on their properties. Therefore, for better understanding and control the electrospinning technique, it is of crucial importance to know more about their particular effects.

Applied voltage

The critical values of applied electromagnetic field needed to overcome the surface tension and formation of Taylor cone varies from polymer to polymer. Generally, formation of smaller-diameter nanofibers is connected with an increase in the voltage values. This is due to higher stretching of the polymer solution in correlation with the charge repulsion within the polymer jet, (Sill and von Recum 2008). However, placing the applied voltage beyond this critical value normally results in the formation of beads or beaded nanofibers because of decrease in the size of the Taylor cone and increase in the jet velocity without changes in the flow rate, (Deitzel et al. 2001).

Flow rate

The flow rate of the polymeric solution also influences the morphology of the electrospun nanofibers. Using optimal flow rate homogenous nanofibers without beads could be obtained. Conversely, increasing the flow rate above the optimum could provoke formation of beads and increase of fiber diameter due to incomplete drying, (Silke Megelski et al. 2002). On the other hand, decreased polymer flow leads sometimes to **receded jet** (a jet that emerges directly from the inside of the needle but not from Taylor cone). Such jets are not stable and, during the electrospinning, they are repetitively replaced by cone jets. The resulting nanofibers normally express non-uniformity in diameter ranges, (Zargham et al. 2012). In addition to bead formation, other structural irregularity can be caused by elevated flow rate. For example ribbon-like defects and unspun droplets can be formed as a result of non- evaporation of the solvent and low stretching of the solution, (Silke Megelski et al. 2002; Zargham et al. 2012). Theron et al. revealed that the flow rate and electric

current are directly related to each other. They showed also that reducing the surface charge density causes merging of nanofibers during their fall toward the collector, (Theron, Zussman, and Yarin 2004).

Needle diameter and needle to collector distance

The distance between the metallic needle tip and collector plays also an essential role in determining the morphology of an electrospun nanofiber. The nanofiber morphology could be easily affected by the distance because it directly correlates with deposition time, evaporation rate, and

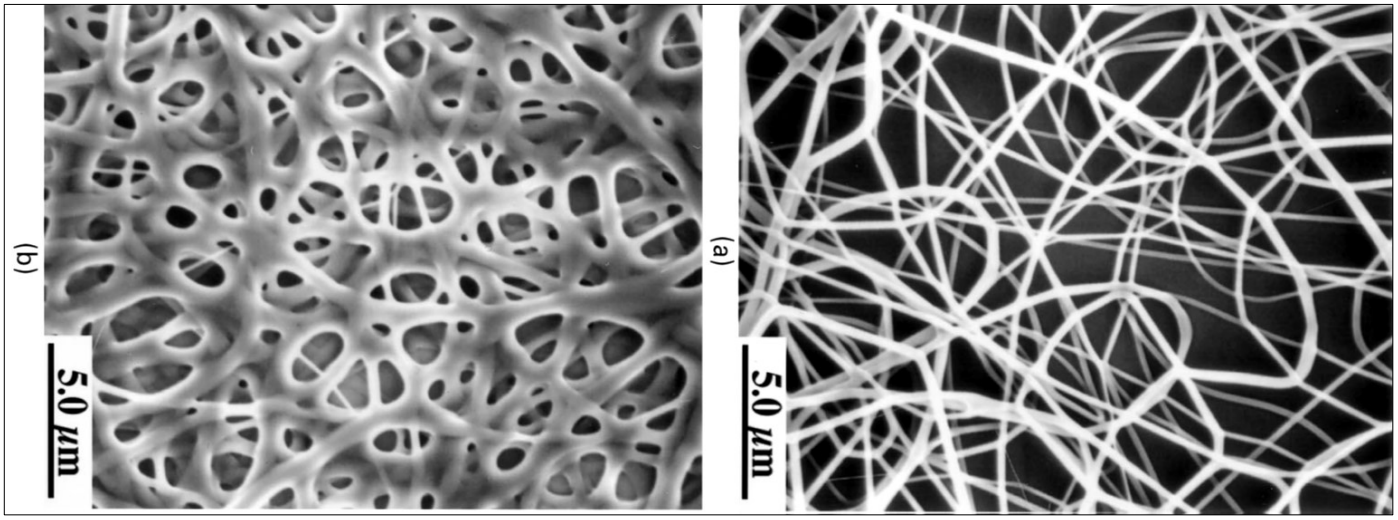

Figure 35. *Morphology of electrospunn nanofibers:* ***(a)*** *- deposited at 2.0 cm;* ***(b)*** *-deposited at 0.5 cm. Adapted from* ***(Buchko et al. 1999)****.*

whipping. Thus, an optimal distance is needed for the production of smooth and uniform electrospun nanofibers. Any changes on either side of the optimal distance will affect the morphology of the nanofibers. Generally, larger-diameter nanofibers are formed when this distance is too short, whereas the diameter of the nanofiber decreases with enlargement of the distance, (Figure 35), (Matabola and Moutloali 2013).

Polymer concentration and viscosity

As electrospinning process relies on the uniaxial stretching of a charged jet it is significantly affected by changing the concentration of the polymeric solution. Low concentration allows that the applied electromagnetic field and the surface tension cause breakage of polymer fibers into fragments before reaching the collector, (Haider et al. 2013; Pillay et al. 2013). Such a fragmentation can result in appearance of beads or beaded nanofibers. Increasing the concentration of the polymer in the solution above the critical level will increase also the viscosity, which subsequently hampers the flow through the needle. The result is defective or beaded nanofibers, (Haider et al. 2013).

Solution conductivity

Solution conductivity is important for both the Taylor cone formation and the diameter of the nanofibers. In low-conductive polymer solutions the surface of the droplet will have no charge to form a Taylor cone and no electrospinning will appear. Increasing the conductivity of the solution to a critical value will increase the charges on the surface of the droplet and will allow to form Taylor cone but also will provoke decrease in the diameter of fibers, (Sun et al. 2014). Increasing the conductivity above the optimal one will hinder again the Taylor cone. This can be explained by interplay of Coulomb force between the charges on the surface of the fluid and the force applied by the external electric field. However, the formation of the Taylor cone is governed largely by the electrostatic force of the surface charges created by the applied external electric field (the component of the field that is tangential to the surface of the fluid induces this electro- static force). Dielectric polymer solution will not have enough charges in the solution to move onto the surface of the fluid; hence, the electrostatic force generated by the applied electric field will not be insufficient to form a Taylor cone and initiate electrospinning process. In contrast, a conductive polymer solution will have sufficient free charges to move onto the surface of the fluid and form a Taylor cone and initiate the electrospinning process. Thus, Coulomb and electrostatic forces together influence the elongating and the stretching of the jet and have a significant influence on the whipping and the diameter of the nanofibers, (Haider et al. 2015).

The conductivity of a polymer solution could be controlled by the addition of an appropriate salt to the solution. The addition of salt affects the electrospinning process by increasing the number of ions in solution (increase of surface charge density) and increasing its conductivity, (Choi et al. 2004).

Solvent

Usage of a proper solvent is a key factors for successful electrospinning. Two parameters are of importance when selecting the proper solvent: **(i)** solubility of the polymer of interest and **(ii)** the boiling point of the solvent that gives an idea about its volatility (evaporation). Generally volatile solvents are preferred as they encourage the easy evaporation. However, too volatile solvents are mostly avoided because very high evaporation rates causes drying of polymer at the needle tip. From other hand, less volatile solvents are also avoided in electrospinning due to their high boiling points that prevent their drying during the nanofiber jet flight. In general, the deposition of non-dried, solvent-containing nanofibers results in the formation of beaded structures on the collector,

(Lannutti et al. 2007; Sill and von Recum 2008). Furthermore, the solvent also plays a vital role if the fabrication of highly porous nanofibers is desired, (Figure 36). This may occur when a polymer is dissolved in two solvents where one of the solvents will act as a non-solvent. The different evaporation rates of the solvent and non-solvent will lead to phase separation and hence will result in the fabrication of highly porous electrospun nanofibers,(Sill and von Recum 2008).

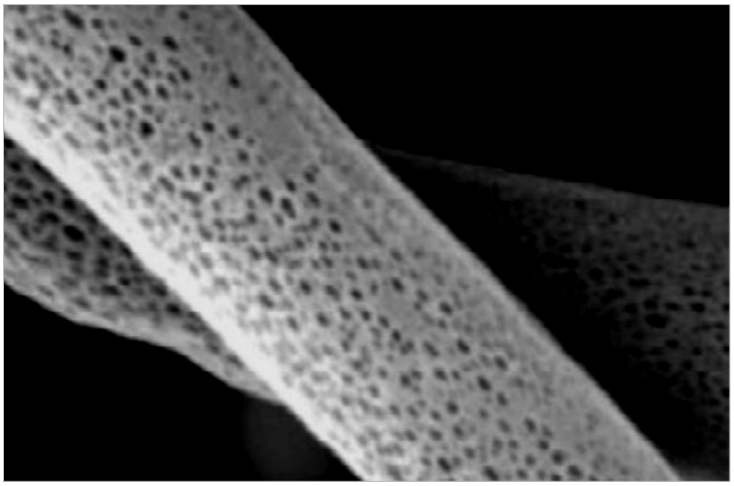

Figure 36. *SEM images of porous poly(vinyl butyral) (PVB) nanofibers prepared from THF/DMSO (9/1, v/v) solution. Adapted from* ***(Gholipour Kanani et al. 2011)****.*

Humidity and temperature

Recently it has been reported that ambient factors such as humidity and temperature also affect the properties of the nanofibers (Huan et al. 2015; Pelipenko et al. 2013). Humidity causes changes in the nanofibers diameter by altering the solidification process of the charged jet. This phenomenon however is strongly dependent on the chemical nature of the polymer. Pelipenko et al studied the change in nanofibers diameter with change in humidity and observed that the diameter of the nanofibers decreased with increase in of humidity. Further increase in humidity however may lead to formation of beaded fibers or obstructed electrospinning without fibers formation, (Pelipenko et al. 2013)

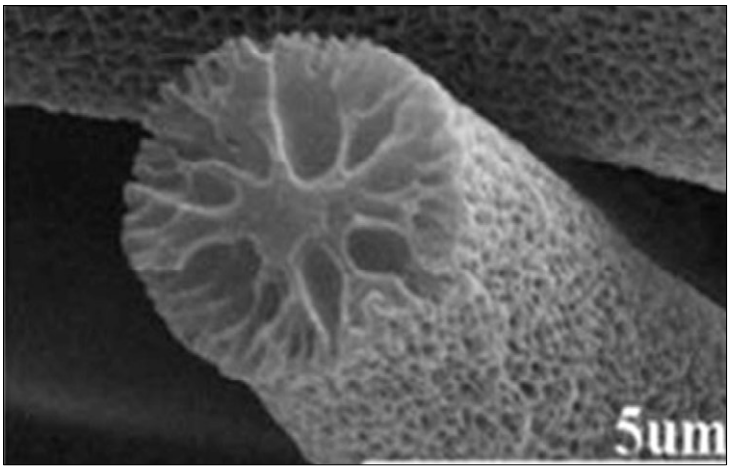

Figure 37. *SEM images of porous electrospun poly(methyl methacrylate) (PMMA) NFs with different humidity. Fiber cross-section* ***(Bae et al., 2013)****.*

Humidity also plays an important role in the creation of porous nanofibers when binary solvents are used. Appearance of the pores is attributed to the different evaporation rates of the two solvent. During electrospinning the more volatile solvent evaporates faster than the less volatile one. This phenomenon has cooling effect and similar to perspiration. The cooling provokes condensation of water vapor into water droplets that deposit on the fibers. The water mixes well with one of the two solvents on the inner and outer surfaces of the fibers. Thus after the complete evaporation of the solvents and the water droplets from the fibers formation of pores was found, (Figure 37), (Bae et al. 2013).

Increasing the temperature usually unlocks two opposing effects to the average diameter of the nanofibers: **(i)** increase the rate of evaporation of solvent and **(ii)** decrease the viscosity of the

solution. Together these effects lead to the decrease in the mean fiber diameter as reported by De Vrieze and co-workers., (De Vrieze et al. 2009).

Polymer consideration

Practically every polymer can be a subject of electrospinning when appropriate solvent and conditions are used. The technique has already been successfully applied to generate nanofibers from more than 100 different types of synthetic or natural polymers, (Burger, Hsiao, and Chu 2006). Synthetic polymers are relatively easy accessible than natural ones, because their lower price, especially when larger amounts are desirable. Most commonly used synthetic polymers for biological applications are poly(caprolactone) (PCL), polyethylene oxide (PEO) and poly(lactic acid) (PLA). Although these polymers are claimed as biocompatible and biodegradable, they may trigger significant inflammation and foreign body reactions when implanted in vivo, (Bergsma et al. 1993). Therefore, natural polymers are more preferred to avoid immune complications. Most abundant natural polymers for electrospinning are collagens I and III, presenting almost one third of the proteins in the human body. Collagens however require cross-linking to maintain their fibrous morphology after electrospinning which is associated with toxicity of crosslinkers, (Barnes, Pemble, et al. 2007).

Fibrinogen is also a preferable choice when considering implication of natural polymers, (D. Gugutkov et al. 2016; D. Gugutkov et al. 2013). However, the mechanical strength of fibrinogen nanofibers is usually limited, (D. Gugutkov et al. 2013; Shields et al. 2004), a problem that may be solved by developing hybrid FBG/polymer nanofibers as shown in the current Thesis, (D. Gugutkov et al. 2016). Principally, the use of precisely tuned blending with synthetic polymers is a popular approach to improve the stability and the mechanical strength of natural polymers allowing their electrospinning in a more stable configuration, (Jin San Choi et al. 2008; D. Gugutkov et al. 2016)

Mechanical properties of electrospun nanofibers

The mechanical properties of electrospun nanofibers depend on number of parameters including the polymer properties and its molecular structure, the size, the density and the orientation of the individual nanofibers, (Mauck et al. 2009). For example, nanofibers made of poly(lactic- co -glycolic acid) (PLGA) are ten folds stiffer than PCL ones, (Li et al. 2006). Ramakrishna and co-workers have found correlation between the rotating speed of the collector and the orientation in the molecular structure within PLA fibers, which consequently led to higher tensile modulus and strength, (Inai et al. 2005). Leong and his group reported an increase in both strength and stiffness with decrease of fiber diameter of PCL-nanofibers, (Chew et al. 2006). Alignment of nanofibers also increases the stiffness in the direction of alignment, an important point when one strives to mimic the anisotropic ECM structure of load-bearing tissues such as tendons and myocardium, (Moffat et al. 2009).

Control on fibers alignment

An important advantage of electrospinning technology is that it provides relatively easy control on nanofibers orientation. Distinct tissue engineering applications require scaffolds made of aligned nanofibers expecting to affect their mechanical properties and cell behavior. Aligned nanofibers are desired for many specific tissue types such as tendon, (Yin et al. 2010), and myocardium (Zong et al. 2005), where collagen fibrils are naturally oriented. However, the alignment of nanofibers can be used also to guide the cell behavior, affecting the orientation, directional migration and overall cells morphology. Such studies were also performed in our lab and included in the present thesis, (Gugutkov et al. 2013, 2016). Aligned nanofibers have been used to guide the outgrowth of neural stem cells (NSCs) (Yang et al. 2005) and to support the differentiation of mouse embryonic stem cells (ESCs) toward neural lineage (Xie et al. 2009). Fibers orientation can also accelerate the wound closure guiding the migration of dermal cells in appropriate direction (Nisbet et al. 2008).

A number of methods have been developed for controlling the alignment of electrospun nanofibers. These methods can be categorized into three classes depending on the type of forces involved, mechanical, electrostatic, or magnetic, (Figure 36):

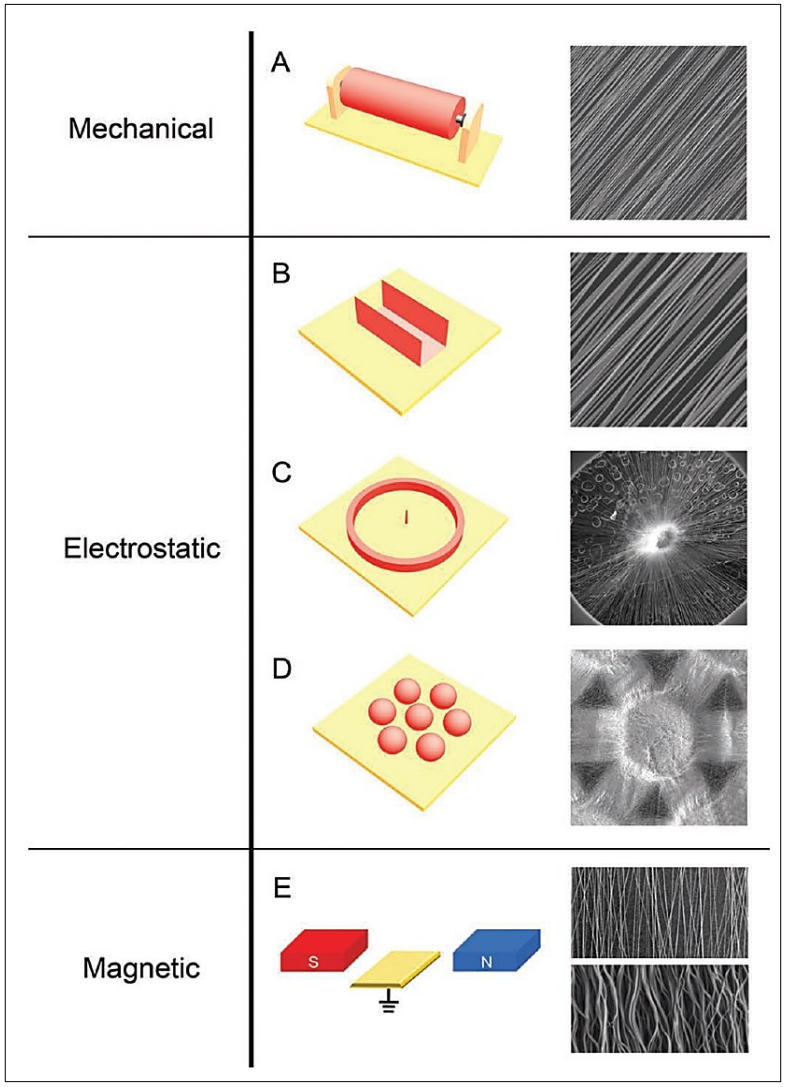

Figure 38. *Control of alignment of electrospun nanofibers using three different forces:* ***(A)*** *mechanical forces through the use of a rotating mandrel;* ***(B) (C) (D).****using different shapes of collector and electrostatic forces;* ***(E)*** *magnetic forces. SEM images in the right column representing typical morphology of. Aligned fibers obtained by respective method. Adapted from (Liu et al. 2012).*

Mechanical forces

This approach most often utilizes a metallic rotating mandrel as collector (Figure 36, A). When the electrospun nanofibers are collected by this way, the rotating speed of the mandrel determines the degree of alignment of the non-woven. Bowlin and co-workers showed that random collagen fibers might be collected at linear velocity lower than 0.16 ms^{-1} , while significant alignment was observed at linear velocities higher than 1.4 ms^{-1}. However, higher speed can result in better alignment to certain level only, as linear velocity higher than 45 ms^{-1} will encourage formation of necks in the

nanofibers because the electrospinning jet may not be slower than the linear velocity of the mandrel. In general, the mechanical alignment by using a simple rotating drum has its limitations, connected mostly with imperfections of alignment as a result of the whipping movements of the nanofibers and difficulties in collecting the electrospun material, (Blond et al. 2008; Na et al. 2009). Thus, for obtaining of uniformly aligned nanofibers, it is essential to optimize the rotation to an appropriate speed, (Barnes, Sell, et al. 2007). Other parameters that can influence the effectiveness of fiber alignment are the size of the mandrel and its conductive properties. Some authors propose the usage of alternated current (AC) to support the alignment process, (Liu, Thomopoulos, and Xia 2012).

Electrostatic forces

Since electrostatic charges are distributed along the electrospinning jet, an external electric field can be used to manipulate and control the alignment of nanofibers, (Liu et al. 2012). The use of collector consisting of two pieces of electrically conducting substrates separated by a gap of an insulating substrate will result in deposition of uniaxially aligned nanofibers. The mechanism of this phenomenon lay on the fact that nanofibers descending from the spinneret will experience two types of electrostatic forces: The first is the electric field pointing towards the two electrodes, which pull the fiber towards the electrodes. However, it also creates opposite charges on the surfaces of the electrodes creating the second force, which stretches the nanofiber across the nonconductive gap to render it perpendicular to the edges of the electrodes (Figure 36, B), (Li and Xia 2004). An advantage of this method of alignment is that it is convenient to collect aligned fibers onto solid substrates. This approach can be applied also for obtaining alignment into other patterns, for example scaffolds made of radially aligned nanofibers or onto arrays of metallic beads used as collector (Figure 36, C and D). In latter case the fibers deposit randomly on the beads and aligned across the gaps between the beads. The resulting non-woven material has concave micro-wells at the positions corresponding to the beads, (Xie et al. 2009). One of the limitations of this technology however is that alignment efficiency decreases with increasing gap between the electrodes.

Magnetic forces

Alignment of nanofibers during electrospinning can also be achieved by applying an external magnetic field (Figure 36, E). Jiang and co-workers showed parallel alignment of magnetized poly(vinyl alcohol) (PVA) fibers using an external magnetic field. The polymer solution was magnetized by adding a small amount (less than 0.5 % in weight) of magnetic nanoparticles. Then the solution was electrospun into nanofibers in magnetic field generated by two parallel permanent magnets. The magnetic field stretched the fibers across the gap to form uniaxially aligned array as they deposited onto the magnets. Electrospinning without magnetic nanoparticles resulted in random distribution without alignment even in presence of magnetic field, (Yang et al. 2007).

References

Alexandrova, Antonina Y. et al. 2008. “Comparative Dynamics of Retrograde Actin Flow and Focal Adhesions: Formation of Nascent Adhesions Triggers Transition from Fast to Slow Flow.” *PloS one* 3(9):e3234. Retrieved November 24, 2016 (http://www.ncbi.nlm.nih.gov/pubmed/18800171).

Altankov, G. and Th Groth. 1994. “Reorganization of Substratum-Bound Fibronectin on Hydrophilic and Hydrophobic Materials Is Related to Biocompatibility.” *Journal of Materials Science: Materials in Medicine* 5(9–10):732–37.

Altankov, George et al. 2010. “Development of Provisional Extracellular Matrix on Biomaterials Interface: Lessons from In Vitro Cell Culture.” Pp. 19–43 in *Media*. Retrieved November 23, 2016 (http://www.springerlink.com/index/10.1007/978-90-481-8790-4).

Altankov, Georgi, Frederick Grinnell, and Thomas Groth. 1996. “Studies on the Biocompatibility of Materials: Fibroblast Reorganization of Substratum-Bound Fibronectin on Surfaces Varying in Wettability.” *Journal of Biomedical Materials Research* 30(3):385–91.

Ambort, Daniel et al. 2010. “Specific Processing of Tenascin-C by the Metalloprotease Meprinβ Neutralizes Its Inhibition of Cell Spreading.” *Matrix Biology* 29(1):31–42. Retrieved January 13, 2017 (http://www.ncbi.nlm.nih.gov/pubmed/19748582).

Ambrosio, A. M., J. S. Sahota, Y. Khan, and C. T. Laurencin. 2001. “A Novel Amorphous Calcium Phosphate Polymer Ceramic for Bone Repair: I. Synthesis and Characterization.” *Journal of biomedical materials research* 58(3):295–301. Retrieved November 15, 2016 (http://www.ncbi.nlm.nih.gov/pubmed/11319744).

Artym, Vira V, Kazue Matsumoto, Susette C. Mueller, and Kenneth M. Yamada. 2011. “Dynamic Membrane Remodeling at Invadopodia Differentiates Invadopodia from Podosomes.” *European journal of cell biology* 90(2–3):172–80. Retrieved November 24, 2016 (http://www.ncbi.nlm.nih.gov/pubmed/20656375).

Askari, Janet A., Patrick A. Buckley, A.Paul Mould, and Martin J. Humphries. 2009. “Linking Integrin Conformation to Function.” *Journal of cell science* 122(Pt 2):165–70. Retrieved (http://www.pubmedcentral.nih.gov/articlerender.fcgi?artid=2714414&tool=pmcentrez&rendertype=abstract).

Assoian, Richard K. 1997. “Anchorage-Dependent Cell Cycle Progression.” *The Journal of Cell Biology* 136(1).

Astrof, Nathan S., Azucena Salas, Motomu Shimaoka, JianFeng Chen, and Timothy A. Springer. 2006. “Importance of Force Linkage in Mechanochemistry of Adhesion Receptors.” *Biochemistry* 45(50):15020–28. Retrieved January 13, 2017 (http://www.ncbi.nlm.nih.gov/pubmed/17154539).

Bae, Hyun-Su et al. 2013. “Fabrication of Highly Porous PMMA Electrospun Fibers and Their

Application in the Removal of Phenol and Iodine." *Journal of Polymer Research* 20(7):158. Retrieved October 11, 2016 (http://link.springer.com/10.1007/s10965-013-0158-9).

Bagavandoss, P. and J. W. Wilks. 1990. "Specific Inhibition of Endothelial Cell Proliferation by Thrombospondin." *Biochemical and biophysical research communications* 170(2):867–72. Retrieved January 11, 2017 (http://www.ncbi.nlm.nih.gov/pubmed/1696478).

Bailey, K., W. T. Astbury, and K. M. Rudall. 1943. "Fibrinogen and Fibrin as Members of the Keratin-Myosin Group." *Nature* 151(3843):716–17. Retrieved January 11, 2017 (http://www.nature.com/doifinder/10.1038/151716a0).

Ball, Vincent and Jeremy J. Ramsden. 1997. "Absence of Surface Exclusion in the First Stage of Lysozyme Adsorption Is Driven through Electrostatic Self-Assembly." *The journal of physical chemistry. B* 101(28):5465–5469.

Ball, Vincent and Jeremy J. Ramsden. 2000. "Analysis of Hen Egg White Lysozyme Adsorption on Si(Ti)O2|aqueous Solution Interfaces at Low Ionic Strength: A Biphasic Reaction Related to Solution Self-Association." *Colloids and Surfaces B: Biointerfaces* 17(2):81–94.

Barczyk, Malgorzata, Sergio Carracedo, and Donald Gullberg. 2010. "Integrins." *Cell and tissue research* 339(1):269–80. Retrieved October 26, 2012 (http://www.pubmedcentral.nih.gov/articlerender.fcgi?artid=2784866&tool=pmcentrez&rendertype=abstract).

Barnard, K. and L. J. Gathercole. 1991. "Short and Long Range Order in Basement Membrane Type IV Collagen Revealed by Enzymic and Chemical Extraction." *International journal of biological macromolecules* 13(6):359–65. Retrieved December 12, 2016 (http://www.ncbi.nlm.nih.gov/pubmed/1772828).

Barnes, Catherine P., Charles W. Pemble, David D. Brand, David G. Simpson, and Gary L. Bowlin. 2007. "Cross-Linking Electrospun Type II Collagen Tissue Engineering Scaffolds with Carbodiimide in Ethanol." *Tissue Engineering* 13(7):1593–1605. Retrieved January 16, 2017 (http://www.liebertonline.com/doi/abs/10.1089/ten.2006.0292).

Barnes, Catherine P., Scott A. Sell, Eugene D. Boland, David G. Simpson, and Gary L. Bowlin. 2007. "Nanofiber Technology: Designing the next Generation of Tissue Engineering Scaffolds." *Advanced Drug Delivery Reviews* 59(14):1413–33. Retrieved January 16, 2017 (http://www.ncbi.nlm.nih.gov/pubmed/17916396).

Bauer, Amy L., Trachette L. Jackson, and Yi Jiang. 2009. "Topography of Extracellular Matrix Mediates Vascular Morphogenesis and Migration Speeds in Angiogenesis." *PLoS computational biology* 5(7):e1000445. Retrieved November 16, 2016 (http://www.ncbi.nlm.nih.gov/pubmed/19629173).

Beglova, Natalia, Stephen C. Blacklow, Junichi Takagi, and Timothy A. Springer. 2002. "Cysteine-Rich Module Structure Reveals a Fulcrum for Integrin Rearrangement upon Activation." *Nature Structural Biology* 9(4):282–87. Retrieved January 13, 2017

(http://www.ncbi.nlm.nih.gov/pubmed/11896403).

Belkin, Alexey M. and Mary Ann Stepp. 2000. “Integrins as Receptors for Laminins.” *Microscopy Research and Technique* 51(3):280–301. Retrieved December 12, 2016 (http://www.ncbi.nlm.nih.gov/pubmed/11054877).

Bergsma, E. J., F. R. Rozema, R. R. Bos, and W. C. de Bruijn. 1993. “Foreign Body Reactions to Resorbable poly(L-Lactide) Bone Plates and Screws Used for the Fixation of Unstable Zygomatic Fractures.” *Journal of oral and maxillofacial surgery : official journal of the American Association of Oral and Maxillofacial Surgeons* 51(6):666–70. Retrieved January 16, 2017 (http://www.ncbi.nlm.nih.gov/pubmed/8492205).

Bettinger, Christopher J., Robert Langer, and Jeffrey T. Borenstein. 2009. “Engineering Substrate Topography at the Micro- and Nanoscale to Control Cell Function.” *Angewandte Chemie (International ed. in English)* 48(30):5406–15. Retrieved November 16, 2016 (http://www.ncbi.nlm.nih.gov/pubmed/19492373).

Bhattacharya, R. et al. 2009. “Recruitment of Vimentin to the Cell Surface by 3 Integrin and Plectin Mediates Adhesion Strength.” *Journal of Cell Science* 122(9):1390–1400. Retrieved January 13, 2017 (http://www.ncbi.nlm.nih.gov/pubmed/19366731).

Bhattarai, Shanta Raj et al. 2004. “Novel Biodegradable Electrospun Membrane: Scaffold for Tissue Engineering.” *Biomaterials* 25(13):2595–2602. (http://www.sciencedirect.com/science/article/pii/S0142961203007816)

Bingham, R. J. et al. 2008. “Crystal Structures of Fibronectin-Binding Sites from Staphylococcus Aureus FnBPA in Complex with Fibronectin Domains.” *Proceedings of the National Academy of Sciences* 105(34):12254–58. Retrieved January 10, 2017 (http://www.ncbi.nlm.nih.gov/pubmed/18713862).

Blond, David et al. 2008. “Strong, Tough, Electrospun Polymer-Nanotube Composite Membranes with Extremely Low Density.” *Advanced Functional Materials* 18(17):2618–24. Retrieved January 16, 2017 (http://doi.wiley.com/10.1002/adfm.200701487).

Bork, P. and R. F. Doolittle. 1992. “Proposed Acquisition of an Animal Protein Domain by Bacteria.” *Proceedings of the National Academy of Sciences of the United States of America* 89(19):8990–94. Retrieved January 2, 2017 (http://www.ncbi.nlm.nih.gov/pubmed/1409594).

Boyle, John. 2005. “Lehninger Principles of Biochemistry (4th Ed.): Nelson, D., and Cox, M.” *Biochemistry and Molecular Biology Education* 33(1):74–75. Retrieved January 20, 2017 (http://doi.wiley.com/10.1002/bmb.2005.494033010419).

Brandenberger, R. et al. 2001. “Identification and Characterization of a Novel Extracellular Matrix Protein Nephronectin That Is Associated with Integrin alpha8beta1 in the Embryonic Kidney.” *The Journal of cell biology* 154(2):447–58. Retrieved January 13, 2017 (http://www.ncbi.nlm.nih.gov/pubmed/11470831).

Buchko, Christopher J., Loui C. Chen, Yu Shen, and David C. Martin. 1999. “Processing and

Microstructural Characterization of Porous Biocompatible Protein Polymer Thin Films." *Polymer* 40(26):7397–7407. Retrieved October 11, 2016 (http://linkinghub.elsevier.com/retrieve/pii/S0032386198008660).

Bülow, Hannes E. and Oliver Hobert. 2006. "The Molecular Diversity of Glycosaminoglycans Shapes Animal Development." *Annual Review of Cell and Developmental Biology* 22(1):375–407. Retrieved January 12, 2017 (http://www.annualreviews.org/doi/10.1146/annurev.cellbio.22.010605.093433).

Burger, Christian, Benjamin S. Hsiao, and Benjamin Chu. 2006. "Nanofibrous Materials and Their Applications." *Annual Review of Materials Research* 36(1):333–68. Retrieved January 16, 2017 (http://www.annualreviews.org/doi/10.1146/annurev.matsci.36.011205.123537).

Calvete, Juan J. et al. 2005. "Snake Venom Disintegrins: Evolution of Structure and Function." *Toxicon* 45(8):1063–74. Retrieved January 13, 2017 (http://www.ncbi.nlm.nih.gov/pubmed/15922775).

Campbell, Iain D. and Martin J. Humphries. 2011. "Integrin Structure, Activation, and Interactions." *Cold Spring Harbor perspectives in biology* 3(3). Retrieved October 30, 2012 (http://www.ncbi.nlm.nih.gov/pubmed/21421922).

Carman, Christopher V and Timothy A. Springer. 2003. "Integrin Avidity Regulation: Are Changes in Affinity and Conformation Underemphasized?" *Current Opinion in Cell Biology* 15(5):547–56.

Chen, L. L. 1999. "Multiple Activation States of Integrin Alpha 4beta 1 Detected through Their Different Affinities for a Small Molecule Ligand." *Journal of Biological Chemistry* 274:13167–75.

Chen, Min and Kathleen L. O'Connor. 2005. "Integrin α6β4 Promotes Expression of autotaxin/ENPP2 Autocrine Motility Factor in Breast Carcinoma Cells." *Oncogene* 24(32):5125–30. Retrieved January 13, 2017 (http://www.ncbi.nlm.nih.gov/pubmed/15897878).

Chen, Victor J. and Peter X. Ma. 2004. "Nano-Fibrous poly(L-Lactic Acid) Scaffolds with Interconnected Spherical Macropores." *Biomaterials* 25(11):2065–73. Retrieved January 16, 2017 (http://www.ncbi.nlm.nih.gov/pubmed/14741621).

Cheng, M. et al. 2007. "Mutation of a Conserved Asparagine in the I-like Domain Promotes Constitutively Active Integrins Lbeta2 and IIbbeta3." *Journal of Biological Chemistry* 282(25):18225–32. Retrieved January 13, 2017 (http://www.ncbi.nlm.nih.gov/pubmed/17468108).

Chew, S. Y., Y. Wen, Y. Dzenis, and K. W. Leong. 2006. "The Role of Electrospinning in the Emerging Field of Nanomedicine." *Current pharmaceutical design* 12(36):4751–70. Retrieved January 16, 2017 (http://www.ncbi.nlm.nih.gov/pubmed/17168776).

Cho, Jaehyung and Deane F. Mosher. 2006. "Enhancement of Thrombogenesis by Plasma Fibronectin Cross-Linked to Fibrin and Assembled in Platelet Thrombi." *Blood* 107(9):3555–63. Retrieved January 10, 2017 (http://www.ncbi.nlm.nih.gov/pubmed/16391013).

Choi, Colin K. et al. 2008. "Actin and α-Actinin Orchestrate the Assembly and Maturation of Nascent

Adhesions in a Myosin II Motor-Independent Manner." *Nature Cell Biology* 10(9):1039–50. Retrieved November 24, 2016 (http://www.nature.com/doifinder/10.1038/ncb1763).

Choi, Jae Shin et al. 2004. "Effect of Organosoluble Salts on the Nanofibrous Structure of Electrospun poly(3-Hydroxybutyrate-Co-3-Hydroxyvalerate)." *International Journal of Biological Macromolecules* 34(4):249–56.

Choi, Jin San, Sang Jin Lee, George J. Christ, Anthony Atala, and James J. Yoo. 2008. "The Influence of Electrospun Aligned Poly(ε-Caprolactone)/collagen Nanofiber Meshes on the Formation of Self-Aligned Skeletal Muscle Myotubes." *Biomaterials* 29(19):2899–2906. Retrieved January 16, 2017 (http://www.ncbi.nlm.nih.gov/pubmed/18400295).

Christopher, R. A., A. P. Kowalczyk, and P. J. McKeown-Longo. 1997. "Localization of Fibronectin Matrix Assembly Sites on Fibroblasts and Endothelial Cells." *Journal of Cell Science* 110(5).

Clark, Richard A. 1989. "Fibronectin." *Cell* 59(5):775–76. Retrieved January 2, 2017 (http://linkinghub.elsevier.com/retrieve/pii/0092867489905990).

Coelho, N. M., V. Llopis-Hernández, M. Salmerón-Sánchez, and G. Altankov. 2016. "Dynamic Reorganization and Enzymatic Remodeling of Type IV Collagen at Cell–Biomaterial Interface." Pp. 81–104 in *Advances in protein chemistry and structural biology*, vol. 105. Retrieved January 16, 2017 (http://www.ncbi.nlm.nih.gov/pubmed/27567485).

Coelho, N.Miranda, C. González-García, J. A. Planell, M. Salmerón-Sánchez, and G. Altankov. 2010. "Different Assembly of Type Iv Collagen on Hydrophilic and Hydrophobic Substrata Alters Endothelial Cells Interaction." *European Cells and Materials* 19(1112):262–72.

Coelho, Nuno Miranda et al. 2013. "Fibroblasts Remodeling of Type IV Collagen at a Biomaterials Interface." *Biomaterials Science* 1(5):494. Retrieved January 24, 2017 (http://xlink.rsc.org/?DOI=c3bm00163f).

Coelho, Nuno Miranda, Cristina González-García, Manuel Salmerón-Sánchez, and George Altankov. 2011. "Arrangement of Type IV Collagen on NH2 and COOH Functionalized Surfaces." *Biotechnology and Bioengineering* 108(12):3009–18. Retrieved January 24, 2017 (http://doi.wiley.com/10.1002/bit.23265).

Collier, I. E. et al. 1988. "H-Ras Oncogene-Transformed Human Bronchial Epithelial Cells (TBE-1) Secrete a Single Metalloprotease Capable of Degrading Basement Membrane Collagen." *The Journal of biological chemistry* 263(14):6579–87. Retrieved January 2, 2017 (http://www.ncbi.nlm.nih.gov/pubmed/2834383).

Cooley, John F. 1899. "Electrical Method of Dispersing Fluids."

Cox, Thomas R. and Janine T. Erler. 2011. "Remodeling and Homeostasis of the Extracellular Matrix: Implications for Fibrotic Diseases and Cancer." *Disease models & mechanisms* 4(2):165–78. Retrieved August 4, 2012 (http://www.pubmedcentral.nih.gov/articlerender.fcgi?artid=3046088&tool=pmcentrez&rendertype=abstract).

Cukierman, E., R. Pankov, D. R. Stevens, and K. M. Yamada. 2001. “Taking Cell-Matrix Adhesions to the Third Dimension.” *Science (New York, N.Y.)* 294(5547):1708–12. Retrieved July 17, 2012 (http://www.ncbi.nlm.nih.gov/pubmed/11721053).

Curino, Alejandro C. et al. 2005. “Intracellular Collagen Degradation Mediated by uPARAP/Endo180 Is a Major Pathway of Extracellular Matrix Turnover during Malignancy.” *The Journal of cell biology* 169(6):977–85. Retrieved November 26, 2016 (http://www.jcb.org/lookup/doi/10.1083/jcb.200411153).

Daley, WP William P., SB Sarah B. Peters, and Melinda Larsen. 2008. “Extracellular Matrix Dynamics in Development and Regenerative Medicine.” *Journal of cell science* 121(Pt 3):255–64. Retrieved November 9, 2012 (http://www.ncbi.nlm.nih.gov/pubmed/18216330).

Darribère, T. et al. 1990. “In Vivo Analyses of Integrin Beta 1 Subunit Function in Fibronectin Matrix Assembly.” *The Journal of cell biology* 110(5):1813–23. Retrieved January 10, 2017 (http://www.ncbi.nlm.nih.gov/pubmed/2186050).

Davies, Jamie A. 2001. “Extracellular Matrix.” *Encyclopedia of Life Sciences* 1–7. Retrieved (www.els.net).

Davies, P. F., A. Robotewskyj, and M. L. Griem. 1994. “Quantitative Studies of Endothelial Cell Adhesion. Directional Remodeling of Focal Adhesion Sites in Response to Flow Forces.” *The Journal of clinical investigation* 93(5):2031–38. Retrieved November 24, 2016 (http://www.ncbi.nlm.nih.gov/pubmed/8182135).

Deitzel, J. .., J. Kleinmeyer, D. Harris, and N. .. Beck Tan. 2001. “The Effect of Processing Variables on the Morphology of Electrospun Nanofibers and Textiles.” *Polymer* 42(1):261–72.

Demanèche, Sandrine, Jean-Paul Chapel, Lucile Jocteur Monrozier, and Hervé Quiquampoix. 2009. “Dissimilar pH-Dependent Adsorption Features of Bovine Serum Albumin and α-Chymotrypsin on Mica Probed by AFM.” *Colloids and Surfaces B: Biointerfaces* 70(2):226–31. Retrieved January 18, 2017 (http://www.ncbi.nlm.nih.gov/pubmed/19186036).

Dickinson, C. D. et al. 1994. “Crystal Structure of the Tenth Type III Cell Adhesion Module of Human Fibronectin.” *Journal of molecular biology* 236(4):1079–92. Retrieved January 2, 2017 (http://www.ncbi.nlm.nih.gov/pubmed/8120888).

Doolittle, Russell F. 1984. “Fibrinogen and Fibrin.” *Annual Reviews in Biochemistry* 53:195–229.

Doshi, Jayesh and Darrell H. Reneker. 1995. “Electrospinning Process and Applications of Electrospun Fibers.” *Journal of Electrostatics* 35(2):151–60.

Dvir, Tal, Brian P. Timko, Daniel S. Kohane, and Robert Langer. 2011. “Nanotechnological Strategies for Engineering Complex Tissues.” *Nature nanotechnology* 6(1):13–22. Retrieved November 8, 2013 (http://www.nature.com/doifinder/10.1038/nnano.2010.246).

Emsley, Jonas, C.Graha. Knight, Richard W. Farndale, Michael J. Barnes, and Robert C. Liddington. 2000. “Structural Basis of Collagen Recognition by Integrin α2β1.” *Cell* 101(1):47–56. Retrieved January 13, 2017 (http://www.ncbi.nlm.nih.gov/pubmed/10778855).

Esemuede, Nowokere, Taeseung Lee, Daphne Pierre-Paul, Bauer E. Sumpio, and Vivian Gahtan. 2004. "The Role of Thrombospondin-1 in Human disease1." *Journal of Surgical Research* 122(1):135–42. Retrieved January 11, 2017 (http://www.ncbi.nlm.nih.gov/pubmed/15522326).

Felding-Habermann, B. and D. A. Cheresh. 1993. "Vitronectin and Its Receptors." *Current opinion in cell biology* 5(5):864–68. Retrieved January 11, 2017 (http://www.ncbi.nlm.nih.gov/pubmed/7694604).

Ffrench-Constant, C. 1995. "Alternative Splicing of Fibronectin—Many Different Proteins but Few Different Functions." *Experimental Cell Research* 221(2):261–71. Retrieved January 2, 2017 (http://www.ncbi.nlm.nih.gov/pubmed/7493623).

van der Flier, A. and A. Sonnenberg. 2001. "Function and Interactions of Integrins." *Cell and tissue research* 305(3):285–98. Retrieved January 13, 2017 (http://www.ncbi.nlm.nih.gov/pubmed/11572082).

Formhals, Anton. 1934. "Process and Apparatus for Preparing Artificial Threads."

Fox, J. W. et al. 1991. "Recombinant Nidogen Consists of Three Globular Domains and Mediates Binding of Laminin to Collagen Type IV." *The EMBO journal* 10(11):3137–46. Retrieved December 12, 2016 (http://www.ncbi.nlm.nih.gov/pubmed/1717261).

Friedland, J. C., M. H. Lee, and D. Boettiger. 2009. "Mechanically Activated Integrin Switch Controls 5 1 Function." *Science* 323(5914):642–44. Retrieved January 13, 2017 (http://www.ncbi.nlm.nih.gov/pubmed/19179533).

Friess, Wolfgang and Monika Schlapp. 2006. "Sterilization of Gentamicin Containing collagen/PLGA Microparticle Composites." *European Journal of Pharmaceutics and Biopharmaceutics* 63(2):176–87.

Fukuda, Tomohiko et al. 2002. "Mice Lacking the EDB Segment of Fibronectin Develop Normally but Exhibit Reduced Cell Growth and Fibronectin Matrix Assembly in Vitro." *Cancer Research* 62(19).

García, Andrés J. 2006. "Interfaces to Control Cell-Biomaterial Adhesive Interactions." Pp. 171–90 in *Polymers for Regenerative Medicine*. Berlin/Heidelberg: Springer-Verlag. Retrieved January 20, 2017 (http://link.springer.com/10.1007/12_071).

Geiger, Benjamin, Joachim P. Spatz, and Alexander D. Bershadsky. 2009. "Environmental Sensing through Focal Adhesions." *Nature reviews. Molecular cell biology* 10(1):21–33. Retrieved November 23, 2016 (http://www.nature.com/doifinder/10.1038/nrm2593).

Geiger, Benjamin and Kenneth M. Yamada. 2011. "Molecular Architecture and Function of Matrix Adhesions." *Cold Spring Harbor perspectives in biology* 3(5). Retrieved July 13, 2012 (http://www.ncbi.nlm.nih.gov/pubmed/21441590).

Gholipour Kanani, A., S.Hajir Bahrami, A. Gholipour Kanani, and S.Hajir Bahrami. 2011. "Effect of Changing Solvents on Poly(-Caprolactone) Nanofibrous Webs Morphology." *Journal of Nanomaterials* 2011:1–10. Retrieved October 11, 2016

(http://www.hindawi.com/journals/jnm/2011/724153/).

Gimona, Mario, Roberto Buccione, Sara A. Courtneidge, and Stefan Linder. 2008. “Assembly and Biological Role of Podosomes and Invadopodia.” *Current Opinion in Cell Biology* 20(2):235–41. Retrieved November 24, 2016 (http://linkinghub.elsevier.com/retrieve/pii/S0955067408000148).

Givant-Horwitz, Vered, Ben Davidson, and Reuven Reich. 2005. “Laminin-Induced Signaling in Tumor Cells.” *Cancer Letters* 223(1):1–10. Retrieved December 12, 2016 (http://www.ncbi.nlm.nih.gov/pubmed/15890231).

Gorkun, O. V, Y. I. Veklich, L. V Medved, A. H. Henschen, and J. W. Weisel. 1994. “Role of the Alpha C Domains of Fibrin in Clot Formation.” *Biochemistry* 33(22):6986–97. Retrieved January 12, 2017 (http://www.ncbi.nlm.nih.gov/pubmed/8204632).

Greiner, Andreas and Joachim H. Wendorff. 2007. “Electrospinning: A Fascinating Method for the Preparation of Ultrathin Fibers.” *Angewandte Chemie International Edition* 46(30):5670–5703. Retrieved January 16, 2017 (http://doi.wiley.com/10.1002/anie.200604646).

Grinnell, F. 1986. “Focal Adhesion Sites and the Removal of Substratum-Bound Fibronectin.” *The Journal of cell biology* 103(6 Pt 2):2697–2706. Retrieved (http://www.pubmedcentral.nih.gov/articlerender.fcgi?artid=2114597&tool=pmcentrez&rendertype=abstract).

Gugutkov, D., G. Altankov, J. C. Rodríguez Hernández, M. Monleón Pradas, and M. Salmerón-Sánchez. 2010. “Fibronectin Activity on Substrates with Controlled --OH Density.” *Journal of biomedical materials research. Part A* 92(1):322–31. Retrieved April 19, 2012 (http://www.ncbi.nlm.nih.gov/pubmed/19189388).

Gugutkov, D., C. Gonzalez-Garcia, G. Altankov, and M. Salmeron-Sanchez. 2011. “Fibrinogen Organization at the Cell-Material Interface Directs Endothelial Cell Behavior.” *Journal of Bioactive and Compatible Polymers* 26(4):375–87. Retrieved April 4, 2012 (http://jbc.sagepub.com/cgi/doi/10.1177/0883911511409020).

Gugutkov, D., J. Gustavsson, M. Cantini, M. Salmeron-Sánchez, and G. Altankov. 2016. “Electrospun Fibrinogen-PLA Nanofibres for Vascular Tissue Engineering.” *Journal of tissue engineering and regenerative medicine*. Retrieved September 23, 2016 (http://www.ncbi.nlm.nih.gov/pubmed/27238477).

Gugutkov, Dencho, Cristina González-García, Jose Carlos Rodríguez Hernández, George Altankov, and Manuel Salmerón-Sánchez. 2009. “Biological Activity of the Substrate-Induced Fibronectin Network: Insight into the Third Dimension through Electrospun Fibers.” *Langmuir : the ACS journal of surfaces and colloids* 25(18):10893–900. Retrieved May 1, 2012 (http://www.ncbi.nlm.nih.gov/pubmed/19735141).

Gugutkov, Dencho, Johan Gustavsson, Maria Pau Ginebra, and George Altankov. 2013. “Fibrinogen Nanofibers for Guiding Endothelial Cell Behavior.” *Biomaterials Science*. Retrieved

July 23, 2013 (http://xlink.rsc.org/?DOI=c3bm60124b).

Gustavsson, Johan et al. 2008. “Surface Modifications of Silicon Nitride for Cellular Biosensor Applications.” *Journal of Materials Science: Materials in Medicine* 19(4):1839–50. Retrieved November 26, 2016 (http://link.springer.com/10.1007/s10856-008-3384-7).

Haider, Adnan, Sajjad Haider, and Inn Kyu Kang. 2015. “A Comprehensive Review Summarizing the Effect of Electrospinning Parameters and Potential Applications of Nanofibers in Biomedical and Biotechnology.” *Arabian Journal of Chemistry*. Retrieved (http://dx.doi.org/10.1016/j.arabjc.2015.11.015).

Haider, Sajjad et al. 2013. “Highly Aligned Narrow Diameter Chitosan Electrospun Nanofibers.” *Journal of Polymer Research* 20(4):105. Retrieved October 11, 2016 (http://link.springer.com/10.1007/s10965-013-0105-9).

Hall, C. E. and H. S. Slayter. 1959. “The Fibrinogen Molecule: Its Size, Shape, and Mode of Polymerization.” *The Journal of biophysical and biochemical cytology* 5(1):11–16. Retrieved January 12, 2017 (http://www.ncbi.nlm.nih.gov/pubmed/13630928).

Hantgan, R. R., P. J. Simpson-Haidaris, C. W. Francis, and V. J. Marder. 2000. “Fibrinogen Structure and Physiology.” Pp. 203–232 in *Hemostasis and Thrombosis: Basic Principles and Clinical Practice*, edited by R.W. Colman, J. Hirsh, V.J. Marder, A.W. Clowes, and J.N. George. Philadelphia: Lippincott, Williams & Wilkins. Retrieved January 12, 2017 (https://books.google.es/books?hl=bg&lr=&id=tG4-BdaCGAUC&oi=fnd&pg=PT65&dq=Fibrinogen+structure+and+physiology.+In+‘“Hemostasis+and+Thrombosis:+Basic+Principles+and+Clinical+Practice”&ots=jDPtISkH8b&sig=YQZqkBLRf3eWPJD7OpnVYVPza6s#v).

Harburger, David S. and David A. Calderwood. 2009. “Integrin Signalling at a Glance.” *Journal of cell science* 122(2):159–63. Retrieved November 24, 2016 (http://jcs.biologists.org/cgi/doi/10.1242/jcs.018093).

Hartgerink, J. D., E. Beniash, and S. I. Stupp. 2001. “Self-Assembly and Mineralization of Peptide-Amphiphile Nanofibers.” *Science* 294(5547):1684–88. Retrieved January 16, 2017 (http://www.ncbi.nlm.nih.gov/pubmed/11721046).

Hartgerink, J. D., E. Beniash, and S. I. Stupp. 2002. “Peptide-Amphiphile Nanofibers: A Versatile Scaffold for the Preparation of Self-Assembling Materials.” *Proceedings of the National Academy of Sciences* 99(8):5133–38. Retrieved January 16, 2017 (http://www.ncbi.nlm.nih.gov/pubmed/11929981).

Hato, T., J. Yamanouchi, Y. Yakushijin, I. Sakail, and M. Yasukawa. 2006. “Identification of Critical Residues for Regulation of Integrin Activation in the beta6-alpha7 Loop of the Integrin beta3 I-like Domain.” *Journal of Thrombosis and Haemostasis* 4(10):2278–80. Retrieved January 13, 2017 (http://www.ncbi.nlm.nih.gov/pubmed/16863536).

Hauck, Christof R., Franziska Agerer, Petra Muenzner, and Tim Schmitter. 2006. “Cellular Adhesion

Molecules as Targets for Bacterial Infection." *European Journal of Cell Biology* 85(3):235–42.

Henschen, Agnes and Jan Mcdonagh. 1986. "Chapter 7 Fibrinogen, Fibrin and Factor XIII." *New Comprehensive Biochemistry* 13:171–241.

Hirano, H. et al. 1983. "Isolation of Genomic DNA Clones Spanning the Entire Fibronectin Gene." *Proceedings of the National Academy of Sciences of the United States of America* 80(1):46–50. Retrieved January 2, 2017 (http://www.ncbi.nlm.nih.gov/pubmed/6572007).

Hodde, Jason P., Stephen F. Badylak, Andrew O. Brightman, and Sherry L. Voytik-Harbin. 1996. "Glycosaminoglycan Content of Small Intestinal Submucosa: A Bioscaffold for Tissue Replacement." *Tissue Engineering* 2(3):209–17. Retrieved January 12, 2017 (http://www.ncbi.nlm.nih.gov/pubmed/19877943).

Honda, S. et al. 2009. "Integrin-Linked Kinase Associated with Integrin Activation." *Blood* 113(21):5304–13. Retrieved January 13, 2017 (http://www.ncbi.nlm.nih.gov/pubmed/19299337).

Huan, Siqi et al. 2015. "Effect of Experimental Parameters on Morphological, Mechanical and Hydrophobic Properties of Electrospun Polystyrene Fibers." *Materials* 8(5):2718–34. Retrieved October 11, 2016 (http://www.mdpi.com/1996-1944/8/5/2718/).

Huang, Jeffrey and Vivian Lee. 2005. "Identification and Characterization of a Novel Human Nephronectin Gene in Silico." *International journal of molecular medicine* 15(4):719–24. Retrieved January 13, 2017 (http://www.ncbi.nlm.nih.gov/pubmed/15754038).

Huang, Y. X., J. Ren, C. Chen, T. B. Ren, and X. Y. Zhou. 2008. "Preparation and Properties of Poly(lactide-Co-Glycolide) (PLGA)/ Nano-Hydroxyapatite (NHA) Scaffolds by Thermally Induced Phase Separation and Rabbit MSCs Culture on Scaffolds." *Journal of Biomaterials Applications* 22(5):409–32.

Hubbell, Jeffrey a. 2007. *Matrix Effects*. Fourth Edi. Elsevier. Retrieved (http://dx.doi.org/10.1016/B978-0-12-398358-9.00021-5).

Hudson, Billy G., Karl Tryggvason, Munirathinam Sundaramoorthy, and Eric G. Neilson. 2003. "Alport's Syndrome, Goodpasture's Syndrome, and Type IV Collagen." *New England Journal of Medicine* 348(25):2543–56. Retrieved November 22, 2016 (http://www.nejm.org/doi/abs/10.1056/NEJMra022296).

Humphries, Jonathan D., Adam Byron, and Martin J. Humphries. 2006. "Integrin Ligands at a Glance." *Journal of cell science* 119(Pt 19):3901–3. Retrieved November 5, 2012 (http://www.ncbi.nlm.nih.gov/pubmed/16988024).

Humphries, M. J. 2000. "Integrin Structure." *Biochemical Society transactions* 28(4):311–39. Retrieved (http://www.ncbi.nlm.nih.gov/pubmed/11078733).

Humphries, Martin J., Emlyn J. H. Symonds, and A.Paul Mould. 2003. "Mapping Functional Residues onto Integrin Crystal Structures." *Current opinion in structural biology* 13(2):236–43. Retrieved January 12, 2017 (http://www.ncbi.nlm.nih.gov/pubmed/12727518).

Hynes, R. O.Richard O. et al. 2002. “Integrins: Bidirectional, Allosteric Signaling Machines.” *Cell* 110(6):673–87. Retrieved November 26, 2016 (http://www.ncbi.nlm.nih.gov/pubmed/12297042).

Hynes, Richard O. 1990. *Fibronectins*. New York, NY: Springer New York. Retrieved January 2, 2017 (http://link.springer.com/10.1007/978-1-4612-3264-3).

Hynes, Richard O. 2009. “The Extracellular Matrix: Not Just Pretty Fibrils.” *Science (New York, N.Y.)* 326(5957):1216–19. Retrieved July 24, 2012 (http://www.ncbi.nlm.nih.gov/pubmed/19965464).

Ido, H. et al. 2007. “The Requirement of the Glutamic Acid Residue at the Third Position from the Carboxyl Termini of the Laminin Chains in Integrin Binding by Laminins.” *Journal of Biological Chemistry* 282(15):11144–54. Retrieved January 13, 2017 (http://www.ncbi.nlm.nih.gov/pubmed/17307733).

Inai, Ryuji et al. 2005. “Structure and Properties of Electrospun PLLA Single Nanofibres.” *Nanotechnology* 16(2):208–13. Retrieved January 16, 2017 (http://stacks.iop.org/0957-4484/16/i=2/a=005?key=crossref.71dfd21f62b0d37e32abfd5d09e09dfb).

Iozzo, Renato V. and Liliana Schaefer. 2015. “Proteoglycan Form and Function: A Comprehensive Nomenclature of Proteoglycans.” *Matrix Biology* 42:11–55.

Ishiguro, Ryo et al. 2005. “Modes of Conformational Changes of Proteins Adsorbed on a Planar Hydrophobic Polymer Surface Reflecting Their Adsorption Behaviors.” *Journal of Colloid and Interface Science* 290(1):91–101.

Jarnagin, W. R., D. C. Rockey, V. E. Koteliansky, S. S. Wang, and D. M. Bissell. 1994. “Expression of Variant Fibronectins in Wound Healing: Cellular Source and Biological Activity of the EIIIA Segment in Rat Hepatic Fibrogenesis.” *The Journal of cell biology* 127(6 Pt 2):2037–48. Retrieved January 2, 2017 (http://www.ncbi.nlm.nih.gov/pubmed/7806580).

Jayaraman, Krishnan, M. Kotaki, Yanzhong Zhang, Xiumei Mo, and S. Ramakrishna. 2004. “Recent Advances in Polymer Nanofibers.” *Journal of nanoscience and nanotechnology* 4(1–2):52–65. Retrieved January 16, 2017 (http://www.ncbi.nlm.nih.gov/pubmed/15112541).

Jones, Frederick Scheetz and Peter Lloyd Jones. 2000. “The Tenascin Family of ECM Glycoproteins: Structure, Function, and Regulation during Embryonic Development and Tissue Remodeling.” *Developmental Dynamics* 218(2):235–59. Retrieved January 13, 2017 (http://www.ncbi.nlm.nih.gov/pubmed/10842355).

Keselowsky, Benjamin G., David M. Collard, and Andrés J. García. 2004. “Surface Chemistry Modulates Focal Adhesion Composition and Signaling through Changes in Integrin Binding.” *Biomaterials* 25(28):5947–54. Retrieved January 20, 2017 (http://www.ncbi.nlm.nih.gov/pubmed/15183609).

Khalili, Amelia Ahmad and Mohd Ridzuan Ahmad. 2015. “A Review of Cell Adhesion Studies for Biomedical and Biological Applications.” *International journal of molecular sciences* 16(8):18149–84. Retrieved November 17, 2016

(http://www.ncbi.nlm.nih.gov/pubmed/26251901).

Khoshnoodi, Jamshid, Jean Philippe Cartailler, Keith Alvares, Arthur Veis, and Billy G. Hudson. 2006. "Molecular Recognition in the Assembly of Collagens: Terminal Noncollagenous Domains Are Key Recognition Modules in the Formation of Triple Helical Protomers." *Journal of Biological Chemistry* 281(50):38117–21.

Khoshnoodi, Jamshid, Vadim Pedchenko, and Billy G. Hudson. 2008. "Mammalian Collagen IV." *Microscopy research and technique* 71(5):357–70. Retrieved November 22, 2016 (http://www.ncbi.nlm.nih.gov/pubmed/18219669).

Kleinman, Hynda K., Deborah Philp, and Matthew P. Hoffman. 2003. "Role of the Extracellular Matrix in Morphogenesis." *Current Opinion in Biotechnology* 14(5):526–32.

Koblinski, Jennifer E., Mamoun Ahram, and Bonnie F. Sloane. 2000. "Unraveling the Role of Proteases in Cancer." *Clinica Chimica Acta* 291(2):113–35.

Kohfeldt, Eddie, Takako Sasaki, Walter Göhring, and Rupert Timpl. 1998. "Nidogen-2: A New Basement Membrane Protein with Diverse Binding Properties." *Journal of Molecular Biology* 282(1):99–109.

Kornblihtt, A. R. et al. 1996. "The Fibronectin Gene as a Model for Splicing and Transcription Studies." *FASEB journal : official publication of the Federation of American Societies for Experimental Biology* 10(2):248–57. Retrieved January 2, 2017 (http://www.ncbi.nlm.nih.gov/pubmed/8641558).

Kosmehl, H., A. Berndt, and D. Katenkamp. 1996. "Molecular Variants of Fibronectin and Laminin: Structure, Physiological Occurrence and Histopathological Aspects." *Virchows Archiv : an international journal of pathology* 429(6):311–22. Retrieved January 2, 2017 (http://www.ncbi.nlm.nih.gov/pubmed/8982375).

Kost, C., W. Stüber, H. J. Ehrlich, H. Pannekoek, and K. T. Preissner. 1992. "Mapping of Binding Sites for Heparin, Plasminogen Activator Inhibitor-1, and Plasminogen to Vitronectin's Heparin-Binding Region Reveals a Novel Vitronectin-Dependent Feedback Mechanism for the Control of Plasmin Formation." *The Journal of biological chemistry* 267(17):12098–105. Retrieved January 10, 2017 (http://www.ncbi.nlm.nih.gov/pubmed/1376317).

Kurban, G. et al. 2008. "Collagen Matrix Assembly Is Driven by the Interaction of von Hippel–Lindau Tumor Suppressor Protein with Hydroxylated Collagen IV Alpha 2." *Oncogene* 27(7):1004–12. Retrieved November 26, 2016 (http://www.nature.com/doifinder/10.1038/sj.onc.1210709).

Kvansakul, M., M. Hopf, A. Ries, R. Timpl, and E. Hohenester. 2001. "Structural Basis for the High-Affinity Interaction of Nidogen-1 with Immunoglobulin-like Domain 3 of Perlecan." *The EMBO journal* 20(19):5342–46. Retrieved December 12, 2016 (http://www.ncbi.nlm.nih.gov/pubmed/11574465).

Lannutti, J., D. Reneker, T. Ma, D. Tomasko, and D. Farson. 2007. "Electrospinning for Tissue Engineering Scaffolds." *Materials Science and Engineering: C* 27(3):504–9. Retrieved

November 7, 2012 (http://linkinghub.elsevier.com/retrieve/pii/S0928493106001421).

Larson, R. S., A. L. Corbi, L. Berman, and T. Springer. 1989. “Primary Structure of the Leukocyte Function-Associated Molecule-1 Alpha Subunit: An Integrin with an Embedded Domain Defining a Protein Superfamily.” *The Journal of cell biology* 108(2):703–12. Retrieved January 12, 2017 (http://www.ncbi.nlm.nih.gov/pubmed/2537322).

Lawler, J. 2000. “The Functions of Thrombospondin-1 and-2.” *Current opinion in cell biology* 12(5):634–40. Retrieved January 11, 2017 (http://www.ncbi.nlm.nih.gov/pubmed/10978901).

Leckband, Deborah and Anil Prakasam. 2006. “Mechanism and Dynamics of Cadherin Adhesion.” *Annual Review of Biomedical Engineering* 8(1):259–87. Retrieved January 12, 2017 (http://www.ncbi.nlm.nih.gov/pubmed/16834557).

Leckband, Deborah and Sanjeevi Sivasankar. 2012. “Cadherin Recognition and Adhesion.” *Current Opinion in Cell Biology* 24(5):620–27. Retrieved January 12, 2017 (http://www.ncbi.nlm.nih.gov/pubmed/22770731).

Lee, J. O., L. A. Bankston, M. A. Arnaout, and R. C. Liddington. 1995. “Two Conformations of the Integrin A-Domain (I-Domain): A Pathway for Activation?” *Structure (London, England : 1993)* 3(12):1333–40. Retrieved January 24, 2017 (http://www.ncbi.nlm.nih.gov/pubmed/8747460).

Leiss, Michael, Karsten Beckmann, Amparo Girós, Mercedes Costell, and Reinhard Fässler. 2008. “The Role of Integrin Binding Sites in Fibronectin Matrix Assembly in Vivo.” *Current opinion in cell biology* 20(5):502–7. Retrieved November 1, 2012 (http://www.ncbi.nlm.nih.gov/pubmed/18586094).

Leitinger, Birgit and Erhard Hohenester. 2007. “Mammalian Collagen Receptors.” *Matrix Biology* 26(3):146–55.

Levental, Kandice R. et al. 2009. “Matrix Crosslinking Forces Tumor Progression by Enhancing Integrin Signaling.” *Cell* 139(5):891–906. Retrieved November 16, 2016 (http://www.ncbi.nlm.nih.gov/pubmed/19931152).

Li, By Dan and Younan Xia. 2004. “Electrospinning of Nanofibers : Reinventing the Wheel.” (14):1151–70.

Li, Shaohua et al. 2002. “Matrix Assembly, Regulation, and Survival Functions of Laminin and Its Receptors in Embryonic Stem Cell Differentiation.” *The Journal of cell biology* 157(7):1279–90. Retrieved December 12, 2016 (http://www.ncbi.nlm.nih.gov/pubmed/12082085).

Li, Shaohua, David Edgar, Reinhard Fässler, William Wadsworth, and Peter D. Yurchenco. 2003. “The Role of Laminin in Embryonic Cell Polarization and Tissue Organization.” *Developmental cell* 4(5):613–24. Retrieved January 24, 2017 (http://www.ncbi.nlm.nih.gov/pubmed/12737798).

Li, Wan-Ju, James A. Cooper, Robert L. Mauck, and Rocky S. Tuan. 2006. “Fabrication and Characterization of Six Electrospun Poly(α-Hydroxy Ester)-Based Fibrous Scaffolds for Tissue Engineering Applications.” *Acta Biomaterialia* 2(4):377–85. Retrieved January 16, 2017 (http://www.ncbi.nlm.nih.gov/pubmed/16765878).

Liao, Y. F., Philip J. Gotwals, Victor E. Koteliansky, Dean Sheppard, and Livingston Van De Water. 2002. "The EIIIA Segment of Fibronectin Is a Ligand for Integrins Alpha 9beta 1 and Alpha 4beta 1 Providing a Novel Mechanism for Regulating Cell Adhesion by Alternative Splicing." *Journal of Biological Chemistry* 277(17):14467–74. Retrieved January 10, 2017 (http://www.ncbi.nlm.nih.gov/pubmed/11839764).

Lin, Jinyou et al. 2012. "Biomimicry via Electrospinning." *Critical Reviews in Solid State and Materials Sciences* 37(2):94–114. Retrieved (http://www.tandfonline.com/doi/abs/10.1080/10408436.2011.627096).

Linton, James M., Gail R. Martin, and Louis F. Reichardt. 2007. "The ECM Protein Nephronectin Promotes Kidney Development via Integrin alpha8beta1-Mediated Stimulation of Gdnf Expression." *Development (Cambridge, England)* 134(13):2501–9. Retrieved January 13, 2017 (http://www.ncbi.nlm.nih.gov/pubmed/17537792).

Liu, Huinan, Elliott B. Slamovich, and Thomas J. Webster. 2006. "Less Harmful Acidic Degradation of Poly(lacticco-Glycolic Acid) Bone Tissue Engineering Scaffolds through Titania Nanoparticle Addition." *International journal of nanomedicine* 1(4):541–45. Retrieved November 15, 2016 (http://www.ncbi.nlm.nih.gov/pubmed/17722285).

Liu, Wenying, Stavros Thomopoulos, and Younan Xia. 2012. "Electrospun Nanofibers for Regenerative Medicine." *Advanced Healthcare Materials* 1(1):10–25.

Llopis-Hernández, Virginia, Patricia Rico, David Moratal, George Altankov, and Manuel Salmerón-Sánchez. 2013. "Role of Material-Driven Fibronectin Fibrillogenesis in Protein Remodeling." *BioResearch open access* 2(5):364–73. Retrieved January 19, 2017 (http://www.ncbi.nlm.nih.gov/pubmed/24083092).

Lord, Megan S., Martina H. Stenzel, Anne Simmons, and Bruce K. Milthorpe. 2006. "The Effect of Charged Groups on Protein Interactions with poly(HEMA) Hydrogels." *Biomaterials* 27(4):567–75.

Lutolf, M. P. and J. a Hubbell. 2005. "Synthetic Biomaterials as Instructive Extracellular Microenvironments for Morphogenesis in Tissue Engineering." *Nature Biotechnology* 23(1):47–55. Retrieved July 12, 2012 (http://www.nature.com/doifinder/10.1038/nbt1055).

M, Del Rosario and H. Tsai. 2015. "Annals of Hematology & Oncology The Case of a Late Bleeder Plasminogen Activator Inhibitor 1 Deficiency." 2(10).

Ma, P. X. and R. Zhang. 1999. "Synthetic Nano-Scale Fibrous Extracellular Matrix." *Journal of biomedical materials research* 46(1):60–72. Retrieved January 16, 2017 (http://www.ncbi.nlm.nih.gov/pubmed/10357136).

Ma, Peter X. 2008. "Biomimetic Materials for Tissue Engineering." *Advanced drug delivery reviews* 60(2):184–98. Retrieved July 17, 2012 (http://www.pubmedcentral.nih.gov/articlerender.fcgi?artid=2271038&tool=pmcentrez&rendertype=abstract).

Ma, Zuwei et al. 2005. “Potential of Nanofiber Matrix as Tissue-Engineering Scaffolds.” *Tissue engineering* 11(1–2):101–9. Retrieved (http://www.ncbi.nlm.nih.gov/pubmed/15738665).

Manabe, R. et al. 2008. “Transcriptome-Based Systematic Identification of Extracellular Matrix Proteins.” *Proceedings of the National Academy of Sciences* 105(35):12849–54. Retrieved January 13, 2017 (http://www.ncbi.nlm.nih.gov/pubmed/18757743).

Manabe, Ri-Ichiroh, Naoko Oh-E, Toshinaga Maeda, Tomohiko Fukuda, and Kiyotoshi Sekiguchi. 1997. “Modulation of Cell-Adhesive Activity of Fibronectin by the Alternatively Spliced EDA Segment.” *The Journal of Cell Biology* 139(1):295–307. Retrieved January 2, 2017 (http://www.jcb.org).

Maneva-Radicheva, L., U. Ebert, N. Dimoudis, and G. Altankov. 2008. “Fibroblast Remodeling of Adsorbed Collagen Type IV Is Altered in Contact with Cancer Cells.” *Histology and histopathology* 23(7):833–42. Retrieved January 16, 2017 (http://www.ncbi.nlm.nih.gov/pubmed/18437682).

Mao, Yong and Jean E. Schwarzbauer. 2005. “Fibronectin Fibrillogenesis, a Cell-Mediated Matrix Assembly Process.” *Matrix biology : journal of the International Society for Matrix Biology* 24(6):389–99. Retrieved March 7, 2012 (http://www.ncbi.nlm.nih.gov/pubmed/16061370).

Marshall, J. F. et al. 1995. “Alpha v Beta 1 Is a Receptor for Vitronectin and Fibrinogen, and Acts with Alpha 5 Beta 1 to Mediate Spreading on Fibronectin.” *Journal of Cell Science* 108(3).

Martin, Ivan et al. 2004. “The Role of Bioreactors in Tissue Engineering.” *Trends in biotechnology* 22(2):80–86. Retrieved November 14, 2016 (http://www.ncbi.nlm.nih.gov/pubmed/14757042).

Matabola, K. P. and R. M. Moutloali. 2013. “The Influence of Electrospinning Parameters on the Morphology and Diameter of Poly(vinyledene Fluoride) Nanofibers- Effect of Sodium Chloride.” *Journal of Materials Science* 48(16):5475–82. Retrieved October 11, 2016 (http://link.springer.com/10.1007/s10853-013-7341-6).

Mauck, Robert L. et al. 2009. “Engineering on the Straight and Narrow: The Mechanics of Nanofibrous Assemblies for Fiber-Reinforced Tissue Regeneration.” *Tissue Engineering Part B: Reviews* 15(2):171–93. Retrieved January 16, 2017 (http://www.liebertonline.com/doi/abs/10.1089/ten.teb.2008.0652).

McEver, R. P. and M. N. Martin. 1984. “A Monoclonal Antibody to a Membrane Glycoprotein Binds Only to Activated Platelets.” *The Journal of biological chemistry* 259(15):9799–9804. Retrieved January 13, 2017 (http://www.ncbi.nlm.nih.gov/pubmed/6746667).

McGrath, Rachel T., Emily McRae, Owen P. Smith, and James S. O’Donnell. 2010. “Platelet von Willebrand Factor - Structure, Function and Biological Importance.” *British Journal of Haematology* 148(6):834–43. Retrieved January 11, 2017 (http://www.ncbi.nlm.nih.gov/pubmed/20067560).

Mecham, Robert P., ed. 2011. *The Extracellular Matrix: An Overview*. Berlin, Heidelberg: Springer Berlin Heidelberg. Retrieved (http://link.springer.com/10.1007/978-3-642-16555-9).

Medved, L. and J. W. Weisel. 2009. “Recommendations for Nomenclature on Fibrinogen and Fibrin.” *Journal of Thrombosis and Haemostasis* 7(2):355–59.

Medved, Leonid, Tatiana Ugarova, Yuri Veklich, Nina Lukinova, and John Weisel. 1990. “Electron Microscope Investigation of the Early Stages of Fibrin Assembly.” *Journal of Molecular Biology* 216(3):503–9. Retrieved January 12, 2017 (http://www.ncbi.nlm.nih.gov/pubmed/2258925).

Meloty-Kapella, Caroline V., Martin Degen, Ruth Chiquet-Ehrismann, and Richard P. Tucker. 2008. “Effects of Tenascin-W on Osteoblasts in Vitro.” *Cell and Tissue Research* 334(3):445–55. Retrieved January 13, 2017 (http://www.ncbi.nlm.nih.gov/pubmed/18985388).

Menrad, Andreas and Hans D. Menssen. 2005. “ED-B Fibronectin as a Target for Antibody-Based Cancer Treatments.” *Expert Opinion on Therapeutic Targets* 9(3):491–500. Retrieved January 2, 2017 (http://www.tandfonline.com/doi/full/10.1517/14728222.9.3.491).

Michael, Kristin E. et al. 2003. “Adsorption-Induced Conformational Changes in Fibronectin Due to Interactions with Well-Defined Surface Chemistries.” *Langmuir* 19(19):8033–8040.

Midwood, K. S. and Jean E. Schwarzbauer. 2002. “Tenascin-C Modulates Matrix Contraction via Focal Adhesion Kinase- and Rho-Mediated Signaling Pathways.” *Molecular Biology of the Cell* 13(10):3601–13. Retrieved January 13, 2017 (http://www.ncbi.nlm.nih.gov/pubmed/12388760).

Minton, A. P. 2001. “Effects of Excluded Surface Area and Adsorbate Clustering on Surface Adsorption of Proteins. II. Kinetic Models.” *Biophysical journal* 80(4):1641–48. Retrieved January 19, 2017 (http://www.ncbi.nlm.nih.gov/pubmed/11259279).

Moffat, Kristen L. et al. 2009. “Novel Nanofiber-Based Scaffold for Rotator Cuff Repair and Augmentation.” *Tissue Engineering Part A* 15(1):115–26. Retrieved January 16, 2017 (http://www.ncbi.nlm.nih.gov/pubmed/18788982).

Mohamed, Mona Mostafa and Bonnie F. Sloane. 2006. “Cysteine Cathepsins: Multifunctional Enzymes in Cancer.” *Nature Reviews Cancer* 6(10):764–75. Retrieved November 26, 2016 (http://www.nature.com/doifinder/10.1038/nrc1949).

Morrison, Peter R., John T. Edsall, and Susan G. Miller. 1948. “Preparation and Properties of Serum and Plasma Proteins. XVIII. The Separation of Purified Fibrinogen from Fraction I of Human Plasma.” *Journal of the American Chemical Society* 70(9):3103–8. Retrieved January 2, 2017 (http://pubs.acs.org/doi/abs/10.1021/ja01189a080).

Morton, William James. 1900. “Method of Dispersing Fluids.”

Mosesson, M. W. and R. A. Umfleet. 1970. “The Cold-I & Oluble Globulin of Human Plasma.” *The Journal of biological chemistry* 245(21):5728–36. Retrieved January 2, 2017 (http://www.ncbi.nlm.nih.gov/pubmed/4097343).

Mosher, Deane F. 1990. “Physiology of Thrombospondin.” *Annual Review of Medicine* 41(1):85–97. Retrieved January 11, 2017 (http://www.ncbi.nlm.nih.gov/pubmed/1691903).

Mosher, Deane F., Jane Sottile, Chuanyue Wu, and John A. McDonald. 1992. “Assembly of Extracellular Matrix.” *Current Opinion in Cell Biology* 4(5):810–18.

Mould, A. P. et al. 2003. “Structure of an Integrin-Ligand Complex Deduced from Solution X-Ray Scattering and Site-Directed Mutagenesis.” *Journal of Biological Chemistry* 278(41):39993–99. Retrieved January 13, 2017 (http://www.ncbi.nlm.nih.gov/pubmed/12871973).

Moyano, J. V et al. 1997. “Fibronectin Type III5 Repeat Contains a Novel Cell Adhesion Sequence, KLDAPT, Which Binds Activated alpha4beta1 and alpha4beta7 Integrins.” *The Journal of biological chemistry* 272(40):24832–36. Retrieved January 10, 2017 (http://www.ncbi.nlm.nih.gov/pubmed/9312081).

Myllyharju, Johanna and Kari I. Kivirikko. 2004. “Collagens, Modifying Enzymes and Their Mutations in Humans, Flies and Worms.” *Trends in Genetics* 20(1):33–43.

Na, Haining, Qunying Li, Hua Sun, Ci Zhao, and Xiaoyan Yuan. 2009. “Anisotropic Mechanical Properties of Hot-Pressed PVDF Membranes with Higher Fiber Alignments via Electrospinning.” *Polymer Engineering & Science* 49(7):1291–98. Retrieved January 16, 2017 (http://doi.wiley.com/10.1002/pen.21368).

Nievers, Mirjam G., Roel Q. J. Schaapveld, and Arnoud Sonnenberg. 1999. “Biology and Function of Hemidesmosomes.” *Matrix Biology* 18(1):5–17.

Nisbet, David R., Kylie E. Crompton, Malcolm K. Horne, David I. Finkelstein, and John S. Forsythe. 2008. “Neural Tissue Engineering of the CNS Using Hydrogels.” *Journal of Biomedical Materials Research Part B: Applied Biomaterials* 87B(1):251–63. Retrieved January 16, 2017 (http://www.ncbi.nlm.nih.gov/pubmed/18161806).

Nishida, Noritaka et al. 2006. “Activation of Leukocyte β2 Integrins by Conversion from Bent to Extended Conformations.” *Immunity* 25(4):583–94. Retrieved January 13, 2017 (http://www.ncbi.nlm.nih.gov/pubmed/17045822).

Nishimura, S. L., D. Sheppard, and R. Pytela. 1994. “Integrin Alpha v Beta 8. Interaction with Vitronectin and Functional Divergence of the Beta 8 Cytoplasmic Domain.” *The Journal of biological chemistry* 269(46):28708–15. Retrieved January 11, 2017 (http://www.ncbi.nlm.nih.gov/pubmed/7525578).

Noh, Hyeran and Erwin A. Vogler. 2006. “Volumetric Interpretation of Protein Adsorption: Mass and Energy Balance for Albumin Adsorption to Particulate Adsorbents with Incrementally Increasing Hydrophilicity.” *Biomaterials* 27(34):5801–12. Retrieved January 20, 2017 (http://www.ncbi.nlm.nih.gov/pubmed/16928398).

Noh, Hyeran and Erwin A. Vogler. 2007. “Volumetric Interpretation of Protein Adsorption: Competition from Mixtures and the Vroman Effect.” *Biomaterials* 28(3):405–22. Retrieved January 18, 2017 (http://www.ncbi.nlm.nih.gov/pubmed/17007920).

O’Brien, Fergal J. 2011. “Biomaterials & Scaffolds for Tissue Engineering.” *Materials Today* 14(3):88–95. Retrieved (http://dx.doi.org/10.1016/S1369-7021(11)70058-X).

O’Leary, J. M. et al. 2004. “Solution Structure and Dynamics of a Prototypical Chordin-like Cysteine-Rich Repeat (von Willebrand Factor Type C Module) from Collagen IIA.” *Journal of Biological*

Chemistry 279(51):53857–66. Retrieved January 2, 2017 (http://www.ncbi.nlm.nih.gov/pubmed/15466413).

Orend, Gertraud and Ruth Chiquet-Ehrismann. 2000. "Adhesion Modulation by Antiadhesive Molecules of the Extracellular Matrix." *Experimental Cell Research* 261(1):104–10. Retrieved January 13, 2017 (http://www.ncbi.nlm.nih.gov/pubmed/11082280).

Ott, Harald C. et al. 2008. "Perfusion-Decellularized Matrix: Using Nature's Platform to Engineer a Bioartificial Heart." *Nature medicine* 14(2):213–21. Retrieved July 12, 2012 (http://www.ncbi.nlm.nih.gov/pubmed/18193059).

Oxvig, C. and T. A. Springer. 1998. "Experimental Support for a Beta-Propeller Domain in Integrin Alpha-Subunits and a Calcium Binding Site on Its Lower Surface." *Proceedings of the National Academy of Sciences of the United States of America* 95(9):4870–75. Retrieved January 12, 2017 (http://www.ncbi.nlm.nih.gov/pubmed/9560195).

Ozhogina, O. A., M. Trexler, L. Bányai, M. Llinás, and L. Patthy. 2001. "Origin of Fibronectin Type II (FN2) Modules: Structural Analyses of Distantly-Related Members of the Kringle Family Idey the Kringle Domain of Neurotrypsin as a Potential Link between FN2 Domains and Kringles." *Protein science : a publication of the Protein Society* 10(10):2114–22. Retrieved January 2, 2017 (http://www.ncbi.nlm.nih.gov/pubmed/11567102).

Page-McCaw, Andrea, Andrew J. Ewald, and Zena Werb. 2007. "Matrix Metalloproteinases and the Regulation of Tissue Remodelling." *Nature reviews. Molecular cell biology* 8(3):221–33. Retrieved November 26, 2016 (http://www.ncbi.nlm.nih.gov/pubmed/17318226).

Palumbo, R.Noelle and Chun Wang. 2006. "Bacterial Invasin: Structure, Function, and Implication for Targeted Oral Gene Delivery." *Current drug delivery* 3(1):47–53. Retrieved January 13, 2017 (http://www.ncbi.nlm.nih.gov/pubmed/16472093).

Pankov, R. et al. 2000. "Integrin Dynamics and Matrix Assembly: Tensin-Dependent Translocation of alpha(5)beta(1) Integrins Promotes Early Fibronectin Fibrillogenesis." *The Journal of cell biology* 148(5):1075–90. Retrieved November 24, 2016 (http://www.ncbi.nlm.nih.gov/pubmed/10704455).

Pankov, R. 2002. "Fibronectin at a Glance." *Journal of Cell Science* 115(20):3861–63. Retrieved March 7, 2012 (http://jcs.biologists.org/cgi/doi/10.1242/jcs.00059).

Pankov, Roumen and Albena Momchilova. 2010. "Cell Adhesions and Signaling: A Tool for Biocompatibility Assessment." Pp. 1–17 in. Springer Netherlands. Retrieved November 24, 2016 (http://link.springer.com/10.1007/978-90-481-8790-4_1).

Paul, J. I. and R. O. Hynes. 1984. "Multiple Fibronectin Subunits and Their Post-Translational Modifications." *The Journal of biological chemistry* 259(21):13477–87. Retrieved January 2, 2017 (http://www.ncbi.nlm.nih.gov/pubmed/6490662).

Pelipenko, Jan, Julijana Kristl, Biljana Janković, Saša Baumgartner, and Petra Kocbek. 2013. "The Impact of Relative Humidity during Electrospinning on the Morphology and Mechanical

Properties of Nanofibers." *International Journal of Pharmaceutics* 456(1):125–34.

Phelps, Edward A., Natalia Landázuri, Peter M. Thulé, W.Robert Taylor, and Andrés J. García. 2010. "Bioartificial Matrices for Therapeutic Vascularization." *Proceedings of the National Academy of Sciences of the United States of America* 107(8):3323–28. Retrieved November 15, 2016 (http://www.ncbi.nlm.nih.gov/pubmed/20080569).

Pickford, A. R. et al. 2001. "The Hairpin Structure of the (6)F1(1)F2(2)F2 Fragment from Human Fibronectin Enhances Gelatin Binding." *The EMBO journal* 20(7):1519–29. Retrieved January 2, 2017 (http://www.ncbi.nlm.nih.gov/pubmed/11285216).

Pillay, Viness et al. 2013. "A Review of the Effect of Processing Variables on the Fabrication of Electrospun Nanofibers for Drug Delivery Applications." *Journal of Nanomaterials* 2013:1–22. Retrieved October 11, 2016 (http://www.hindawi.com/journals/jnm/2013/789289/).

Place, Elsie S., Nicholas D. Evans, and Molly M. Stevens. 2009. "Complexity in Biomaterials for Tissue Engineering." *Nature materials* 8(6):457–70. Retrieved July 12, 2012 (http://www.ncbi.nlm.nih.gov/pubmed/19458646).

Plow, E. F., T. a Haas, L. Zhang, J. Loftus, and J. W. Smith. 2000. "Ligand Binding to Integrins." *The Journal of biological chemistry* 275(29):21785–88. Retrieved November 6, 2012 (http://www.ncbi.nlm.nih.gov/pubmed/10801897).

Poincloux, R., F. Lizarraga, and P. Chavrier. 2009. "Matrix Invasion by Tumour Cells: A Focus on MT1-MMP Trafficking to Invadopodia." *Journal of Cell Science* 122(17):3015–24. Retrieved November 24, 2016 (http://jcs.biologists.org/cgi/doi/10.1242/jcs.034561).

Pöschl, E. et al. 1996. "Site-Directed Mutagenesis and Structural Interpretation of the Nidogen Binding Site of the Laminin gamma1 Chain." *The EMBO journal* 15(19):5154–59. Retrieved December 12, 2016 (http://www.ncbi.nlm.nih.gov/pubmed/8895559).

Preissner, Klaus T. 1991. "Structure and Biological Role of Vitronectin." *Annual Review of Cell Biology* 7(1):275–310. Retrieved January 10, 2017 (http://www.annualreviews.org/doi/10.1146/annurev.cb.07.110191.001423).

Prime, KL and GM Whitesides. 1991. "Self-Assembled Organic Monolayers: Model Systems for Studying Adsorption of Proteins at Surfaces." *Science* 252(5009).

Privalov, P. L. and L. V Medved. 1982. "Domains in the Fibrinogen Molecule." *Journal of molecular biology* 159(4):665–83. Retrieved January 12, 2017 (http://www.ncbi.nlm.nih.gov/pubmed/7143446).

Rabe, Michael et al. 2009. "Surface-Induced Spreading Phenomenon of Protein Clusters." *Soft Matter* 5(5):1039. Retrieved January 19, 2017 (http://xlink.rsc.org/?DOI=b814053g).

Ramirez, Francesco and Lynn Y. Sakai. 2010. "Biogenesis and Function of Fibrillin Assemblies." *Cell and tissue research* 339(1):71–82. Retrieved January 12, 2017 (http://www.ncbi.nlm.nih.gov/pubmed/19513754).

Rao, S. P.Sudhakar. et al. 1991. "Fibrinogen Structure in Projection at 18 Å Resolution: Electron

Density by Co-Ordinated Cryo-Electron Microscopy and X-Ray Crystallography." *Journal of Molecular Biology* 222(1):89–98.

Reddig, Peter J. and Rudy L. Juliano. 2005. "Clinging to Life: Cell to Matrix Adhesion and Cell Survival." *Cancer and Metastasis Reviews* 24(3):425–39. Retrieved January 13, 2017 (http://link.springer.com/10.1007/s10555-005-5134-3).

Reinhardt, D. et al. 1993. "Mapping of Nidogen Binding Sites for Collagen Type IV, Heparan Sulfate Proteoglycan, and Zinc." *The Journal of biological chemistry* 268(15):10881–87. Retrieved December 12, 2016 (http://www.ncbi.nlm.nih.gov/pubmed/8496153).

Reisenauer, Anita et al. 2007. "Increased Carcinogenic Potential of Myeloid Tumor Cells Induced by Aberrant TGF-β1-Signaling and Upregulation of Cathepsin B." *Biological Chemistry* 388(6):639–50. Retrieved November 26, 2016 (http://www.degruyter.com/view/j/bchm.2007.388.issue-6/bc.2007.072/bc.2007.072.xml).

Reneker, Darrell H. et al. 1996. "Nanometre Diameter Fibres of Polymer, Produced by Electrospinning." *Nanotechnology* 7(3):216–23. Retrieved January 16, 2017 (http://stacks.iop.org/0957-4484/7/i=3/a=009?key=crossref.b62a3c509c723c5a2561f1e345fc1706).

Rhee, Sangmyung and Frederick Grinnell. 2007. "Fibroblast Mechanics in 3D Collagen Matrices." *Advanced drug delivery reviews* 59(13):1299–1305. Retrieved November 26, 2016 (http://www.ncbi.nlm.nih.gov/pubmed/17825456).

Rico, Patricia et al. 2009. "Substrate-Induced Assembly of Fibronectin into Networks: Influence of Surface Chemistry and Effect on Osteoblast Adhesion." *Tissue engineering. Part A* 15(11):3271–81. Retrieved January 19, 2017 (http://www.ncbi.nlm.nih.gov/pubmed/19382854).

Rosen, Steven D. and Carolyn R. Bertozzi. 1994. "The Selectins and Their Ligands." *Current Opinion in Cell Biology* 6(5):663–73.

Ross, Tyler D. et al. 2013. "Integrins in Mechanotransduction." *Current Opinion in Cell Biology* 25(5):613–18.

Rowlands, A. S., S. A. Lim, D. Martin, and J. J. Cooper-White. 2007. "Polyurethane/poly(lactic-Co-Glycolic) Acid Composite Scaffolds Fabricated by Thermally Induced Phase Separation." *Biomaterials* 28(12):2109–21.

Rozario, Tania and Douglas W. Desimone. 2011. "Dynamic View." 341(1):126–40.

Sadler, J.Evan. 1998. "BIOCHEMISTRY AND GENETICS OF VON WILLEBRAND FACTOR." *Annual Review of Biochemistry* 67(1):395–424. Retrieved January 11, 2017 (http://www.ncbi.nlm.nih.gov/pubmed/9759493).

Salmeron-Sanchez, Manuel, George Altankov, and Daniel Eberli. 2010. "Cell-Protein-Material Interaction in Tissue Engineering." *Tissue Engineering* 77–103. Retrieved November 26, 2016 (http://www.intechopen.com/books/tissue-engineering/cell-protein-material-interaction-in-tissue-engineering).

Santore, Maria M. and Christian F. Wertz. 2005. “Protein Spreading Kinetics at Liquid−Solid Interfaces via an Adsorption Probe Method.” *Langmuir* 21(22):10172–78. Retrieved January 18, 2017 (http://www.ncbi.nlm.nih.gov/pubmed/16229542).

Sato, Y. et al. 2009. “Molecular Basis of the Recognition of Nephronectin by Integrin 8 1.” *Journal of Biological Chemistry* 284(21):14524–36. Retrieved January 13, 2017 (http://www.ncbi.nlm.nih.gov/pubmed/19342381).

Schéele, Susanne et al. 2007. “Laminin Isoforms in Development and Disease.” *Journal of Molecular Medicine* 85(8):825–36. Retrieved December 12, 2016 (http://link.springer.com/10.1007/s00109-007-0182-5).

Schvartz, I., D. Seger, and S. Shaltiel. 1999. “Vitronectin.” *The international journal of biochemistry & cell biology* 31(5):539–44. Retrieved January 10, 2017 (http://www.ncbi.nlm.nih.gov/pubmed/10399314).

Schwartz, M. A. and R. K. Assoian. 2001. “Integrins and Cell Proliferation: Regulation of Cyclin-Dependent Kinases via Cytoplasmic Signaling Pathways.” *Journal of cell science* 114(Pt 14):2553–60. Retrieved January 13, 2017 (http://www.ncbi.nlm.nih.gov/pubmed/11683383).

Schwarz-Linek, Ulrich, Magnus Höök, and Jennifer R. Potts. 2004. “The Molecular Basis of Fibronectin-Mediated Bacterial Adherence to Host Cells.” *Molecular Microbiology* 52(3):631–41. Retrieved January 10, 2017 (http://www.ncbi.nlm.nih.gov/pubmed/15101971).

Seiffert, D., K. Crain, N. V Wagner, and D. J. Loskutoff. 1994. “Vitronectin Gene Expression in Vivo. Evidence for Extrahepatic Synthesis and Acute Phase Regulation.” *The Journal of biological chemistry* 269(31):19836–42. Retrieved January 23, 2017 (http://www.ncbi.nlm.nih.gov/pubmed/7519600).

Sethuraman, Ananthakrishnan and Georges Belfort. 2005. “Protein Structural Perturbation and Aggregation on Homogeneous Surfaces.” *Biophysical journal* 88(2):1322–33. Retrieved January 18, 2017 (http://www.ncbi.nlm.nih.gov/pubmed/15542559).

Sharma, A., J. A. Askari, M. J. Humphries, E. Y. Jones, and D. I. Stuart. 1999. “Crystal Structure of a Heparin- and Integrin-Binding Segment of Human Fibronectin.” *The EMBO journal* 18(6):1468–79. Retrieved January 11, 2017 (http://www.ncbi.nlm.nih.gov/pubmed/10075919).

Shattil, Sanford J., Chungho Kim, and Mark H. Ginsberg. 2010. “The Final Steps of Integrin Activation: The End Game.” *Nature reviews. Molecular cell biology* 11(4):288–300. Retrieved (http://linkinghub.elsevier.com/retrieve/pii/S0734975011001534%5Cnhttp://www.nature.com/doifinder/10.1038/nrm2871%5Cnhttp://www.ncbi.nlm.nih.gov/pubmed/20308986%5Cnhttp://www.pubmedcentral.nih.gov/articlerender.fcgi?artid=PMC3929966).

Shi, Jian et al. 2010. “Incorporating Protein Gradient into Electrospun Nanofibers As Scaffolds for Tissue Engineering.” *ACS Applied Materials & Interfaces* 2(4):1025–30. Retrieved January 16, 2017 (http://pubs.acs.org/doi/abs/10.1021/am9007962).

Shields, Kelly J., Matthew J. Beckman, Gary L. Bowlin, and Jennifer S. Wayne. 2004. “Mechanical

Properties and Cellular Proliferation of Electrospun Collagen Type II." *Tissue Engineering* 10(9–10):1510–17. Retrieved January 16, 2017 (http://www.ncbi.nlm.nih.gov/pubmed/15588410).

Sicari, Brian M., Ricardo Londono, and Stephen F. Badylak. 2014. *Extracellular Matrix as a Bioscaffold for Tissue Engineering*. Second Edi. Elsevier Inc. Retrieved (http://linkinghub.elsevier.com/retrieve/pii/B9780124201453000055).

Silke Megelski, †, † Jean S. Stephens, ‡ and D. Bruce Chase, and † John F. Rabolt*. 2002. "Micro- and Nanostructured Surface Morphology on Electrospun Polymer Fibers." *Macromolecules* 35(22):8456–8466.

Sill, Travis J. and Horst A. von Recum. 2008. "Electrospinning: Applications in Drug Delivery and Tissue Engineering." *Biomaterials* 29(13):1989–2006. Retrieved November 12, 2012 (http://www.ncbi.nlm.nih.gov/pubmed/18281090).

Sipe, Jean D. 2002. "Tissue Engineering and Reparative Medicine." *Annals of the New York Academy of Sciences* 961:1–9. Retrieved (http://www.ncbi.nlm.nih.gov/pubmed/12081856).

Smith, L. A. and P. X. Ma. 2004. "Nano-Fibrous Scaffolds for Tissue Engineering." *Colloids and Surfaces B: Biointerfaces* 39(3):125–31. Retrieved January 16, 2017 (http://www.ncbi.nlm.nih.gov/pubmed/15556341).

Sottile, Jane and Denise C. Hocking. 2002. "Fibronectin Polymerization Regulates the Composition and Stability of Extracellular Matrix Fibrils and Cell-Matrix Adhesions." *Molecular biology of the cell* 13(10):3546–59. Retrieved November 26, 2016 (http://www.ncbi.nlm.nih.gov/pubmed/12388756).

Sousa, S. R., M.Manuela Brás, P. Moradas-Ferreira, and M. A. Barbosa. 2007. "Dynamics of Fibronectin Adsorption on TiO $_2$ Surfaces." *Langmuir* 23(13):7046–54. Retrieved January 20, 2017 (http://www.ncbi.nlm.nih.gov/pubmed/17508764).

Springer, T. A. 2011. "Biology and Physics of von Willebrand Factor Concatamers." *Journal of Thrombosis and Haemostasis* 9:130–43. Retrieved January 11, 2017 (http://www.ncbi.nlm.nih.gov/pubmed/21781248).

Sriramarao, P., M. Mendler, and M. A. Bourdon. 1993. "Endothelial Cell Attachment and Spreading on Human Tenascin Is Mediated by Alpha 2 Beta 1 and Alpha v Beta 3 Integrins." *Journal of cell science* 1001–12. Retrieved January 13, 2017 (http://www.ncbi.nlm.nih.gov/pubmed/7693733).

Steiner, Gerald, Sibel Tunc, Manfred Maitz, and Reiner Salzer. 2007. "Conformational Changes during Protein Adsorption. FT-IR Spectroscopic Imaging of Adsorbed Fibrinogen Layers." *Analytical Chemistry* 79(4):1311–16. Retrieved January 20, 2017 (http://www.ncbi.nlm.nih.gov/pubmed/17297929).

Stewart, Phoebe L. and Glen R. Nemerow. 2007. "Cell Integrins: Commonly Used Receptors for Diverse Viral Pathogens." *Trends in Microbiology* 15(11):500–507. Retrieved January 13, 2017 (http://www.ncbi.nlm.nih.gov/pubmed/17988871).

Sun, B. et al. 2014. “Advances in Three-Dimensional Nanofibrous Macrostructures via Electrospinning.” *Progress in Polymer Science* 39(5):862–90.

Swenson, Stephen, Swapnika Ramu, and Francis S. Markland. 2007. “Anti-Angiogenesis and RGD-Containing Snake Venom Disintegrins.” *Current pharmaceutical design* 13(28):2860–71. Retrieved January 13, 2017 (http://www.ncbi.nlm.nih.gov/pubmed/17979731).

Tadokoro, S. et al. 2003. “Talin Binding to Integrin Tails: A Final Common Step in Integrin Activation.” *Science* 302(5642):103–6. Retrieved January 13, 2017 (http://www.ncbi.nlm.nih.gov/pubmed/14526080).

Takagi, Junichi, Benjamin M. Petre, Thomas Walz, and Timothy A. Springer. 2002. “Global Conformational Rearrangements in Integrin Extracellular Domains in Outside-In and Inside-Out Signaling.” *Cell* 110(5):599–611.

Tancred, D. C., B. a McCormack, and a J. Carr. 1998. “A Synthetic Bone Implant Macroscopically Identical to Cancellous Bone.” *Biomaterials* 19(24):2303–11. Retrieved (http://www.ncbi.nlm.nih.gov/pubmed/9884044).

Than, Manuel E. et al. 2002. “The 1.9-A Crystal Structure of the Noncollagenous (NC1) Domain of Human Placenta Collagen IV Shows Stabilization via a Novel Type of Covalent Met-Lys Cross-Link.” *Proceedings of the National Academy of Sciences of the United States of America* 99(10):6607–12. Retrieved November 26, 2016 (http://www.ncbi.nlm.nih.gov/pubmed/12011424).

Theron, S. A., E. Zussman, and A. L. Yarin. 2004. “Experimental Investigation of the Governing Parameters in the Electrospinning of Polymer Solutions.” *Polymer* 45(6):2017–30.

Timpl, Rupert et al. 2000. “Structure and Function of Laminin LG Modules.” *Matrix Biology* 19(4):309–17.

Timpl, Rupert and Judith C. Brown. 1996. “Supramolecular Assembly of Basement Membranes.” *BioEssays* 18(2):123–32. Retrieved December 12, 2016 (http://doi.wiley.com/10.1002/bies.950180208).

Tomasini-Johansson, Bianca R., Douglas S. Annis, and Deane F. Mosher. 2006. “The N-Terminal 70-kDa Fragment of Fibronectin Binds to Cell Surface Fibronectin Assembly Sites in the Absence of Intact Fibronectin.” *Matrix Biology* 25(5):282–93. Retrieved January 10, 2017 (http://www.ncbi.nlm.nih.gov/pubmed/16567085).

Tomasini, B. R. and D. F. Mosher. 1991. “Vitronectin.” *Progress in hemostasis and thrombosis* 10:269–305. Retrieved January 10, 2017 (http://www.ncbi.nlm.nih.gov/pubmed/1706881).

Toromanov, Georgi, Cristina González-García, George Altankov, and Manuel Salmerón-Sánchez. 2010. “Vitronectin Activity on Polymer Substrates with Controlled -OH Density.” *Polymer* 51(11):2329–36.

Tsang, Kwok Yeung, Martin C. H. Cheung, Danny Chan, and Kathryn S. E. Cheah. 2010. “The Developmental Roles of the Extracellular Matrix: Beyond Structure to Regulation.” *Cell and*

Tissue Research 339(1):93–110. Retrieved November 15, 2016 (http://link.springer.com/10.1007/s00441-009-0893-8).

Tsapikouni, Theodora S. and Yannis F. Missirlis. 2007. "pH and Ionic Strength Effect on Single Fibrinogen Molecule Adsorption on Mica Studied with AFM." *Colloids and Surfaces B: Biointerfaces* 57(1):89–96.

Tzoneva, Rumiana, Thomas Groth, George Altankov, and Dieter Paul. 2002. "Remodeling of Fibrinogen by Endothelial Cells in Dependence on Fibronectin Matrix Assembly. Effect of Substratum Wettability." *Journal of materials science. Materials in medicine* 13(12):1235–44. Retrieved (http://www.ncbi.nlm.nih.gov/pubmed/15348671).

Tzu, Julia and M.Peter Marinkovich. 2008. "No Title." 40(2):199–214. Retrieved December 12, 2016 (http://www.ncbi.nlm.nih.gov/pubmed/17855154).

Vandenberg, P. et al. 1991. "Characterization of a Type IV Collagen Major Cell Binding Site with Affinity to the Alpha 1 Beta 1 and the Alpha 2 Beta 1 Integrins." *The Journal of cell biology* 113(6):1475–83. Retrieved November 22, 2016 (http://www.ncbi.nlm.nih.gov/pubmed/1646206).

Velling, T. 2002. "Polymerization of Type I and III Collagens Is Dependent On Fibronectin and Enhanced By Integrins Alpha 11beta 1 and Alpha 2beta 1." *Journal of Biological Chemistry* 277(40):37377–81. Retrieved November 26, 2016 (http://www.jbc.org/cgi/doi/10.1074/jbc.M206286200).

Vestweber, D. and J. E. Blanks. 1999. "Mechanisms That Regulate the Function of the Selectins and Their Ligands." *Physiological reviews* 79(1):181–213. Retrieved January 12, 2017 (http://www.ncbi.nlm.nih.gov/pubmed/9922371).

Vogel, Tikva et al. 1993. "Modulation of Endothelial Cell Proliferation, Adhesion, and Motility by Recombinant Heparin-Binding Domain and Synthetic Peptides from the Type I Repeats of Thrombospondin." *Journal of Cellular Biochemistry* 53(1):74–84. Retrieved January 11, 2017 (http://www.ncbi.nlm.nih.gov/pubmed/8227183).

De Vrieze, S. et al. 2009. "The Effect of Temperature and Humidity on Electrospinning." *Journal of Materials Science* 44(5):1357–62. Retrieved October 11, 2016 (http://link.springer.com/10.1007/s10853-008-3010-6).

Wagenaar-Miller, R. A. et al. 2007. "Complementary Roles of Intracellular and Pericellular Collagen Degradation Pathways In Vivo." *Molecular and Cellular Biology* 27(18):6309–22. Retrieved November 26, 2016 (http://mcb.asm.org/cgi/doi/10.1128/MCB.00291-07).

Walsh, Frank S. and Patrick Doherty. 1997. "Neural Cell Adhesion Molecules of the Immunoglobulin Superfamily: Role in Axon Growth and Guidance." *Annual Review of Cell and Developmental Biology* 13(1):425–56. Retrieved January 12, 2017 (http://www.ncbi.nlm.nih.gov/pubmed/9442880).

Wang, Min. 2003. "Developing Bioactive Composite Materials for Tissue Replacement."

Biomaterials 24(13):2133–51.

Wang, R., M. H. Stromer, and T. W. Huiatt. 1998. “Integrin Expression in Developing Smooth Muscle Cells.” *The journal of histochemistry and cytochemistry : official journal of the Histochemistry Society* 46(1):119–26. Retrieved November 24, 2016 (http://www.ncbi.nlm.nih.gov/pubmed/9405501).

Wang, Xianfeng, Bin Ding, and Bingyun Li. 2013. “Biomimetic Electrospun Nanofibrous Structures for Tissue Engineering.” *Materials Today* 16(6):229–41. Retrieved (http://dx.doi.org/10.1016/j.mattod.2013.06.005).

Watt, Fiona M. 2002. “Role of Integrins in Regulating Epidermal Adhesion, Growth and Differentiation.” *The EMBO journal* 21(15):3919–26. Retrieved December 12, 2016 (http://www.ncbi.nlm.nih.gov/pubmed/12145193).

Wei, Y. et al. 1994. “Identification of the Urokinase Receptor as an Adhesion Receptor for Vitronectin.” *The Journal of biological chemistry* 269(51):32380–88. Retrieved January 23, 2017 (http://www.ncbi.nlm.nih.gov/pubmed/7528215).

Weisel, By John W. 2005. “FIBRINOGEN AND FIBRIN.” *Advances in Protein Chemistry* 70(4):247–99.

Weisel, J. W., C. V Stauffacher, E. Bullitt, and C. Cohen. 1985. “A Model for Fibrinogen: Domains and Sequence.” *Science (New York, N.Y.)* 230(4732):1388–91. Retrieved January 12, 2017 (http://www.ncbi.nlm.nih.gov/pubmed/4071058).

Werner, Carsten, Tilo Pompe, and Katrin Salchert. 2006. “Modulating Extracellular Matrix at Interfaces of Polymeric Materials.” Pp. 63–93 in *Polymers for Regenerative Medicine*. Berlin/Heidelberg: Springer-Verlag. Retrieved January 20, 2017 (http://link.springer.com/10.1007/12_089).

Williams, David F. 2008. “On the Mechanisms of Biocompatibility.” *Biomaterials* 29(20):2941–53. Retrieved November 14, 2012 (http://www.ncbi.nlm.nih.gov/pubmed/18440630).

Williams, Michael J. et al. 1994. “Solution Structure of a Pair of Fibronectin Type 1 Modules with Fibrin Binding Activity.” *Journal of Molecular Biology* 235(4):1302–11.

Xiao, Tsan, Junichi Takagi, Barry S. Coller, Jia-Huai Wang, and Timothy A. Springer. 2004. “Structural Basis for Allostery in Integrins and Binding to Fibrinogen-Mimetic Therapeutics.” *Nature* 432(7013):59–67. Retrieved (http://dx.doi.org/10.1038/nature02976).

Xie, Jingwei et al. 2009. “The Differentiation of Embryonic Stem Cells Seeded on Electrospun Nanofibers into Neural Lineages.” *Biomaterials* 30(3):354–62. Retrieved January 16, 2017 (http://www.ncbi.nlm.nih.gov/pubmed/18930315).

Xiong, J. P. et al. 2002. “Crystal Structure of the Extracellular Segment of Integrin Alpha Vbeta 3 in Complex with an Arg-Gly-Asp Ligand.” *Science* 296(5565):151–55. Retrieved January 12, 2017 (http://www.ncbi.nlm.nih.gov/pubmed/11884718).

Xu, Jielin et al. 2009. “Display of Cell Surface Sites for Fibronectin Assembly Is Modulated by Cell

Adherence to 1F3 and C-Terminal Modules of Fibronectin" edited by Rory Edward Morty. *PLoS ONE* 4(1):e4113. Retrieved January 10, 2017 (http://dx.plos.org/10.1371/journal.pone.0004113).

Yang, D., B. Lu, Y. Zhao, and X. Jiang. 2007. "Fabrication of Aligned Fibrous Arrays by Magnetic Electrospinning." *Advanced Materials* 19(21):3702–6. Retrieved January 16, 2017 (http://doi.wiley.com/10.1002/adma.200700171).

Yang, F., R. Murugan, S. Wang, and S. Ramakrishna. 2005. "Electrospinning of Nano/micro Scale Poly(l-Lactic Acid) Aligned Fibers and Their Potential in Neural Tissue Engineering." *Biomaterials* 26(15):2603–10.

Yin, Zi et al. 2010. "The Regulation of Tendon Stem Cell Differentiation by the Alignment of Nanofibers." *Biomaterials* 31(8):2163–75. Retrieved January 16, 2017 (http://www.ncbi.nlm.nih.gov/pubmed/19995669).

Yu, Hongmei, Janna Kay Mouw, and Valerie M. Weaver. 2011. "Forcing Form and Function: Biomechanical Regulation of Tumor Evolution." *Trends in Cell Biology* 21(1):47–56. Retrieved (http://dx.doi.org/10.1016/j.tcb.2010.08.015).

Yurchenco, P. D. and H. Furthmayr. 1984. "Self-Assembly of Basement Membrane Collagen." *Biochemistry* 23(8):1839–50. Retrieved November 22, 2016 (http://www.ncbi.nlm.nih.gov/pubmed/6722126).

Yurchenco, P. D. and J. J. O'Rear. 1994. "Basement Membrane Assembly." *Methods in enzymology* 245:489–518. Retrieved December 12, 2016 (http://www.ncbi.nlm.nih.gov/pubmed/7760748).

Yurchenco, P. D. and G. C. Ruben. 1987. "Basement-Membrane Structure Insitu - Evidence for Lateral Associations in the Type-Iv Collagen Network." *Journal of Cell Biology* 105(6):2559–68.

Yurchenco, Peter D. and William G. Wadsworth. 2004. "Assembly and Tissue Functions of Early Embryonic Laminins and Netrins." *Current Opinion in Cell Biology* 16(5):572–79. Retrieved December 12, 2016 (http://www.ncbi.nlm.nih.gov/pubmed/15363809).

Zaidel-Bar, Ronen and Benjamin Geiger. 2010. "The Switchable Integrin Adhesome." *Journal of cell science* 123(Pt 9):1385–88. Retrieved November 24, 2016 (http://www.ncbi.nlm.nih.gov/pubmed/20410370).

Zaidel-Bar, Ronen, Shalev Itzkovitz, Avi Ma'ayan, Ravi Iyengar, and Benjamin Geiger. 2007. "Functional Atlas of the Integrin Adhesome." *Nature Cell Biology* 9(8):858–67. Retrieved November 24, 2016 (http://www.ncbi.nlm.nih.gov/pubmed/17671451).

Zaidel-Bar, Ronen, Ron Milo, Zvi Kam, and Benjamin Geiger. 2007. "A Paxillin Tyrosine Phosphorylation Switch Regulates the Assembly and Form of Cell-Matrix Adhesions." *Journal of cell science* 120(Pt 1):137–48. Retrieved November 24, 2016 (http://www.ncbi.nlm.nih.gov/pubmed/17164291).

Zamir, E. et al. 1999. "Molecular Diversity of Cell-Matrix Adhesions." *Journal of cell science* 112 (pt11):1655–69.

Zargham, Shamim, Saeed Bazgir, Amir Tavakoli, Abo Saied Rashidi, and Rogheih Damerchely. 2012. “The Effect of Flow Rate on Morphology and Deposition Area of Electrospun Nylon 6 Nanofiber.” *Journal of Engineered Fibers and Fabrics* 4(7):42.

Zeleny, John. 1914. “The Electrical Discharge from Liquid Points, and a Hydrostatic Method of Measuring the Electric Intensity at Their Surfaces.” *Physical Review* 3(2):69–91. Retrieved January 16, 2017 (http://link.aps.org/doi/10.1103/PhysRev.3.69).

Zhang, Jing and Xiang Y. Liu. 2003. “Effect of Protein–protein Interactions on Protein Aggregation Kinetics.” *The Journal of Chemical Physics* 119(20):10972–76. Retrieved January 19, 2017 (http://aip.scitation.org/doi/10.1063/1.1622380).

Zhang, Shuguang. 2003. “Fabrication of Novel Biomaterials through Molecular Self-Assembly.” *Nature Biotechnology* 21(10):1171–78. Retrieved January 16, 2017 (http://www.ncbi.nlm.nih.gov/pubmed/14520402).

Zheng, X., T. L. Saunders, S. A. Camper, L. C. Samuelson, and D. Ginsburg. 1995. “Vitronectin Is Not Essential for Normal Mammalian Development and Fertility.” *Proceedings of the National Academy of Sciences of the United States of America* 92(26):12426–30. Retrieved January 11, 2017 (http://www.ncbi.nlm.nih.gov/pubmed/8618914).

Zhou, Aiwu, James A. Huntington, Navraj S. Pannu, Robin W. Carrell, and Randy J. Read. 2003. “How Vitronectin Binds PAI-1 to Modulate Fibrinolysis and Cell Migration.” *Nature Structural Biology* 10(7):541–44. Retrieved January 10, 2017 (http://www.ncbi.nlm.nih.gov/pubmed/12808446).

Zhu, C. Q. et al. 2007. “Integrin 11 Regulates IGF2 Expression in Fibroblasts to Enhance Tumorigenicity of Human Non-Small-Cell Lung Cancer Cells.” *Proceedings of the National Academy of Sciences* 104(28):11754–59. Retrieved January 13, 2017 (http://www.ncbi.nlm.nih.gov/pubmed/17600088).

Zhu, Jianghai et al. 2008. “Structure of a Complete Integrin Ectodomain in a Physiologic Resting State and Activation and Deactivation by Applied Forces.” *Molecular Cell* 32(6):849–61. Retrieved January 24, 2017 (http://www.ncbi.nlm.nih.gov/pubmed/19111664).

Zong, X. et al. 2005. “Electrospun Fine-Textured Scaffolds for Heart Tissue Constructs.” *Biomaterials* 26(26):5330–38. Retrieved January 16, 2017 (http://www.ncbi.nlm.nih.gov/pubmed/15814131).

CHAPTER 2

FIBRONECTIN ACTIVITY ON SUBSTRATES WITH CONTROLLED –OH DENSITY

Published in
Journal of Biomedical Materials Research Part A, 2009

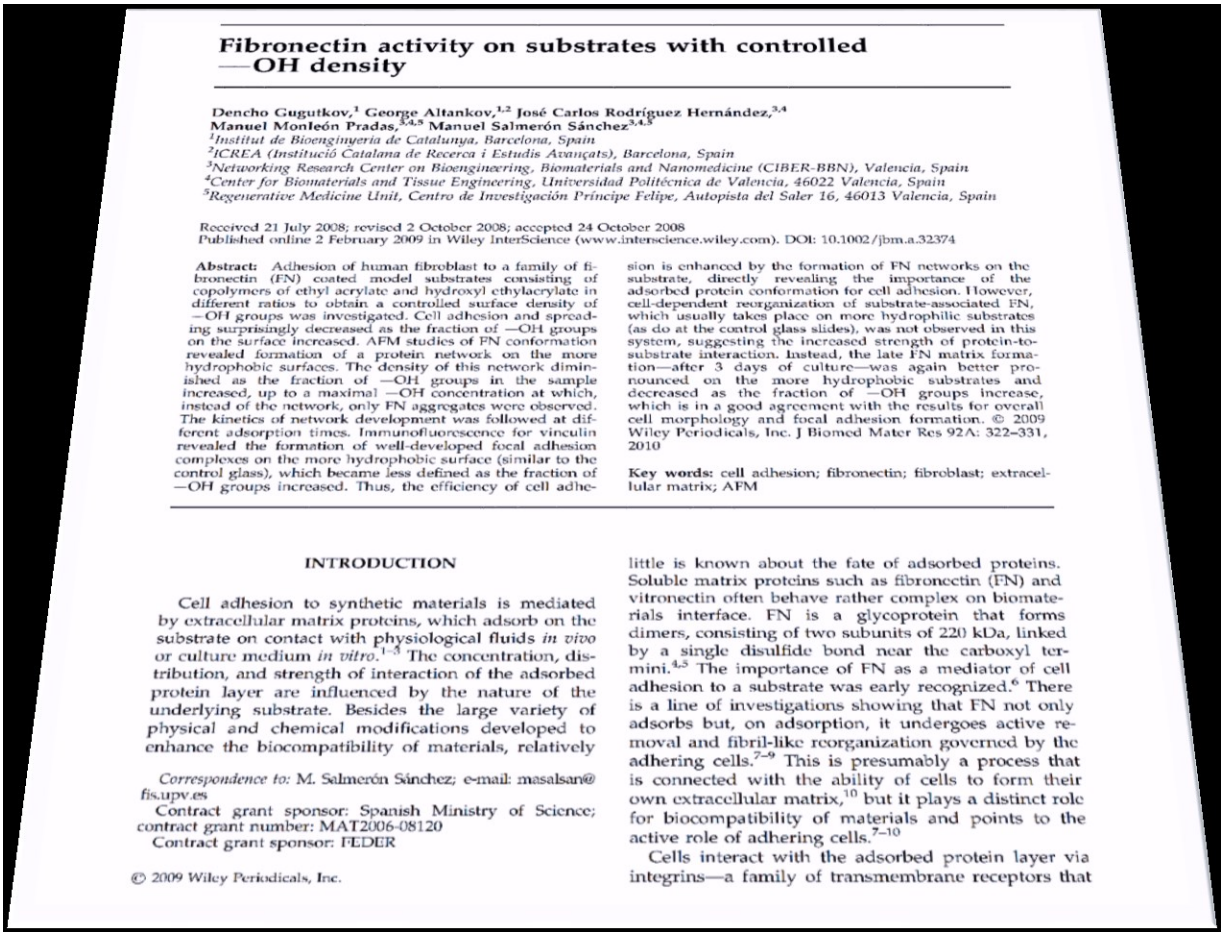

Fibronectin activity on substrates with controlled —OH density

Dencho Gugutkov,[1] George Altankov,[1,2] José Carlos Rodríguez Hernández,[3,4] Manuel Monleón Pradas,[3,4,5] Manuel Salmerón Sánchez[3,4,5]
[1]*Institut de Bioenginyeria de Catalunya, Barcelona, Spain*
[2]*ICREA (Institució Catalana de Recerca i Estudis Avançats), Barcelona, Spain*
[3]*Networking Research Center on Bioengineering, Biomaterials and Nanomedicine (CIBER-BBN), Valencia, Spain*
[4]*Center for Biomaterials and Tissue Engineering, Universidad Politécnica de Valencia, 46022 Valencia, Spain*
[5]*Regenerative Medicine Unit, Centro de Investigación Príncipe Felipe, Autopista del Saler 16, 46013 Valencia, Spain*

Received 21 July 2008; revised 2 October 2008; accepted 24 October 2008
Published online 2 February 2009 in Wiley InterScience (www.interscience.wiley.com). DOI: 10.1002/jbm.a.32374

Abstract: Adhesion of human fibroblast to a family of fibronectin (FN) coated model substrates consisting of copolymers of ethyl acrylate and hydroxyl ethylacrylate in different ratios to obtain a controlled surface density of —OH groups was investigated. Cell adhesion and spreading surprisingly decreased as the fraction of —OH groups on the surface increased. AFM studies of FN conformation revealed formation of a protein network on the more hydrophobic surfaces. The density of this network diminished as the fraction of —OH groups in the sample increased, up to a maximal —OH concentration at which, instead of the network, only FN aggregates were observed. The kinetics of network development was followed at different adsorption times. Immunofluorescence for vinculin revealed the formation of well-developed focal adhesion complexes on the more hydrophobic surface (similar to the control glass), which became less defined as the fraction of —OH groups increased. Thus, the efficiency of cell adhesion is enhanced by the formation of FN networks on the substrate, directly revealing the importance of the adsorbed protein conformation for cell adhesion. However, cell-dependent reorganization of substrate-associated FN, which usually takes place on more hydrophilic substrates (as do at the control glass slides), was not observed in this system, suggesting the increased strength of protein-to-substrate interaction. Instead, the late FN matrix formation—after 3 days of culture—was again better pronounced on the more hydrophobic substrates and decreased as the fraction of —OH groups increase, which is in a good agreement with the results for overall cell morphology and focal adhesion formation. © 2009 Wiley Periodicals, Inc. J Biomed Mater Res 92A: 322–331, 2010

Key words: cell adhesion; fibronectin; fibroblast; extracellular matrix; AFM

INTRODUCTION

Cell adhesion to synthetic materials is mediated by extracellular matrix proteins, which adsorb on the substrate on contact with physiological fluids *in vivo* or culture medium *in vitro*.[1–3] The concentration, distribution, and strength of interaction of the adsorbed protein layer are influenced by the nature of the underlying substrate. Besides the large variety of physical and chemical modifications developed to enhance the biocompatibility of materials, relatively little is known about the fate of adsorbed proteins. Soluble matrix proteins such as fibronectin (FN) and vitronectin often behave rather complex on biomaterials interface. FN is a glycoprotein that forms dimers, consisting of two subunits of 220 kDa, linked by a single disulfide bond near the carboxyl termini.[4,5] The importance of FN as a mediator of cell adhesion to a substrate was early recognized.[6] There is a line of investigations showing that FN not only adsorbs but, on adsorption, it undergoes active removal and fibril-like reorganization governed by the adhering cells.[7–9] This is presumably a process that is connected with the ability of cells to form their own extracellular matrix,[10] but it plays a distinct role for biocompatibility of materials and points to the active role of adhering cells.[7–10]

Cells interact with the adsorbed protein layer via integrins—a family of transmembrane receptors that

Correspondence to: M. Salmerón Sánchez; e-mail: masalsan@fis.upv.es
Contract grant sponsor: Spanish Ministry of Science; contract grant number: MAT2006-08120
Contract grant sponsor: FEDER

Published online 2 February 2009 in Wiley InterScience (www.interscience.wiley.com)
J Biomed Mater Res A. 2010; 92(1):322-31
DOI: 10.1002/jbm.a.32374

Preface to Chapter 2

As stated in the Introduction, one considerable achievement of our group was the disclosure of fact that **material-driven protein assembly** might be used to obtain control over the biological activity of matrix proteins. It shall be clearly admitted however that this work was performed in a close cooperation with the group of Prof. Salmeron-Sanchez (Polytechnic University of Valencia and currently The University of Glasgow) contributing particularly on the nanoindentation of the observed phenomenon. Without their contribution it would be not possible to understand neither to explain the obtained biological consequences. Applying the established by this group family of model substrates with **varying density of surface –OH groups**, in fact, we described for the first time that fibronectin molecules may undergo **lateral interaction** provoked on some distinct chemistries, which leads to unique **FN network** formation. This phenomenon is also a matter of additional studies performed in the group of Prof Sanchez, which are separate and are not included in this Thesis. Here we found that the material driven FN networks formation depends not only on the surface density of –OH groups, but also affects significantly the biological performance of FN. Utilizing human fibroblast as model system we showed that cell adhesion and spreading to FN surprisingly declines as the fraction of –OH groups increases, contrarily to the classical trend for the behavior of FN on biomaterials, and that this is a specific result from the FN network assembly. Revealing this effect was the particular contribution of our group performed by the author of this Thesis. The more stable FN network was formed the better interaction of cells was observed. Conversely, as the density of network diminished (with increasing the fraction of –OH) the cellular interaction dramatically decline. Thus we showed for the first time that through controlling the density of –OH groups at biomaterials interface we can obtain control over the cellular interaction through altering the FN networks assembly. The complete details for this study are to find in the original paper ***"Fibronectin activity on substrates with controlled –OH density"***, presented in this Chapter.

Abstract

Adhesion of human fibroblast to a family of fibronectin (FN) coated model substrates consisting of copolymers of ethyl acrylate and hydroxyl ethyl acrylate in different ratios to obtain a controlled surface density of –OH groups was investigated. Cell adhesion and spreading surprisingly decreased as the fraction of –OH groups on the surface increased. AFM studies of FN conformation revealed formation of a protein network on the more hydrophobic surfaces. The density of this network diminished as the fraction of –OH groups in the sample increased, up to a maximal –OH concentration at which, instead of the network, only FN aggregates were observed. The kinetics of network development was followed at different adsorption times. Immunofluorescence for vinculin revealed the formation of well-developed focal adhesion complexes on the more hydrophobic surface (similar to the control glass), which became less defined as the fraction of –OH groups increased. Thus, the efficiency of cell adhesion is enhanced by the formation of FN networks on the substrate, directly revealing the importance of the adsorbed protein conformation for cell adhesion. However, cell-dependent reorganization of substrate-associated FN, which usually takes place on more hydrophilic substrates (as do at the control glass slides), was not observed in this system, suggesting the increased strength of protein-to-substrate interaction. Instead, the late FN matrix - formation - after 3 days of culture, was again better pronounced on the more hydrophobic substrates and decreased as the fraction of –OH groups increase, which is in a good agreement with the results for overall cell morphology and focal adhesion formation.

*Key words: *cell adhesion; fibronectin; fibroblast; extracellular matrix; AFM*

Introduction

Cell adhesion to synthetic materials is mediated by extracellular matrix proteins, which adsorb on the substrate on contact with physiological fluids in vivo or culture medium in vitro [1–3]. The concentration, distribution, and strength of interaction of the adsorbed protein layer are influenced by the nature of the underlying substrate. Besides the large variety of physical and chemical modifications developed to enhance the biocompatibility of materials, relatively little is known about the fate of adsorbed proteins. Soluble matrix proteins such as fibronectin (FN) and vitronectin often behave rather complex on biomaterials interface. FN is a glycoprotein that forms dimers, consisting of two subunits of 220 kDa, linked by a single disulfide bond near the carboxyl termini [4, 5]. The importance of FN as a mediator of cell adhesion to a substrate was early recognized [6]. There is a line of investigations showing that FN not only adsorbs but, on adsorption, it undergoes active removal and fibril-like reorganization governed by the adhering cells [7–9]. This is presumably a process that is connected with the ability of cells to form their own extracellular matrix[10], but it plays a distinct role for biocompatibility of materials and points to the active role of adhering cells [7–10]. Cells interact with the adsorbed protein layer via integrins - a family of transmembrane receptors that govern the interaction of cells with the extracellular matrix (ECM). Integrin-mediated adhesion is a complex process that involves integrin association with the actin cytoskeleton and clustering into supramolecular complexes, focal adhesions, which contain structural proteins (vinculin, talin, tensin, etc.) and signaling molecules [11, 12]. Integrin-FN interaction, governed mainly by the $\alpha_5\beta_1$ dimer, often leads to the reorganization of the adsorbed FN into extracellular matrix fibrils [13]. The β_1 integrin-mediated FN fibrillogenesis on the surface of a synthetic material depends on the wettability of the surface: fibroblasts are able to remove and reorganize adsorbed FN from some hydrophilic surfaces but not on other more hydrophobic ones [7-9]. Cell-mediated FN reorganization on a synthetic material seems to be an important factor to determine the biocompatibility of a material, because poor cell adhesion and spreading has been found in cases when integrin-mediated rearrangement of FN did not occur during ECM formation [7, 10].Many studies have shown the importance of FN in promoting cell adhesion and regulating cell survival and phenotype expression on different surfaces.14–21 The hydrophobic/hydrophilic nature of the surface is able to modulate FN conformation,[14] which is said to adsorb preferentially on hydrophobic surfaces[22] and that it undergoes greater extension of its dimer arms on hydrophilic than on hydrophobic glass[23]in a conformation which favors the cell-material interaction.[24]It is well documented that physicochemical properties of biomaterials surfaces have a great impact on protein adsorption and subsequent adhesion and proliferation of cells.[2,14,15,19–21] In particular, the substrate wettability, as characterized by water contact angle, has been found to be a clue parameter [2,7–10,20]. In general, wettable surfaces support cellular adhesion, which presumably is connected with the appropriate conformation of adsorbed proteins [20]. However, this is not always straightforward because materials with very high

wettability, which usually bind much water-like hydrogels - do not support the adsorption of proteins and cell adhesion [25]. It seems that several factors collectively contribute to cellular interaction, and it is often difficult to distinguish them; for example, surface chemistry[11,12,14,15], surface charge [25,26] and even the micro/nano-surface roughness [27,28] have been shown to influence FN adsorption and its biological activity. This work investigates the role of –OH groups on cell-to-substrate interaction using human fibroblasts and a set of FN-coated surfaces with controlled fraction of hydroxyl groups. Cell adhesion and spreading, overall cell morphology and focal adhesions formation, as well as the fate of substrate associated FN, including its initial reorganization by the cells and subsequent fibrillar matrix formation, are studied and correlated with the conformation of adsorbed FN as directly observed by atomic force microscopy.

Materials and methods

Substrate preparation

Copolymer sheets were obtained by polymerization of a solution of both monomers ethyl acrylate, EA, (99% pure, Aldrich, Steinheim, Germany) and hydroxyethyl acrylate, HEA (96% pure, Aldrich), with the desired proportion, using 0.1 wt % of benzoin (98% pure, Scharlau, Barcelona, Spain) as photoinitiator and a 2 wt % of ethylene glycol dimethacrylate EGDMA (Aldrich, 98% pure) as crosslinking agent. The polymerization was carried out up to limiting conversion. Five monomer feed compositions were chosen, given by the weight fraction of HEA in the initial mixture of 1, 0.7, 0.5, 0.3, and 0 (hereafter, $–OH_X$ will refer to the sample with fraction x of HEA in the copolymer). After polymerization, low molecular mass substances were extracted from the material by boiling in ethanol for 24 h and then drying in vacuum to constant weight. Small disks were cut from the polymerized sheets to be used in the protein adsorption and cell adhesion studies. The samples were sterilized with gamma radiation (25 kGy) before the experiments.

Atomic force microscopy

AFM experiments were performed using a Multimode AFM equipped with NanoScope IIIa controller from Veeco (Manchester, UK) operating in tapping mode in air; the Nanoscope 5.30r2 software version was used. Si-cantilevers from Veeco (Manchester, UK) were used with force constant of 2.8 N/m and resonance frequency of 75 kHz. The phase signal was set to zero at a frequency 5–10% lower than the resonance one. Drive amplitude was 200 mV, and the amplitude set point A_{sp} was 1.4 V. The ratio between the amplitude set-point and the free amplitude A_{sp}/A_0 was kept equal to 0.7. Fibronectin from human plasma (Roche, Mannheim, Germany) was adsorbed on the different substrates by immersing the material sheets in 20 μg/mL physiological solution (NaCl 0.9%) for 10 min. The influence of the adsorption time on the conformation of the adsorbed protein was investigated by immersing the PEA (–OH X_0) sheet in protein solutions at different times: 10 s, 30 s, 1 min, and 3 min. After protein adsorption, samples were rinsed three times in the physiological solution to eliminate the non-adsorbed protein. Remaining drops on the surface were dried by exposing the sample to a nitrogen flow for 2–3 min. AFM was performed in the tapping mode in air

TABLE I
Equilibrium Water Content (EWC) and Water Contact Angle (WCA) for the Different Substrates

x_{OH}	EWC (%)	WCA (°)	R_{max} (nm)	RMS (nm)
0	1.7 ± 0.4	89 ± 1	24.3	3.1
0.3	7.6 ± 0.9	80 ± 2	8.5	1.5
0.5	18.2 ± 1.7	67 ± 1	10.6	1.1
0.7	40.6 ± 0.4	55 ± 1	17.1	1.5
1	134 ± 5	45 ± 2	6.9	1.2

immediately after sample preparation. Both height and phase magnitudes were recorded for each image. Mean values and their standard deviations are reported for both EWC and WCA. The last two columns show the roughness parameters (R_{max}, the difference between the highest and lowest heights; RMS, root mean square, the standard deviation of the height values) for the different samples calculated on 1 x 1 μm^2 before fibronectin adsorption.

Contact angle measures

Water (Sigma-Aldrich, reagent grade) contact angle experiments were performed making use of the optical contact angle measuring device DataPhysics OCA 10 (Filderstadt, Germany). The sessile drop method was used to evaluate the static contact angle with constant drop volumes at room conditions. Measurements were performed in triplicate for each sample after gamma radiation.

Cells

Human dermal fibroblast cell line CCD-25SK was obtained from the American Type Culture Collection (ATCC, Rockville, MD). Cells were maintained in Dulbecco's modified Eagle medium (Gibco, 11960-044) supplemented with 10% fetal bovine serum (FBS), 1% penicillin / streptomycin, 2 mM L-glutamine, and 1 mM sodium pyruvate (Gibco, 11360-039), in a humidified atmosphere of 5% CO_2in air. Around confluence the cells were detached with trypsin-EDTA (Gibco, 25200-072) that was inactivated with FBS after 5 min. The cells were then re-plated or used for experiments. For cell experiments, the polymer substrates were sterilized in 70% ethanol during 10 min and then copiously rinsed with sterile phosphate buffered saline solution (PBS). The samples were placed individually in 24-well tissue culture plates with a culture area of 1.9 cm^2 , (Nunc, 142475).

Cell adhesion

To investigate initial cell adhesion and morphology, 2.0 x 10^4 cells/well were seeded to each sample in 2.0 mL serum free medium. One set of samples had been precoated with FN (20 µg/mL) for 30 min at 37 ºC. After 2 h of incubation, the living cells were labeled with fluorescein diacetate (FDA) by adding 10 µL/mL from a stock of 1 mg/mL FDA in acetone to the medium. Under these conditions, the vital cells convert FDA in a fluorescent analogue via their esterases. Representative pictures of the adhered cells were then taken with a fluorescent micro- scope, (Nikon, Eclipse E600), using the green channel. At least three representative pictures of each sample were made. Cell density and cell spreading were quantified by image analysis by calculating the average cell area on the different substrates.

FITC-Fibronectin reorganization

Human plasma FN, (Sigma, F2006), was dissolved in 0.1M sodium bicarbonate buffer (pH 5 9.0) at 1 mg/mL, then 10 µL of fluorescein isotiocianate (FITC), (Sigma, F7378) dissolved in

dimethylsulfoxide to 10 mg/mL was added and left for 2 h at room temperature. The labeled FN was separated from non-conjugated dye on a Sephadex G-25 desalting column equilibrated with PBS. The final protein concentration was estimated by measuring the absorbance at 280 nm, while the degree of FITC-labeling was calculated against the absorbance at 494 nm. Aliquots were then stored at -20 ºC. The ability of fibroblasts to reorganize adsorbed FITC-

FN (i.e., early matrix) was monitored by coating all samples with 40 μg/mL for 30 min at 37 ºC, then rinsing with PBS twice, before seeding with 2.0×10^4 cells/well in serum containing medium. After 4 h of incubation, the samples were fixed using 3% paraformaldehyde, mounted in Mowiol (Sigma, 324590) and viewed and photographed with a fluorescent microscope (Nikon, Eclipse E600). As a positive control, a regular round shaped glass coverslip was used (Menzel GmbH, 15 mm diameter).

Fibronectin matrix formation

The ability of fibroblasts to secrete and deposit FN into the extracellular matrix fibrils (i.e., late matrix) was examined via immunofluorescence. For that, 3.0×10^4 cells/well were cultured on the different substrates for 3 days in serum containing medium. At the end of incubation, the cells were rinsed with PBS three times before fixed with 3% paraformaldehyde for 5 min. The samples were then washed as above and saturated with 1% bovine serum albumin (BSA) for 15 min. Subsequently, they were stained with a polyclonal rabbit anti-FN antibody (Santa Cruz, 9068) dissolved in 1% BSA in PBS for 30 min, followed by goat anti-rabbit Cy3-conjugated secondary antibody for 30 min before washed and mounted with Mowiol.

Focal adhesions formation

All samples were fixed with 3% paraformaldehyde (5 min) and permeabilized with 0.5% Triton X-100 in PBS (5 min) before saturation with 10% albumin in PBS. Immunofluoresecence for vinculin was performed according to standard protocol (30 min, 37 ºC) applying mouse monoclonal anti-vinculin antibody 1:100 (Invitrogen) followed by goat anti-mouse Cy2-conjugated secondary antibody (Sigma) before washing and mounting with Mowiol.

Results

Figure 1 shows the overall cell morphology on the different FN-coated substrates and the control glass after 2 h of culture. Cell density and spreading depend strongly on the –OH fraction on the surface (Table II). However, most elongated cells, similar to those on the control glass, are observed

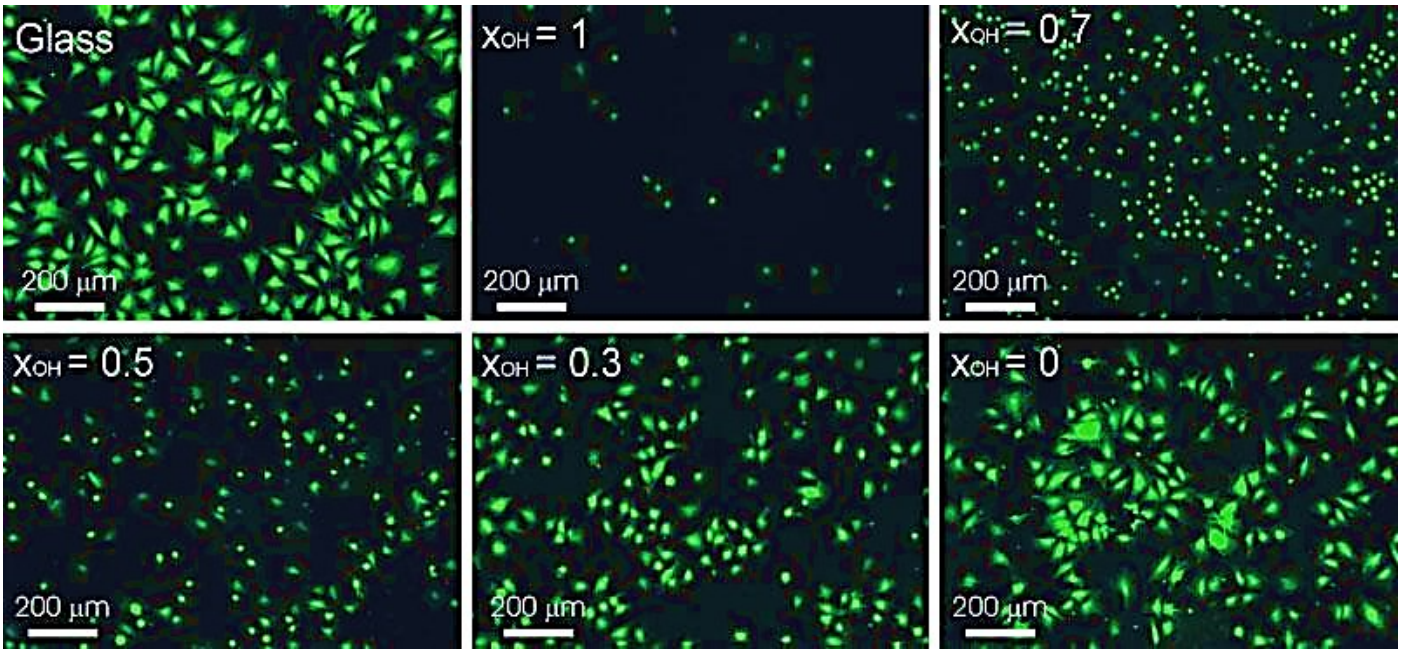

Figure 1. *FDA vital staining of fibroblast on the different substrates and the control glass. The density of –OH groups (xOH) is shown on each picture for the different substrates.*

on the most hydrophobic substrate $–OH_0$; as the fraction of –OH groups in the material increases, the number of attached cells reduces and spreading diminishes. As expected, the substrate wettability clearly drops (see Table I) with reducing the –OH density. Only rounded cells are observed on the more hydrophilic systems ($–OH_{50}$ and $–OH_{70}$) even if the cell density does not differ significantly among them. The organization of cellular proteins involved in the formation of focal adhesion complexes provides an opportunity to learn more about the effectiveness of cell-to-substrate interaction. Figure 2 shows the distribution of vinculin in fibroblasts adhering on the different model substrates. Well-defined focal adhesions were found only on the more hydrophobic

TABLE II
Cell Density and Spreading Area as Calculated From Image Analysis of Figure 1

x_{OH}	Cell Area (μm^2)	Cell Density (cells/mm^2)
0	27 ± 17	142
0.3	21 ± 8	144
0.5	13 ± 4	112
0.7	7 ± 2	175
1	14 ± 5	26
Glass	43 ± 14	150

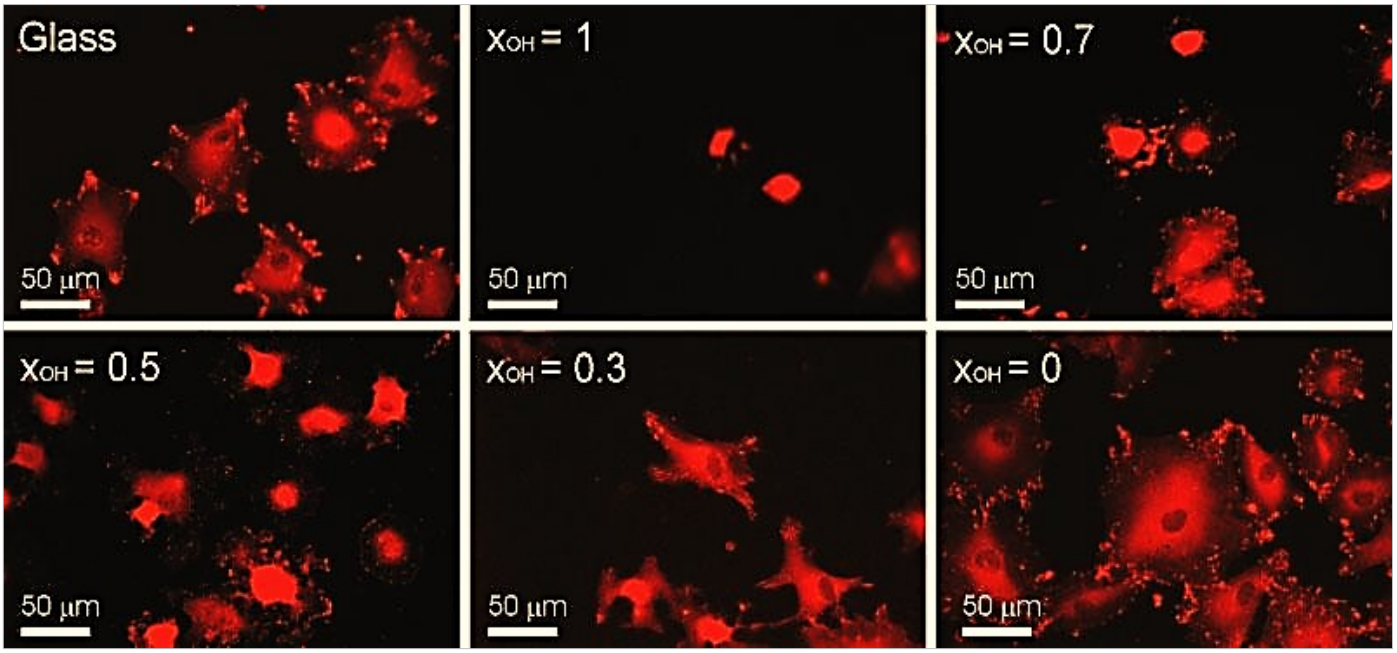

Figure 2. *Focal adhesion formation of fibroblast on the different substrates and the control glass through inmunofluorescence for vinculin. The density of ÀÀOHgroups (xOH) is shown on each picture for the different substrate.*

substrates (–OH_0, –OH_{30}, Fig. 2) and on the control glass (Fig. 2). Even if vinculin is expressed also in the more hydrophilic substrates, it is not organized into focal contacts but randomly distributed along the cell periphery. Late FN matrix formation, for example after 3 days of culture, was also followed via immunofluorescence on the different samples. It was found that the cells are able to synthesize and deposit FN matrix fibrils on some of the material surfaces (Fig. 3) (hereafter, the term fibril will refer to the assembly of individual FN molecules through protein–protein interactions, which constitute a stable supramolecular entity. The formation of FN fibrils, the so-called fibrillogenesis, is a process either mediated by integrins or, as it is accounted for in the paper,

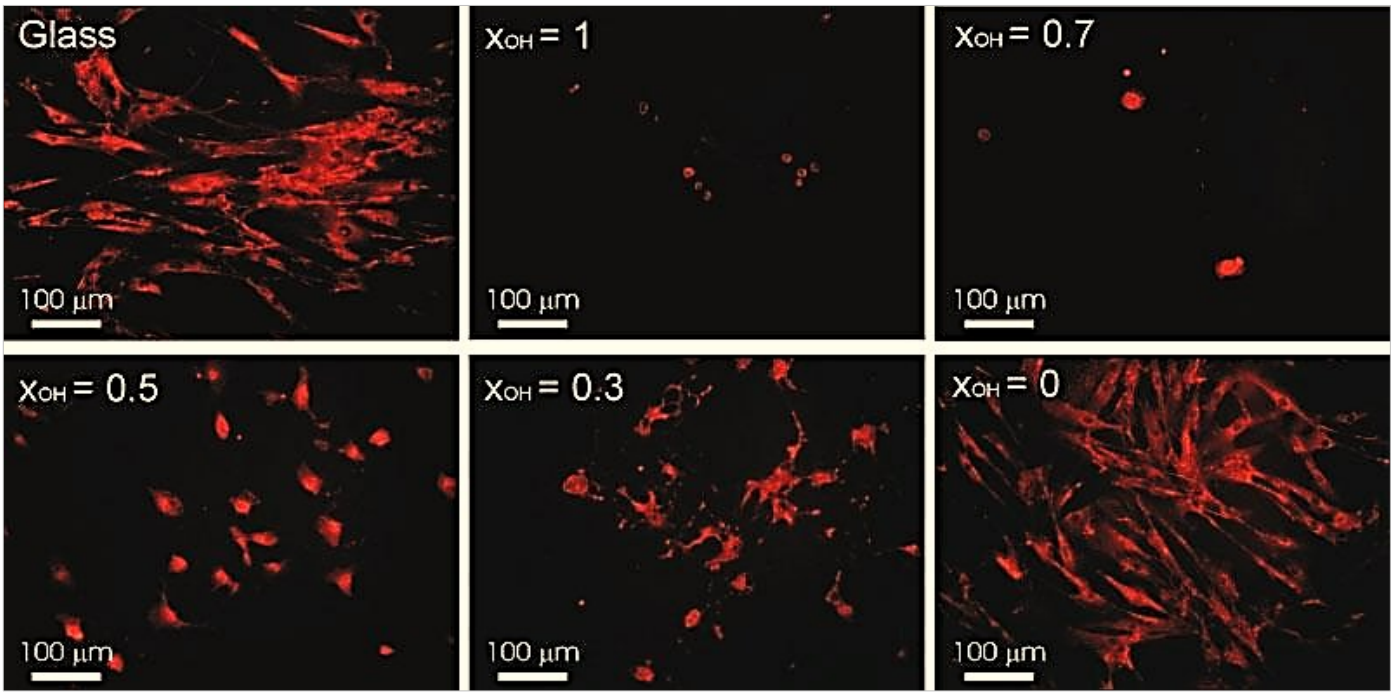

Figure 3. *Fibronectin matrix formation by fibroblast on the different substrates and the control glass after 3 days of culture. The mass fraction of –OH groups (xOH) is shown on each picture for the different substrates.*

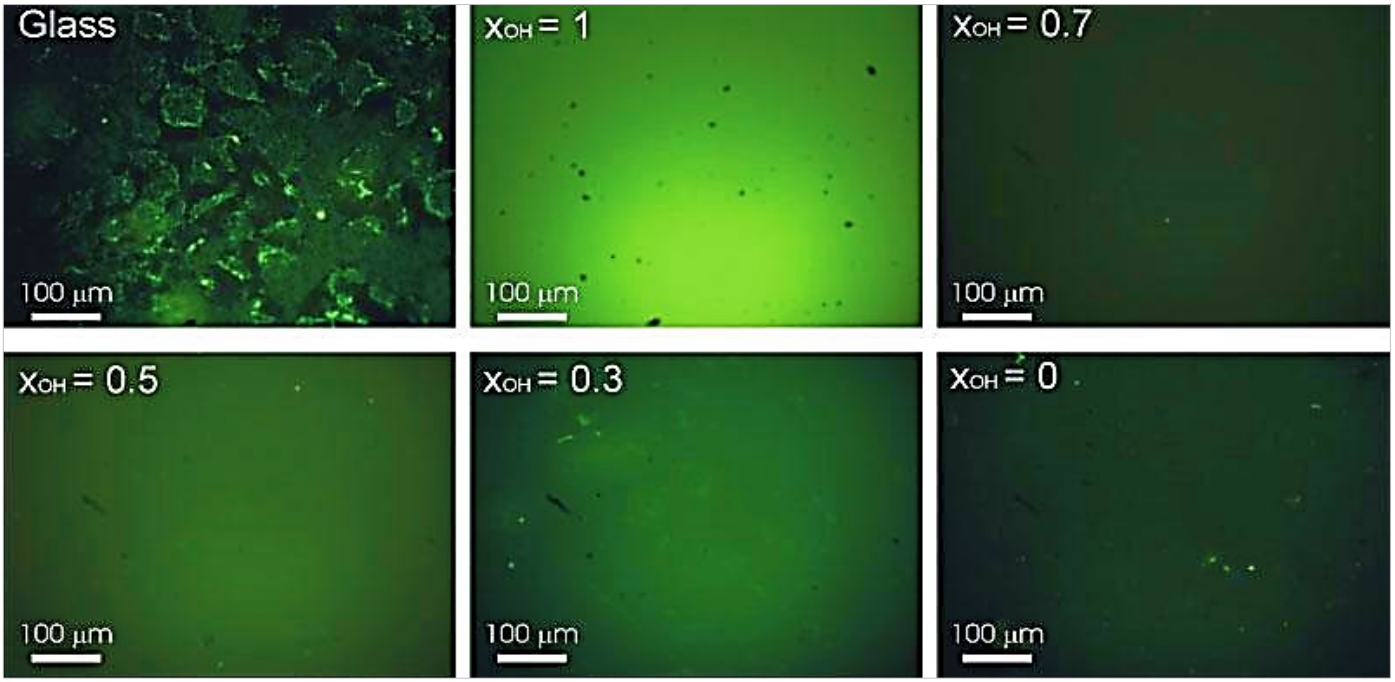

Figure 4. *Reorganization of fluorescent fibronectin by fibroblast on the different substrates and the control glass after 2 h. The mass fraction of –OH groups is shown on each picture for the different substrates.*

induced by the substrate). However, FN fibrils could not be found on the more hydrophilic samples [$–OH_{100}$ and $–OH_{70}$, Fig. 3(b, c)] while on the sample with intermediate composition, $–OH_{70}$, the fibroblasts deposit only small fibrils, located mostly beneath the cells [Fig. 3(d)]. As the hydroxyl fraction decreases the FN deposition increases, which moreover is organized into a typical matrix-like structure [Fig. 3(e, f)] similar to those on the control glass [Fig. 3(a)]. Figure 4 shows the cellular reorganization of adsorbed FITC-FN after 2 h of culture. As inferred from the homogeneous fluorescence of the substrate, no reorganization of FN takes place whatever the hydroxyl fraction of groups in the sample, that is, FN reorganization does not depend on the hydrophilicity for this family of substrates [Fig. 4(b-f)]. Conversely, FN reorganization is well pronounced on the control glass

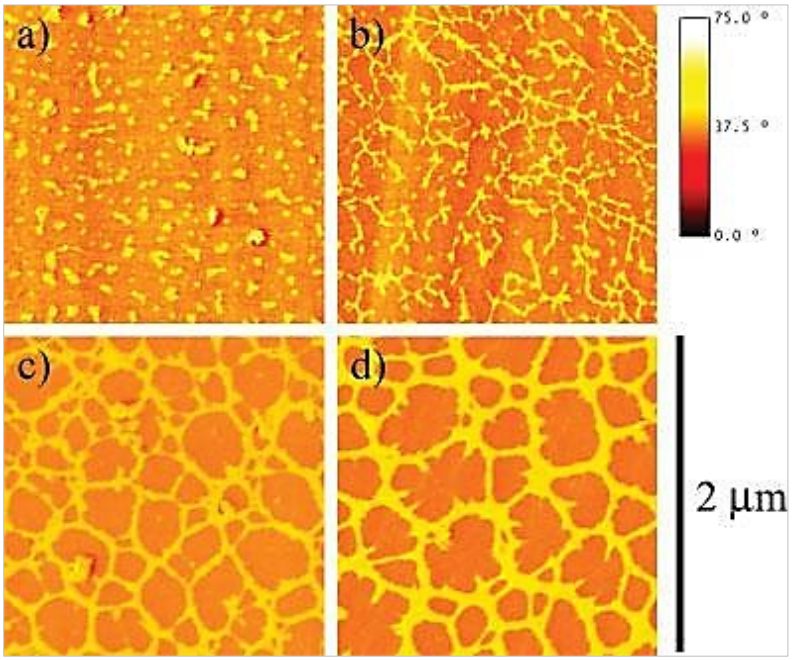

Figure 5. *Dynamics of fibronectin fibrillogenesis on PEA (–OH0) as revealed by the phase magnitude in AFM. The protein was adsorbed from a solution of concentration 20 μg/mL for different times* ***(a)*** *10 s* ***(b)*** *30 s* ***(c)*** *1 min, and* ***(d)*** *3 min.*

surface, an effect well documented in previous studies, [7–9] as indicated by the dark areas of FN removal by the cells and organization into bright fibril-like structures [Fig. 4(a)]. Figure 5 shows the AFM images of the FN adsorbed on the most hydrophobic substrate ($–OH_0$) after different adsorption times (10, 30, 60, and 180 s) from 20 μg/mL protein solution. Previous studies show that AFM phase signal reveals protein conformation when substrata's surfaces are not completely smooth (i.e., when their roughness blurs the small features due to adsorbed proteins) [28]. The overall FN conformation on the surface changes as adsorption time goes by. At the very beginning of the adsorption process [Fig. 5(a), 10 s], isolated globular FN molecules are homogeneously distributed on the material. After 30 s of adsorption, FN globular molecules tend to align suggesting the initial formation of intramolecular connections, which result in protein–protein contacts through the surface [Fig. 5(b)]. FN conformation on Figure 5(c) reveals the formation of a protein network on the material after 60 s of adsorption. Increasing the adsorption time results in thickening the fibrils, which make up the protein network [Fig. 5(d), 3 min]. Surface density of –OH groups (X_{OH}) influences

FN conformation on the substrates. Figure 6 shows protein conformation and distribution after adsorption for 10 min on the different substrates at different magnifications from a 20 μg/mL protein solution, which was the concentration previously employed for coating the substrates in cell

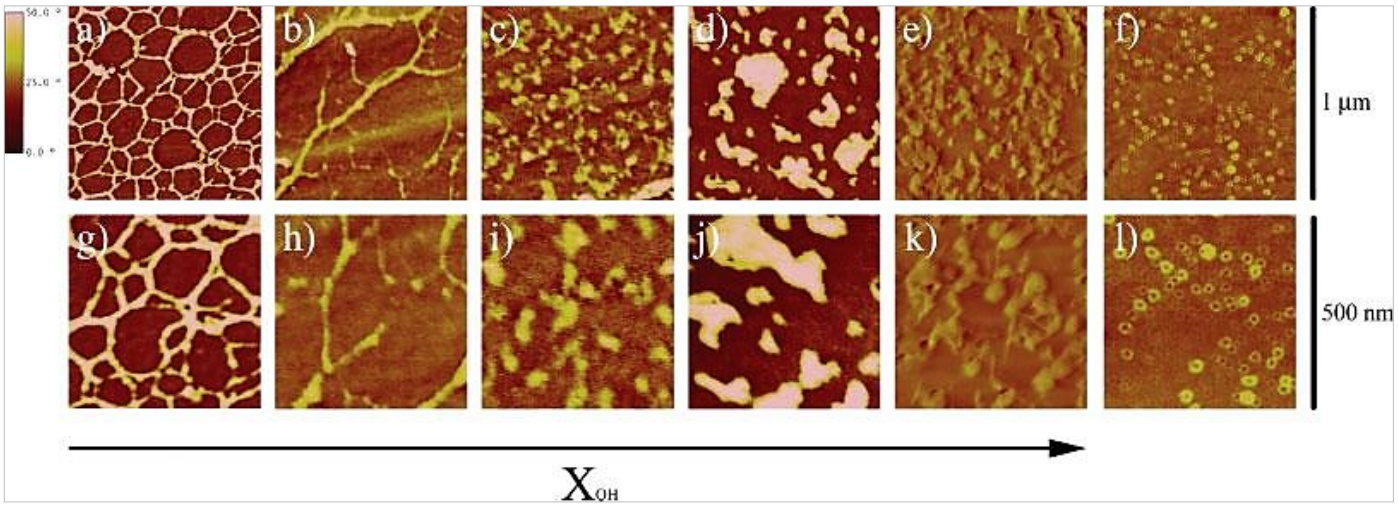

Figure 6. *Fibronectin conformation as revealed by the phase magnitude in AFM. The protein was adsorbed for 10 min from a solution of concentration 20 μg/mL on substrates with increasing fraction of –OH groups.* ***(a,g)*** *PEA; XOH = 0,* ***(b,h)*** *XOH = 0.30,* ***(c,i)*** *XOH = 0.50,* ***(d,j)*** *XOH = 0.70,* ***(e,k)*** *XOH = 1,* ***(f,l)*** *control glass.*

adhesion studies. The more hydrophobic surfaces induce the formation of protein networks, whose density decreases as the fraction of –OH groups increases. FN network is well developed on the PEA ($–OH_0$) substrates [Fig. 6(a, g)]. Protein molecules with elongated shape, in the form of long fibrils, are still formed on the ÀÀOH_{30}surface, but only weakly connected protein filaments are identified [Fig. 6(b, h)].

Higher amounts of hydroxyl groups (from X_{OH}=0.5 on) prevent the formation of a protein network on the materials surface and only disperse (nano) aggregates of the protein are observed on the $–OH_{50}$, $–OH_{70}$ and PHEA substrates. Isolated globular molecules, homogeneously dispersed

throughout the surface lacking FN–FN interactions, are observed on the control glass [Fig. 6(f, l)]. It must be remarked here the perfectly, ring-shaped, FN conformations observed on the control glass which is suggested to be a consequence of the protein-material interaction on hydrated surfaces.[28]

Discussion

The initial cell-material interaction is a process driven by the soluble ECM proteins such as fibronectin and vitronectin, which rapidly adsorb on their surface.[2,10,20,29,30] The quantity, distribution, conformation and strength of interaction between these ECM proteins and the material's surface determine the cell response to artificial substrates.[7,8] In solution, before adsorption, FN is in a compact conformation [5,31]; substrate chemistry is known to influence FN conformation on a synthetic material leading to either the extension of the protein arms when favorable interactions between the surface chemistry and the protein takes place or, on the contrary, keeping the overall compact solution in other cases.[14,21]

To learn more about the particular role of –OH groups on the surface behavior of adsorbed matrix proteins, we have copolymerized ethyl acrylate and hydroxyethyl acrylate monomers, which have a vinyl backbone chain with the side groups $–COOCH_2CH_3$ and $–COOCH_2CH_2OH$, respectively. Their copolymerization gives rise to a substrate in which the surface density of –OH groups can be varied without modifying any other chemical functionality of the system. Substrate's hardness, sheet thickness, and roughness are known to influence protein adsorption. Our substrates were sheets $1 mm thickness in the rubber state (room temperature is well-above the glass transition temperature), so their moduli are those of an elastomer ($1 MPa, independently of composition).[32]Moreover, the effect of gamma radiation on the physic-chemical properties of the system was shown to be negligible for this system.[33]

The concentration of –OH groups determines both the wettability and the hydrophilicity of the substrate, whereas the surface roughness remains unaffected (Table I). The interaction of the protein domains with the chemical functionalities of the substrate and with water determines the molecule's adsorbed conformation. That is to say, proteins will perceive not only the differences in the –OH groups of the polymeric structure, but also strong differences in the content of water molecules on the surface.

In contrast with results of previous studies, [7–10] dramatically altered fibroblast adhesion and focal adhesions formation were found on the most hydrophobic substrates. It was surprising, as it is generally agreed that some wettability enhances cellular interaction. [2, 7–10] However, this is valid for moderate wettable substrata (about 30–60º WCA), and further decrease of WCA is either ineffective or leads to diminish cellular interaction.[2, 34, 35] Materials with too high wettability, like hydrogels[34]or PEG grafted substrates,[18, 21] which carry too much water, do not support cell adhesion, because they acquire repelling properties for proteins and cells. Conversely, too high hydrophobicity also does not favor cellular interaction because may induce conformational changes of FN molecules resulting in altered biological properties. [2, 10, 20] The relatively high equilibrium water content of pure PHEA in our system could explain the low cell attachment. It is noteworthy, however, that the values for the wettability of these samples (WCA 45º) correspond to values that are optimal for the cellular

interaction in other systems.[2, 10, 20, 35] Conversely, surfaces with about 90º WCA, characteristic for pure PEA, and where the best cellular interaction was found, usually abrogate cellular interaction.[7–10, 20, 35] All this points to the different behavior surface associated FN in our system.

Indeed, we found that FN is able to form a network on the more hydrophobic surfaces ($–OH_0$, $–OH_{300}$) whose density decreases as the fraction of the hydroxyl groups on the surface increases. FN fibrillogenesis, for example, the formation of a FN matrix, has been described as a process driven only by cells,[7] which occurs when integrins interact with the RGD domains of the FN molecule and extend their subunits giving rise to the formation of fibrils.[13] In this way, the FN that is synthesized by fibroblasts assembles into a fibril network,[6, 14, 15, 17] this cell-mediated FN assembly obviously also takes place on our model surfaces (Fig. 3). During this assembly, however, FN needs to undergo distinct conformational changes[14, 15, 17] which on adsorption to the substrate can be limited. This may explain why materials surfaces affect FN matrix formation.[8] A line of previous studies suggests that to be biocompatible, materials need to adsorb proteins loosely, for example, in such a way that cells can easily remove and organize in matrix fibrils.[7–10] Our results, however, show that FN fibrillogenesis can take place as a consequence of the sole interaction between the protein molecules and a material surface, that is, without the need of cell involvement. Moreover, this material-induced fibrillogenesis is a dynamic process that depends strongly on the amount of protein adsorbed on the substrate and the time: as the FN is adsorbed its organization changes from a globular-like morphology to a more elongated one, and finally, the formation of the protein network takes place (Fig. 5). It seems, however, that from a certain concentration of hydroxyl groups on (X_{OH} = 0.5 or higher), the interaction between FN domains and the substrate surface keeps the protein molecules in a globular like conformation, and the protein network is not formed anymore. We cannot discard the formation of FN globular aggregates in the more hydrophilic samples as a consequence of the drying process, which could lead to lateral reorganization of the adsorbed layer at the air-liquid interface; this process could be favored on very hydrophilic surfaces due to the absence of strong enough protein-surface interactions to prevent the protein relaxation during water release.[36] Nevertheless, this dehydration-generated change of conformation does not take place on the more hydrophobic substrates, on which the substrate-induced fibrillogenesis is stable.

It is noteworthy that the biological activity of the above observed FN network differs significantly from what we know for FN behavior on other set of surfaces.[10] The strength of the interaction between the protein and the substrate depends on the conformation of the protein after the adsorption process. Besides, it has been suggested that protein adsorption takes place more strongly on hydrophobic substrates.[35] Nonetheless, it is suggested that the formation of a protein network on the most hydrophobic substrate ($–OH_0$) must increase the strength of the material-protein interaction: cells are able to adhere and spread in a similar way as on the control glass [Fig. 1(a)] although residing on strongly hydrophobic substrate [$–OH_0$, Fig. 1(f)]; however, cell mediated FN-reorganization could only take place on the control glass but not on $–OH_0$ substrate [Fig. 4(a)],

which suggests that FN is rather strongly bound compared to control glass, where it adsorbs more loosely.[7–10] Nevertheless, focal adhesion contacts are well developed on both surfaces (Fig. 2). Thus, very different FN conformations on the substrate may result in a similar cell response, which suggests that protein conformation and the strength of cellular interaction cannot be simply correlated (or even considered independently) when one tries to understand cell-material interactions, that is, excellent cell adhesion may occur even if cells are unable to reorganize adsorbed FN before rendering their own matrix as long as the protein-material interaction lead to the adequate protein conformation of the substrate. As the amount of $–OH_0$ groups on the surface increases cell adhesion and spreading diminish (Table II), as well as the number of focal adhesion points. On the $–OH_{30}$substrate, pre-adsorbed FN is still able to form interconnected fibrils in a network like fashion which correlated with relatively good cell spreading [Fig. 1(e)] and focal adhesion formation [Fig. 2(e)] even if cell-mediated FN reorganization cannot take place on the substrate [Fig. 4(e)]. Higher amounts of hydroxyl groups (above 50%: $–OH_{50}$, $–OH_{70}$, $–OH_{100}$) lead to poor cell adhesion and, consequently, to poorer spreading and focal adhesion formation [see Figs. 1, 2, and 4(b–d)]. AFM data show that on these substrates FN adsorption takes place in a globular-like conformation and there is no protein network formation [Fig. 5(d–f)]. For this group of substrates, cell-mediated FN reorganization does not take place presumably because of the conformation of the adsorbed FN is not good enough to allow initial cell adhesion, which are required before starting the matrix reorganization process.[10, 37]

Late FN matrix formation-after 3 days of culture was again excellent on the more hydrophobic substrates and decreased as the fraction of –OH groups increased in good agreement with cell adhesion and focal adhesions formation. Cells are also able to secrete their own extracellular matrix on the control glass. Altogether this suggests that even unable to organize the preadsorbed FN on the substrate, the fibroblasts respond on this FN network, presumably because the conformation of the protein provides the adequate signals which stimulate their normal matrix-forming activity.[10]

Our results suggest that the distinction between hydrophilic and hydrophobic features of a substrate is insufficient to explain the general trends underlying the cell-material interaction, and more factors must be taken into account. For instance, it has been reported that the ability of fibroblasts to secrete ECM proteins is greatly reduced on hydrophobic substrates, [9] even if cell adhesion takes place, what clearly differs from the results in this work. Rather, fibroblast functional behavior on a synthetic substrate depends in a subtle way on the particular substrate chemistry that influences the process of protein adsorption. Both protein conformation on the substrate and the intensity of the protein-material bond play a fundamental role on cell behavior: the adequate protein conformation on the substrate — leading to a substrate induced FN fibrillogenenis — results in excellent cell adhesion and matrix formation (for low –OH contents in this work), even if pre-adsorbed FN cannot be removed by cells. Alternatively, if protein conformation is good enough so as to support initial cell adhesion, cells will be able to remove the initial FN layer and secrete their

own extracellular matrix (as it happens in the control glass). Higher –OH fractions in the substrate lead to inadequate protein conformation on the substrate, which does not support good cell adhesion and consequently leads to diminished functionality.

Conclusions

FN conformation depends on the substrate density of hydroxyl groups. On the more hydrophobic substrates, FN is capable of establishing FN–FN interactions, which lead to the formation of a protein network, directly revealed by AFM, enhancing the protein-material interaction. The kinetics of FN fibrillogenesis was observed by AFM after different adsorption times. The presence of a protein network on the material favors fibroblast adhesion and late matrix formation, even if cells are not able to reorganize the preadsorbed FN layer. Higher amounts of hydroxyl groups on the substrate diminished cell adhesion and functionality: protein conformation is not adequate to cluster integrins and to direct adequate signals to the cell interior.

AFM was performed under the technical guidance of the Microscopy Service at the Universidad Politecnica de Valencia, whose advice is greatly appreciated. Image analysis was performed by Dr. David Moratal.

References

1. Gumbiner BM. Cell adhesion: The molecular basis of tissue architecture and morphogenesis. Cell 1996; 84:345–357.
2. Garcı´a AJ. Interfaces to control cell-biomaterial adhesive interactions. Adv Polym Sci 2006; 203:171–190.
3. Werner C, Pompe T, Salchert K. Modulating extracellular matrix at interfaces of polymeric materials. Adv Polym Sci 2006; 203:63–93.
4. Erickson HP, McDonagh J. Fibronectin molecule visualized in electron microscopy: A long, thin, flexible strand. J Cell Biol 1981; 91:673–678.
5. Erickson HP, Carell NA. Fibronectin in extended and com pact conformations. Electron microscopy and sedimentation analysis. J Biol Chem 1983; 258:14539–14544.
6. Pearlstein E, Gold LI, Garcia-Pardo A. Fibronectin: A review of its structure and biological activity. Mol Cell Biochem 1980; 29:103–128.
7. Altankov G, Groth T. Reorganization of substratum-bound fibronectin on hydrophilic and hydrophobic materials is related to biocompatibility. J Mater Sci Mater Med 1994; 5: 732–737.
8. Altankov G, Groth T. Fibronectin matrix formation and the biocompatibility of materials. J Mater Sci Mater Med 1996; 7: 425–429.
9. Altankov G, Grinnell F, Groth T. Studies of the biocompatibility of materials: Fibroblast reorganization of substratum - bound fibronectin on surfaces varying in wettaability. J Biomed Mater Res 1996; 30:385–391.
10. Tzoneva R, Groth T, Altankov G, Paul D. Remodeling of fibrinogen by endothelial cells in dependence on fibronectin matrix assembly. Effect of substratum wettability. J Mater Sci: Mater Med 2002; 13:1235–1244.
11. Garcia AJ. Get a grip: Integrins in cell-biomaterial interactions. Biomaterials 2005; 26:7525–7529.
12. Hynes RO. Integrins: Bidirectional, allosteric signaling machines. Cell 2002; 110:673–687.
13. Mao Y, Schwarzbauer JE. Fibronectin fibrillogenesis, a cell-mediated matrix assembly process. Matrix Biol 2005; 24:389–399.
14. Keselowsky BG, Collard DM, Garcı´a AJ. Surface chemistry modulates fibronectin conformation and directs integrin binding and specificity to control cell adhesion. J Biomed Mater Res A 2003; 66:247–259.
15. Michael KE, Vernekar VN, Keselowsky BG, Meredith JC, Latoru RA, Garcı´a AJ. Adsorption-induced conformational changes in fibronectin due to interactions with well-defined surface chemistries. Langmuir 2003; 19:8033–8040.
16. Garcia AJ, Boettiger DB. Integrin-fibronectin interactions at the cell-material interface: Initial

integrin binding and signaling. Biomaterials 1999; 20:2427–2433.

17. Toworfe GK, Composto RJ, Adams CS, Shapiro IM, Ducheyne P. Fibronectin adsorption on surface-activated poly(dimethylsiloxane) and its effect on cellular function. J Biomed Mater Res 2004; 71A:449–461.
18. Baugh L, Vogel L. Structural changes of fibronectin adsorbed to model surfaces probed by fluorescence resonance energy transfer. J Biomed Mater Res 2004; 69A:525–534.
19. Lan MA, Gersbach CA, Michael KE, Keselowsky BG, Garcia AJ. Myoblast proliferation and differentiation on fibronectin-coated selfassembled monolayers presenting different surface chemistries. Biomaterials 2005; 26:4523–4531.
20. Grinnell F, Feld MK. Fibronectin adsorption on hydrophilic and hydrophobic surfaces detected by antibody binding and analyzed during cell adhesion in serum-containing medium. J Biol Chem 1982; 257:4888–4893.
21. Altankov G, Thom V, Groth T, Jankova K, Jonsson G, Ulbricht M. Modulating the biocompatibility of polymer surfaces with poly (ethylene glycol): Effect of fibronectin. J Biomed Mater Res A 2000; 52:219–230.
22. Toworfe GK, Composto RJ, Adams CS, Shapiro IM, Ducheyne P. Fibronectin adsorption on surface-activated poly(dimethylsiloxane) and its effect on cellular function. J Biomed Mater Res 2004; 71A:449–46.
23. Baugh L, Vogel L. Structural changes of fibronectin adsorbed to model surfaces probed by fluorescence resonance energy transfer. J Biomed Mater Res 2004; 69A:525–534.
24. Kowalczynska HM, Nowak-Wyrzykowska M, Kolos R, Dobkowski J, Kaminski J. Fibronectin adsorption and arrangement on copolymer surfaces and their significance in cell adhesion. J Biomed Mater Res 2005; 72A:228–236.
25. Altankov G, Richau K, Groth T. The role of surface zeta potential and substratum chemistry for regulation of dermal fibroblast interaction. Mater Eng 2003; 34:1120–1128.
26. Khang D, Yeol K, Liu-Snyder P, Palmore TR, Durbin SM, Webster TJ. Enhanced fibronectin adsorption on carbon nanotube/poly(carbonate) urethane: Independent role of surface nano-roughness and associated surface energy. Biomaterials 2007; 28:4756–4768.
27. Costa Martinez E, Rodriguez Hernandez JC, Machado M, Sanchez M. Tissue Eng 2008; 14:1751–1762.
28. Gomez Ribelles JL, Monleon Pradas M. Substrate chemistry- dependent conformation of single laminin molecules on polymer surfaces are revealed by the phase signal of atomic force microscopy. Biophys J 2007; 93:202–207.
29. Groth T, Altankov G. Studies on cell-biomaterials interactions: Role of tyrosine phosphorylation during fibroblast spreading on surfaces varying in wettability. Biomaterials 1996; 17:1277–1234.
30. Groth T, Altankov G. Cell surface interactions and the tissue compatibility of biomaterials. In:

Harris PI, Chapman D, editors. New Biomedical Materials - Basic and Applied Studies, Biomedical and Health Research, Vol. XVI. Amsterdam, The Netherlands: IOS Press; 1998. p 12–23.

31. Johnson KJ, Sage H, Briscoe G, Erickson HP. The compact conformation of fibronectin is determined by intramolecular ionic interactions. J Biol Chem 1999; 274:15473–15479.
32. Campillo Fernandez F, Salmeron Sanchez M, Sabater I, Serra R, Meseguer Duenas JM, Gomez Ribelles JL. Water-induced nanophase separation in poly(ethyl acrylate-co-hydroxyethyl acrylate) copolymer networks. Eur Polym J 2003; 44:1996–2004.
33. Brıgido Diego R, Salmeron Sanchez M, Gomez Ribelles JL, Monleon Pradas M. Effect of γ-irradiation on the structure of poly(ethyl acrylate-co-hydroxyethyl methacrylate) copolymer networks for biomedical applications. J Mater Sci: Mater Med 2007; 18:693–698.
34. Tamada Y, Ikada Y. Fibroblast growth on polymer surfaces and biosynthesis of collagen. Biomed Mater Res 1994; 28:783–789.
35. Arima Y, Iwata H. Effect of wettability and surface functional groups on protein adsorption and cell adhesion using well-defined mixed self-assembled monolayers. Biomaterials 2007; 28:3074–3082.
36. Ortega-Vinuesa JL, Tengvall P, Lundström I. Aggregation of HSA. IgG and fibrinogen on methylated silicon surfaces. J Colloid Interface Sci 1998; 207:228–239.
37. Groth T, Altankov G. Studies on cell-biomaterials interactions: Role of tyrosine phosphorylation during fibroblast spreading on surfaces varying in wettability. Biomaterials 1996; 17:1227–1234.

CHAPTER 3

BIOLOGICAL ACTIVITY OF THE SUBSTRATE-INDUCED FIBRONECTIN NETWORK: INSIGHT INTO THE THIRD DIMENSION THROUGH ELECTROSPUN FIBERS

Published in
Langmuir, 2009

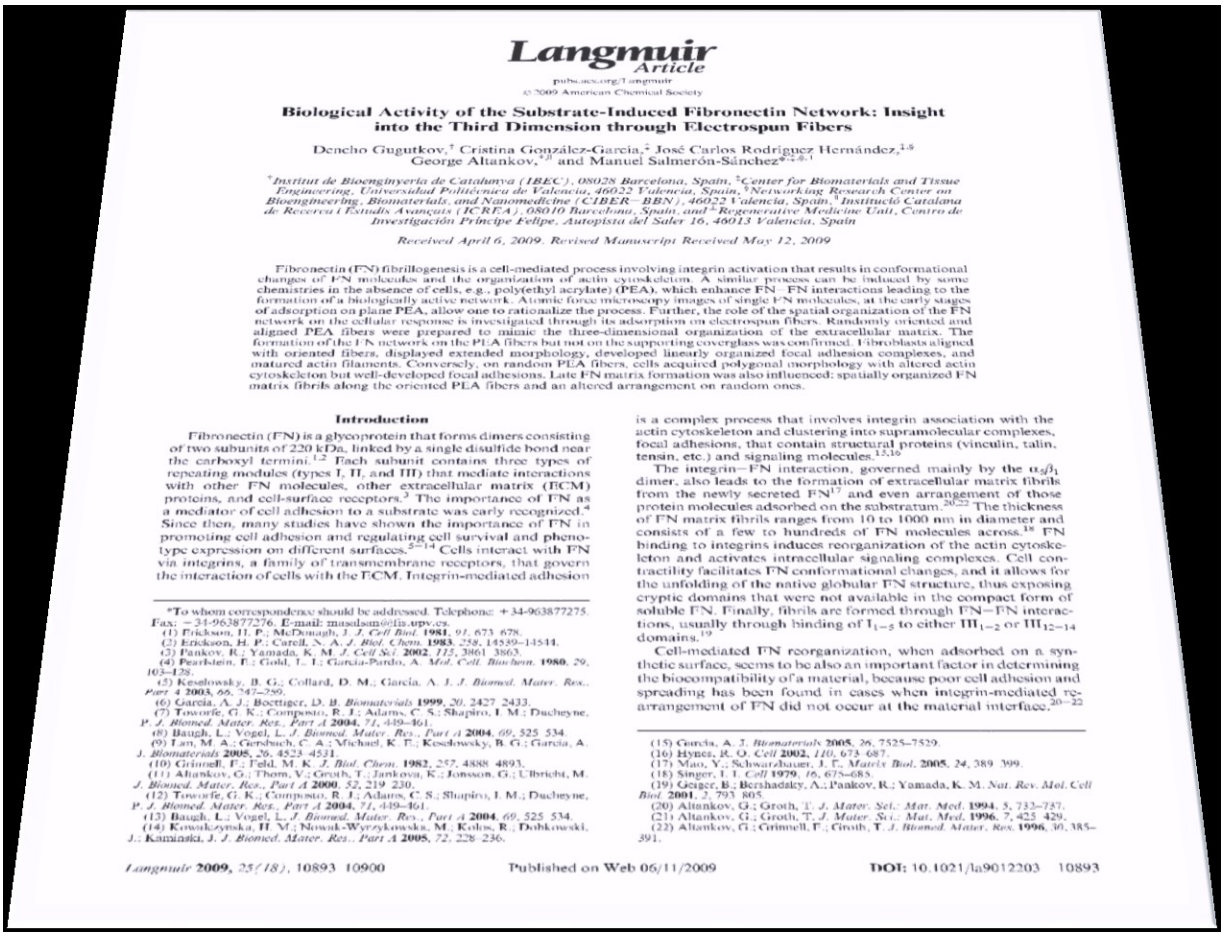

Langmuir
Article
pubs.acs.org/Langmuir
© 2009 American Chemical Society

Biological Activity of the Substrate-Induced Fibronectin Network: Insight into the Third Dimension through Electrospun Fibers

Dencho Gugutkov,† Cristina González-García,‡ José Carlos Rodríguez Hernández,†,§ George Altankov,*,†,∥ and Manuel Salmerón-Sánchez*,⊥,#

†Institut de Bioenginyeria de Catalunya (IBEC), 08028 Barcelona, Spain, ‡Center for Biomaterials and Tissue Engineering, Universidad Politécnica de Valencia, 46022 Valencia, Spain, §Networking Research Center on Bioengineering, Biomaterials, and Nanomedicine (CIBER–BBN), 46022 Valencia, Spain, ∥Institució Catalana de Recerca i Estudis Avançats (ICREA), 08010 Barcelona, Spain, and ⊥Regenerative Medicine Unit, Centro de Investigación Príncipe Felipe, Autopista del Saler 16, 46013 Valencia, Spain

Received April 6, 2009. Revised Manuscript Received May 12, 2009

Fibronectin (FN) fibrillogenesis is a cell-mediated process involving integrin activation that results in conformational changes of FN molecules and the organization of actin cytoskeleton. A similar process can be induced by some chemistries in the absence of cells, e.g., poly(ethyl acrylate) (PEA), which enhance FN−FN interactions leading to the formation of a biologically active network. Atomic force microscopy images of single FN molecules, at the early stages of adsorption on plane PEA, allow one to rationalize the process. Further, the role of the spatial organization of the FN network on the cellular response is investigated through its adsorption on electrospun fibers. Randomly oriented and aligned PEA fibers were prepared to mimic the three-dimensional organization of the extracellular matrix. The formation of the FN network on the PEA fibers but not on the supporting coverglass was confirmed. Fibroblasts aligned with oriented fibers, displayed extended morphology, developed linearly organized focal adhesion complexes, and matured actin filaments. Conversely, on random PEA fibers, cells acquired polygonal morphology with altered actin cytoskeleton but well-developed focal adhesions. Late FN matrix formation was also influenced: spatially organized FN matrix fibrils along the oriented PEA fibers and an altered arrangement on random ones.

Introduction

Fibronectin (FN) is a glycoprotein that forms dimers consisting of two subunits of 220 kDa, linked by a single disulfide bond near the carboxyl termini.[1,2] Each subunit contains three types of repeating modules (types I, II, and III) that mediate interactions with other FN molecules, other extracellular matrix (ECM) proteins, and cell-surface receptors.[3] The importance of FN as a mediator of cell adhesion to a substrate was early recognized.[4] Since then, many studies have shown the importance of FN in promoting cell adhesion and regulating cell survival and phenotype expression on different surfaces.[5−14] Cells interact with FN via integrins, a family of transmembrane receptors, that govern the interaction of cells with the ECM. Integrin-mediated adhesion is a complex process that involves integrin association with the actin cytoskeleton and clustering into supramolecular complexes, focal adhesions, that contain structural proteins (vinculin, talin, tensin, etc.) and signaling molecules.[15,16]

The integrin−FN interaction, governed mainly by the $\alpha_5\beta_1$ dimer, also leads to the formation of extracellular matrix fibrils from the newly secreted FN[17] and even arrangement of those protein molecules adsorbed on the substratum.[20,22] The thickness of FN matrix fibrils ranges from 10 to 1000 nm in diameter and consists of a few to hundreds of FN molecules across.[18] FN binding to integrins induces reorganization of the actin cytoskeleton and activates intracellular signaling complexes. Cell contractility facilitates FN conformational changes, and it allows for the unfolding of the native globular FN structure, thus exposing cryptic domains that were not available in the compact form of soluble FN. Finally, fibrils are formed through FN−FN interactions, usually through binding of I_{1-5} to either III_{1-2} or III_{12-14} domains.[19]

Cell-mediated FN reorganization, when adsorbed on a synthetic surface, seems to be also an important factor in determining the biocompatibility of a material, because poor cell adhesion and spreading has been found in cases when integrin-mediated rearrangement of FN did not occur at the material interface.[20−22]

*To whom correspondence should be addressed. Telephone: +34-963877275. Fax: −34-963877276. E-mail: maselsan@ifa.upv.es.

(1) Erickson, H. P.; McDonagh, J. *J. Cell Biol.* **1981**, *91*, 673–678.
(2) Erickson, H. P.; Carrell, N. A. *J. Biol. Chem.* **1983**, *258*, 14539–14544.
(3) Pankov, R.; Yamada, K. M. *J. Cell Sci.* **2002**, *115*, 3861–3863.
(4) Pearlstein, E.; Gold, L. I.; García-Pardo, A. *Mol. Cell. Biochem.* **1980**, *29*, 103–128.
(5) Keselowsky, B. G.; Collard, D. M.; García, A. J. *J. Biomed. Mater. Res., Part A* **2003**, *66*, 247–259.
(6) García, A. J.; Boettiger, D. *B. Biomaterials* **1999**, *20*, 2427–2433.
(7) Towsoffe, G. K.; Composto, R. J.; Adams, C. S.; Shapiro, I. M.; Ducheyne, P. *J. Biomed. Mater. Res., Part A* **2004**, *71*, 449–461.
(8) Baugh, L.; Vogel, L. *J. Biomed. Mater. Res., Part A* **2004**, *69*, 525–534.
(9) Lan, M. A.; Gersbach, C. A.; Michael, K. E.; Keselowsky, B. G.; García, A. J. *Biomaterials* **2005**, *26*, 4523–4531.
(10) Grinnell, F.; Feld, M. K. *J. Biol. Chem.* **1982**, *257*, 4888–4893.
(11) Altankov, G.; Thorn, V.; Groth, T.; Jankova, K.; Jonsson, G.; Ulbricht, M. *J. Biomed. Mater. Res., Part A* **2000**, *52*, 219–230.
(12) Towsoffe, G. K.; Composto, R. J.; Adams, C. S.; Shapiro, I. M.; Ducheyne, P. *J. Biomed. Mater. Res., Part A* **2004**, *71*, 449–461.
(13) Baugh, L.; Vogel, L. *J. Biomed. Mater. Res., Part A* **2004**, *69*, 525–534.
(14) Krwalczynska, H. M.; Nowak-Wyrzykowska, M.; Kolos, R.; Dobkowski, J.; Kamiński, J. *J. Biomed. Mater. Res., Part A* **2005**, *72*, 228–236.
(15) García, A. J. *Biomaterials* **2005**, *26*, 7525–7529.
(16) Hynes, R. O. *Cell* **2002**, *110*, 673–687.
(17) Mao, Y.; Schwarzbauer, J. T. *Matrix Biol.* **2005**, *24*, 389–399.
(18) Singer, I. I. *Cell* **1979**, *16*, 675–685.
(19) Geiger, B.; Bershadsky, A.; Pankov, R.; Yamada, K. M. *Nat. Rev. Mol. Cell Biol.* **2001**, *2*, 793–805.
(20) Altankov, G.; Groth, T. *J. Mater. Sci.: Mat. Med.* **1994**, *5*, 732–737.
(21) Altankov, G.; Groth, T. *J. Mater. Sci.: Mat. Med.* **1996**, *7*, 425–429.
(22) Altankov, G.; Grinnell, F.; Groth, T. *J. Biomed. Mater. Res.* **1996**, *30*, 385–391.

Published online 06 November 2009 in www.pubs.acs.org/Langmuir
Langmuir 2009, 25(18), 10893–10900
DOI: 10.1021/la9012203 10893

Preface to Chapter 3

The results provided in the previous Chapter 2 clearly suggested that the **fibronectin network** is strongly **bioactive** and can be used for guiding the behavior of cells by simply varying the efficiency of its formation on the material interface. The FN network applied in this study however, is a two dimensional (2D) structure formed on a model planar substratum, while the natural cellular environment in most cases is three-dimensional (3D). Therefore, in the present study we strived to switch the system to the **third dimension** by providing the cells with a **bioactive nanofibrous environment**. Indeed, we succeed to produce nanofibers from pure PEA – the polymer supporting best of FN network formation – using the classical vertical electrospinning technology, but in our own set-up and original technique for production of aligned fibers (see illustration). Thus, we could electrospun PEA nanofibers with different organization, random and aligned, which gave us opportunity to compare their effects on the cells. The rationale behind is that we were looking for a geometric cell response as indirect proof that cells recognize the **substratum assembled FN network**, now provided in 3D form.

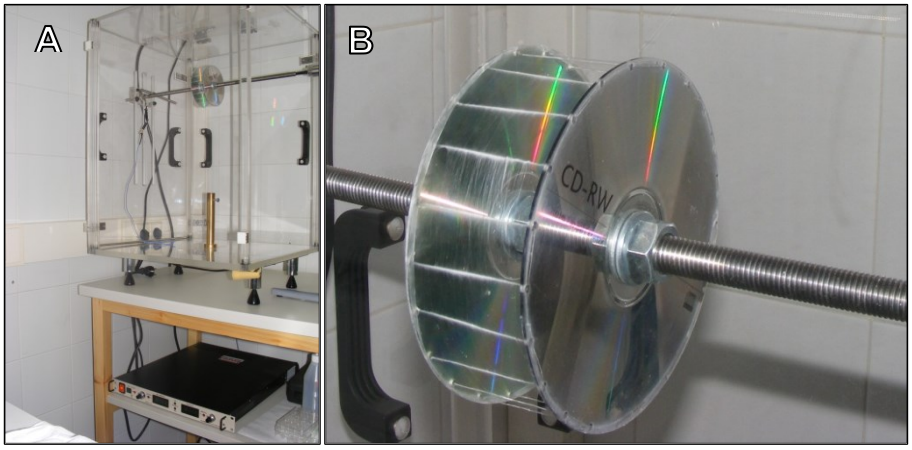

*Illustration of our Electrospinning set-up used for the production of nanofibers **(A);** Tailor made rotating collector for production of aligned nanofibers **(B),** originally designed by the author of this Thesis*

We note again, this work was performed in very close cooperation with Prof Salmeron-Sanchez group contributing particularly on the characterization of nanofibers and the nanoindentation of the FN network.

Indeed, the results obtained clearly suggest that fibroblasts respond strictly to the third dimension, acquiring distinct morphology (stellate-like on random and extended on aligned), which imply on the biological significance of the signal originating from the FN network. Interestingly the fibers orientation affected also the organization of the lately synthesized fibroblast FN matrix, which further confirms the applicability of material driven FN network formation for guiding the cell behavior in a long-term. Details for this study may be found in the original paper ***"Biological activity of the substrate-induced fibronectin network: insight into the third dimension through electrospun fibers"***, presented in this Chapter.

Abstract

Fibronectin (FN) fibrillogenesis is a cell-mediated process involving integrin activation that results in conformational changes of FN molecules and the organization of actin cytoskeleton. A similar process can be induced by some chemistries in the absence of cells, e.g., poly(ethyl acrylate) (PEA), which enhance FN-FN interactions leading to the formation of a biologically active network. Atomic force microscopy images of single FN molecules, at the early stages of adsorption on plane PEA, allow one to rationalize the process. Further, the role of the spatial organization of the FN network on the cellular response is investigated through its adsorption on electrospun fibers. Randomly oriented and aligned PEA fibers were prepared to mimic the three-dimensional organization of the extracellular matrix. The formation of the FN network on the PEA fibers but not on the supporting coverglass was confirmed. Fibroblasts aligned with oriented fibers, displayed extended morphology, developed linearly organized focal adhesion complexes, and matured actin filaments. Conversely, on random PEA fibers, cells acquired polygonal morphology with altered actin cytoskeleton but well-developed focal adhesions. Late FN matrix formation was also influenced: spatially organized FN matrix fibrils along the oriented PEA fibers and an altered arrangement on random ones.

Introduction

Fibronectin (FN) is a glycoprotein that forms dimers consisting of two subunits of 220 kDa, linked by a single disulfide bond near the carboxyl termini.[1, 2] Each subunit contains three types of repeating modules (types I, II, and III) that mediate interactions with other FN molecules, other extracellular matrix (ECM) proteins, and cell-surface receptors.[3] The importance of FN as a mediator of cell adhesion to a substrate was early recognized.[4] Since then, many studies have shown the importance of FN in promoting cell adhesion and regulating cell survival and phenotype expression on different surfaces.[5]-14 Cells interact with FN via integrins, a family of transmembrane receptors, that govern the interaction of cells with the ECM. Integrin-mediated adhesion is a complex process that involves integrin association with the actin cytoskeleton and clustering into supramolecular complexes, focal adhesions, that contain structural proteins (vinculin, talin, tensin, etc.) and signaling molecules.[15, 16]

The integrin-FN interaction, governed mainly by the $\alpha_5\beta_1$ dimer, also leads to the formation of extracellular matrix fibrils from the newly secreted FN[17]and even arrangement of those protein molecules adsorbed on the substratum.[20, 22] The thickness of FN matrix fibrils ranges from 10 to 1000 nm in diameter and consists of a few to hundreds of FN molecules across.[18] FN binding to integrins induces reorganization of the actin cytoskeleton and activates intracellular signaling complexes. Cell contractility facilitates FN conformational changes, and it allows for the unfolding of the native globular FN structure, thus exposing cryptic domains that were not available in the compact form of soluble FN. Finally, fibrils are formed through FN-FN interactions, usually through binding of $I_{1\text{-}5}$ to either $III_{1\text{-}2}$ or $III_{12\text{-}14}$ domains.[19]

Cell-mediated FN reorganization, when adsorbed on a synthetic surface, seems to be also an important factor in determining the biocompatibility of a material, because poor cell adhesion and spreading has been found in cases when integrin-mediated rearrangement of FN did not occur at the material interface.[20 – 22]

Article

Previous investigations have shown that fibroblasts and endothelial cells tend to rearrange adsorbed matrix proteins, such as FN and fibrinogen, in a fibril-like pattern. Using model surfaces, mostly self-assembled monolayers (SAMs), it is shown that cellular activity is mainly dependent upon the surface properties of materials, such as wettability, surface chemistry, and charge.[23,25] This evidence raises the possibility that tissue compatibility of materials may be connected to the allowance of cells to remodel surface-associated proteins, presumably as an attempt to form their own provisional matrix; e.g., materials that bind proteins loosely will support the organization of a provisional ECM. This concept, however, raises many limitations to the biomaterials selection; therefore, to obtain a system that supports spontaneous fibrillogenesis of surface-associated FN is highly desirable.

It has been shown that the existence of mechanical tension is necessary for efficient integrin-mediated FN fibrillogenesis.[26, 27] Fibrillar networks of FN have been generated also in the absence of cells by means of interactions with the underlying substrate that involves mechanical events at the molecular scale. FN fibrillogenesis upon contact with a lipid monolayer was explained through mechanical tension caused by domain separation in the lipid monolayer that pulls the protein into an extended conformation. [28] The assembly of FN into fibers was obtained also by applying forces to FN molecules via poly(dimethylsiloxane) (PDMS) micropillars at different stages of fibrillogenesis.[29] We have recently shown that FN fibrillogenesis can take place as a consequence of the sole interaction between the protein molecules and a material surface with the appropriate surface chemistry; in concrete, a spontaneous formation of biologically active FN network was found in vitro after its adsorption on poly(ethyl acrylate) (PEA).[30, 31]

This work further assesses the biological activity of the substrate-induced FN network assembled on electrospun PEA fibers. The electrospinning technique allows for the production of very thin fibers with very large specific surface areas. The technique has gained importance in recent years for biomedical applications, such as tissue engineering, drug release, wound dressing, and enzyme immobilization.[32, 33] Random and aligned PEA fibers have been deposited on glass coverslips. FN fibrillogenesis on this electrospun substrate was directly observed by atomic force microscopy (AFM). The biological activity of the protein was assessed by *in vitro* culture of fibroblasts that respond to fiber organization as a consequence of FN network-cell interaction.

Experimental section

Substrate preparation

Polymer sheets were obtained by polymerization of a solution of ethyl acrylate (EA, 99% pure, Aldrich, Steinheim, Germany) using 0.1 wt % of benzoin (98% pure, Scharlau, Barcelona, Spain) as a photoinitiator. The polymerization was carried out up to limiting conversion. After polymerization, low-molecular-mass substances were extracted from the material by boiling in ethanol for 24 h and then drying in vacuum to a constant weight.

PEA was dissolved in hexafluoroisopropanol (HFP) at 30 mg/mL at room temperature. Randomly deposited PEA microfibers with a size in the range of 2-3 μm (see Figure 3) were obtained by electrospinning the polymer solution for 2 min onto 15 mm round-shaped glass coverslips (Termo Scientific/Menzel-Glaser, Germany) placed on grounded aluminum foil. The applied voltage was 20 kV; the distance to the collector was 125 mm; and the flow rate was 300 μL/h. Aligned fibers were obtained under the same conditions, but the polymer solutions were electrospun for 5-6 min onto a rotating drum (1000 rpm) consisting of two parallel plastic discs (120 mm diameter) spaced at 15 mm that are mounted at one and the same axis and connected in their periphery with 0.5 mm grounded coiled metal wire (21 parallel coils in a distance of 16 mm). The fibers, which align perpendicularly between the wires, were finally collected with glass coverslips.

Scanning Electron Microscopy (SEM)

SEM analysis of the electrospun fibers was carried out in a Jeol JSM-5410 scanning electron microscope. Samples were coated with a conductive layer of sputtered gold. The micrographs were taken at an accelerating voltage of 10 kV to ensure a suitable image resolution.

Fast Fourier transformation (FFT) analysis of the SEM pictures was used to characterize the alignment of the fibers. A graphical description of the FFT frequency distribution was performed by placing a circular projection on the FFT output image using the Oval Profile plug-in and collecting the radial sums of the pixel intensities for each degree between 0° and 360°, in 1° step increments.[34]Analysis of the SEM micrographs was performed with ImageJ software (NIH, http://rsb.info.nih.gov/ij) with installed Oval Profile plug-in (authored by William O'Connell). All FFT data were normalized to a baseline value and plotted in arbitrary units, allowing different data sets to be directly compared.

AFM

AFM experiments were performed using a Multimode AFM equipped with a NanoScope IIIa controller from Veeco (Manchester, U.K.) operating in tapping mode in air; the Nanoscope 5.30r2 software version was used. Si-cantilevers from Veeco (Manchester, U.K.) were used with a force

constant of 2.8 N/m and resonance frequency of 75 kHz. The phase signal was set to zero at a frequency of 5-10% lower than the resonance one. The drive amplitude was 600 mV, and the amplitude set point A_{sp} was 1.6 V. The ratio between the amplitude set point and the free amplitude A_{sp}/A_0 was kept equal to 0.7.

FN from human plasma (Roche, Mannheim, Germany) was adsorbed on the different substrates by immersing the material sheets in 20 µg/mL physiological solution (NaCl 0.9%) for 10 min.

After protein adsorption, samples were rinsed 3 times in the physiological solution to eliminate the non-adsorbed protein. Remaining drops on the surface were dried by exposing the sample to a nitrogen flow for 2-3 min. AFM was performed in the tapping mode in air immediately after sample preparation. Both height, phase, and amplitude magnitudes were recorded for each image.

Cells

Human dermal fibroblasts (PromoCell, Germany, catalog number C-12302) were cultured in Dulbecco's modified Eagle's medium (DMEM) supplemented with 10% fetal bovine serum (FBS), 1 mM sodium pyruvate, 2 mM L-glutamine, and penicillin-streptomycin, all of them purchased from Invitrogen.

Cell Adhesion and Overall Morphology

To investigate the initial cell adhesion and overall cell morphology, 5 x 10^4cells/well were seeded in 24-well TC plates (Nunc, Denmark) containing the samples of PEA fibers and control glass slides at a final volume of 1 mL serum-free medium. All samples were precoated with FN (20 µg/mL) for 30 min at 37 °C. After 2h of incubation, the cells were fixed with 4% paraformaldehyde (5 min), permeabilized with 0.5% Triton X-1000 (5 min), and stained with FITC-Phaloidin (Invitrogen) (dilution 1:100) for 30 min to visualize actin cytoskeleton before washed and mounted with Mowiol (Polysciences, Inc.). Representative pictures of the adhered cells were then taken at low magnification (10x) using the green channel (excitation BP, 450-490 nm; beam splitter FT, 510 nm; emission LP, 515 nm) of a fluorescent microscope (Zeiss, Axiovert 40) equipped with digital camera IMag (Inrey Solutins, Bulgaria) and the corresponding software.

Visualization of Focal Adhesions

The cells were seeded as described above. To visualize focal adhesions, fixed and permeabilized samples were saturated with 1% albumin in phosphate- buffered saline (PBS) (15 min) and immunofluorencently stained for vinculin using monoclonal anti vinculin antibody (Sigma, catalog number V9131) dissolved in 1% BSA in PBS for 30 min followed Cy3-conjugated goat anti-mouse IgG (H + L) (Jackson ImmunoResearch, catalog number 115-165-062) as a secondary antibody (30 min). To simultaneously visualize actin, FITC-phalloidin (Invitrogen) was added to the secondary

antibody solution at a final concentration of 1:100. The samples were viewed and photographed on an inverted fluorescent microscope as above. Representative images were acquired on the green and red channel (excitation BP, 530-585 nm; beam splitter FT, 600 nm; emission LP, 615nm) and superimposed with ImageJ software.

FN Matrix Formation

The ability of fibroblasts to secrete and deposit FN into the extracellular matrix fibrils (i.e., late matrix) was examined also via immunofluorescence. For that, 3 x 10^4 cells/well were cultured on the different substrates for 3 days in serum-containing medium. At the end of incubation, the cells were fixed and saturated as previously described and further stained with a polyclonal rabbit anti-FN antibody (Santa Cruz Inc., 9068) dissolved in 1% bovine serum albumin (BSA) in PBS for 30 min, followed by goat anti-rabbit Cy3-conjugated (Jackson ImmunoResearch) secondary antibody for 30 min before being washed and mounted with Mowiol.

Results

Randomly and aligned fibers were prepared with similar diameters (approximately 3 μm). Figure 1 shows the SEM micrographs of the electrospun PEA fibers on glass coverslips. Even if simple observation of the SEM pictures allows one to appreciate the distribution of the fibers, the existence of a characteristic direction in the case of Figure 1B and the lack of any principal direction in Figure 1A were assessed by calculating the FFT output for each case, which result in the existence of a

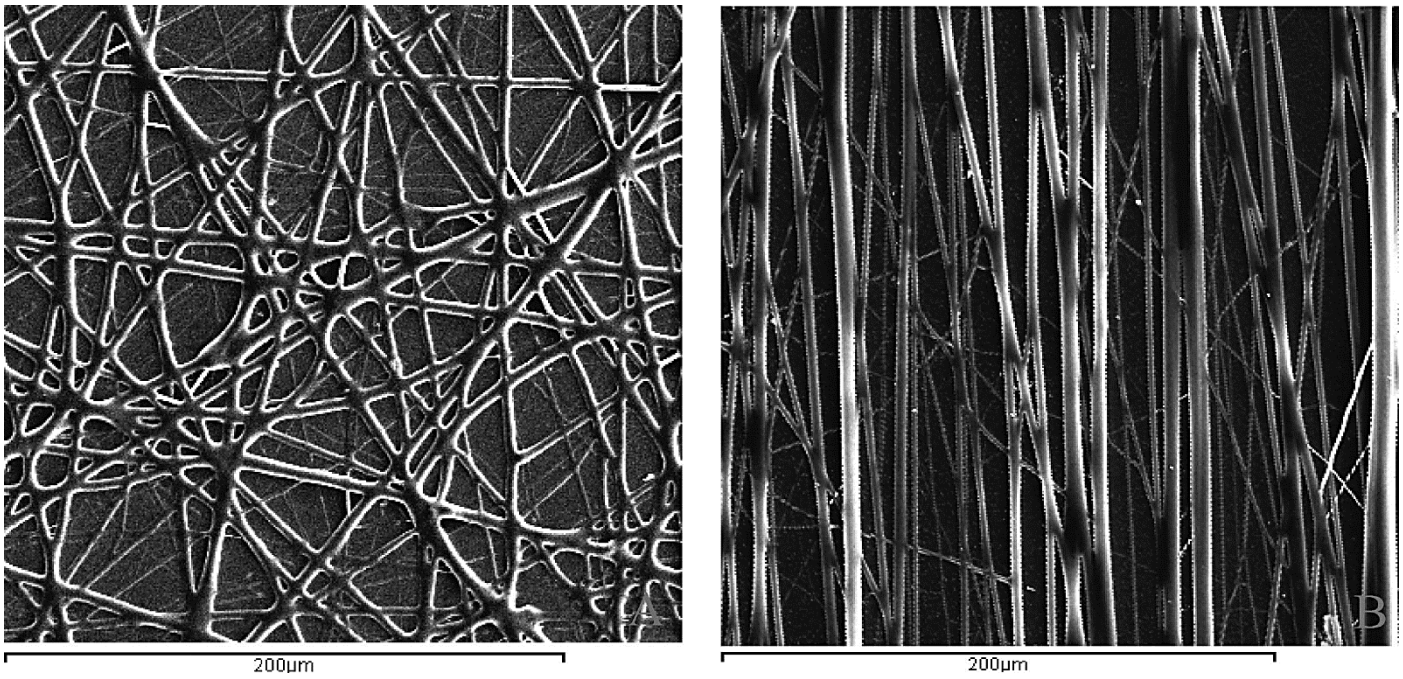

Figure 1. *SEMmicrographs of PEA fibers **(A)** randomly distributed and **(B)** aligned on glass coverslips.*

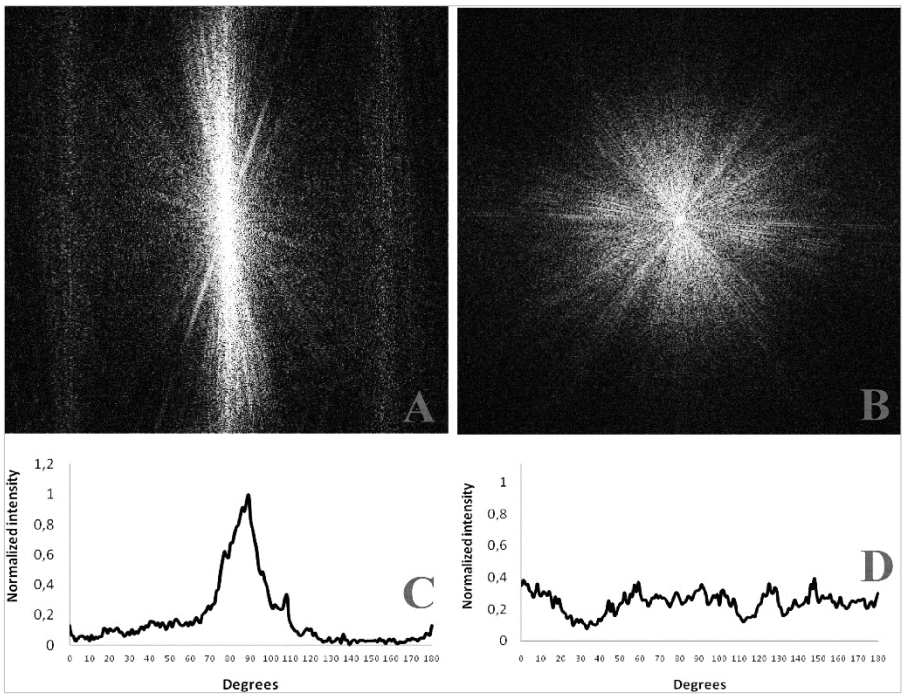

Figure 2. *FFT output images of **(A)** aligned and **(B)** randomly deposited PEA microfibers on glass coverslips. Normalized angular intensity distribution of **(C)** aligned and **(D)** randomly deposited fibers.*

maximum for pixel intensity distribution for the aligned fibers, that corresponds to the direction of alignment and the lack of any characteristic direction for the so-called randomly distributed electrospun fibers (Figure 2).

Figure 3 shows the three-dimensional view of the aligned and randomly distributed electrospun

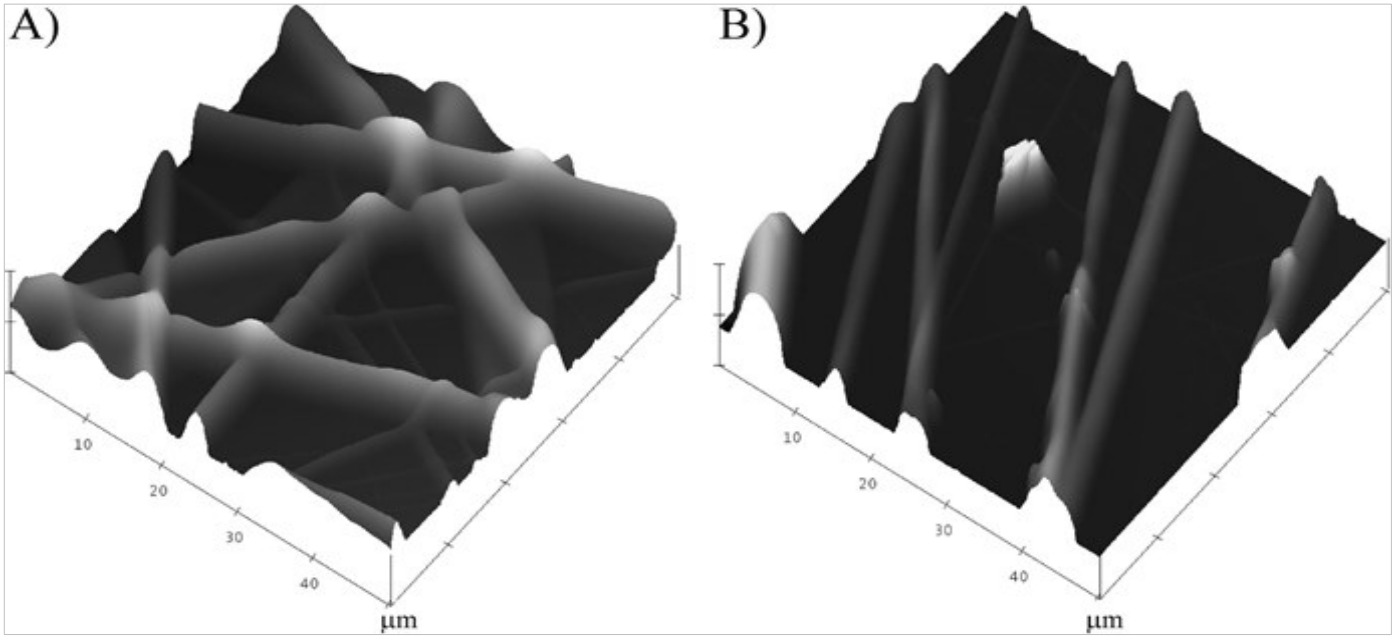

Figure 3. *Three-dimensional view of the electrospun PEA fibers by AFM:* ***(A)*** *randomly distributed and* ***(B)*** *aligned fibers on glass coverslips. The vertical scale is 2 µm.*

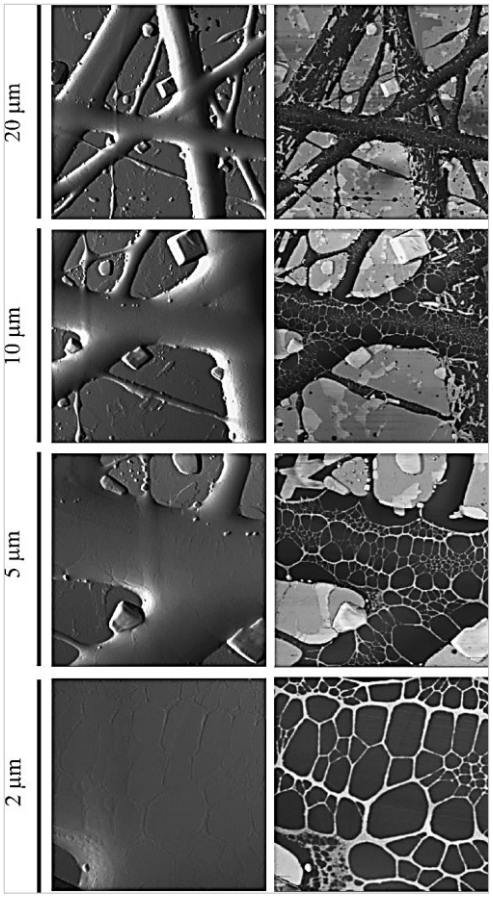

Figure 4. *FN assembly on PEA fibers as observed by AFM (phase, right; amplitude, left). PEA fibers were electrospun on glass coverslips, and FN was adsorbed for 10 min from a solution with a concentration of 20 µg/mL. The FN network is only assembled on the PEA fibers and not on the underlying glass substrate.*

fibers. This figure 3 allows one to infer the real three dimensionality of the fibers, on which protein adsorption and cell adhesion is going to be investigated. The height of the fibers is approximately 2 μm.

Figure 4 shows AFM pictures (different magnifications, phase, and amplitude magnitudes) of the PEA fibers after FN adsorption from a solution with a concentration of 20 μg/mL for 10 min. Large fiber topography prevents FN to be identified from the height magnitude in AFM. Nevertheless, the phase magnitude reveals the existence of a FN network assembled on the electrospun PEA fibers: a substrate-induced FN fibrillogenesis *in vitro* in the absence of cells.[30, 31] Only some salts were observed on the underlying glass substrate without any trace of the protein network on it. FN distribution on the substrate is not well-observed from the amplitude magnitude, even if some traces can be identified from the 2 μm image (Figure 4). However, the amplitude magnitude is appropriate for identification of the electrospun PEA fibers.

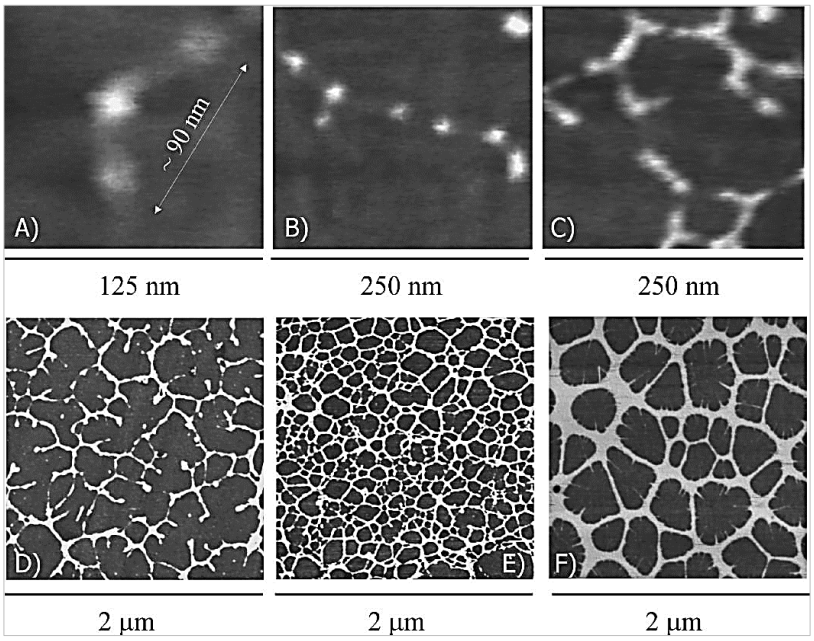

Figure 5. *AFM phase image of single FN molecules on PEA:* ***(A)*** *isolated molecule,* ***(B)*** *two FN molecules interacting through the amino terminal (I_1-5) domains,* ***(C)*** *assembly of FN molecules into an incipient network,* ***(D)*** *assembly of FN into a non-completely interconnected network,* ***(E)*** *interconnected FN network, and* ***(F)*** *thickening of protein arms at higher concentrations. FN was adsorbed for 10 min from solutions with a concentration of 2, 2.5, 3.3, 5, 20, and 50 μg/mL, respectively.*

Figure 5 shows the AFM images of FN adsorbed on plane PEA substrates after immersion for 10 min at protein solutions of different concentrations: 2, 2.5, 3.3, 5, 20, and 50 μg/mL. The lowest concentration (Figure 5A) results in isolated extended FN molecules homogeneously distributed on the material. For a concentration of 2.5 μg/mL (Figure 5B), FN molecules are observed in a higher density. However, extended FN molecules tend to align, suggesting the initial formation of intermolecular connections (Figure 5B). FN conformation in Figure 5C suggests the incipient formation of a protein network on the material when FN was adsorbed from a solution with a concentration of 3.3 μg/mL. Protein adsorption from higher solution concentrations gives rise to the

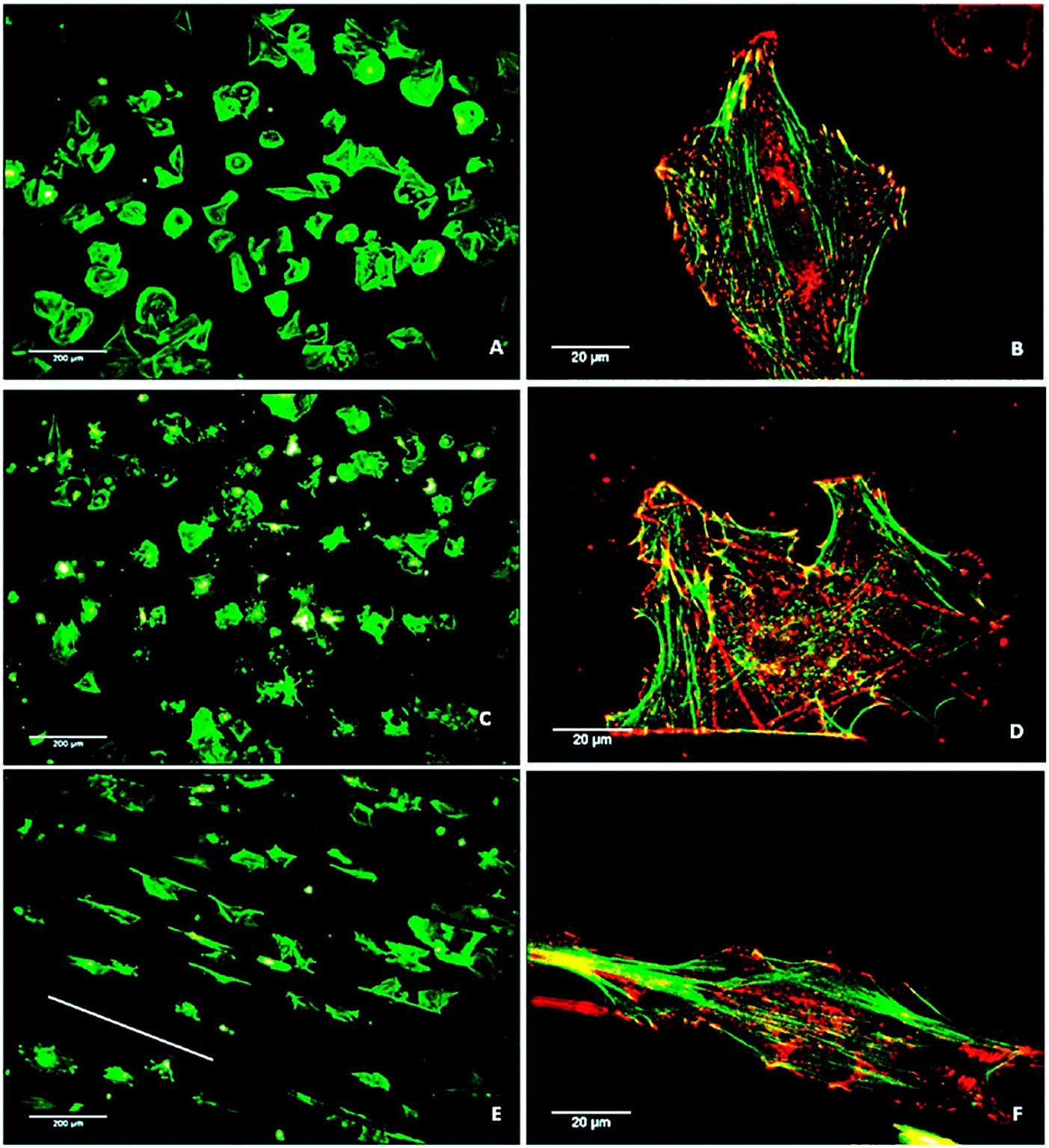

Figure 6. *Overall morphology of fibroblasts adhering on **(C and D**) random and **(E and F)** aligned FN-coated PEA fibers compared to the **(A and B)** control of FN-coated glass vizualized by actin (A, C, and E) or double stained for vinculin (red) and actin (green) **(B, D, and F)**. The line in E represents the main direction of PEA fiber alignment. Magnification for A, C, and E, 10x; bar, 200 µm. Magnification for B, D, and E, 100x; bar, 20 µm.*

formation of FN networks on the material with higher cross-link density, i.e., a higher number of cross-link point and lower distance between them (panels D-F of Figure 5).

The left column in Figure 6 represents the overall morphology of fibroblasts adhering for 2h on FN-coated PEA fibers and control glass, visualized via staining for actin. Irregularly spread cells representing multiple projections were typically observed on randomly dispersed PEA fibers (Figure 6C), presumably resembling early stellate morphology, apart from the fibroblasts on control glass

(Figure 6A), which shows a typical (for 2D substrata) flattened and polarized morphology without prevalent orientation of cells. Conversely, an extended cell shape, parallel to the orientation of the fibers, was observed on aligned PEA fibers (Figure 6E). Cells linearly organize focal adhesion complexes, particularly in the contact zones with PEA fibers (Figure 6F), and well-developed actin stress fibers inserting into the focal adhesions mostly at the extended cell edges (in yellow). On random PEA fibers (Figure 6D), the cells represent less oriented but prominent actin cytoskeleton with well-developed focal adhesion complexes following the multiple directions of the fibers. On control FN- coated glass (Figure 6B), as expected, the fibroblasts represent prominent actin stress fibers inserting to the well-developed focal adhesion at cell edges.[30] It must be remarked here that, if the same experiment is performed without adsorbing any FN on PEA, no cell adhesion is found.

Late FN matrix formation after 3 days of culture was also followed via immunofluorescence (Figure

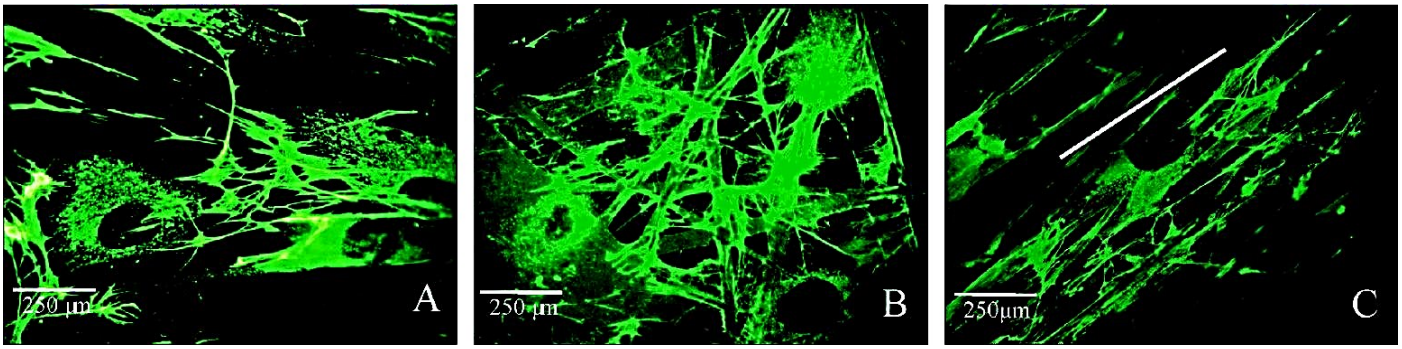

Figure 7. *FN matrix formation by NHD fibroblast on FN-coated PEA fibers after 3 days of culture:* ***(A)*** *control glass,* ***(B)*** *randomly deposited fibers, and* ***(C)*** *aligned fibers. The line in (C) shows the direction of electrospun fibers.*

7). It was found that the cells are able to synthesize and deposit FN matrix fibrils on both the randomly distributed and aligned PEA fibers as well as the control glass. However, matrix distribution is not spatially organized either in the randomly distributed fibers or on the control glass, but FN fibrils clearly follow the direction of PEA fibers when deposited on the aligned samples (Figure 7C).

Discussion

It is well-accepted that FN fibrillization, i.e., the formation of a FN matrix, is a process driven by living cells taking place because of the bidirectional interaction between integrins and the adhesion motifs of the FN molecule [e.g., arginine-glycine-aspartate (RGD) sequence] from one site and the actin cytoskeleton from the other.[17] We have recently shown that FN is able to self-assemble into a network on hydrophobic plane PEA in the absence of cells; that is to say, as a consequence of the protein-material interaction, leading to a so-called substrate-induced FN fibrillogenesis.[30, 31] Moreover, this material-induced fibrillogenesis is a dynamic process that strongly depends upon the amount of protein adsorbed on the substrate and the adsorption time.[30]

This work shows that the formation of a FN network on a PEA substrate is not restricted to plane surfaces but that FN fibrillogenesis can take place on topographic cues, e.g., the electrospun 3D fibers, either randomly distributed or aligned. Moreover, FN fibrillogenesis does not occur on the underlying glass, although the protein is also adsorbed on this surface,[30] but only on the fraction of the substrate covered by PEA fibers (Figure 4). This feature supports the hypothesis that the phenomenon occurs only independently of the topological (2D/3D) disposition of the substrate.

The development of a FN network in the absence of cells gains a distinct bioengineering interest because it is a way to improve the biocompatibility of materials. It is well-documented that cells recognize faster and with higher affinity already assembled FN fibrils versus adsorbed protein.[17-19, 34-36] The existence of cell-free routes able to induce the formation of FN fibrils from isolated molecules have been described in the literature and include (i) the exposition of sulfhydryl groups (able to form disulfide-bonded FN multimers) by adding denaturants, e.g., guanidine 3M,[35] (ii) reduction of disulfide bonds that promotes unfolding of the molecule and non-covalent binding interactions among FN molecules,[36] and (iii) the addition of a fragment from the first type-III repeat of FN that induces spontaneous disulfide cross-linking of the molecule into multimers.[37] Apart from these biochemical routes to induce FN assembly, it has been shown that FN can be assembled into networks after adsorption on certain substrates,(iv) underneath dipalmitoyl phosphatidylcholine (DPPC) monolayers, which resemble the major lipid fraction of cell membranes,[28] and (v) a super hydrophobic surface made of elastic micropillars.[29] Both of these situations require the existence of mechanical tension to drive the process. The formation of FN networks on PEA (Figure 4) must be a consequence of the following sequence of events:

(1) Conformational change upon FN adsorption on PEA. It is known that FN has a compact folded structure in physiological buffer that is stabilized through ionic interactions between arms.[38] The FN (a vinyl backbone with $–COOCH_2CH_3$side chain) gives rise to conformational changes in the molecule that lead to the extension of the protein arms (Figure 5A). Adsorption

of FN on slightly charged surfaces (negative neat group in the $-COO^-$ group) gives rise to elongated structures of the molecule, as obtained for $SiO_2$and glass.[13,39] It is likely that FN orients at the surface, so that its hydrophobic segments interact with the methyl groups in PEA, maybe throughout the heparin-binding fragment, as proposed for the FN-DPPC interaction,[28] but with more efficient arm extension results because of the neat negative charge of the surface.

(2) Enhanced FN-FN interaction on the PEA substrate. The adequate conformation of individual FN molecules as the adsorption process continues favors FN- FN interactions, probably throughout the interaction between I_{1-5} and III_{1-2} domains located near their amino side [3]. Figure 5B shows the relative orientation of two FN molecules compatible with this hypothesis.

(3) New proteins are preferentially adsorbed in close contact to FN molecules already present on the substrate (Figure 5C), probably as a consequence of the presence of polar-oriented FN molecules enhancing the collision rate of FN self-assembly sites,[28] which finally gives rise to the initial formation of a protein network on the substrate. This process leads to a well-interconnected network of FN on the surface of the substrate regardless of its topographic disposition (Figure 4).[30,31]

Figure 8 sketches the above-described sequence of events leading to this substrate-induced FN fibrillogenesis. Adsorption from solutions of higher concentrations leads to the formation of a protein network with thicker arms (panels D-F of Figure 5). The formation of a FN network on PEA is not a universal property of this protein. For example, a similar network was found for fibrinogen,[40] but only globular-isolated molecules were observed after laminin adsorption.[41]

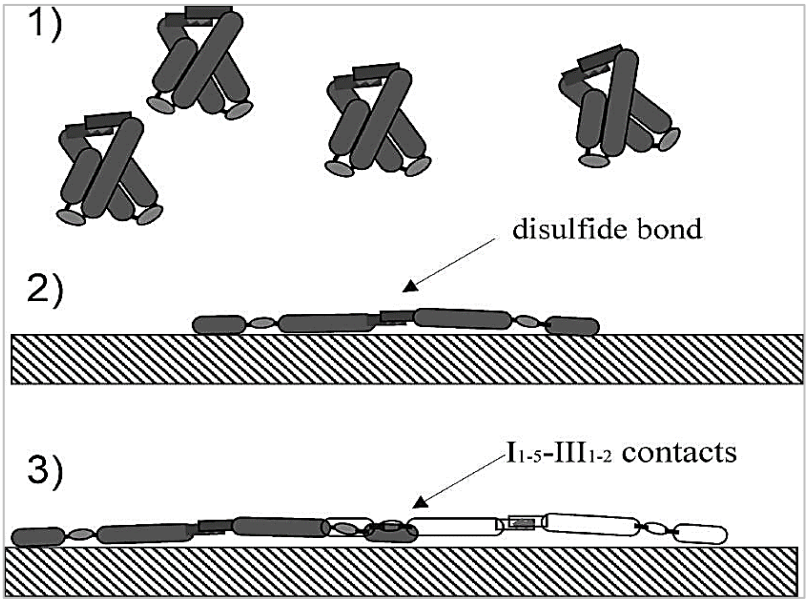

Figure 8. *Sketch of the process leading to FN assembly on PEA surfaces.* ***(1)*** *FN molecules are in compact (folded)conformation in solution.* ***(2)*** *Adsorption of (individual) first FN molecules on PEA results in unfolding of the protein and extension of its arms.* ***(3)*** *FN-FN interactions are enhanced on the substrate leading to a self-assembled FN network.*

More importantly however is that this FN network that assemblies spontaneously on PEA fibers is biologically active (Figure 6) even more than FN directly adsorbed on the underlying glass (Figure 6), but still the substrate-induced FN network cannot be considered to be equivalent to that assembled by cells (even if some characteristic features are shown; e.g., both of them are deoxycholate-insoluble). It is evident that cells tend to interact with PEA fibers rather than glass and start to orient, modifying their characteristic spread morphology, following the fibers direction (panels E and F of Figure 6). Complementary material shows a movie of living cells, which migrate throughout the surface, in a real tactile exploration, until a PEA fiber is found. Afterward, cell morphology is modified to adapt cell-substrate contact along the electrospun PEA fiber. The well-developed focal adhesion complexes and the insertions of actin stress fibers in these complexes point to a proper transmission of signals by integrins to the cell interior. Interestingly, when adhering on random PEA fibers, cells tend to develop a rounded morphology with multiple projections, which resemble stellate morphology, characteristic for cells in the 3D environment. This also means that cells receive proper signals coming from the FN network on the PEA fibers. Moreover, it applies to the oriented fibers as well because fibroblasts immediately acquire extended morphology with asymmetrical organization of the adhesive complexes (Figure 6F), suggesting activation of their motility. In fact, fibroblast movement on PEA fibers is well-demonstrated in the complementary movie (see the Supporting Information); also, the cells may “jump” from the supporting glass to the PEA fibers, e.g., preferring to move on the FN network.

Late FN matrix formation, after 3 days of culture, was again influenced by the formation of the FN network on the PEA fibers, reflecting the high biological activity of the pre-organized protein. Matrix formation was excellent on both the PEA fibers and control glass; however, in agreement with the initial cell adhesion, newly synthesized FN is preferentially deposited on PEA fibers, as is clearly visible in panels B and C of Figure 7 for both types of substrates. Thus, one can assume that, by tailoring the fiber orientation, we can control the organization of the provisional FN matrix secreted by the cells.

Conclusions

We have further investigated self-assembly of FN on PEA leading to the formation of a protein network, e.g., a case of spontaneous FN fibrillogenesis without cell involvement. AFM images of individual molecules during the first stages of the process suggest a mechanism in which FN molecules (from a folded conformation in solution) assemble on the substrate as a consequence of protein unfolding upon adsorption. We have obtained FN network formation on electrospun PEA fibers, which allows one to conclude that the process is not dependent upon topological constraints (2D versus 3D) and, moreover, provides a direct way to proof the biological activity of the assembled FN; cells respond to it and to the topographical work by orienting themselves in contact with the adsorbed protein layer. However, it is by no means discarded that other proteins that do not induce the formation of a FN network lead to cell orientation on polymer fibers as a consequence of the complex cell-material interaction process that involves reorganization of the initial protein layer.

Cells interact well with the assembled FN network on the PEA fibrils, which leads to their alignment and deposition of the spatially oriented FN matrix, one route to control their behavior in the long term.

Acknowledgment

AFM was performed under the technical guidance of the Microscopy Service at the Universidad Politecnica de Valencia, whose advice is greatly appreciated. The support of the Spanish Ministry of Science through project *MAT2006-08120* (including the FEDER financial support) is kindly acknowledged. This work has been partly financed through *“Convenio de colaboracion entre el Instituto de Salud Carlos III, la Conselleria de Sanidad de la Generalitat Valenciana y la Fundacion de la Comunidad Valenciana Centro de Investigacion Prıncipe Felipe para la investigacion basica y traslacional en medicina regenerativa”.*

Supporting information available

A movie showing cell migration from underlying glass to electrospun PEA fibers. This material is available free of charge via the Internet at http://pubs.acs.org.

References

1. Erickson, H. P.; McDonagh, J. J. Cell Biol. 1981, 91, 673–678.
2. Erickson, H. P.; Carell, N. A. J. Biol. Chem. 1983, 258, 14539–14544.
3. Pankov, R.; Yamada, K. M. J. Cell Sci. 2002, 115, 3861–3863.
4. Pearlstein, E.; Gold, L. I.; Garcia-Pardo, A. Mol. Cell. Biochem. 1980, 29, 103–128.
5. Keselowsky, B. G.; Collard, D. M.; Garcıa, A. J. J. Biomed. Mater. Res., Part A 2003, 66, 247–259.
6. Garcıa, A. J.; Boettiger, D. B. Biomaterials 1999, 20, 2427–2433.
7. Toworfe, G. K.; Composto, R. J.; Adams, C. S.; Shapiro, I. M.; Ducheyne, P. J. Biomed. Mater. Res., Part A 2004, 71, 449–461.
8. Baugh, L.; Vogel, L. J. Biomed. Mater. Res., Part A 2004, 69, 525–534.
9. Lan, M. A.; Gersbach, C. A.; Michael, K. E.; Keselowsky, B. G.; Garcıa, A. J. Biomaterials 2005, 26, 4523–4531.
10. Grinnell, F.; Feld, M. K. J. Biol. Chem. 1982, 257, 4888–4893.
11. Altankov, G.; Thom, V.; Groth, T.;Jankova,K.; Jonsson, G.; Ulbricht, M. J. Biomed. Mater. Res., Part A 2000, 52, 219–230.
12. Toworfe, G. K.; Composto, R. J.; Adams, C. S.; Shapiro, I. M.; Ducheyne, P. J. Biomed. Mater. Res., Part A 2004, 71, 449–461.
13. Baugh, L.; Vogel, L. J. Biomed. Mater. Res., Part A 2004, 69, 525–534.
14. Kowalczynska, H. M.; Nowak-Wyrzykowska, M.; Kolos, R.;Dobkowski, J.; Kaminski, J. J. Biomed. Mater. Res., Part A 2005, 72, 228–236.
15. Garcıa, A. J. Biomaterials 2005, 26, 7525–7529.
16. Hynes, R. O. Cell 2002, 110, 673–687.
17. Mao, Y.; Schwarzbauer, J. E. Matrix Biol. 2005, 24, 389–399.
18. Singer, I. I. Cell 1979, 16, 675–685.
19. Geiger, B.; Bershadsky, A.; Pankov,R.; Yamada,K.M.Nat. Rev. Mol. Cell Biol. 2001, 2, 793–805.
20. Altankov, G.; Groth, T. J. Mater. Sci.: Mat. Med. 1994, 5, 732–737.
21. Altankov, G.; Groth, T. J. Mater. Sci.: Mat. Med. 1996, 7, 425–429.
22. Altankov, G.; Grinnell, F.; Groth, T. J. Biomed. Mater. Res. 1996, 30, 385–
23. Altankov, G.; Groth, T.; Krasteva, N.; Albrecht, W.; Paul, D. J. Biomat. Sci., Polym. Ed. 1997, 8, 721–740.
24. Tzoneva, R.; Groth, T.;Altankov, G.; Paul, D. J. Mater. Sci.: Mater. Med. 200213, 1235–1244.
25. Pompe, T.; Keller, K.; Mitdank, C.; Werner, C. Eur. Biophys. J. 2005, 34, 1049–1056.
26. Erickson, H. P. J. Muscle Res. Cell Motil. 2002, 23, 575–580.

27. Smith, M. L.; Gourdon, D.; Little, W. C.; Kubow, K. E.; Eguiluz, R. A.; Luna-Morris, S.; Vogel, V. PLoS Biol. 2007, 5, 2243–2254.
28. Baneyx, G.; Vogel,V. Proc. Natl. Acad. Sci. U.S.A. 1999, 96, 12518–12523.
29. Ulmer, J.; Geiger, B.; Spatz, J. P. Soft Matter 2008, 4, 1998–2007.
30. Gugutkov, D.; Altankov, G.; Rodrıguez Hernandez, J. C.; Monleon Pradas, M.; Salmeron-Sanchez, M. J. Biomed. Mater. Res., Part A, 2009, DOI: 10.1002/jbm.a.32374.
31. Rico, P.; Rodrıguez Hernandez, J. C.; Moratal, D.; Altankov, G.; Monleon Pradas, M.; Salmeron-Sanchez, M. Tissue Eng., Part A, 2009, DOI: 10.1089/ten. TEA.2009.0141.
32. Agarwal, S.; Wendorff, J.; Greiner, A. Polymer 2008, 49, 5603–5621.
33. Sill, T. J. S.; von Recum, H. A. Biomaterials 2008, 29, 1989–2006.
34. Alexander, J. K.; Fuss, B.; Colello, R. J. Neuron Glia Biol. 2006, 2, 93–103.
35. Mosher, D. F.; Johnson, R. B. J. Biol. Chem. 1983, 258, 6595–6601.
36. Williams, E. C.; Janmey, P. A.; Johnson, R. B.; Mosher, D. F. J. Biol. Chem. 1983, 258, 5911–5914.
37. Morla, A.; Zhang, Z.; Rouslahti, E. Nature 1994, 367, 193–196.
38. Johnson, K. J.; Sage, H.; Briscoe, G.; Erikson, H. P. J. Biol. Chem. 1999, 274, 15473–15479.
39. Bergkvist, M.; Carlsson, J.; Oscarsson, S. J. Biomed. Mater. Res., Part A 2003, 64, 349–356.
40. Rico, P.; Rodrıguez Hernandez, J. C.; Moratal, D.; Monleon Pradas, M.; Salmeron-Sanchez, M. Macromol. Biosci. 2009, DOI: 10.1002/mabi.200800332.
41. Rodrıguez Hernandez, J. C.; Salmeron-Sanchez, M.; Soria, J. M.; Gomez Ribelles, J. L.; Monleon Pradas, M. Biophys. J. 2007, 93, 202–207.

CHAPTER 4

FIBRINOGEN ORGANIZATION AT THE CELL–MATERIAL INTERFACE DIRECTS ENDOTHELIAL CELL BEHAVIOR

Published in
Journal of Bioactive and Compatible Polymers, 2011

Article

Fibrinogen organization at the cell–material interface directs endothelial cell behavior

Dencho Gugutkov[1], Cristina González-García[2], George Altankov[1,3] and Manuel Salmerón-Sánchez[2,4,5]

Journal of Bioactive and Compatible Polymers
26(4) 375–387

DOI: 10.1177/0883911511409020
jbc.sagepub.com
SAGE

Abstract
Fibrinogen (FG) adsorption on surfaces with controlled fraction of —OH groups was investigated with AFM and correlated to the initial interaction of primary endothelial cells (HUVEC). The —OH content was tailored making use of a family of copolymers consisting of ethyl acrylate (EA) and hydroxyl ethyl acrylate (HEA) in different ratios. The supramolecular distribution of FG changed from an organized network-like structure on the most hydrophobic surface ($—OH_0$) to dispersed molecular aggregate one as the fraction of —OH groups increases, indicating a different conformation by the adsorbed protein. The best cellular interaction was observed on the most hydrophobic ($—OH_0$) surface where FG assembled in a fibrin-like appearance in the absence of any thrombin. Likewise, focal adhesion formation and actin cytoskeleton development was poorer as the fraction of hydroxy groups on the surface was increased. The biological activity of the surface-induced FG network to provide 3D cues in a potential tissue engineered scaffold, making use of electrospun PEA fibers ($—OH_0$), seeded with human umbilical vein endothelial cells was investigated. The FG assembled on the polymer fibers gave rise to a biologically active network able to direct cell orientation along the fibers (random or aligned), promote cytoskeleton organization and focal adhesion formation.

Keywords
fibrinogen, cell–material interactions, HUVEC, electrospun fibers, fibrinogen organization, cell–material interface, endothelial cell behavior, ethyl acrylate, hydroxyl ethyl acrylate

[1]Institut de Bioenginyeria de Catalunya, Barcelona, Spain
[2]Center for Biomaterials and Tissue Engineering, Universidad Politécnica de Valencia, Spain
[3]ICREA (Institució Catalana de Recerca i Estudis Avançats), Catalonia, Spain
[4]CIBER de Bioingeniería, Biomateriales y Nanomedicina (CIBER-BBN), Valencia, Spain
[5]Regenerative Medicine Unit, Centro de Investigación Príncipe Felipe, Valencia, Spain

Corresponding author:
Manuel Salmerón-Sánchez, Center for Biomaterials and Tissue Engineering, Universidad Politécnica de Valencia, Spain
Email: masalsan@fis.upv.es

Published online 14 June 2011 in www.jbc.sagepub.com
Journal of Bioactive and Compatible Polymers 2011, 26(4), 375–387
DOI: 10.1177/08839115114090

Preface to Chapter 4

This paper is a result from our further ongoing research with the group of Prof Sanchez connected with the nanoscale behavior of ECM proteins on surfaces with controlled density of -OH groups. In this case the adsorbed protein was **fibrinogen** (FBG), chosen because of its unique multifunctional properties. Besides important blood clotting factor, FG acts also as a soluble ECM protein having strong impact on tissue regeneration and wound healing. In this work we showed that, similarly to FN, the supramolecular organization of FG changed from an organized network-like structure on the **most hydrophobic poly(ethyl acrylate) (PEA)** surface ($-OH_0$) to dispersed molecular aggregates as the fraction of -OH groups increases. Its biological activity was further corroborated utilizing human umbilical vein endothelial cells (HUVEC) as model system, showing the best cellular interaction on pure PEA. This result confirmed our observations that laterally associated networks of ECM proteins are strongly bioactive - a property that we further explored, likewise the FN network before, making use of **electrospun PEA nanofibers** in order to provide 3D cues to the cells in a putative tissue engineered scaffold.

In summary, the FG network assembled on the polymer fibers gave rise to a strongly bioactive scaffold able to direct cell orientation along the fibers (random or aligned), and to promote cytoskeleton organization and focal adhesions formation. Details for this study may be found in the original paper presented below. Details for this study may be found in the original paper ***"Fibrinogen organization at the cell–material interface directs endothelial cell behavior"***, presented in this Chapter.

Abstract

Fibrinogen (FG) adsorption on surfaces with controlled fraction of –OH groups was investigated with AFM and correlated to the initial interaction of primary endothelial cells (HUVEC). The –OH content was tailored making use of a family of copolymers consisting of ethyl acrylate (EA) and hydroxyl ethyl acrylate (HEA) in different ratios. The supramolecular distribution of FG changed from an organized network-like structure on the most hydrophobic surface ($–OH_0$) to dispersed molecular aggregate one as the fraction of –OH groups increases, indicating a different conformation by the adsorbed protein. The best cellular interaction was observed on the most hydrophobic ($–OH_0$) surface where FG assembled in a fibrin-like appearance in the absence of any thrombin. Likewise, focal adhesion formation and actin cytoskeleton development was poorer as the fraction of hydroxy groups on the surface was increased. The biological activity of the surface- induced FG network to provide 3D cues in a potential tissue engineered scaffold, making use of electrospun PEA fibers ($–OH_0$), seeded with human umbilical vein endothelial cells was investigated. The FG assembled on the polymer fibers gave rise to a biologically active network able to direct cell orientation along the fibers (random or aligned), promote cytoskeleton organization and focal adhesion formation. –OH

Keywords: fibrinogen, cell–material interactions, HUVEC, electrospun fibers, fibrinogen organization, cell–material interface, endothelial cell behavior, ethyl acrylate, hydroxyl ethyl acrylate

Introduction

Fibrinogen (FG) is a fibrous glycoprotein normally present in blood plasma and involved in several key biological functions including hemostasis, wound healing, inflammation, and angiogenesis.[1]FG influences endothelial cell adhesions, motility, and growth during events associated with blood-coagulation and wound repair,[2-4] and, therefore, is recognized as fundamental for maintaining the balance between prothrombotic and fibrinolytic properties of endothelium during wound repair.[4-6]

The FG molecule consists of three pairs of polypeptide chains, designed as Aα, Bβ, and γ, with molecular masses of 66, 52, and 46 kDa, respectively, which are linked by 29 disulfide bonds.[1] These six polypeptides are organized into independently folded units: a central E-domain, which includes the N-terminus of all six polypeptide chains, and two terminal D-domains which include the Bβ- and γ-chains. The carboxyl-terminal of the Aα-chain – the Cα-domain – departs from the D fragment and either associate to the E-domain to form a single globular domain or alternatively, form appendages with a certain degree of mobility.[7] The cleavage of the small A and B sequences from the Aa- and Bb-chains by thrombin in the E-domain yields fibrin, which is able to polymerize. The length of an individual FG molecule is 45–60 nm.[8, 9]

The interaction of FG with a broad range of material surfaces has been extensively studied during the recent decade through different techniques,[10] including Atomic Force Microscopy (AFM).[11–14] The wettability of material surfaces is considered to be one of the most important parameters affecting the biological response of adsorbed proteins. However, FG adsorption has led to inconsistent conclusions, especially in terms of its conformation at the material interfaces.[2,15,16,17]

In a recent investigation of FG adsorption and distribution on a family of model polymer surfaces consisting of poly(ethyl acrylate) (PEA) and poly(hydroxyl ethyl acrylate) (PHEA) in different ratios, we tailored the wettability by changing the number of hydroxy groups present in the system without modifying any other chemical functionality.[18] We found that the amount of FG adsorbed on these substrates decreased as the fraction of –OH groups increased,[18] which is a general trend observed in the literature.[19,20] However, we also found good cellular interaction on the most hydrophobic surface of pure PEA (e.g., in the absence of –OH groups) due to the spontaneous formation of FG networks.[18]

In this study, we investigated, in detail, the biological activity of the FG network depending on the fraction of –OH groups and as well as the dimensions of the substrate using human umbilical vein endothelial cells (HUVEC). The HUVEC were chosen based on their role in determining the neovascularization potential of implants[21,22] which is particularly important in tissue engineering strategies.22,23 To date, blood contacting devices including small diameter vascular grafts, stents, and heart valves, suffer from a common defect – the lack of significant endothelial cells ingrowth, resulting in an accelerated device failure.[24]Consequently, the organization of FG at the material

interface is critical for bioengineering successful interactions with endothelial cells[25]– which should be considered to mimic the natural organization of vessel wall.

The overall morphology, focal adhesion formations, and cytoskeleton development of HUVEC adhering on model surfaces with different OH contents were followed. We used FG-coated PEA fibers obtained via electrospinning to demonstrate the potential of cellular interaction in 3D of these scaffolds for tissue engineering applications.[26, 27]

Materials and methods

Preparation of ethyl acrylate (EA) and hydroxyethyl acrylate (HEA) copolymers

The copolymer sheets were obtained by the copolymerization of both monomers EA (Aldrich, 99% pure) and HEA (Aldrich 96% pure), in predetermined proportions; the photoinitiator was benzoin (0.1 wt%, Scharlau, 98% pure) with 2 wt% ethylene glycol dimethacrylate (Aldrich, 98% pure) as the cross-linking agent. Five monomer feeds were chosen, based on the weight fraction of HEA in the initial mixture of 1, 0.7, 0.5, 0.3, and 0 (hereafter $–OH_x$, will refer to the sample with percentage x of HEA in the copolymer). After polymerization, low molecular mass substances were extracted from the material by refluxing in ethanol for 24 h and then drying in vacuum to a constant weight. Small disks (~10 mm diameter) were cut from the polymerized plates for the protein adsorption and cell adhesion studies.

PEA was dissolved in hexafluoroisopropanol at 30 μg/mL at room temperature. Randomly deposited PEA microfibers with size in the range of 2–3 mm were obtained by electrospinning the polymer solution for 2 min onto a 15 mm round-shaped glass coverslips (Thermo Scientific/Menzel-Glaser, Germany) placed on a grounded aluminum foil. The applied voltage was 20 kV, 125 mm from the collector, and the flow rate 300 μL/h. Aligned fibers were obtained under the same conditions but the polymer solutions were electrospun for 5–6 min onto a rotating drum (1000 rpm) consisting of two parallel plastic disks (120 mm diameter) spaced at 15 mm that are mounted to the same axis and connected in their periphery with 0.5 mm grounded coiled metal wire (21 parallel coils in 16 mm). The fibers, which align perpendicularly between the wires, were collected on glass coverslips.

Characterization of Poly(ethyl acrylate-co-hydroxylethyl acrylate)

Scanning electron microscopy.

The scanning electron microscopy (SEM) analysis of the electrospun fibers was carried out on a Jeol JSM-5410 scanning electron microscope. Samples were coated with a conductive layer of sputtered gold. The micrographs were taken at an accelerating voltage of 15 kV for suitable image resolution.

Swelling and contact angle measurements

The equilibrium water content (mass of water absorbed by the dry mass of the substrate) and the water contact angle (WCA) were measured (Dataphysics OCA) for the different substrates. Each experiment was performed in triplicate at room temperature.

X-ray photoelectron spectroscopy.

The X-ray photoelectron spectroscopy (XPS) experiments were performed on a PHI 5500 Multi-technique System (from Physical Electronics) with a monochromatic X-ray source and calibrated using the $3d_{5/2}$line of Ag. The analyzed area was a circle of 0.8 mm diameter, and the selected resolution for the spectra was 23.5 eV of pass energy and 0.1 eV step$^{\text{À}}$1. All measurements were made in an ultra-high vacuum chamber. The XPS elemental sensitivity factors, according to the MULTIPAK program for PHI instruments, were used. An automatic XPS signal-fitting software (developed under MATLAB v7.2, The MathWorks Inc., Natick, MA, USA) was used to deconvolute the spectra.[28] The fitting software makes use of an independent Voigt function per peak (which, in our case, means four Voigt functions to fit the C 1s spectra and three Voigt functions to fit the O 1s peaks).

Atomic force microscopy.

Surfaces for AFM were prepared as follows. FG from human plasma (Sigma) was adsorbed on the different substrates by immersing the material disks in 20 μg/mL solutions of phosphate-buffered saline (PBS) for 10 min. AFM was performed in a NanoScope III from Digital Instruments (Santa Barbara, CA) operating in the tapping mode; the Nanoscope 5.30r2 software version was used. Si-cantilevers from Veeco (Manchester, UK) were used with force constant of 2.8 N/m and resonance frequency of 75 kHz. The phase signal was set to zero at a frequency 5–10% lower than the resonance one. Drive amplitude was 200 mV and the amplitude setpoint (A_{sp}) 1.4 V. The ratio between the amplitude set point and the free amplitude (A_{sp}/A_0) was kept equal to 0.7.

Cell cultures

HUVEC (PromoCell) were cultured in endothelial cell growth medium supplemented with SupplementMix (PromoCell) containing 0.4% ECGS/H, 2% fetal calf serum, 1 ng/mL epidermal growth factor, 1 mg/mL hydrocortison, and 1 ng/mL basic fibroblast factor. For the adhesion experiments, the cells were detached from around confluent flasks with Trypsin/EDTA (Invitrogen) and the remained trypsin activity was stopped with 100% FBS before washing two times with medium without supplements. The cells were then counted and reconstituted.

Cell adhesion and overall morphology

To determine the overall cell morphology of HUVEC adhering to different samples, 5 x 10^4 cells/well were seeded in 24-well TC plates (Costar) containing the samples for 2 h in serum free medium. The cells were then fixed with 4% paraformaldehyde (10 min) and permeabilized with 0.5% Triton X-100 for 5 min. The actin cytoskeleton was stained with 20 μg/mL AlexaFluor-488 phalloidin (Molecular Probes) in PBS before the samples were washed and mounted in Mowiol (Polysciences

Inc.). Images of the adhered cells were obtained at low magnification (10x to get the overall cell morphology), or at higher magnification (63x to follow the organization of actin filaments), using the green channel of a fluorescent microscope (Zeiss, Axiovert 40) equipped with digital camera IMag (InRey Solutions, Bulgaria) and the corresponding software.

Visualization of focal adhesions

To visualize focal adhesions, the fixed and permeabilized samples were saturated with 1% albumin in PBS (15 min) and immunofluorescently stained for vinculin with monoclonal anti-vinculin antibody (Sigma, cat no. V9131) dissolved in 1% BSA in PBS for 30 min, followed by Cy3-conjugated Goat Anti-Mouse IgG (H+L) (Jackson ImmunoResearch, cat. no 115-165-062) as secondary antibody (30 min). To simultaneously visualize actin, FITC-labeled phalloidin (Invitrogen) was added to the secondary antibody solution at a final concentration 1:100. The samples were viewed and photographed with an inverted fluorescent microscope. Representative images were acquired on the green and red channel and superimposed with ImageJ software.

Results

The data presented in Table 1 show a significant decrease in the WCA with increasing amounts of HEA in the copolymer, from 89 for pure PEA ($–OH_0$) to 45 for pure PHEA ($–OH_{100}$). Topography of the surfaces, which is known to be a parameter able to influence cell behavior, was examined by AFM prior to protein adsorption and yielded similar roughness parameters regardless the polymer composition. The roughness parameters were $R_a = 18 \pm 4$ nm and $R_{ms} = 22 \pm 4$ nm (R_a is the average height deviations; R_{ms} is the standard deviation of the height values).

Table 1. Equilibrium water content (EWC) and WCA for the different substrates varying in density of –OH groups

–OHx	EWC (%)	WCA (°)	–OHx (XPS)	FG (μg/cm^2)
0	1.7 ± 0.4	89 ± 1	0	1.20 ± 0.10
0.3	7.6 ± 0.9	80 ± 2	0.25	0.37 ± 0.05
0.5	18.2 ± 1.7	67 ± 1	0.45	0.20 ± 0.04
0.7	40.6 ± 0.4	55 ± 1	0.68	0.16 ± 0.05
1	134 ± 5	45 ± 2	1	0.14 ± 0.08

Column (1) is the fraction of HEA units used in the copolymerization process; Column (4) is the fraction of HEA units available on the material surface as obtained from XPS analysis. Column (5) has the surface densities of adsorbed FG on the substrates.[18]

The fraction of –OH groups on all the surfaces was assessed by XPS (Table 1). The fraction of hydrophilic units on the surface was similar to the initial ratio of HEA in the feeding mixture of co-monomers. Thus, most of the hydroxyl groups in the system remain available to interact with the biological media.

FG distribution on surfaces with tailored –OH content

The FG distribution (Figure 1) is observed by AFM after adsorption on the different substrates from a 20 mg/mL solution, which is the concentration afterwards employed for cell culture purposes. This protein concentration does not reveal the conformation of single FG proteins since FG fibrils are present in all samples: rather than single FG molecules, the AFM images show protein patterns with different topologies. The formation of a FG network takes place on pure PEA ($–OH_0$), the degree

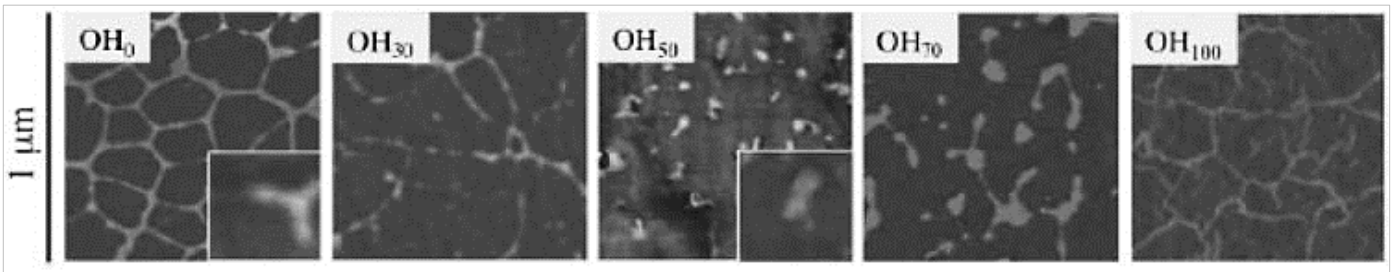

Figure 1. *Phase signal AFM images after FG adsorption on substrates with controlled OH surface densities. Insets show individual FG molecules representative of extended (for OH0and OH30) and globular (for OH50, OH70, and OH100) conformations.*

of interconnection of the protein fibrils is diminished for samples with higher hydroxy contents, while it is enhanced again on the most hydrophilic surface ($–OH_{100}$). Detailed information on this process can be found in Hernandez et al.[18] Furthermore, the adsorption from lower concentration solutions (2 μg/mL) provided the identification of FG molecules in an extended conformation on $–OH_0$ and $–OH_{30}$ while being mostly globular-like aggregates on $–OH_{50}$ and $–OH_{70}$ (Figure 1, inset).

Cellular interaction depending on surface –OH content

Substrates were immersed overnight in a FG solution (20 mg/mL) prior to cell culture. The cell morphology of the HUVEC on the different FG-coated substrates and the control glass, after culturing and actin staining, is shown in Figure 2. The cell density and spreading depended on the –OH fraction on the surface. However, most elongated cells, similar to those on the control glass, were only observed on the most hydrophobic substrate $–OH_0$; as the –OH fraction in the material increased, the number of attached cells reduced and the spreading diminished. The substrate wettability clearly dropped (Table 1) as the –OH density decreased. Only rounded cells were observed on the more hydrophilic systems ($–OH_{50}$and $–OH_{70}$) even when the cell density did not differ significantly (Figure 2).

The development of an actin cytoskeleton was observed at higher magnification (Figure 3) which allowed us to establish the degree of maturation of the F-actin fibers on the different FG-coated substrates. On the more hydrophobic polymers ($–OH_0$ and $–OH_{30}$), the cells spread on the surface displaying a well-defined and developed actin cytoskeleton with mature F-actin cables (Figure 3). Higher fractions of hydroxyl groups in the substrate lead to a less spread morphology and only initial-peripheric trends of F-actin were visible ($–OH_{50}$and $–OH_{70}$). Cells on the most wettable

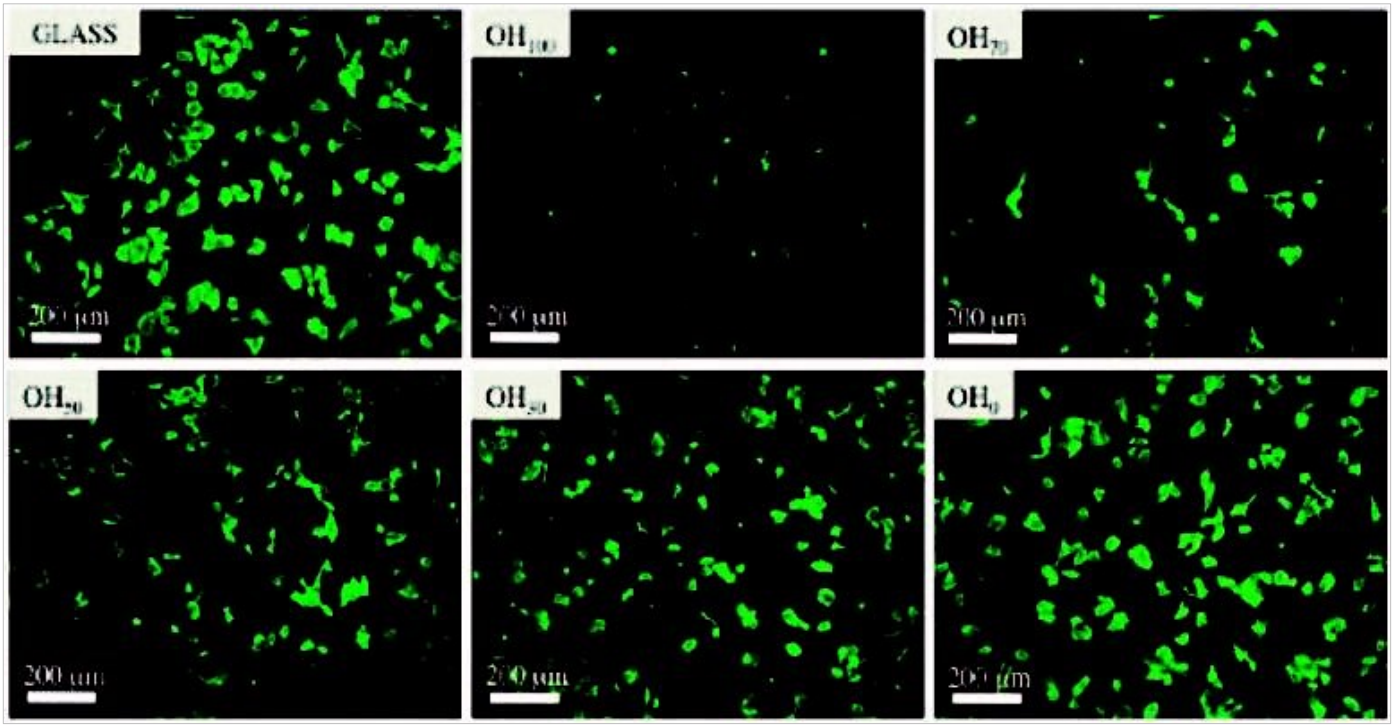

Figure 2. *Distribution of HUVEC on the material surfaces after a 3 h culture after phalloidin staining for actin.*

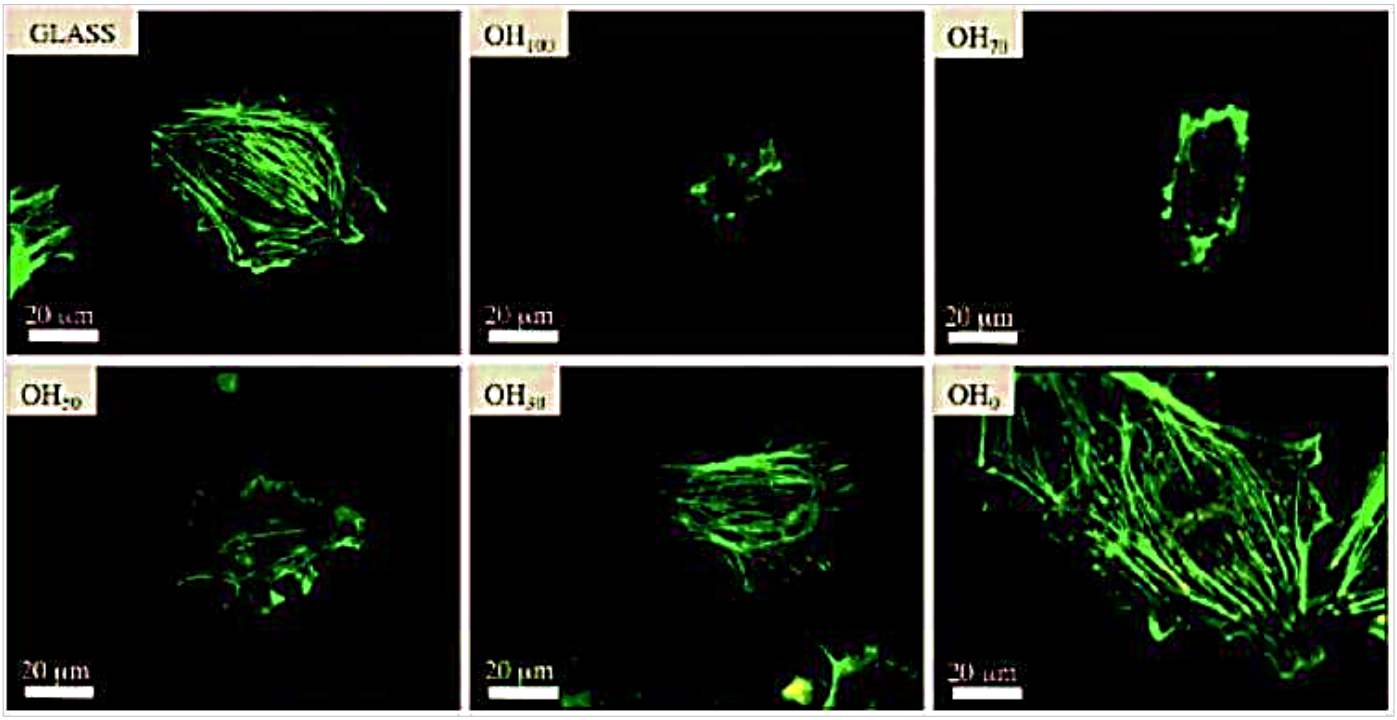

Figure 3. *F-actin cytoskeleton development of HUVEC on the different substrates with controlled fraction of hydroxy groups.*

substrate (–OH_{100}) had round shapes with only a shadow of non-polymerized actin.

The organization of cellular proteins involved in the formation of the focal adhesion complexes provided an opportunity to observe the effectiveness of cell-to-substrate interactions. The distribution of vinculin in fibroblasts adhering on the FG - coated substrates is shown in Figure 4. Well-defined focal adhesions were found only on the more hydrophobic surfaces (–OH_0, and –OH_{30}) and on the control glass. Even if vinculin had been expressed in the more hydrophilic

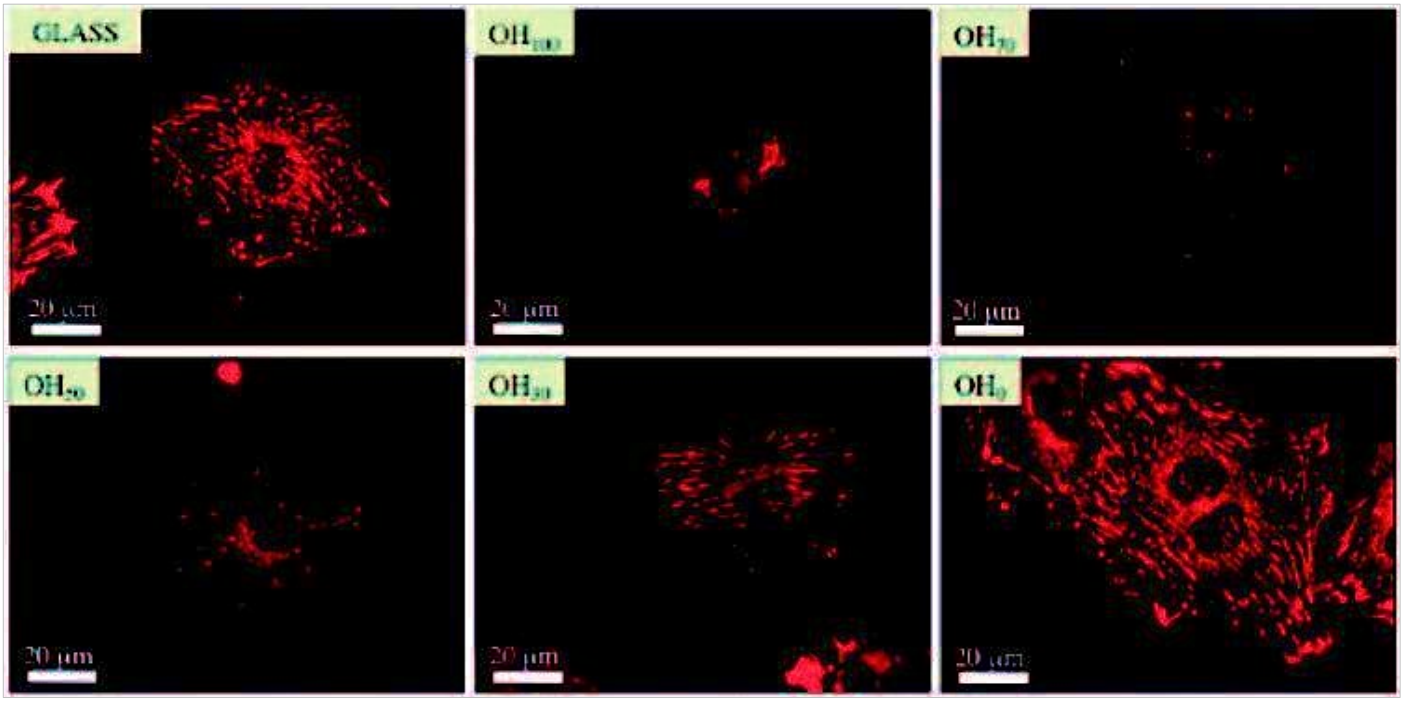

Figure 4. *Focal adhesion formation for HUVEC on the different substrates and the control glass through immunofluorescence for vinculin*

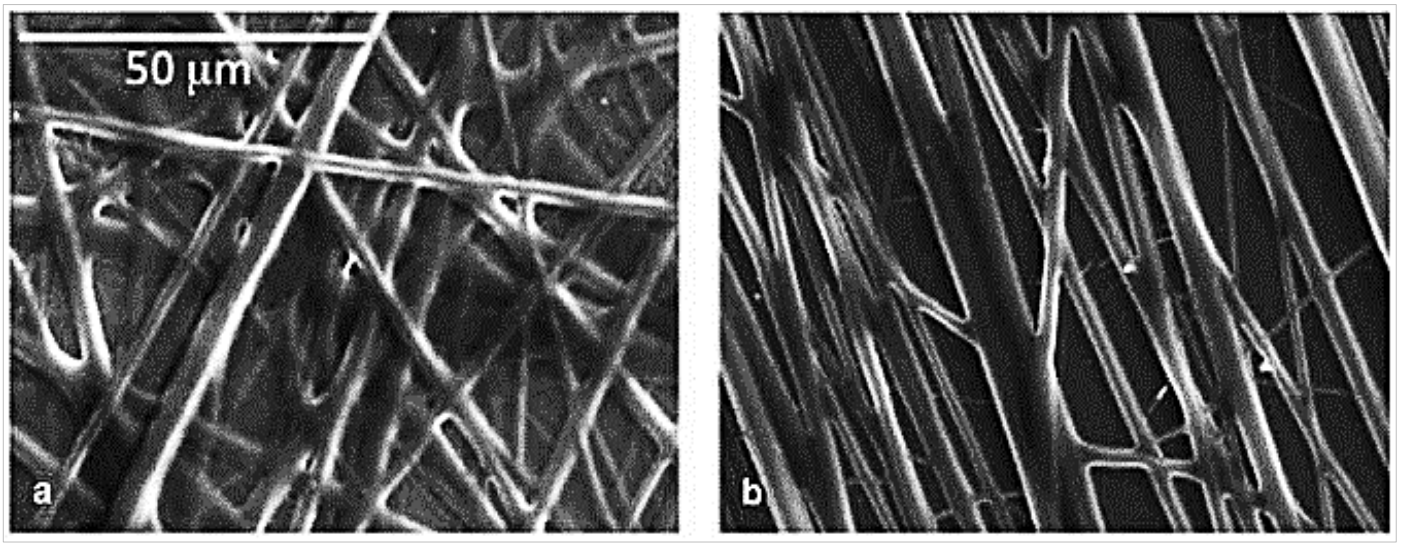

Figure 5. *SEM micrographs of PEA fibers* ***(a)*** *randomly distributed and* ***(b)*** *aligned on glass coverslips*

substrates, it was not organized into focal contacts but randomly distributed along the cell periphery (Figure 4).

Electrospun PEA microfibers (OH_0) coated with FG

Random and aligned PEA fibers were prepared via electrospinning with diameters of approximately 3 mm. Representative SEM micrographs of electrospun PEA fibers on glass coverslips are seen in Figure 5. The SEM images show the distribution of the fibers, the existence of a characteristic direction in the case of Figure 5(b) and the lack of any principal direction in Figure 5(a).

AFM images (different magnifications, phase, and magnitude of the amplitude) of the PEA electrospun fibers after FG adsorption from a solution of concentration 20 mg/mL are shown in

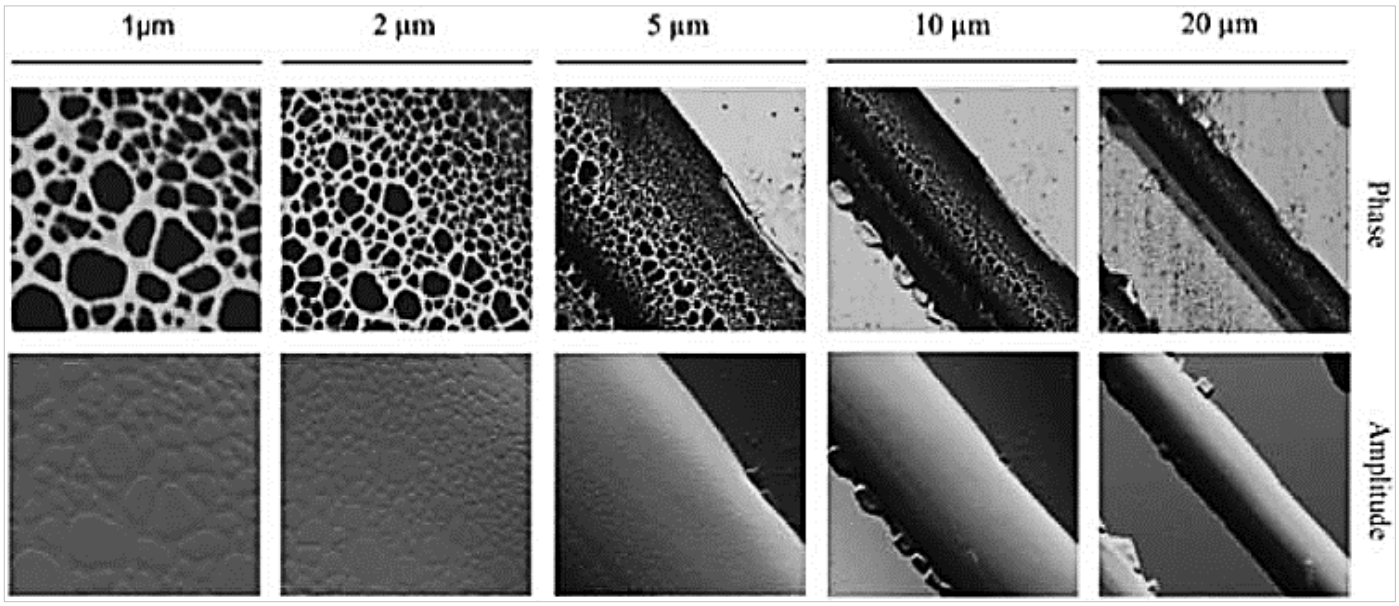

Figure 6. *FG assembly on PEA fibers as observed by AFM (phase and amplitude). PEA fibers were electrospun on glass coverslips, and FG was adsorbed for 10 min from a 20 mg/mL solution. The FG network only assembled on the PEA fibers and not on the underlying glass substrate.*

Figure 6. Large fiber topography prevented FN to be identified. However, the phase magnitude revealed the existence of a FG network assembled on the electrospun PEA fibers, in the absence of thrombin or cells, as a consequence of the protein–material interactions. Some salt crystals were observed on the underlying glass substrate without a trace of the protein network on it. FG distribution on the PEA substrate was not observable at this magnitude of the amplitude, although some topographic signs were identified in the 2 mm image (Figure 6). However, this magnitude of the amplitude was sufficient to identify the electrospun PEA fibers.

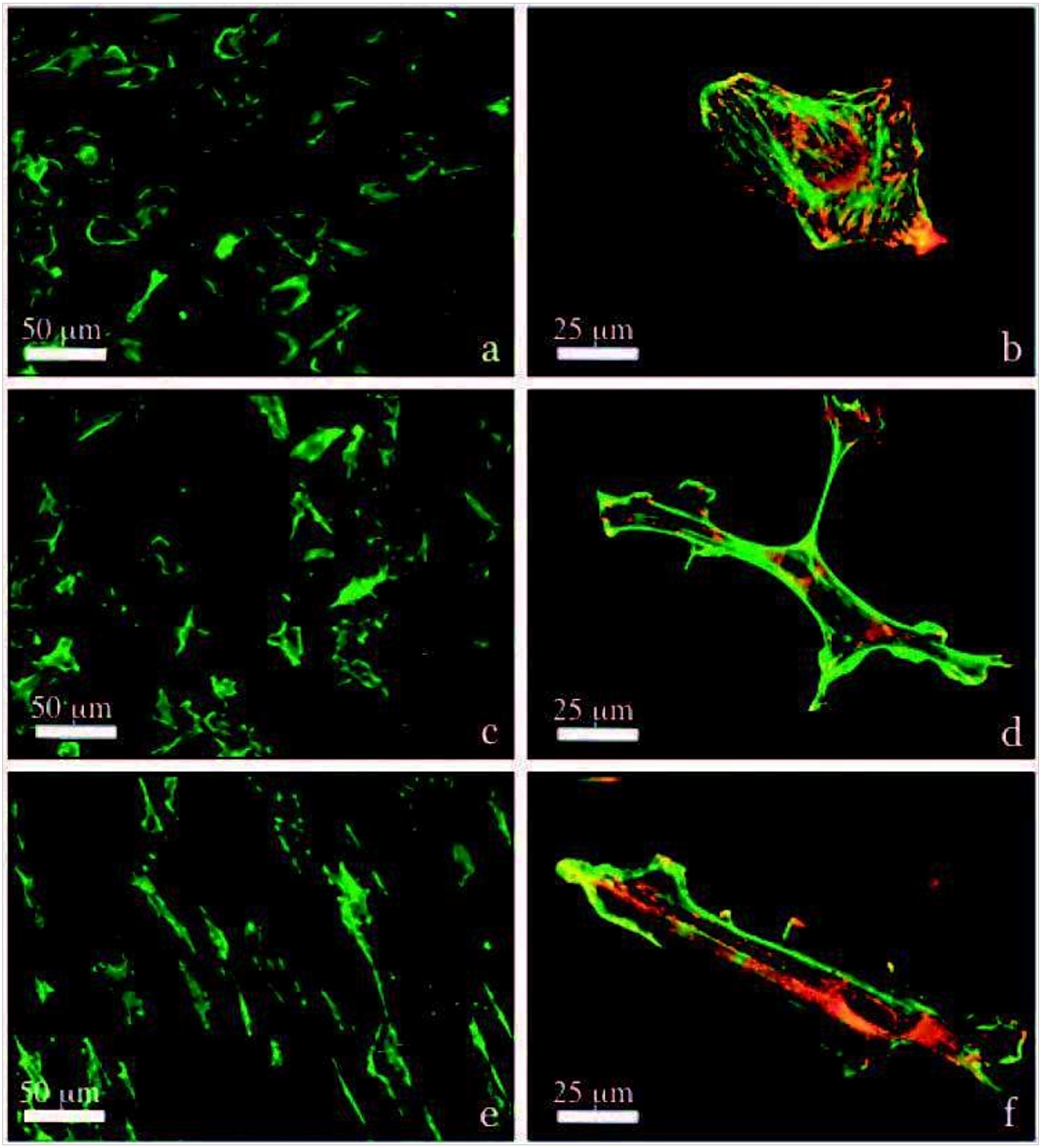

Figure 7. *Overall morphology of HUVEC adhering on* ***(c, d)*** *random and* ***(e, f)*** *aligned FG-coated PEA fibers compared to the* ***(a, b)*** *control of FG-coated glass visualized by actin* ***(a, c,*** *and* ***e)*** *or double stained for vinculin (red) and actin (green)* ***(b, d,*** *and* ***f)****.*

Cellular interaction with electrospun PEA microfibers

The left column in Figure 7 represents the overall morphology of HUVEC adhering after 2 h on the FG-coated (electrospun) PEA fibers and control glass samples for comparison, visualized via staining for actin. Irregularly spread cells representing multiple projections were typically on the randomly dispersed PEA fibers (Figure 7(c)), presumably resembling early stellate morphology in response to the underlying substrate, apart from the cells on the control glass (Figure 7(a)), had a typical (2D substrata) flattened and polarized morphology without prevalent orientation of the cells. Conversely, an extended cell shape, parallel to the orientation of the fibers, was observed on the aligned PEA fibers (Figure 7(e)) that corroborated with the focal adhesion complexes and well-developed actin stress fibers inserting into them (in yellow), particularly in the contact zones with PEA fibers (Figure 7(f)). Conversely, on random PEA fibers (Figure 7(d)), actin cytoskeletons were rather cortically accumulated, combined with well-developed longitudinal stress fibers inserting into the prominent focal adhesion plaques that follow multiple directions of the underlying polymer fibers. On the control FG-coated glass (Figure 7(b)), the cells were ‘classical’ actin cytoskeleton with stress fibers inserting into regularly dispersed focal adhesion at cell edges.

Discussion

Biofunctionalization of blood contact devices is a strategy used to achieve endothelialization and to prevent failure upon implantation.[29–31] We found that FG adsorption in vitro can be triggered by the amount of OH groups in the surface and that endothelial cell behavior is then directed in this way.

It is known that protein adsorption on a synthetic surfaces triggers the biological response of the material.[32,33,34] The copolymer substrates employed in this study were based on the random combination of ethyl acrylate and HEA monomers that have vinyl backbone chains with $–COOCH_2CH_3$ and $–COOCH_2CH_2OH$ side groups. The surface density of –OH groups is easily varied without modifying any other chemical functionality of the system. The sequential incorporation of hydroxyl groups on the material surface was assessed by XPS (Table 1). The concentration of –OH groups determines both the wettability and the hydrophilicity of the substrate, while the surface roughness remains unaffected (Table 1).

We found that both the FG adsorption and distribution on this family of polymers determined the initial interaction with endothelial cells. The amount of adsorbed FG decreased monotonically as the fraction of hydroxyl groups increased (Table 1).[18–20] However, the different distributions of FG on the surface led to different cell behaviors; the cells spread well on the hydrophobic substrate with excellent adhesion, but round cells were found on the hydrophilic one (Figures 2 and 3). It is known that, excluding platelets, cell adhesion to FG is mediated by the $\alpha_v\beta_3$ integrin which recognizes the RGD sequence near the C-terminus of the $A\alpha$ chain of the FG molecules, (RGDF at $A\alpha$ 95-98 and RGDS at $A\alpha$ 572-575).[35–39] The conformation of the adsorbed FG on the most hydrophobic substrates permitted the recognition of the RGD sequence by the integrins, which was prevented on the hydrophilic surfaces.[19, 20]

Endothelial cell interactions on the FG-coated substrates containing up to 30% hydroxyl groups ($–OH_0$, $–OH_{30}$) was accompanied by the formation of the actin cytoskeleton, focal adhesion plaques, and spread morphology. This indicated that the conformation of the protein was able to enhance the cell–FG interactions, even if the number of cells adhered on the substrate was lower as the surface density of adsorbed FG (Figures 1 and 2 and Table 1).

High amounts of hydroxyl groups in the substrate (samples $–OH_{50,}$ $–OH_{70}$, and OH_{100}) resulted in a qualitative change of the cell–material interactions; the cells, which barely adhered to the substrate, had rounded morphology and lacked focal adhesion contacts and actin cytoskeleton. Since the amount of adsorbed FG on the higher hydroxyl content in the substrate was only slightly lower (Table 1), we ascribed this behavior to the different distributions and conformation of the protein on the substrate.

Interestingly, the FG organized into a biological active protein network upon adsorption on PEA

(Figure 1), with patterns similar to those found by Gettens et al.[6] and to those observed by Sit and Marchant [40] in the process of fibrin assembly on graphite in the presence of thrombin. One way to establish intermolecular interactions between FG molecules involves the electrostatic bonds between the globular C-termini (which are negatively charged) and the overall positive charge of the E-domain.[41] Similarly, the C-termini were also able to bind to themselves.[7] The extended conformation of the FG molecules on PEA supported the formation of intermolecular interactions after protein adsorption on the material surface (Figure 1, inset). This study shows that the formation of a FG network on a PEA substrate is not restricted to plane surfaces but that it can resemble distinct topographic cues that are recognized by endothelial cells, when deposited on the electrospun 3D fibers (Figure 3).

Other ECM proteins were previously investigated on this family of polymers concerning protein adsorption by AFM.[18,42,43,44] Particular features were obtained that reflect the difficulty in establishing general rules concerning the effect of material properties on protein adsorption.

More importantly, the FG network that assembled spontaneously on the PEA fibers is biologically active (Figure 7). Evidently, the cells interacted with the PEA fibers and started to orient, modifying their characteristic flattened morphology on glass, following the fibers direction (Figure 7(e) and (f)). The cell morphology was then modified to adapt cell-substrate contact along the electrospun PEA fiber. The well-developed focal adhesion complexes and the insertions of actin stress fibers in these complexes point to a proper transmission of signals by the integrins to the cell interior. Interestingly, when adhering to random PEA fibers, the cells tend to develop a rounded morphology with multiple projections, which resemble stellate morphology, characteristic of cells in a 3D environment. In fact, this protein network represents a rather 2.5 D substrate (for cellular dimensions), which means that the cells receive proper signals from the FG network. Moreover, it also applies to the oriented fibers where endothelial cells immediately acquire extended morphology with asymmetrical organization of the adhesive complexes (Figure 7(f)), thus indicating activation of their motility.

Conclusions

FG was organized into a network-like structure upon adsorption on PEA. The fraction of OH groups in the system was increased by copolymerizing with HEA which led to a different distributions of FG on the substrate (globular-like pattern) and lower surface density of adsorbed protein. A lower number of attached cells, without focal adhesion plaques and scarce actin cytoskeleton, were found as the fraction of OH groups in the copolymer increased. After adsorption on the electrospun PEA fibers the network organization of FG on the material interface provided specific 3D cues that triggered endothelial cell behavior. The cellular interactions with this FG structure gave rise to the formation of extended morphologies, well-developed focal adhesion plaques and polarized cytoskeleton following the underlying FG-coated electrospun polymer.

Acknowledgement

AFM was performed under the technical guidance of the Microscopy Service at the Universidad Politecnica de Valencia, whose advice is greatly appreciated. The work was supported by the Spanish Ministry of Science and Innovation through projects № *MAT2009-14440-C02-01, MAT2009-14440-C02-02* and *EULANEST PIM2010EEU-00111.*

References

1. Weisel JW. Fibrinogen and fibrin. Adv Prot Chem 2005; 70: 247–299.
2. Agnihotri A and Siedlecki CA. Time-dependent conformational changes in fibrinogen measured by atomic force microscopy. Langmuir 2004; 20: 8846–8852.
3. Cacciafesta P, Humphris ADL, Jandt KD and Miles MJ. Human plasma fibrinogen adsorption on ultraflat titanium oxide surfaces studied with atomic force microscopy. Langmuir 2000; 16: 8167–8175.
4. Tzoneva R, Groth T, Altankov G and Paul D. Remodeling of fibrinogen by endothelial cells in dependence on fibronectin matrix assembly. Effect of substratum wettability. J Mater Sci. Mater Med 2002; 13: 1235–1244.
5. Tunc S, Maitz MF, Steiner G, Vazquez L, Pham MT and Salzer R. In situ conformational analysis of fibrinogen adsorbed on Si surfaces. Colloid Surf B 2005; 42: 219–225.
6. Gettens RTT, Bai Z and Gilbert JL. Quantification of the kinetics and thermodynamics of protein adsorption using atomic force microscopy. J Biomed Mater Res A 2005; 72: 246–257.
7. Veklich YI, Gorkun OV, Medved LV, Nieuwenhuizen W and Weisel JW. Carboxyl-terminal portions of the α chains of fibrinogen and fibrin: localization by electron microscopy and the effects of isolated αC fragments on polymerization. J Biol Chem 1993; 268: 13577–13585.
8. Ta TC and McDermott M. Mapping interfacial chemistry induced variations in protein adsorption with scanning force microscopy. Anal Chem 2000; 72: 2627–2634.
9. Ishizaki T, Saito N, Sato Y and Takai O. Probing into adsorption behavior of human plasma fibrinogen on self-assembled monolayers with different chemical properties by scanning probe microscopy. Surf Sci 2007; 601: 3861–3865.
10. Brash JL and Horbett TA. In protein at interfaces II: fundamentals and applications. In: Brash JL and Horbett TA. (eds). *ACS Symposium Series* No. 602. Washington, DC: American Chemical Society, 1995Chapter 1.
11. Gettens RTT and Gilbert JL. Quantification of fibrinogen adsorption onto 316L stainless steel. J Biomed Mater Res A 2007; 81: 465–473.
12. Ortega-Vinuesa JL, Tengvall P and Lundstrom I. Aggregation of HSA, IgG, and fibrinogen on methylated silicon surfaces. J Colloid Interface Sci 1998; 207: 228–239.
13. Mitsakakis K, Lousinian S and Logothetidis S. Early stages of human plasma proteins adsorption probed by atomic force microscope. Biomol Eng 2007; 24: 119–124.
14. Sit PS and Marchant RE. Surface-dependent conformations of human fibrinogen observed by atomic force microscopy under aqueous conditions. Thromb Haemost 1999; 82: 1053–1060.
15. Marchin KL and Berrie CL. Conformational changes in the plasma protein fibrinogen upon adsorption to graphite and mica investigated by atomic force microscopy. Langmuir 2003; 19:

9883–9888.

16. Wertz CF and Santore MM. Effect of surface hydrophobicity on adsorption and relaxation kinetics of albumin and fibrinogen: single-species and competitive behavior. Langmuir 2001; 17: 3006–3016.
17. Wertz CF and Santore MM. Fibrinogenadsorption on hydrophilic and hydrophobic surfaces: geometrical and energetic aspects of interfacial relaxations. Langmuir 2002; 18: 706–715.
18. Hernandez JCR, Rico P, Moratal D, Pradas MM and Salmeron-Sanchez M. Fibrinogen patterns and activity on substrates with tailored hydroxyl density. Macromol Biosci 2009; 9: 766–775.
19. Slack SM and Horbett TA. Changes in fibrinogen adsorbed to segmented polyurethanes and hydroxyethylmethacrylate-ethylmethacrylate copolymers. J Biomed Mater Res 1992; 26: 1633–1649.
20. Rodrigues SN, Goncalves IC, Martins MCL, Barbosa MA and Ratner B. Fibrinogen adsorption, platelet adhesion andactivation on mixed hydroxyl-/methyl-terminated self-assembled monolayers. Biomaterials 2006; 27: 5357–5367.
21. Daley WP, Peters SB and Larsen M. Extracellular matrix dynamics in development and regenerative medicine. J Cell Sci 2008; 121: 255–264.
22. Rivron NC, Liu J, Rouwkema J, de Boer J and van Blitterswijk CA. Engineering vascularized tissues in vitro. Eur Cells Mater 2008; 15: 27–40.
23. Sephel GC, Kennedy R and Kudravi S. Expression of capillary basement membrane components during sequential phases of wound angiogenesis. Matrix Biol 1996; 15: 263–279.
24. Keresztes Z, Rouxhet PG, Remacle C and Dupont- Gillain C. Supramolecular assemblies of adsorbed collagen affect the adhesion of endothelial cells. J Biomed Mater Res A 2006; 76: 223–233.
25. Tzoneva R, Seifert B, Albrecht W, Richau K, Lendlein A and Groth T. Poly(ether imide) membranes: studies on the effect of surface modification and protein pre-adsorption on endothelial cell adhesion, growth and function. J Biomater Sci Polym Ed 2008; 19: 837–852.
26. Volpato ZF, Lopes S, Ramos F, Motta A and Migliaresi C. Physical and in-vitro biological evaluation of a PA6/MWCNT electrospun composite for biomedical applications. J Bioact Compat Polym 2011; 26(1): 35–47.
27. Puppi D, Piras AM, Detta D, Ylikauppila H, Nikkola L, Ashammakhi N, et al. Poly(vinyl alcohol)-based electrospun meshes as potential candidate scaffolds in regenerative medicine. J Bioact Compat Polym 2011; 26: 20–34.
28. Gonzalez-Garcıa C, Latorre L, Moratal D, Pradas MM and Salmeron-Sanchez M. Poly (L-lactide) substrates with tailored surface chemistry by plasma copolymerisation of acrylic monomers. Plasma Polym Proc 2009; 6: 190–198.
29. de Mel A, Jell G, Stevens MM and Seifalian AM. Biofunctionalization of biomaterials for

accelerated in situ endothelialization: a review. Biomacromolecules 2008; 9: 2969–2979.

30. Griffith LG and Naughton G. Tissue engineering– current challenges and expanding opportunities. Science 2002; 295: 1009–1014.
31. Sipe JD. Tissue engineering and reparative medicine. Ann NY Acad Sci 2002; 961: 1–9.
32. Altankov G and Groth T. Reorganization of substratum-bound fibronectin on hydrophilic and hydrophobic materials is related to biocompatibility. J Mater Sci Mater Med 1994; 5: 732–737.
33. Altankov G and Groth T. Fibronectin matrix formation and the biocompatibility of materials. J Mater Sci Mater Med 1996; 7: 425–429.
34. Grinnell F and Feld MK. Fibronectin adsorption on hydrophilic and hydrophobic surfaces detected by antibody binding and analyzed during cell adhesion in serum-containing medium. J Biol Chem 1982; 257: 4888–4893.
35. Farell DH, Thiagarajan P, Chung DW and Davie EW. Role of fibrinogen alpha and gamma chain sites in platelet aggregation. Proc Natl Acad Sci 1992; 89: 10729–10732.
36. Cheresh D. Human endothelial cells synthesize and express an Arg-Gly-Asp-directed adhesion receptor involved in attachment to fibrinogen and von Willebrand factor. Proc Natl Acad Sci 1987; 84: 6471–6475.
37. Cheresh D, Berliner S, Vicente V and Ruggery Z. Recognition of distinct adhesive sites on fibrinogen by related integrins on platelets and endothelial cells. Cell 1989; 58: 945–953.
38. Gailit F, Clarke C, Newman D, Tonnesen MG, Mosesson MW and Clark RAF. Human fibroblasts bind directly to fibrinogen at RGD sites through integrin avb3. Exp Cell Res 1997; 232: 118–126.
39. Doolittle RF, Watt KWK, Cottrell BA, Strong DD and Riley M. The amino acid sequence of the a-chain of human fibrinogen. Nature 1979; 280: 464–468.
40. Sit PS and Marchant RE. Surface-dependent differences in fibrin assembly visualized by atomic force microscopy. Surf Sci 2001; 491: 421–432.
41. Toscano A and Santore M. Fibrinogen adsorption on three silica-based surfaces: conformation and kinetics. Langmuir 2006; 22: 2588–2597.
42. Gugutkov D, Gonzalez-Garcıa C, Hernandez JCR, Altankov G and Salmeron-
43. Sanchez M. Biological activity of the substrate- induced fibronectin network: insight into the third dimension through electrospun fibers. Langmuir 2009; 25: 10893–10900.
44. Toromanov G, Gonzalez-Garcıa C, Altankov G and Salmeron-Sanchez M. Vitronectin activity on polymer substrates with controlled –OH density. Polymer 2010; 51: 2329–2336.
45. Hernandez JCR, Salmeron-Sanchez M, Soria JM, Ribelles JLG and Pradas MM. Substrate chemistry-dependent conformations of single laminin molecules on polymer surfaces are revealed by the phase signal of atomic forcemicroscopy. Biophys J 2007; 93: 202–207.

CHAPTER 5

FIBRINOGEN NANOFIBERS FOR GUIDING ENDOTHELIAL CELL BEHAVIOR

Published in
Biomaterials Science, 2013

Biomaterials Science

RSC Publishing

PAPER

View Article Online
View Journal | View Issue

Cite this: Biomater. Sci., 2013, 1, 1065

Fibrinogen nanofibers for guiding endothelial cell behavior†

Dencho Gugutkov,[a,b] Johan Gustavsson,[a] Maria Pau Ginebra[b,c] and George Altankov[a,d,e]

This paper describes the biological consequences of presenting electrospun fibrinogen (FBG) to endothelial cells as a spatially organized nanofibrous matrix. Aligned and randomly oriented FBG nanofibers with an average diameter of less than 200 nm were obtained by electrospinning of native FBG solution. Electrophoretic profiling confirmed that the electrospun FBG resembled the native protein structure, and fluorescent tracing of FITC-labeled FBG showed that electrospun fibers withstood immersion in physiological solutions reasonably well for several days. With respect to cellular interactions, the nanofibrous FBG matrix provided better conditions for initial recognition by human umbilical vein endothelial cells compared to pre-adsorbed FBG on a flat surface. Furthermore, the spatial organization of electrospun FBG fibers presented opportunities for guiding the cellular behavior in a way that is not possible when the protein is presented in another form (*e.g.* adsorbed or soluble). For example, on aligned FBG fibers, cells rapidly oriented themselves along the fibers, and time-lapse recordings revealed pronounced cellular movements restricted to the fiber direction. In great contrast, on randomly deposited fibers, cells acquired a stellate-like morphology and became locally immobilized by the fibers. We also show that the FBG fiber orientation significantly influenced both the cytoskeleton organization in confluent cell layers and the orientation of the extracellular fibronectin matrix secreted by the cells. In conclusion, this study demonstrates that electrospun FBG nanofibers can be a promising tool for guiding endothelial cell behavior for tissue engineering applications.

Received 10th May 2013,
Accepted 17th June 2013
DOI: 10.1039/c3bm60124b
www.rsc.org/biomaterialsscience

Introduction

Cellular interactions with foreign materials initially rely on fundamental processes such as protein adsorption[1] and ligand–receptor interactions[2] which determine the subsequent cellular interaction and response. In fact, those initial events mimic to a certain extent the natural interaction of cells with the extracellular matrix (ECM),[3] a notion that is required not only for understanding biocompatibility, but also for biology and medicine in general, since tissue development in multicellular animals heavily relies on the ability of cells to synthesize and organize ECM – a fact that cannot be underestimated in biomaterials science.

Basically, the ECM is a structure consisting of glycosaminoglycans (a gel-like matter) and spatially organized matrix fibrils (*e.g.* collagen, laminin, fibronectin, *etc.*) whose length in some cases greatly exceeds that of individual cells.[4] The importance of correct regulation of fibril deposition is exemplified by diseases such as osteogenesis imperfecta (caused by mutations in collagen genes), fibrosis (*i.e.*, ectopic accumulation of ECM), as well as by its frequent appearance in degenerative tissue disorders.[5,6] The biological relevance of fibrillar nanostructures is also clearly reflected in the efforts made in the fields of biomaterials and tissue engineering to reproduce and apply ECM-like fibers, *e.g.* by electrospinning[7] or by self-assembly.[8] Despite the promise of such techniques, there is still a need to understand how cells respond to complex structures that contain both spatial and biological information.

Among the different fibrillar proteins, fibrinogen (FBG)[9] is of particular interest for tissue engineering applications due to its many biological functions. FBG is a soluble protein secreted into the plasma in high amounts mainly by hepatocytes, and it plays a key role in the coagulation cascade and as a bridging molecule for platelet aggregation.[10] FBG and its derivative fibrin also serve as a provisional ECM in some injured tissues,[11] and is involved in wound healing,[12] tissue

[a]Institute for Bioengineering of Catalonia, Barcelona, Spain
[b]Universitat Politècnica de Catalunya, Barcelona, Spain
[c]Centro de Investigación Biomédica en Red en Bioingeniería, Biomateriales y Nanomedicina (CIBER-BBN), Zaragoza, Spain
[d]Institució Catalana de Recerca i Estudis Avançats (ICREA), Barcelona, Spain. E-mail: George.Altankov@barcrea.cat; Fax: +34 93 403 98 73; Tel: +34 93 403 97 09
†Electronic supplementary information (ESI) available: Videos 1–4; one figure. See DOI: 10.1039/c3bm60124b

Published online 08 Jul 2013 in www.rsc.org/biomaterialsscience
Biomater. Sci. 2013, 1, 1065-1073
DOI: 10.1039/C3BM6012

Preface to Chapter 5

This part of the Thesis reflects the **switch in our concept** to a more efficient geometric control of the cellular interaction, using **nanofibers consisting of natural ECM protein**. Indeed, our previous studies clearly showed that cells are able to accept organizational stimuli from the substratum on which they attach, and this is a way to control their behavior. However, the cells also respond to the **mechanical properties** of their environment, which is difficult to control on planar substrata. On the other hand, when ECM proteins polymerize *in vivo,* they usually generate a complex fibrillar structures, possessing except distinct mechanics also some recognition sequences that are specific for the ECM proteins themselves. Such a setting is sensed directly by the cellular adhesive machinery. A large and growing body of evidences shows that when facing fibrillar environment, the cells utilize different signaling mechanisms and this is further complicated by the fact that they recognize such signals in a 3D system. Accordingly, we anticipate that the fibrillar structuring not only influences the ECM organization, but also possess specific recognition cues that effect cellular behavior. Therefore in this study, utilizing an original protocol for electrospinning, we used native fibrinogen (FBG) as material to produce nanofibers considering that it is a natural ECM protein specifically recognized by the cells (via αvβ3 integrin). Moreover, FBG interacts very well with endothelial cells (HUVEC), already demonstrated in Chapter 4, which cells we used again here as a model system considering easier translation of results for **vascular tissue engineering purposes**, (see Chapter 6). We showed that native FBG nanofibers not only provoke faster cellular interaction (compared to FBG coated planar substrata), but also affect the spatial orientation of cells, likewise previously observed with PEA nanofibers, (see Chapter 3 and Chapter 4). Furthermore, here we provide for the first time evidence (time-laps movie) that the aligned FBG nanofibers may be used as tool for guiding the directional movement of endothelial cells.

Details for this study may be found in the original paper ***"Fibrinogen nanofibers for guiding endothelial cell behavior"***, presented in this Chapter.

Abstract

This paper describes the biological consequences of presenting electrospun fibrinogen (FBG) to endothelial cells as a spatially organized nanofibrous matrix. Aligned and randomly oriented FBG nanofibers with an average diameter of less than 200 nm were obtained by electrospinning of native FBG solution. Electrophoretic profiling confirmed that the electrospun FBG resembled the native protein structure, and fluorescent tracing of FITC-labeled FBG showed that electrospun fibers withstood immersion in physiological solutions reasonably well for several days. With respect to cellular interactions, the nanofibrous FBG matrix provided better conditions for initial recognition by human umbilical vein endothelial cells compared to pre-adsorbed FBG on a flat surface. Furthermore, the spatial organization of electrospun FBG fibers presented opportunities for guiding the cellular behavior in a way that is not possible when the protein is presented in another form (e.g. adsorbed or soluble). For example, on aligned FBG fibers, cells rapidly oriented themselves along the fibers, and time-lapse recordings revealed pronounced cellular movements restricted to the fiber direction. In great contrast, on randomly deposited fibers, cells acquired a stellate-like morphology and became locally immobilized by the fibers. We also show that the FBG fiber orientation significantly influenced both the cytoskeleton organization in confluent cell layers and the orientation of the extracellular fibronectin matrix secreted by the cells. In conclusion, this study demonstrates that electrospun FBG nanofibers can be a promising tool for guiding endothelial cell behavior for tissue engineering applications.

Introduction

Cellular interactions with foreign materials initially rely on fundamental processes such as protein adsorption [1] and ligand–receptor interactions [2], which determine the subsequent cellular interaction and response. In fact, those initial events mimic to a certain extent the natural interaction of cells with the extracellular matrix (ECM) [3], a notion that is required not only for understanding biocompatibility, but also for biology and medicine in general, since tissue development in multicellular animals heavily relies on the ability of cells to synthesize and organize ECM – a fact that cannot be underestimated in biomaterials science.

Basically, the ECM is a structure consisting of glycosaminoglycans (a gel-like matter) and spatially organized matrix fibrils (e.g. collagen, laminin, fibronectin, etc.) whose length in some cases greatly exceeds that of individual cells.[4] The importance of correct regulation of fibril deposition is exemplified by diseases such as osteogenesis imperfecta (caused by mutations in collagen genes), fibrosis (i.e., ectopic accumulation of ECM), as well as by its frequent appearance in degenerative tissue disorders.[5,6] The biological relevance of fibrillar nanostructures is also clearly reflected in the efforts made in the fields of biomaterials and tissue engineering to reproduce and apply ECMlike fibers, e.g. by electrospinning[7] or by self-assembly.8 Despite the promise of such techniques, there is still a need to understand how cells respond to complex structures that contain both spatial and biological information.

Among the different fibrillar proteins, fibrinogen (FBG)[9] is of particular interest for tissue engineering applications due to its many biological functions. FBG is a soluble protein secreted into the plasma in high amounts mainly by hepatocytes, and it plays a key role in the coagulation cascade and as a bridging molecule for platelet aggregation.[10] FBG and its derivative fibrin also serve as a provisional ECM in some injured tissues,[11] and is involved in wound healing,[12] tissue regeneration,[13] inflammatory cell response,[14] and angiogenesis.[15] Thus, the consistency of using fibrin(-ogen) as a tissue sealant and/or scaffold for cellular therapies[16] has been explored for example in cardiovascular, bone, cartilage, and skin tissue engineering applications.[17–20] Interestingly, extrahepatic cells such as lung, intestinal and cervical epithelial cells also secrete FBG[21–23] which then can integrate as a recognizable part of the natural ECM of these cells in the form of non-covalently assembled fibrils.[24] Finally, considering the previously established fact in our laboratory that FBG undergoes significant spatial organization and remodeling into fibrillar structures in contact with endothelial cells,[25] we anticipated that the organization of FBG molecules in matrixlike configurations could have significant impact on subsequent cell behavior. Therefore the aim of this paper was to carefully explore how endothelial cells, here using primary human umbilical vein endothelial cells (HUVECs) as a model system, respond to spatially organized nanofibers produced from electrospinning of pure FBG solution. For that purpose, we built on the work of Bowlin and coworkers[26] who first succeeded in preparing electrospun native FBG nanofibers. Although it has

been previously described that cells such as fibroblasts easily colonize electrospun FBG scaffolds,[27] the fiber stability in aqueous environments and the cellular recognition and locomotor activity toward spatially organized FBG nanofibers are unknown. In this study we address these questions, which comprise the novelty of the obtained results.

Materials and methods

Electrospinning of fibrinogen nanofibers

Fibrinogen nanofibers were prepared as previously described.[26] Briefly, fibrinogen from bovine plasma (Sigma-Aldrich) was dissolved at 100 mg mL^{-1} in 1-1-1,3-3-3-hexafluoroisopropanol (HFIP) (Sigma-Aldrich) mixed (9 : 1) with 10× concentrated DMEM (Invitrogen). The obtained FBG solution was centrifuged at 4000 rpm for 10 minutes and the supernatant was loaded in a conventional 10 mL syringe (BD-Scientific). For electrospinning of that solution we used a home-made setup based on a high voltage supply (Glassman High Voltage Inc.), a syringe pump (AITECS), and a grounded collector. Randomly deposited FBG nanofibers were obtained by vertical electrospinning of the polymer solution onto glass coverslips (ϕ 15 mm, Thermo Scientific) placed on aluminum foil that covered the collector. The applied voltage was 20–25 kV, the distance between the needle tip and the collector was 125 mm, and the pump flow rate was 0.3 mL h^{-1}. Aligned fibers were obtained using the same spinning conditions, but with an original and simple method of collection based on a rotating drum (Fig. S1). Basically, two plastic discs (ϕ 120 mm) were mounted on a common axis and separated by 100 mm. Thin metal wires were stretched between the disc peripheries to form parallel strings at 16 mm distance from each other. While rotating the common axis (600–800 rpm), the nanofibers aligned between the metal wires, and they could thereafter be easily collected onto glass coverslips.

Morphological fiber characterization

The electrospun FBG fibers were morphologically characterized by scanning electron microscopy (SEM, Jeol JSM-5410) at the Center for Biomaterials and Tissue Engineering at the Technical University of Valencia (Spain). Before analysis, the samples were coated with a conductive layer of sputtered gold. The SEM micrographs were taken at an accelerating voltage of 15 kV in order to ensure good image resolution. Fast Fourier Transformation (FFT) outputs of the scanning electron micrographs were then used to characterize the alignment of the fibers.[28] The analysis of the SEM micrographs was performed with ImageJ (NIH) and the oval profile plug-in (authored by William O'Connnell). Briefly, a circular projection was placed on the FFT frequency distribution outputs of the micrographs and the radial sums of the pixel intensities for each degree between 0 and 180° were collected. The pixel intensity was then plotted as a function of its angle of acquisition. Distribution data were normalized to a baseline value and plotted in arbitrary units, allowing different data sets to be directly compared.

Chemical fiber characterization

The effect of the electrospinning process on the protein configuration was investigated using classical SDS-PAGE for pure FBG, electrospun FBG nanofibers, and fibrin gel under reducing conditions. Fibrin gel was obtained by adding thrombin (Sigma-Aldrich; 2.0 NIHU mL^{-1}) and 2.5 mM $CaCl_2$ to a 2 mg mL^{-1} fibrinogen solution. The reduced protein samples were prepared by adding 10% (v/v) of 5% β-mercaptoethanol in sample buffer to the protein samples, and after boiling the obtained samples at 100 °C for 5 minutes, they were loaded in a 10% polyacrylamide gel, electrophoresed using vertical slab apparatus (BioRad), and thereafter stained by Coomassie Blue.

To estimate the chemical stability of the FBG nanofibers under physiological-like conditions, fluorescein isothiocyanate-labeled FBG (FITC-FBG) was added to the FBG polymer solution (0.14 mg mL^{-1}) before electrospinning. In this way, FITC-FBG/FBG nanofibers were obtained as random fibers on glass coverslips. The weight of each sample was measured before and after the electrospinning process to ensure equal mass of nanofibers on each coverslip (1.0 mg). The samples were then incubated in a standard culture environment (37 °C, 5% CO_2) in 0.5 mL of either PBS or culture medium(EndoGRO, Invitrogen) for different time periods: 5, 24, and 72 hours, respectively. After incubation, the supernatant was removed and the remaining nanofibers were dried at room temperature. Then all the samples, including fresh control samples not exposed to any aqueous environments, were immersed in 0.2 M NaOH until the fibers were completely dissolved and no visible debris were present in the solution (48 hours at 37 °C). Finally, the sample extracts were resuspended and analyzed fluorometrically (FluoroMax-4, HoribaJobin Yvon; excitation 494 nm, emission 525 nm).

Cells

Human umbilical vein endothelial cells (HUVECs) were purchased from MilliPore (Spain), and cultured at 37 °C and with 5% CO_2 in complete EndoGRO medium containing 2% fetal bovine serum (FBS). For experiments, cells were harvested and washed two times in FBS-free medium. Typically, the cell seeding density was 5×10^4 cells per sample in 2.0 mL of culture medium in 24-well TCPS plates (Nunc) containing the samples.

Fast cell adhesion assay

To investigate the initial cellular recognition of the nanofibers, a fast cell adhesion assay was performed as previously described.[29] Briefly, cells were seeded in serum-free EndoGRO medium on randomly deposited FBG nanofibers and on glass coverslips coated with FBG (50 μg mL^{-1}). At 5 and 20 minutes after plating, cells were washed, fixed with 4% paraformaldehyde, permeabilized with 0.5% Triton-X 100, and stained for the actin cytoskeleton and nuclei with FITC-phalloidin (Invitrogen) and Hoechst 34580 (Invitrogen) dissolved in PBS containing 1% albumin. Stained cells

were photographed using an inverted fluorescent microscope (Axio Observer Z1, Zeiss), and cells were counted from 20 randomly chosen microscopic fields on each sample.

Overall cell morphology and alignment to fibers

The overall morphology of HUVECs cultured on randomly and aligned electrospun FBG fibers was evaluated after 2 hours of incubation under serum-free conditions. For that purpose, cells were washed, fixed, and stained for actin and nuclei as described in the previous section, and at least three representative images of cells were acquired under each magnification and sample condition. Cell orientation on both aligned and random nanofibers was evaluated by analyzing 40 randomly chosen cells from one representative image using ImageJ (NIH). Briefly, the image of the cell on aligned nanofibers was rotated so that the approximate fiber direction was set perpendicular to the horizontal image baseline which was used as a reference direction (i.e. 0°). Images of cells on random samples were not rotated because of the absence of a reference direction. The longitudinal axis of each cell and its angle against the baseline were then determined. The data were finally normalized and plotted in a distribution histogram between 0 and 180° at 20° intervals. In this way, a perfect cell alignment to the fibers occurred at 90° (i.e. the interval 80–100°).

Visualization of focal adhesion complexes

To visualize focal adhesions, fixed and permeabilized cells were saturated with 1% BSA in PBS for 15 minutes and stained with monoclonal anti-vinculin antibody (Sigma) (dilution 1 : 800) for 30 minutes followed by another 30 minutes of incubation with secondary goat anti-mouse AlexaFluor® 555-conjugated antibody (Abcam). In addition, FITC-phalloidin was used as described above to stain for the actin cytoskeleton.

Time-lapse recording

To monitor cellular movements on the random and aligned FBG nanofibers, cells growing in the culture flask were fluorescently labeled overnight with CellTracker Green CMFDA (Invitrogen) according to the supplier's instructions. The stained cells were harvested and seeded onto random and aligned nanofiber samples for 2 h in serum-free medium. Live imaging of the cells was then initiated using an inverted fluorescent microscope (Axio Observer Z1) equipped with an onstage mini-chamber providing appropriate culture conditions (37 °C, humidified atmosphere, 5% CO_2). Consecutive images were recorded using AxioVision software (Zeiss) every five minutes during a total period of six hours.

Cell motility

To characterize the patterns of cellular movement, the timelapse movies were analyzed using the ImageJ Manual Tracking plugin (developed by FP Cordelières, Institut Curie, Orsay, France). Path

trajectories of 20 randomly chosen cells were analyzed, and from it the main track length was calculated. The main track orientation was measured as for cell alignment (see above) and plotted in the distribution histogram between 0 and 180° at 20° intervals.

Long-term cultures

To follow the long-term behaviour of HUVECs on FBG nanofibers, 3×10^4 cells were cultured on random and aligned samples for up to 7 days in complete EndoGRO medium. At the end of the incubation the cells were fixed and stained for actin and the nucleus as described above.

Fibronectin matrix formation

HUVECs secretion of the fibronectin (FN) matrix was examined via immunofluorescence. For that purpose, 3×10^4 cells per sample were cultured for three days in complete EndoGRO medium. At the end of the incubation, the cells were washed, fixed, and stained with a polyclonal rabbit anti-FN antibody (Santa Cruz) for 30 minutes, followed by secondary goat antirabbit AlexaFluor® 555-conjugated antibody (Abcam).

Statistical analysis

Each datum is expressed as mean ± standard deviation if not indicated otherwise. Statistical significance was determined by a two-tailed independent Student's t-test and $p < 0.05$.

Results

Characterization of electrospun FBG fibers

Electrospinning of 100 mg mL^{-1} FBG in HFIP allowed for the production of homogeneous nanofibers with an average diameter of 192 ± 46 nm (n = 50) as determined from SEM micrographs. By changing the way the fibers were collected during the electrospinning process, it was possible to

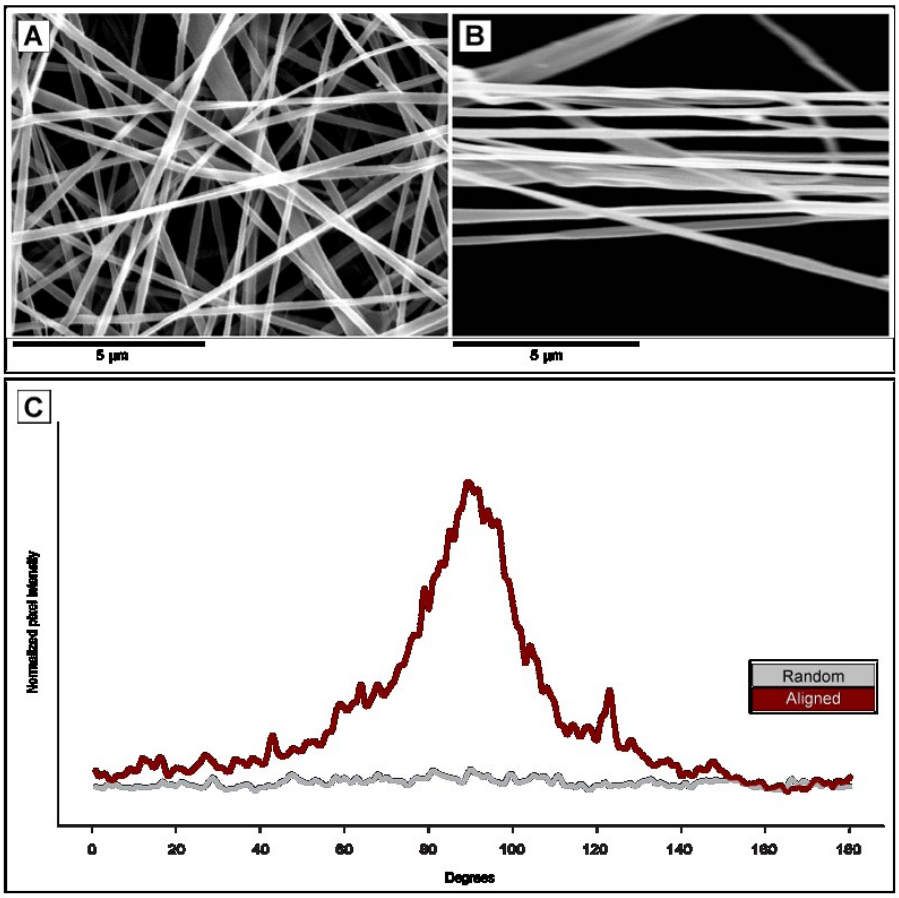

Figure 1. *SEM imaging depicted the spatial organization of electrospun FBG fibers in random **(A)** and aligned **(B)** configurations. The spatial organization of fibers was characterized by FFT analysis and then plotted as pixel intensity against the angle of acquisition **(C)**.*

obtain fibers that were either randomly deposited over the sample or aligned along a common direction (Fig. 1). Specifically, the pixel intensity distribution obtained from FFT analyses of the SEM micrographs revealed that 50% more fibers were oriented in the range of 85 to 95° on aligned samples compared to random samples. To study the influence of the electrospinning process on the FBG structure, a SDS-PAGE was performed (Fig. 2a). The electrophoretic profile of electrospun FBG (dissolved in sample buffer) was observed to be identical to the profile of native FBG protein. In contrast, fibrin (i. e. thrombin-treated FBG) displayed an additional band (between B′β′ and γ) due to fibrinopeptide loss from the polymer backbone. The stability of the FBG nanofibers in aqueous solutions was estimated by extracting FITC-FBG from electrospun FBG/ FITC-FBG nanofibers that had been immersed in PBS or EndoGRO medium for different time periods (Fig. 2b). It was found that the fluorescent signal measured in the extracted samples decreased with time in both solutions, representing a loss of FITC-FBG from the electrospun fibers into solution. After 72 hours of

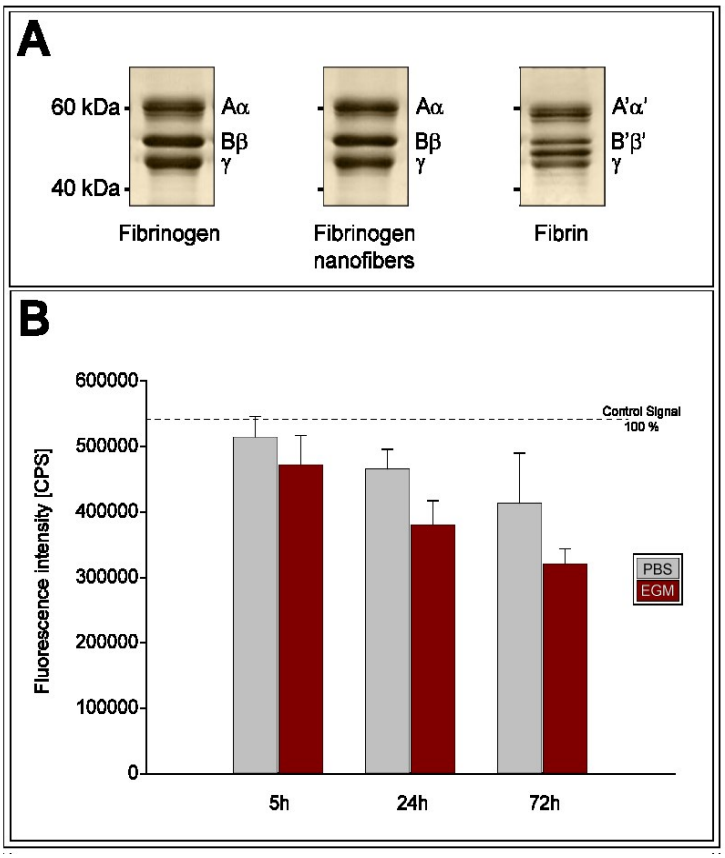

Figure 2. *Characterization of the stability of electrospun FBG fibers.* ***(A)*** *SDS-PAGE profiles of pure FBG, electrospun FBG, and fibrin.* ***(B)*** *Fluorescence intensity was measured in counts per second (CPS) of extracted electrospun FBG/FITC-FBG incubated in PBS or EndoGRO medium (EGM) for different time periods. Error bars show standard error.*

incubation, 24% of fluorescent signal was lost in fibers incubated in PBS. In EndoGRO medium, the fluorescent signal was, in general, weaker at all time points, and by 72 hours the fluorescent signal had decreased to 36% of its original intensity.

Cellular interactions with FBG nanofibers

The cellular recognition and response to the FBG nanofibers were first evaluated using the so-called “fast adhesion” assay, i.e. cell adhesion was measured when any differences in the affinity of

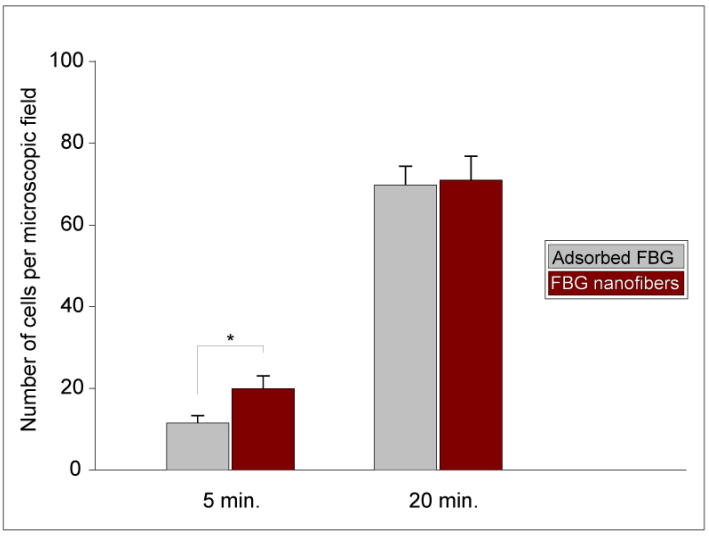

Figure 3. *HUVEC attachment to FBG-coated glass coverslips (grey bars) and electrospun FBG nanofibers (red bars) at 5 and 20 minutes after plating. Data show the average cell number per microscopic field.*

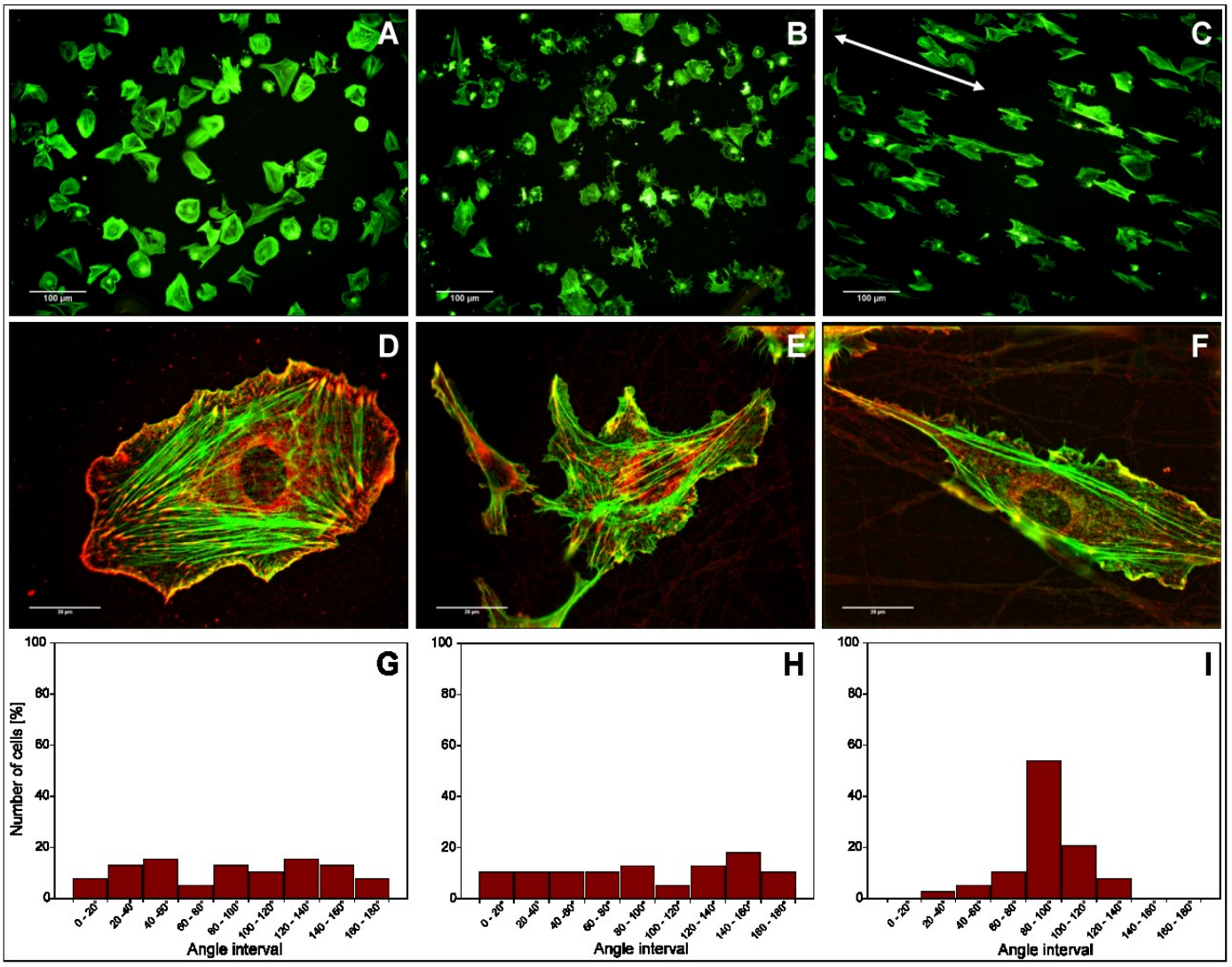

Figure 4. *Cellular interactions with FBG nanofibers after 2 hours of incubation in serum-free medium.* ***(A–C)*** *Overall cell morphology of HUVECs on adsorbed FBG* ***(A)****, randomly deposited nanofibers* ***(B)****, and aligned nanofibers* ***(C)****, where the direction of fiber alignment is indicated by the white arrow.* ***(D–F)*** *Immunofluorescent micrographs showing the development of focal adhesion complexes (vinculin in red) and the actin cytoskeleton (phalloidin in green) on adsorbed FBG* ***(D)****, random nanofibers* ***(E)****, and aligned nanofibers* ***(F)****.* ***(G–I)*** *Distribution of cell orientation on adsorbed FBG* ***(G)****, randomly deposited nanofibers* ***(H)****, and aligned nanofibers* ***(I)****, measured as the angle between the longitudinal cell axis and the line perpendicular to the nanofiber direction*

integrin receptors to their ligand might be easily distinguished, and which typically occurs within a few minutes after seeding.[29] As shown in Fig. 3, after five minutes of incubation almost two times more cells were counted on FBG nanofibers compared to regular FBG-coated samples. However, already after 20 minutes of incubation, cell adhesion on FBG nanofibers and regular FBG-coating was equilibrated. After two hours of incubation, cells had been given enough time to develop their shape, and we then examined the overall cell morphology. When adhered to regular FBG-coated samples the cells presented a typical flattened morphology (Fig. 4a) comprising random cell polarization and a well- developed cytoskeleton with actin fibers that inserted into focal adhesions complexes (Fig. 4d). In sharp contrast, adhesion to random nanofibers promoted an irregular cell shape with multiple cytoplasmic projections extending towards differently oriented fibers (Fig. 4b). The cell protrusions showed high accumulation of actin that co-localized with vinculin in the focal adhesions (Fig. 4e) which often inserted long actin fibers with centripetal organization, suggesting that cells insert some traction over the nanofibers. On aligned FBG nanofibers, the cells acquired a

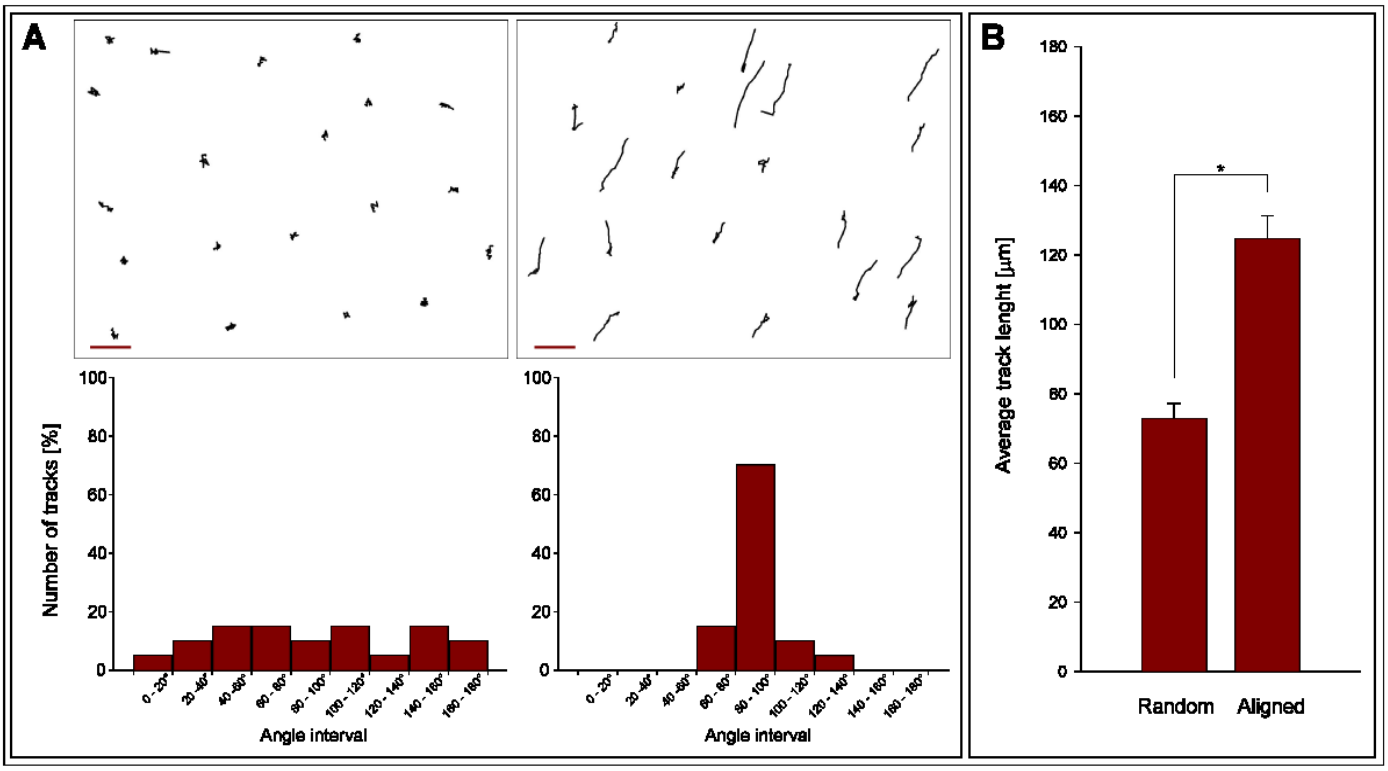

Figure 5. *Cell motility on FBG nanofibers.* ***(A)*** *HUVEC cell tracks on random (upper left) and aligned nanofibers (upper right). Scale bars represent 100 µm. The distributions of the cell track orientation on random and aligned fibers are shown below each graph.* ***(B)*** *Average cell track length on random and aligned FBG*

morphology strongly associated with the spatial organization of the underlying nanofibers. They typically presented an extended morphology that strongly followed the fibers orientation (Fig. 4c). The elongated cell shape corresponded to the highly extended actin stress fibers that were inserting into relatively small focal adhesion complexes located mostly at the polarized cell edges (Fig. 4f). Analysis of cell orientation with respect to the underlying fibers showed that cells oriented along the distributed in all directions (aligned fibers (Fig. 4i), while on random fibers and the regular FBG-coated sample the cell orientation was equally Fig. 4g and 4h).

Cell motility

Time-lapse recordings demonstrated that the cells were highly motile on the aligned FBG nanofibers (see ESI videos 1 and 2†), with individual cells undergoing the typical motile cycle of extending a leading cell edge, followed by traction of the tail cell edge. While most of the cells on aligned FBG nanofibers carried out a linear path of translocation, cells on random nanofibers performed rather oscillatory and relatively short movements and in different directions (see ESI videos 3 and 4). Quantitative analysis of cell motions confirmed that cellular movements on aligned nanofibers clearly coincided with the fiber orientation, while cells on random nanofibers did not display any preferred direction of movement (Fig. 5a). Moreover, cells on aligned nanofibers were confirmed to traverse significantly longer distances (track length) than cells on random nanofibers (Fig. 5b)

Long-term cell culture on FBG nanofibers

To follow the long-term fate of HUVECs grown on FBG nanofibers, cells were cultured on both random and aligned samples for up to 7 days. First, to learn whether the orientation of underlining nanofibers affected the ECM deposition, the cell layers were stained for FN after three days of

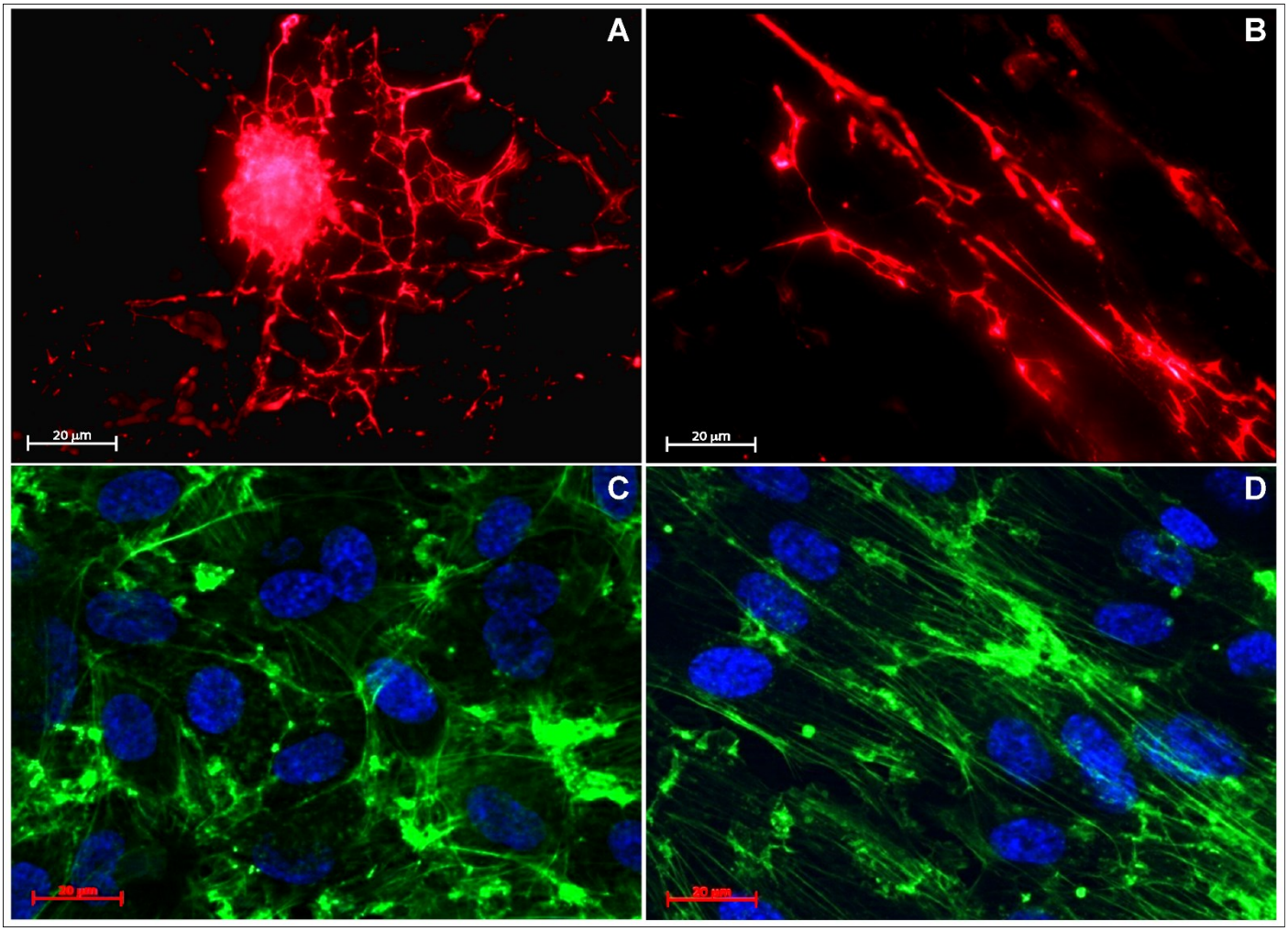

Figure 6. *Deposition of fibronectin secreted by HUVECs cultured for 3 days on random **(A)** and aligned FBG nanofibers **(B)**. Indirect immunofluorescent staining of HUVEC cultured for 7 days on random **(C)** and aligned FBG nanofibers **(D)** with phalloidin (green) and Hoechst (blue).*

incubation. On random fibers, the cell-secreted FN was rather stochastically distributed (Fig. 6a) while on aligned nanofibers the FN matrix clearly assembled along the main fiber direction (Fig. 6b). When cells were cultured further in time, they formed confluent layers on both aligned and random nanofibers within 5–7 days. By staining the cells for their actin cytoskeleton at the end of the culture period, remarkable differences in the organization of cells within the confluent cell layers depending on the spatial organization of the fibers could be observed. On aligned samples, the orientation of the actin cytoskeleton was dominated by the direction of underlying nanofibers, resulting in a uniform linear pattern coinciding with the cell polarization (Fig. 6d).In contrast, on random samples there was no specific orientation of the actin bundles (Fig. 6c).

Discussion

Successful cell–biomaterials interaction is critical for all tissue engineering applications, and depends not only on the adsorption of adhesive proteins,[1] but also on the spatial organization of the proteins.[29] Therefore, spatial engineering of cell– materials interfaces via reconstruction of supramolecular ECM protein structures is, in general, highly sought for,[8,30] and precise reproduction of the fibrillar ECM organization is of specific importance as the ECM is by nature a fibrous structure. In that context, electrospinning of polymer solutions is known to be a potent engineering approach for a simple and fast production of biomimetic nanofibers that resemble natural ECM fibrils,[31] and it has been repetitively used to create ultrathin fibers from a variety of different matrix proteins,[32] including fibrinogen and fibrin.[26,33] The latter achievements are of interest for multiple reasons. For example, fibrin(ogen) is the main component of the provisional ECM during wound healing, and it is also a well-characterized acute phase protein of the innate immune response that attracts many adhesive glycoproteins to serve as a reservoir for growth factors, proteases, and protease inhibitors.[34,35] Moreover, FBG acts as regular ECM for several epithelial cells where it, interestingly, assembles into non-covalent fibrils,[24] which emphasizes the importance of the spatial organization of the protein itself. That observation raises the question: to what extent cells recognize and respond to spatially organized FBG sized in the range of natural ECM fibrils? At the same time, little is still known about the role of fibrillar FBG structures that are not formed via the traditional conversion of FBG into insoluble fibrin, i.e. by enzymatic cleavage by thrombin and further stabilized by transglutaminase (i.e. factor XIII).[9] To address those questions, we herein used tailor-made technology for deposition of FBG nanofibers in either random or aligned configurations. Using established protocols[26] we obtained fibers with an average diameter of 192 nm, which compares well with previously reported values between 80 and 700 nm depending on the FBG concentration (80–170 mg mL^{-1}).[26] However, two important aspects of electrospun FBG need to be clarified: (1) the influence of the electrospinning process on the protein structure and (2) the long-term stability of the electrospun fibers in physiological aqueous environments. In this context, one has to remember that it is still not clear how FBG becomes insoluble during electrospinning. One possibility is that FBG is normally cleaved to fibrin if traces of thrombin are present in commercial FBG. Here, our electrophoretic data clearly showed that FBG did not convert to fibrin during electrospinning as it did not display the additional band present in fibrin caused by the fibrinopeptide loss [9]. This observation confirms that FBG molecules within the electrospun nanofibers assemble and become insoluble by other mechanisms. One can consider the possibility that electrospinning provides the conditions where FBG molecules polymerize by van der Waals forces of attraction that overcome the electrostatic forces of repulsion, giving rise to a peculiar amyloid-like product (aggregate) similar to those described under some pathological conditions (e.g. Alzheimer's disease).[36] It should also be kept in mind that extrahepatic FBG assembles into an insoluble matrix fibrils in presence of cells

(fibroblasts, lung and mammary epithelial cells), in a process where cryptic beta residues are exposed to form FBG fibrils.[35] However, the relevance of such an assembly mechanism in absence of cells is not clear.

With respect to the second issue mentioned above, i.e. the long-term stability of electrospun FBG fibers under aqueous conditions, it has been detailed by Baker et al. that the mechanical properties of electrospun FBG fibers decrease significantly when the fibers are immersed in wet environments (e.g., the stiffness decreases more than 1000 times).[37] Therefore, to understand how aqueous conditions affected the electrospun FBG fibers, we used FITC-labeled FBG for fluorescent tracing of the protein under physiological solutions. That approach revealed that approximately 5% of the protein fibers dissolved during 24 hours of incubation. In our view, that degradation rate is not an obstacle as initial cellular interactions go very fast, typically within minutes (Fig. 3), and also the endothelial cells will secrete many other matrix proteins (e.g. fibronectin, von Willebrand factor, etc.) during the first 24 hours from seeding, which will follow the initial fiber orientation and thus contribute to the cellular response. Indeed, our study demonstrates coextensive organization of FN matrix fibrils at the third day of incubation (Fig. 6). Nevertheless, upon prolonged incubation times, about 30% of the electrospun FBG fibers were dissolved, and such degradation has to be carefully considered for potential biomedical applications.

Following the initial characterization of the electrospun fibers in acellular environments, we then turned our attention to cellular interactions with the electrospun FBG fibers. It is known that FBG expresses a number of cell-binding domains identified on Aα, Bβ and γ-chains. Specifically, the RGD integrin-binding sequence in the Aα-chain and the heparin binding domain within the Bβ-chain particularly mediate cell–matrix interactions.[35,38] According to the electrophoretic profile of FBG fibers, the Aα, Bβ and γ-chains were maintained intact after electrospinning, and thus the electrospun FBG fibers were expected to efficiently promote cell adhesion. Indeed, our data showed that cells adhered equally well on FBG fibers as on glass coverslips coated with FBG. Interestingly, we also showed that the adhesion process went significantly faster on fibrillar FBG compared to FBG adsorbed on a flat surface (Fig. 3). Considering that the fibers were deposited in a random layer dense enough to not permit penetration of cells (i.e. cell adhesion was constrained to a limited surface area), and that the ligand-concentrations on both fibrillar and flat substrata were saturated with respect to optimal cell adhesion (about 30 μg mL^{-1} is sufficient to give maximal cell adhesion according to our own experience), the observed fast cell adhesion on fibrillar FBG indicates an important role of the spatial ligand organization to rapidly engage in integrin activation. Similar observations were made by Cukierman et al.[29] proposing that cell–matrix interactions in three-dimensions occur as a combination of normal focal adhesions and fibrillar adhesions that together mediate cell adhesion much more efficiently than any of those mechanisms do alone. It seems that such advanced matrix-binding structures are pre-synthesized during culture, and when cells are back in a matrix-like environment they rapidly regenerate them.[29] Such adhesion mechanisms could

explain the improved fast cellular interactions with nanofibrous FBG, although one also has to consider the pure geometrical response to the (nano) fibrous environment.[43] Recent studies indicate that cells sense and respond to different nanofiber geometries. For example, Li et al. showed that chondrocytes secrete an increased amount of ECM when seeded on nanofibers compared with the microfiber matrix.[44] It is still not clear how cells recognize and respond to certain fibrillar patterns, which should not be equalized with “classical” topographic environments as they differ in many aspects. For example, microscopic analysis and time-lapse imaging revealed that an isotropic topography (having identical values of a property in all directions) did not alter cell morphology but highly induced cell motility.[45] Our studies, however, with random nanofibers clearly show that multidirectional fiber orientation affects cell morphology, accompanied by cell immobilization. On the other hand, an anisotropic environment can have variable impact on cell behavior (e.g. depending on the ridge–groove ratio), while the highly aligned FBG nanofibers induced elongated cell morphology, and importantly provoked directional cell movement. It is generally difficult to match the topographic cell response with the bioactivity of nanofibers. Nevertheless, our results confirm the relevance of studying and learning more about the reciprocal and adaptive interactions between cells and the surrounding matrix in the interface between two and three dimensional environments.[39,43]

Another important issue that we want to stress on, and which connects with the above observation, is the morphological response of adhering endothelial cells. We found clear differences in the overall cell morphology depending on the spatial organization of fibers. On aligned fibers, cells presented an extended morphology that strongly followed the fiber orientation, while on random nanofibers, cells spread in multiple directions. The presence of highly extended actin stress fibers inserting into focal adhesions suggests that endothelial cells on aligned nanofibers exert traction over the fibers. Also on randomly oriented fibers, cells were shown to form protrusions containing focal adhesions, suggesting strong cellular interaction with the substratum. Interestingly, the overall shape of endothelial cells on random fibers resembles, to a large extent, the stellate-like morphology characteristic for cells residing in three dimensional environments,[39] suggesting that cells read the geometry of the underlining nanofibrous substratum (i.e., 2.5D). One should also consider that nanofibers do not provide enough surface area for larger clustering of integrins and thus resemble more the natural 3D ECM environment.[40] On both aligned and random fibers we observed small focal adhesion complexes (explained by the small surface area of the fiber itself, rather than insufficient contact), which resemble the natural matrix contacts. Collectively, this study provides morphological evidence for well-established focal adhesion complexes and even for the development of matrix contacts that could explain the facilitated initial adhesion of endothelial cells on FBG nanofibers.

Beyond the events of initial cellular adhesion and subsequent spreading, time-lapse studies revealed the patterns of cell migration on the FBG nanofibers. Understanding the factors that control

cell migration is, in general, important when designing implants for optimal cellular infiltration and integration with native tissue. In accordance with other studies,[41] we show that endothelial cells not only oriented themselves well to aligned nanofibers, but also that they moved significantly along them. Conversely, on randomly deposited fibers, cells were locally immobilized and their accumulated traversed distance was reduced, presumably by their strong anchorage from multiple projections extended to differently oriented fibers. Nevertheless, while guiding the movement of cells in a specific direction is important for recruitment of endothelial cells, e.g. for colonization of scaffolds or angiogenesis, local immobilization of cells may also be of interest for tissue engineering applications, e.g. for controlled cell behavior on blood contacting devices where up-regulation of the adhesive phenotype might be very important.[42] Our data indicate that abrogated motility of HUVECs on random fibers could support their local immobilization to the device. In our present work we are now exploring how the balance of adhesive and motile phenotypes influences the cellular differentiation, trying to address the problem of endothelial cells dedifferentiation.

We finally explored whether FBG nanofibers were able to affect the long-term behavior of endothelial cells. For that purpose we cultured HUVECs on random and aligned nanofibers for one week, and interestingly, the orientations of the underlying nanofibers were clearly reflected in the organization of the confluent cellular layers. Not only was the cellular actin cytoskeleton well-aligned with the fiber direction, but the newly generated fibronectin fibrils also followed the organization of the cytoskeleton and the nanofiber direction. Those observations suggest that the described aligned FBG nanofibers are a promising template for oriented ECM deposition.

Conclusions

This study provides insights into how endothelial cells respond to spatially organized ECM-like stimuli such as pure FBG nanofibers. Being relatively stable for several days under physiological conditions, FBG nanofibers were well recognized by HUVECs and showed a clear ability to modulate cell behavior via the orientation of the fibers. Collectively, this study shows that FBG nanofibers have potential for tissue engineering applications, but also that they represent a simple model system that can allow for further explorations of the natural interaction between cells and their extracellular environment.

Acknowledgments

This work was supported by CIBER-BBN via the European Commission through the FP7 Industry-Academia Partnerships and Pathways (IAPP) project 324386 (FIBROGELNET) and the EuroNanoMed project STRUCTGEL.

Electronic supplementary information (ESI) available

Supplementary videos 1 to 4 and a supplementary figure are available at http://pubs.rsc.org

References

1. C. J. Wilson, R. E. Clegg, D. I. Leavesly and M. J. Pearcy, Tissue Eng., 2005, 11, 1.
2. A. L. Berrier and K. M. Yamada, J. Cell. Physiol., 2007, 213, 565.
3. W. P. Daley, S. B. Peters and M. Larsen, J. Cell Sci., 2008, 121, 255.
4. C. Frantz, K. M. Steward and V. M. Weaver, J. Cell Sci., 2010, 123, 4195.
5. H. Järveläinen, A. Sainio, M. Koulu, T. N. Wight and R. Penttinen, Pharmacol. Rev., 2009, 61, 198.
6. P. Lu, K. Takai, V. M. Weaver and Z. Werb, Cold SpringHarbor Perspect. Biol., 2011, 3, a005058.
7. 7 S. Agarwal, J. H. Wendorff and A. Greiner, Polymer, 2008, 49, 5603.
8. G. A. Silva, C. Czeisler, K. L. Niece, E. Beniash, D. A. Harrington, J. A. Kessler and S. I. Stupp, Science, 2004, 303, 1352.
9. M. W. Mosesson, J. Thromb. Haemostasis, 2005, 3, 1894. 10 T. Lisman, C. Weetering and P. G. de Groot, Front. Biosci., 2005, 10, 2504.
10. J. W. Weisel, Adv. Protein Chem., 2005, 70, 247.
11. R. Raghow, FASEB J., 1994, 8, 823.
12. K. M. Yamada and R. A. F. Clark, in The Molecular and Cellular Biology of Wound Repair, ed. R. A. F. Clark, Plenum, New York, 2nd edn, 1996, pp. 51–93.
13. M. J. Flick, X. Du, D. P. Witte, M. Irouskova, D. A. Soloviev, S. J. Busuttil, E. F. Plow and J. L. Degen, J. Clin. Invest., 2004, 113, 1596.
14. V. W. van Hinsbergh, A. Collen and P. Koolwijk, Ann. N. Y. Acad. Sci., 2001, 936, 426.
15. M. Dietrich, J. Heselhaus, J. Wozniak, S. Weinandy, P. Mela, B. Tschoeke, T. Schmitz-Rode and S. Joeckenhoevel, Tissue Eng., Part C, 2013, 3, 216.
16. Q. Ye, G. Zünd, P. Benedikt, S. Jockenhoevel,
17. S. P. Hoerstrup, S. Sakyama, J. A. Hubbell and M. Turina, Eur. J. Cardio-Thorac., 2000, 17, 587.
18. H. E. Davis, S. L. Miller, E. M. Case and J. K. Leach, Acta Biomater., 2011, 7, 691.
19. C. J. Hunter, J. K. Mouw and M. E. Levenston, Osteoarthr. Cartilage, 2004, 12, 117.
20. M. Hojo, S. Inokuchi, M. Kidokoro, N. Fukuyama, E. Tanaka, C. Tsuji, M. Miyasaka, R. Tanino and H. Nakazawa, Plast. Reconstr. Surg., 2003, 111, 1638.
21. S. O. Lawrence and P. J. Simpson-Haidaris, Thromb. Haemost., 2004, 92, 234.
22. E. P. Molmenti, T. Ziambaras and D. H. Perlmutter, J. Biol. Chem., 1993, 268, 14116.
23. S. Y. Lee, K. P. Lee and J. W. Lim, Thromb. Haemost., 1996, 75, 466.
24. M. Pereira, B. J. Rybarczyk, T. M. Odrljin, D. C. Hocking, J. Sottile and P. J. Simpson-Haidaris, J. Cell Sci., 2002, 115, 609.
25. R. Tzoneva, T. Groth, G. Altankov and D. Paul, J. Mater. Sci.: Mater. Med., 2002, 13, 1235.

26. G. E. Wnek, M. E. Carr, D. G. Simpson and G. L. Bowlin, Nano Lett., 2003, 3, 213.
27. M. C. Mcmanus, E. D. Boland, D. G. Simpson, C. P. Barnes and G. L. Bowlin, J. Biomed. Mater. Res. Part A, 2007, 81, 299.
28. C. Ayers, G. L. Bowlin, S. C. Henderson, L. Taylor, J. Shultz, J. Alexander, T. Telemeco and D. G. Simpson, Biomaterials, 2006, 27, 5524.
29. E. Cukierman, R. Pankov, D. R. Stevens and K. Yamada,
30. Science, 2001, 294, 1708.
31. K. Salchert, U. Streller, T. Pompe, N. Herold, M. Grimmer and C. Werner, Biomacromolecules, 2004, 5, 1350. 31 Q. P. Pham, U. Sharma and A. G. Mikos, Tissue Eng., 2006, 12, 1197.
32. S. A. Sell, P. S. Wolfe, K. Garg, J. M. McCool, I. A. Rodriguez and G. L. Bowlin, Polymer, 2010, 2, 522.
33. S. R. Perumcherry, K. P. Chennazhi, S. V. Nair, D. Menon and R. Afeesh, Tissue Eng., Part C, 2011, 17, 1121.
34. N. Laurens, P. Koolwijk and P. M. de Maat, Thromb. Haemostasis, 2006, 4, 932.
35. B. J. Rybarczyk, S. O. Lawrence and P. J. Simpson-Haidaris, Blood, 2003, 102, 4035.
36. M. Fändrich, Cell. Mol. Life Sci., 2007, 64, 2066.
37. S. Baker, J. Sigley, C. C. Helms, J. Stitzel, J. Berry, K. Bonin and M. Guthold, Mater. Sci. Eng., C, 2012, 32, 215.
38. T. M. Odrljin, C. W. Francis, L. A. Sporn, L. A. Bunce, V. J. Marder and P. J. Simpson-Haidaris, Arterioscler., Thromb., Vasc. Biol., 1996, 16, 1544.
39. F. Grinnell, Trends Cell Biol., 2003, 13, 264.
40. B. Geiger, J. P. Spatz and A. D. Bershadsky, Nat. Rev. Mol. Cell Biol., 2009, 10, 21.
41. H. G. Sundararaghavan, R. L. Saunders, D. A. Hammer and J. A. Burdick, Biotechnol. Bioeng., 2013, 110, 1249.
42. A. de Mel, G. Jell, M. M. Stevens and A. M. Seifalian, Biomacromolecules, 2008, 9, 2969.
43. L. G. Griffith and M. Swartz, Nat. Rev. Mol. Cell Biol., 2006, 7(3), 211.
44. W.-J. Li, Y. J. Jiang and R. S. Tuan, Tissue Eng., 2006, 12, 1775.
45. E. Lamers, R. Van Horssen, J. Te Riet, F. C. Van Delft, R. Luttge, X. F. Walboomers and J. Jansen, Eur. Cell. Mater., 2010, 20, 329.

CHAPTER 6

ELECTROSPUN FIBRINOGEN–PLA NANOFIBERS FOR VASCULAR TISSUE ENGINEERING

Published in
Journal of Tissue Engineering and Regenerative Medicine, 2016

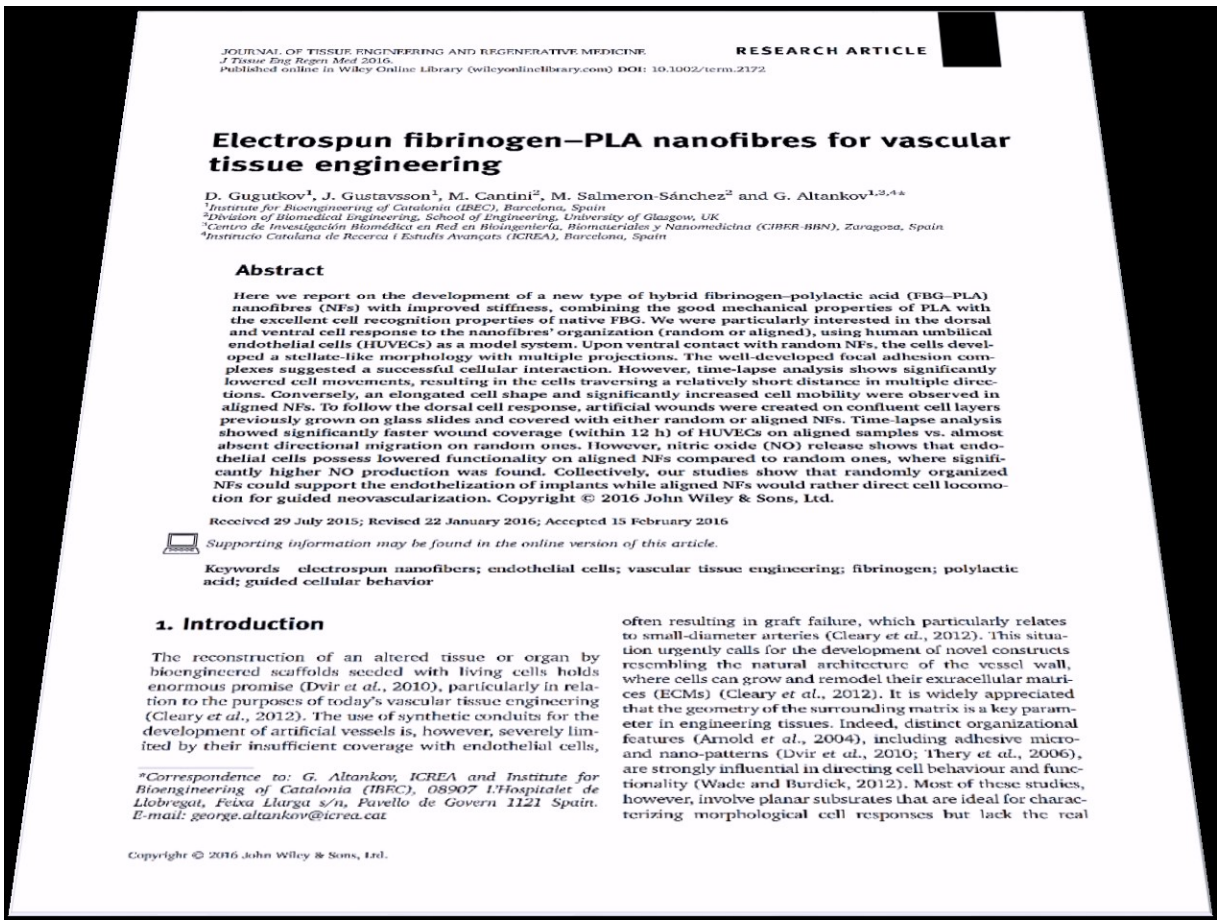

JOURNAL OF TISSUE ENGINEERING AND REGENERATIVE MEDICINE
J Tissue Eng Regen Med 2016.
Published online in Wiley Online Library (wileyonlinelibrary.com) DOI: 10.1002/term.2172

RESEARCH ARTICLE

Electrospun fibrinogen–PLA nanofibres for vascular tissue engineering

D. Gugutkov[1], J. Gustavsson[1], M. Cantini[2], M. Salmeron-Sánchez[2] and G. Altankov[1,3,4]*
[1]*Institute for Bioengineering of Catalonia (IBEC), Barcelona, Spain*
[2]*Division of Biomedical Engineering, School of Engineering, University of Glasgow, UK*
[3]*Centro de Investigación Biomédica en Red en Bioingeniería, Biomateriales y Nanomedicina (CIBER-BBN), Zaragoza, Spain*
[4]*Instituto Catalana de Recerca i Estudis Avançats (ICREA), Barcelona, Spain*

Abstract

Here we report on the development of a new type of hybrid fibrinogen–polylactic acid (FBG–PLA) nanofibres (NFs) with improved stiffness, combining the good mechanical properties of PLA with the excellent cell recognition properties of native FBG. We were particularly interested in the dorsal and ventral cell response to the nanofibres' organization (random or aligned), using human umbilical endothelial cells (HUVECs) as a model system. Upon ventral contact with random NFs, the cells developed a stellate-like morphology with multiple projections. The well-developed focal adhesion complexes suggested a successful cellular interaction. However, time-lapse analysis shows significantly lowered cell movements, resulting in the cells traversing a relatively short distance in multiple directions. Conversely, an elongated cell shape and significantly increased cell mobility were observed in aligned NFs. To follow the dorsal cell response, artificial wounds were created on confluent cell layers previously grown on glass slides and covered with either random or aligned NFs. Time-lapse analysis showed significantly faster wound coverage (within 12 h) of HUVECs on aligned samples vs. almost absent directional migration on random ones. However, nitric oxide (NO) release shows that endothelial cells possess lowered functionality on aligned NFs compared to random ones, where significantly higher NO production was found. Collectively, our studies show that randomly organized NFs could support the endothelization of implants while aligned NFs would rather direct cell locomotion for guided neovascularization. Copyright © 2016 John Wiley & Sons, Ltd.

Received 29 July 2015; Revised 22 January 2016; Accepted 15 February 2016

Supporting information may be found in the online version of this article.

Keywords electrospun nanofibers; endothelial cells; vascular tissue engineering; fibrinogen; polylactic acid; guided cellular behavior

1. Introduction

The reconstruction of an altered tissue or organ by bioengineered scaffolds seeded with living cells holds enormous promise (Dvir *et al.*, 2010), particularly in relation to the purposes of today's vascular tissue engineering (Cleary *et al.*, 2012). The use of synthetic conduits for the development of artificial vessels is, however, severely limited by their insufficient coverage with endothelial cells, often resulting in graft failure, which particularly relates to small-diameter arteries (Cleary *et al.*, 2012). This situation urgently calls for the development of novel constructs resembling the natural architecture of the vessel wall, where cells can grow and remodel their extracellular matrices (ECMs) (Cleary *et al.*, 2012). It is widely appreciated that the geometry of the surrounding matrix is a key parameter in engineering tissues. Indeed, distinct organizational features (Arnold *et al.*, 2004), including adhesive micro- and nano-patterns (Dvir *et al.*, 2010; Thery *et al.*, 2006), are strongly influential in directing cell behaviour and functionality (Wade and Burdick, 2012). Most of these studies, however, involve planar substrates that are ideal for characterizing morphological cell responses but lack the real

*Correspondence to: G. Altankov, ICREA and Institute for Bioengineering of Catalonia (IBEC), 08907 L'Hospitalet de Llobregat, Feixa Llarga s/n, Pavello de Govern 1121 Spain. E-mail: george.altankov@icrea.cat

Published online 30 May 2016 in www.onlinelibrary.wiley.com
Journal of Tissue Engineering and Regenerative Medicine 2016
DOI: 10.1002/term.21

Preface to Chapter 6

This chapter does not provide any new concept, neither different cellular system. It is dedicated on the **development of a new type of hybrid nanofibers** considered for vascular tissue engineering and stress on their application.

As shown in the previous Chapter 5 we have successfully electrospun native fibrinogen nanofibers. However, although these fibers were well recognized by endothelial cells, they presented poor mechanical properties, being too soft and easily breakable in contact with liquids. This was a reason why we could not study the **dorsal cell response**, i.e. the situation when cells receive a signal from the 3rd dimension. Here we reported the development of novel hybrid fibrinogen / polylactic acid (FBG/PLA) nanofibers with improved mechanical properties, but retaining the good cell-recognition properties of native FBG. This part of the Thesis describes some technological aspects of their production alongside with their biological characterization. The emphasis is on the role of the nanofibers organization upon contact with the dorsal and ventral cell surfaces, using HUVEC as a relevant cell model and time-laps microscopy to follow their motility. The functional tests showed that endothelial cells possess lowered activity (decreased nitric oxide (NO) secretion) when cultured on aligned nanofibers, presumably as a consequence of increased cell mobility that was also observed. This suggests that randomly organized nanofibers are these that may support the **endothelialization** of implants, while aligned nanofibers are more suitable for **guided neovascularization** promoted by the improved directional migration of the cells on them.

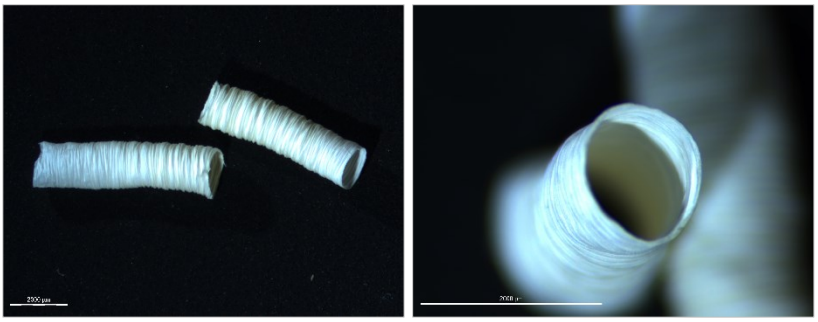

Electrospun tubes made of hybrid PLA/FBG nanofibers and produced in our laboratory by original technique, developed by the auther of this Thesis

Note: The described composite FBG/PLA nanofibers were successfully applied in two European projects in the field of Tissue engineering conducted in our group, namely: STRUCTGEL (FP7 Euronanomed) and FIBROGELNET (FP7-PEOPLE-2012-IAPP). These projects are dealing with the development of soft nanofibrous construct for cellular therapy of degenerative skeletal disorders, which demonstrates applicability of the hybrid nanofibers far beyond the scope of the present work.

Complete details for this study may be found in the original paper ***"Electrospun FBG–PLA nanofibers for vascular tissue engineering"***, presented in this Chapter.

Abstract

Here we report on the development of a new type of hybrid fibrinogen–polylactic acid (FBG–PLA) nanofibers (NFs) with improved stiffness, combining the good mechanical properties of PLA with the excellent cell recognition properties of native FBG. We were particularly interested in the dorsal and ventral cell response to the nanofibers' organization (random or aligned), using human umbilical endothelial cells (HUVECs) as a model system. Upon ventral contact with random NFs, the cells developed a stellate-like morphology with multiple projections. The well-developed focal adhesion complexes suggested a successful cellular interaction. However, time-lapse analysis shows significantly lowered cell movements, resulting in the cells traversing a relatively short distance in multiple directions. Conversely, an elongated cell shape and significantly increased cell mobility were observed in aligned NFs. To follow the dorsal cell response, artificial wounds were created on confluent cell layers previously grown on glass slides and covered with either random or aligned NFs. Time-lapse analysis showed significantly faster wound coverage (within 12 h) of HUVECs on aligned samples vs. almost absent directional migration on random ones. However, nitric oxide (NO) release shows that endothelial cells possess lowered functionality on aligned NFs compared to random ones, where significantly higher NO production was found. Collectively, our studies show that randomly organized NFs could support the endothelization of implants while aligned NFs would rather direct cell locomotion for guided neovascularization.

Keywords: electrospun nanofibers; endothelial cells; vascular tissue engineering; fibrinogen; polylactic acid; guided cellular behavior

Introduction

The reconstruction of an altered tissue or organ by bioengineered scaffolds seeded with living cells holds enormous promise, (Dvir et al., 2010), particularly in relation to the purposes of today's vascular tissue engineering, (Cleary et al., 2012). The use of synthetic conduits for the development of artificial vessels is, however, severely limited by their insufficient coverage with endothelial cells, often resulting in graft failure, which particularly relates to small-diameter arteries (Cleary et al., 2012). This situation urgently calls for the development of novel constructs resembling the natural architecture of the vessel wall, where cells can grow and remodel their extracellular matrices (ECMs) (Cleary et al., 2012). It is widely appreciated that the geometry of the surrounding matrix is a key parameter in engineering tissues. Indeed, distinct organizational features (Arnold et al., 2004), including adhesive micro and nano-patterns, (Dvir et al., 2010; Thery et al., 2006),

Most of these studies, however, involve planar substrates that are ideal for characterizing morphological cell responses but lack the real three-dimensional (3D) architecture necessary for the establishment of a functional tissue, (Dvir et al., 2010). Conversely, studies on cells encapsulated in hydrogel systems provide an adequate 3D micro-environment but lack the hierarchical fibrillar organization of ECM and its mechanical properties, (Lutolf and Hubbell, 2005; Dvir et al., 2010). Fibrillar structures provoke cellular interactions, apart from providing better mechanical support. They can also guide directional cell movements, (Dvir et al., 2010). Therefore, the implications of electrospining technology for producing fibrous scaffolds have received much attention in tissue engineering, due to the morphological and dimensional similarity of synthesized nanofibers to the natural ECM (recently reviewed by Liu et al., 2013). Moreover, during electrospinning the nanofibers can be orientated depending on the fiber collection set-up, (Baji et al., 2010) and recent studies have shown that such orientated nanofibers can guide the spatial arrangement of cytoskeletal proteins, resulting in their elongation along the direction of fibers orientation, (Liu et al., 2009; Guelcher and Goldstein, 2009). However, relatively little is known about whether fiber orientation can influence overall cell behavior and cell-specific functionality, (Fu and Wang, 2012), particularly of endothelial cells, which are a principal cellular component of the vessel wall, (Fang et al., 2011). Current studies in the field show that nanofibrous scaffolds should be considered as ideal candidates for the engineering of the vessel wall because they mimic the fibrillar structure of the ECM, (Ma et al., 2005; Steven and George, 2005; Swartz et al., 2005), provide the desired mechanical stability (Edelman, 1999) and topographical features that encourage the interaction and growth of endothelial cells, (Chiu et al., 2005; Nisbet et al., 2007; Kumar and Krishnan, 2001).

Utilizing established protocols, (Wnek et al., 2003; He et al., 2011; Perumcherry et al., 2011), we have previously electrospun native fibrinogen (FBG) nanofibers (NFs) in consideration of distinct in vitro studies on cell behavior and potential vascular tissue engineering applications, (Gugutkov et

al., 2013). Although these fibers were well recognized by endothelial cells, they presented poor mechanical properties, being too soft and easily breakable in contact with cells. Here we report on the development of a novel type of hybrid fibrinogen–polylactic acid (FBG– PLA) nanofibers with improved mechanical properties, but at the same time retaining the good cell-recognition characteristics of native FBG. This paper describes some aspects of their production and biological characterization, emphasizing the role of NFs organization upon contact with the dorsal or ventral cell surfaces, using human umbilical endothelial cells (HUVECs) as a relevant cell model.

Materials and methods

Electrospinning of FBG–PLA nanofibers

For the production of composite FBG–PLA nanofibers, fibrinogen from bovine plasma (Sigma-Aldrich) and poly-LDL-lactic acid 70:30 (PURAC) were separately dissolved in 1,1,1,3,3,3-hexafluoroisopropanol (HFIP; Sigma-Aldrich). PLA (4% w/v) was dissolved overnight at room temperature under continuous agitation. Fibrinogen (100 mg/ml) was dissolved in a 9:1 mixture of HFIP and 10× Dulbecco's modified Eagle's medium (DMEM; Invitrogen) and centrifuged at 4000 rpm for 10 min. The supernatant was carefully collected, mixed with the PLA solution (1:1 v/v) and loaded into a syringe pump (AITECS). For electrospinning, we used a conventional set-up based on a high voltage supply (Glassman High Voltage Inc.) and a grounded collector. Randomly deposited nanofibers were obtained by vertical electrospinning onto 15 mm round glass coverslips (Thermo Scientific) placed on aluminum foil. Aligned fibers were obtained using an original method of collection, as recently described (Gugutkov et al., 2013). The applied voltage in both cases was 25–30 kV, the distance between the needle tip and the collector was 125 mm, and the pump flow rate was set to 0.5 ml/h.

Characterization of nanofibers

Fiber morphology and alignment

The electrospun FBG–PLA fibers were coated with a conductive layer of sputtered gold and then viewed by scanning electron microscopy (SEM) at 15 kV (Jeol JSM-5410). Fast Fourier transform (FFT) outputs of the SEM micrographs were used to characterize fiber alignment (ImageJ with Oval profile plug-in). Briefly, a circular projection was placed on the FFT frequency distribution outputs and the radial sums of the pixel intensities for each angle (0–180°) were calculated. Pixel intensity was then plotted as a function of its angle of acquisition. Distribution data were normalized to a baseline value and plotted in arbitrary units.

Atomic force microscopy

Nanofibers of different composition (composite FBG–PLA, pure FBG and pure PLA, respectively) were incubated at 37°C in phosphate-buffered saline (PBS) for either 1 day or 1 week, to characterize their stability. After incubation, the fibers were dried under a nitrogen flow and their morphology and mechanical properties were evaluated using atomic force microscopy (AFM). For that purpose, a Nanowizard® 3 Bioscience AFM (JPK Instruments AG) was used in the quantitative imaging (QI™) mode, with a set-point of 0.4 V, a Z length of 0.7 μm and an extend/retract time of 7 ms. Cantilevers with a spring constant of 2.8 N/m (Bruker) were used. The height, slope and

adhesion images were obtained from the force spectroscopy curves recorded for each pixel of the scanned areas (256 × 256 pixels).

The mechanical stiffness of the nanofibers was measured through nanoindentation experiments performed via AFM. Nanoindentations were carried out in a MultiMode AFM from Bruker (Billerica, MA, USA), using cantilevers (OTR8 from Bruker) with a 0.57 N/m spring constant and a square pyramidal tip with a half-angle of 35°. Calibration of the tip sensitivity was performed under the same conditions as the experiments, using a flat rigid surface, and the value was used to correct the force–height curves for the deflection of the cantilever. The stiffness was then calculated using the slope of the force–penetration curves, as described elsewhere (Forner et al., 2009).

Stability

To determine the stability of FBG-containing nanofibers in aqueous surroundings, we labelled FBG with fluorescein isothiocyanate (FITC; 0.1 mg/ml) before electrospinning. Nanofibers containing known amounts of FITC–FBG (0.2% from the total protein) were then electrospun in controlled quantities (1.0 mg) and thereafter incubated at 37°C in PBS for up to 72 h. After incubation, the supernatant was collected and its fluorescence was measured (494 nm excitation, 525 nm emission; FluoroMax-4, Horiba-Jobin Yvon). Pure FBG nanofiber samples, obtained as previously described (Gugutkov et al., 2013) and containing the same amount of FITC-labelled FBG, were used as the control.

Cells

Human umbilical vein endothelial cells (HUVECs) were obtained from MilliPore and cultured in complete EndoGRO medium (MilliPore) with 2% fetal bovine serum (FBS). For the experiments, cells were harvested with trypsin–EDTA, which was subsequently inactivated by FBS, and washed twice in FBS-free medium. The cells were seeded on nanofiber samples placed in standard 24-well plates, typically using 2.0 ml medium.

Cell morphology and visualization of focaladhesion complexes

Overall cell morphology on randomly and aligned electrospun FBG–PLA nanofibers was evaluated after 2 h of incubation in serum-free conditions (cell seeding density 5×10^4 cells/sample) and also after 7 days of incubation in the presence of FBS (cell seeding density 3×10^4 cells/sample). After incubation, the cells were washed with PBS, fixed with 4% paraformaldehyde, permeabilized with 0.5% Triton-X100, and stained with FITC–phalloidin (Invitrogen) for actin cytoskeleton and Hoechst 34580 (Invitrogen) for nuclei. Focal adhesions were visualized with monoclonal anti-vinculin antibody (Sigma-Aldrich) followed by goat anti-mouse AlexaFluor® 555-conjugated secondary antibody (Abcam). Cells were photographed using an inverted fluorescent microscope (Axio

Observer Z1, Zeiss) and at least three representative images were acquired for each sample condition.

Nitric oxide production

A Nitric Oxide Assay Kit (Enzo, Life Science) based on the Griess reaction was used to colorimetrically determine total nitrate levels in the culture supernatants after 1 and 3 days of cell culture on random and aligned FBG–PLA NFs. As no significant difference in cell growth was found between random and aligned NFs and a control sample (glass coated with 50 µg/ml FBG at 37°C for 30 min) after 7 days of culture, direct comparison of the photometric signals without normalization to cell numbers was done.

Long-term cultures

To follow the long-term cell response to random and aligned NFs, 3×10^4 cells were seeded on the samples and cultured for 7 days in complete EndoGRO medium, which was exchanged each second day. At the end of incubation the cells were fixed and stained for actin and nuclei, as described above. In addition, cell-produced fibronectin (FN) matrix was visualized by immunofluorescence, using polyclonal anti-FN antibody (Sigma, cat. no. F3648) followed by AlexaFluor® 555 anti-rabbit secondary antibody (Invitrogen, cat. no. A21428). Cell density was determined by counting the cell nuclei in four randomly chosen squares from low-magnification fluorescent images.

Cell mobility

To investigate how FBG–PLA nanofibers influence cell mobility, we distinguished between dorsally and ventrally applied nanofibers. In the latter case, time-lapse recordings of HUVECs were initiated 1 h after cell seeding (3×10^4 cells/sample) on FBG–PLA nanofibers and proceeded for 6 h (12 images/h), using an on-stage mini-chamber coupled to the microscope (Axio Observer Z1, Zeiss) to assure appropriate cell culture conditions (37°C, humidified atmosphere and 5% CO_2). To investigate the dorsal cell response to nanofibers, confluent layers of HUVECs produced on glass slides were scratched with a sterile pipette tip to produce an artificial wound (ca. 1 mm wide). The cell layers were then covered with random or aligned nanofibers deposited onto 10 mm cylindrical Teflon rings, to ensure intimate contact of the cells with the NFs, and recorded as above for up to 12 h. Time-lapse recordings were processed using the MTrackJ plugin of ImageJ (developed by the Biomedical Imaging Group of Erasmus University Medical Centre, Rotterdam, The Netherlands). Path trajectories of 15 (ventral experiment) and 20 (dorsal experiment) randomly chosen cells were traced manually, following their positions at each tenth frame of the time-lapse records to analyze their motile behavior.

Statistical analysis

Data are expressed as mean ± standard deviation (SD) unless indicated otherwise. Statistical significance was determined by two-tailed independent Student's t-test ($p < 0.05$).

Results

Morphology and mechanical properties of electrospun FBG–PLA nanofibers

Composite FBG–PLA nanofibers were obtained by electrospinning a mixture of FBG and PLA in HFIP, collected as a homogeneous layer of either random or aligned fibers (Figure 1A, B). In the latter case, pixel intensity distribution obtained from FFT analyses of representative SEM fiber images revealed that the majority of the fibers aligned within 10° of the major fiber direction (Figure 1C, D). The main fiber diameters determined from SEM images are shown in Figure 1E; 398 ± 128 nm for random fibers and 250 ± 160 nm for aligned ones (n = 100). The mechanical properties of dry nanofibers were determined by nano-indentations, using AFM. Figure 1F shows that reinforcement of FBG nanofibers with PLA substantially increased the local stiffness of the fibers from 30 ± 10 Nm to 275 ± 50 Nm. Meanwhile, pure PLA fibers were significantly stiffer than composite nanofibers (4000 ± 400 Nm).

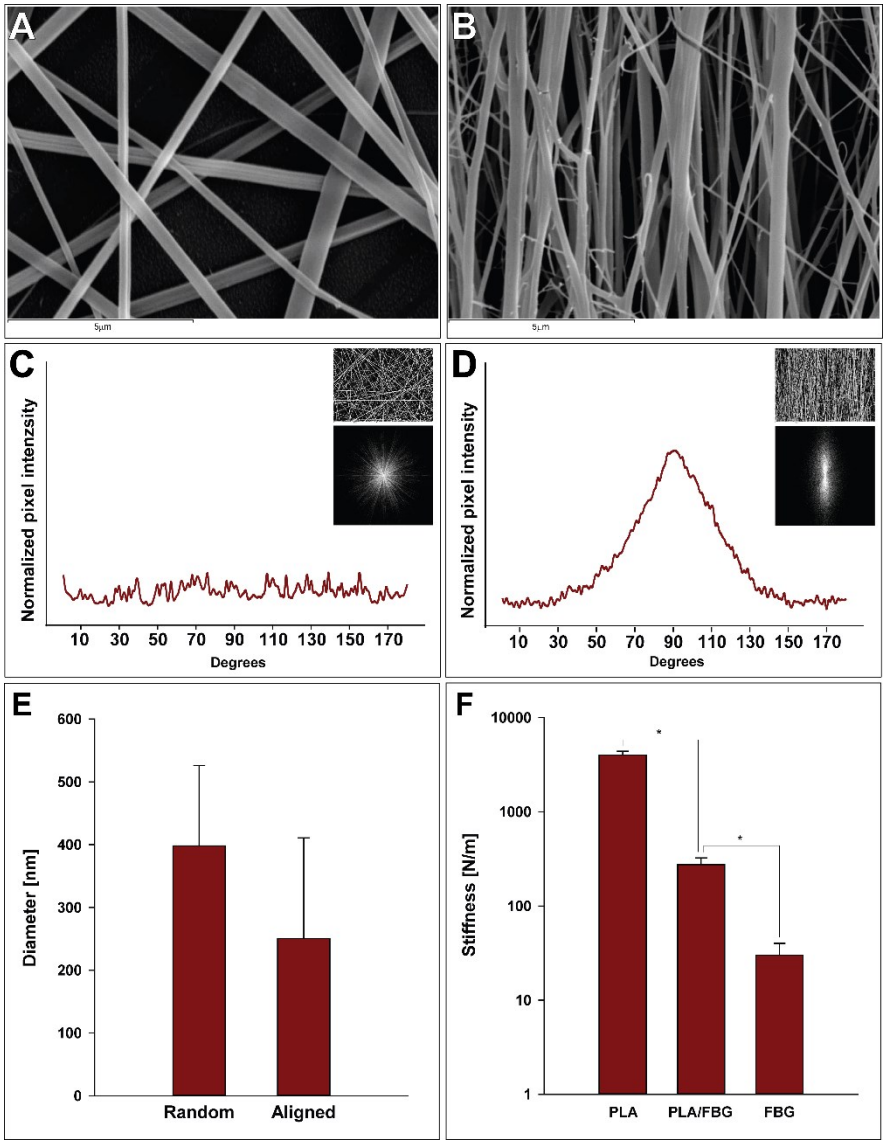

Figure 1. *SEM images representing the spatial organization of electrospun FBG–PLA nanofibers in **(A)** random and **(B)** aligned configurations. The spatial organization of fibers is characterized by FFT analysis: **(C)** pixel intensity plotted against the angle of acquisition; **(D)** pixel intensity around 90° indicates fiber alignment, which is absent in the random samples in **(C)**. **(E)** Average fiber diameter and **(F)** stiffness of the pure PLA, composite FBG–PLA and pure FBG nanofibers measured by AFM; *statistically significant difference (p< 0.05)*

Stability of electrospun fibers in physiological solution

The stability of composite and pure nanofibers in aqueous solutions was initially estimated from morphological changes using AFM. After 7 days of incubation in PBS at 37°C, both FBG and FBG–PLA fibers presented clear changes in their morphology, as judged by AFM adhesion strength magnitude images. Over the same period, pure PLA fibers remained unaltered (Figure 2). However, AFM height images did not reveal any significant differences in surface roughness, suggesting less sensitivity of this approach, but also implying that degradation is rather negligible. No evidence for degradation was found at intermediate times (data not shown), indicating that the samples were unaltered over shorter periods of incubation. Fiber stability was further characterized by measuring fluorescence release from electrospun FBG–PLA composite fibers containing FITC–FBG. For comparison, pure FBG nanofibers containing the same amount of FITC–FBG (0.2% from the total protein) and prepared according to a previously described protocol (Gugutkov et al. 2013) were

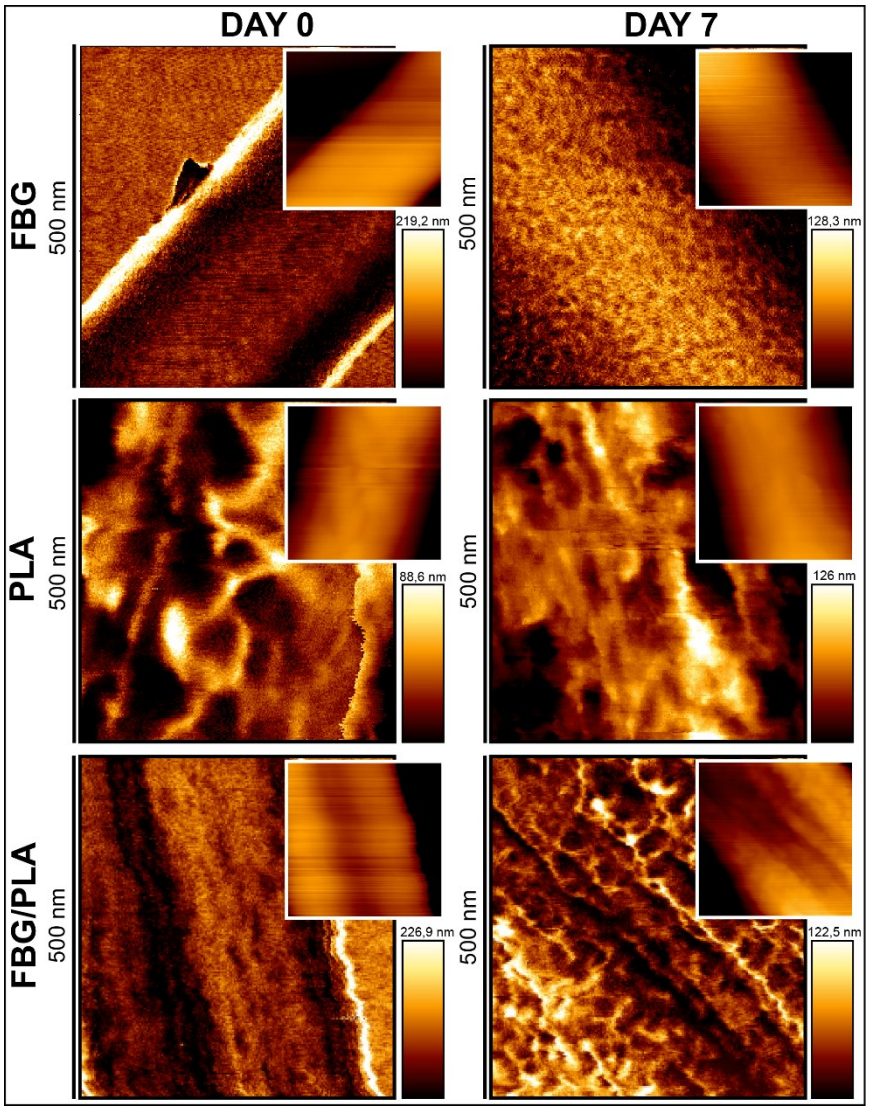

Figure 2. *AFM adhesion images of pure FBG (upper row), pure PLA (middle row) and composite FBG–PLA nanofibers (lower row) at days 0 (left) and 7 (right), i.e. after incubation of the samples for 1 week in PBS. No signs of degradation were observed for the pure PLA samples, but slightly rougher surfaces can be obtained on pure FBG and composite FBG–PLA fibers after 1 week. However, from the inserts showing AFM height images of the same samples, a rather unnoticeable change in morphology was observed, implying very little degradation*

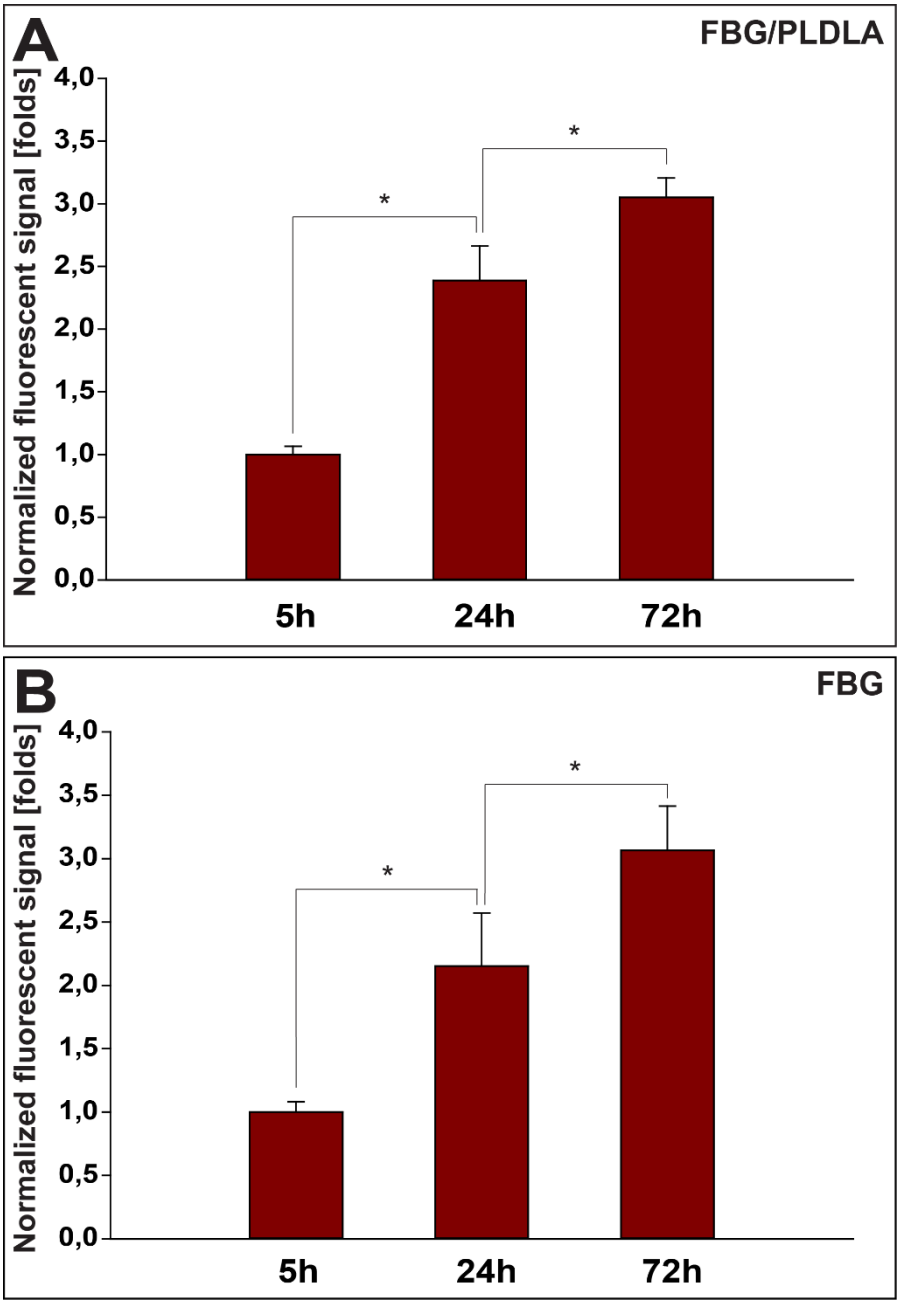

Figure 3. *Characterization of the stability of electrospun FBG-PLA fibers. Kinetics of FITC–FBG release from **(A)** composite FBG–PLA and **(B)** pure FBG samples. Fibers containing 1% FITC-labelled FBG were incubated for 5, 24 and 72 h in PBS and the fluorescence intensity of the supernatants was measured. The values for 24 and 72 h were normalized to the signal of 5 h, accepted as reference; *statistically significant difference ($p < 0.05$)*

used. As shown in Figure 3, the fluorescence signal in the supernatant increased gradually with incubation time, and the kinetics of FITC–FBG release were very similar for pure FBG and composite FBG–PLA nanofibers.

Cellular response upon ventral contact with FBG–PLA nanofibers

The response of HUVECs to ventral contact with composite nanofibers was first evaluated morphologically in a short-term experiment. After 2 h of incubation, adhesion to random nanofibers promoted an irregular cell shape, with multiple cytoplasmic projections extending towards differently orientated fibers (Figure 4A, C). The cell protrusions showed high accumulation of actin that co-

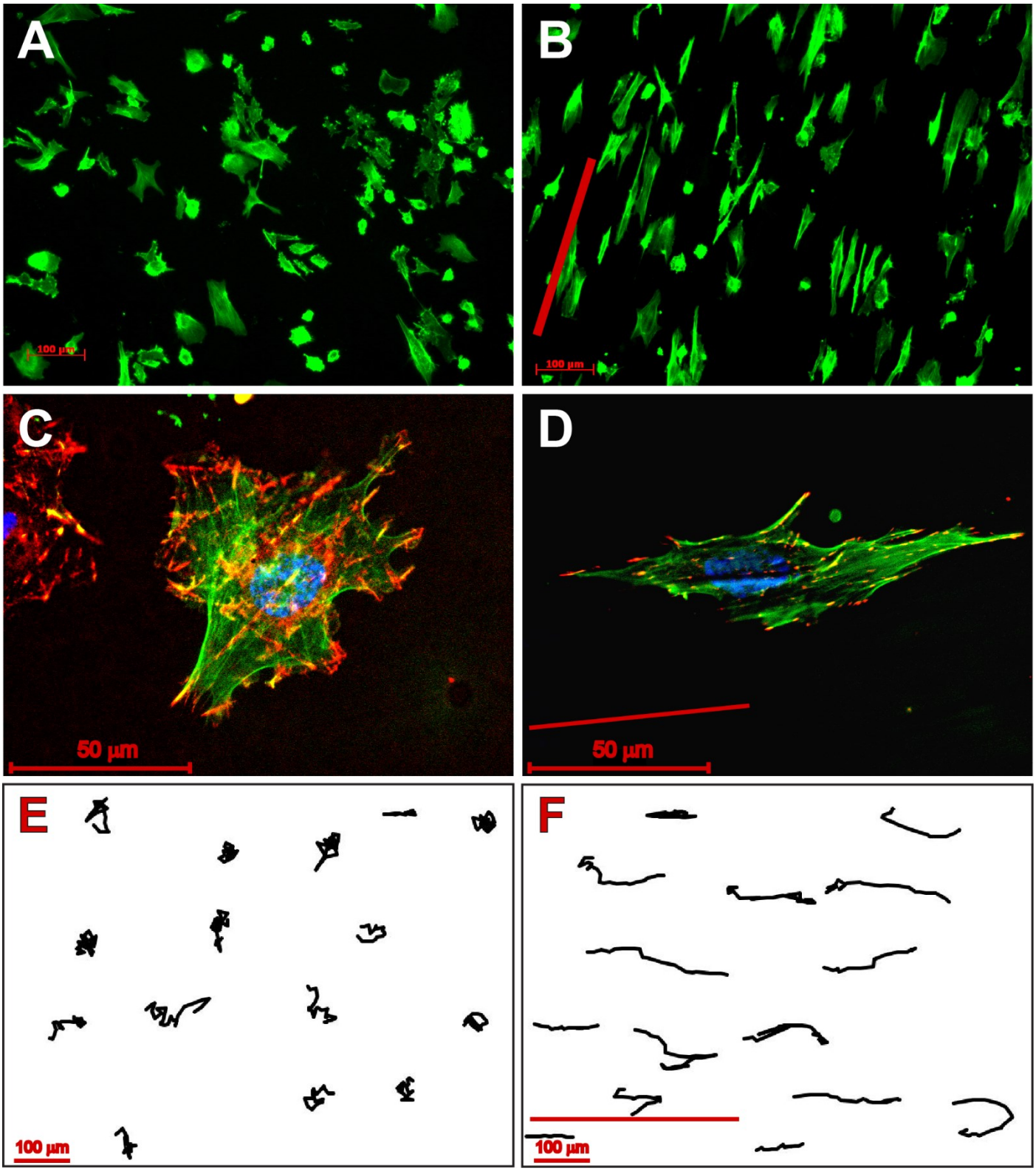

Figure 4. *Cellular interactions with FBG–PLA nanofibers. Overall morphology of HUVECs after 2 h of incubation on **(A)** random and **(B)** aligned nanofibers. Visualization of focal adhesion complexes by vinculin (red) and actin cytoskeleton (green) on **(C)** random and **(D)** aligned nanofibers; nuclei are stained with Hoechst (blue). Visualization of cell tracks on **(E)** random and **(F)** aligned nanofibers; time lapses were recorded using phase-contrast (magnification = × 10); the direction of alignment of the fibers (if any) is indicated by a red line*

localized with vinculin in focal adhesions (Figure 4C), where long actin fibers with centripetal organization inserted, suggesting firm adhesive interaction with the fibers. On aligned fibers (Figure 4B, D) the cells acquired an extended morphology that strongly followed the orientation of the fibers. The highly extended actin stress fibers inserted into well-developed focal adhesion complexes

(Figure 4D) indicate that the cells exercised traction over the nanofibers. Time-lapse recordings further demonstrated that HUVECs were highly motile on aligned FBG–PLA nanofibers (see supporting information, Video S1), with individual cells undergoing the typical motile cycle of extending a leading cell edge, followed by traction of the tail cell edge. While most of the cells on aligned FBG–PLA nanofibers carried out a linear path of translocation (Figure 4F), tracking analysis of cell motion (see supporting information, Video S2) showed that cells on random nanofibers performed restricted movements in arbitrary directions (Figure 4E), resulting in a shorter travelled distance than cells on aligned nanofibers.

Cellular response to dorsal contact with FBG–PLA nanofibers

To study the cellular response to dorsal application of FBG– PLA nanofibers (i.e. 3D response), we overlaid random or aligned nanofibers on artificial wounds created in confluent cell layers and then recorded cell migration (see supporting information, Videos S3 and S4). Tracking analysis revealed that the HUVECs moved without any preferred direction, i.e. showing disorientated

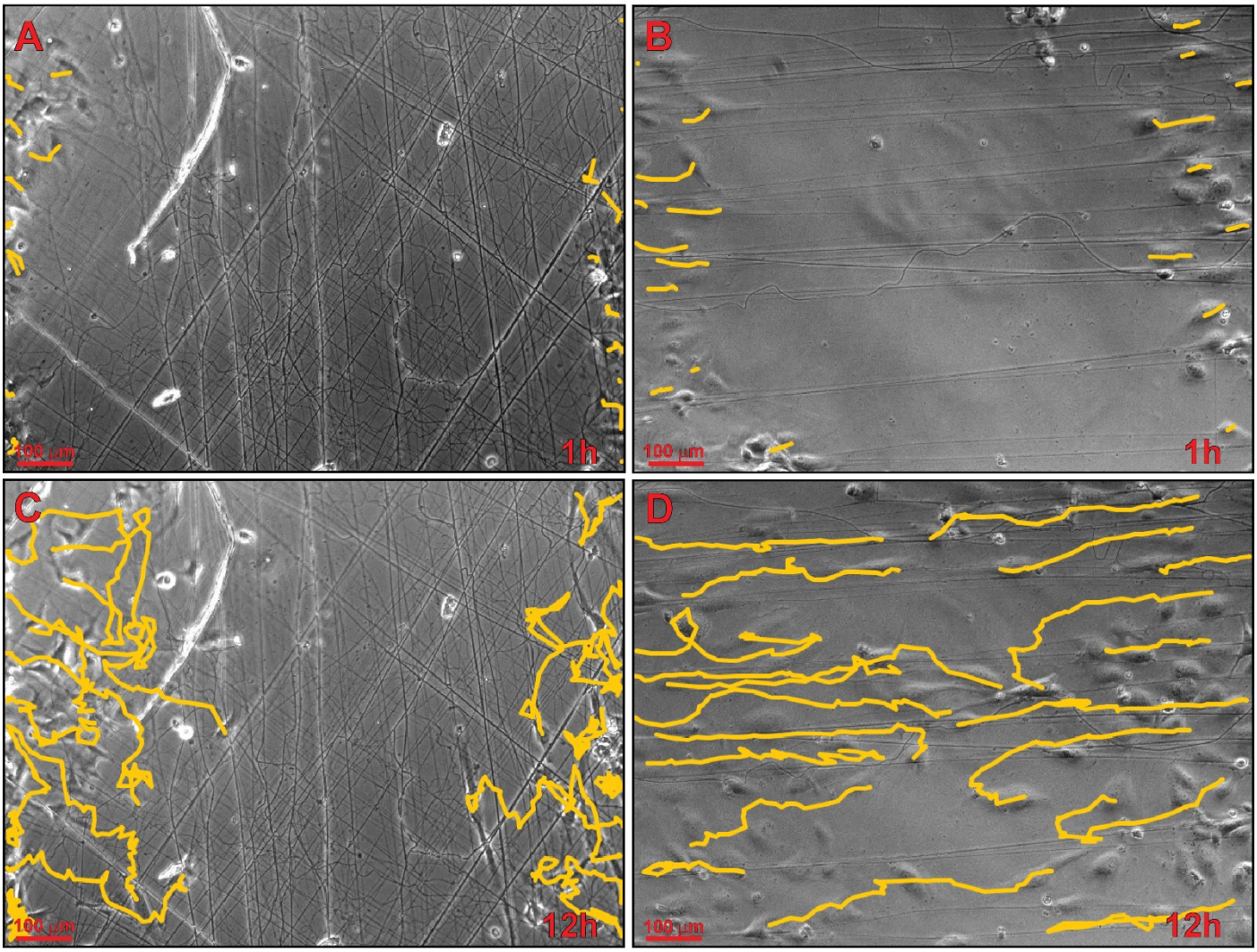

Figure 5. *Cell-tracks analysis during the wound-healing experiment. Random **(A, C)** and aligned **(B, D)** FBG–PLA nanofibers were applied to the dorsal cell surface of the confluent HUVECs layer where artificial wounds were previously created (see Materials and methods). Cell tracks (yellow) were obtained by analysis of the time-lapse movies (MTrack, ImageJ) during the first 1 h **(A, B)** and after 12 h **(C, D)** of incubation*

migration within 12 h of recording, when coated with random nanofibers (Figure 5A,C).As a consequence, the cells traversed relatively short distances on random fibers and remained near the altered wound edges. Conversely, when the cells were covered with aligned nanofibers (Figure 5 B,D) they were confined to traversing significantly longer distances, resulting in uniform wound coverage within 12 h.

Long-term cell culture on FBG–PLA nanofibers

No significant difference in cell growth was found between random and aligned NFs as well as control samples of FBG-coated glass substrata, even after 7 days of culture (see Table1). Fiber orientation was, however, observed to affect both cellular organization and ECM deposition in long-term cultures. The actin cytoskeleton aligned with the fiber direction, resulting in stochastic orientation of cellular actin bundles of cells grown on random fibers (Figure 6A) or in a uniform linear

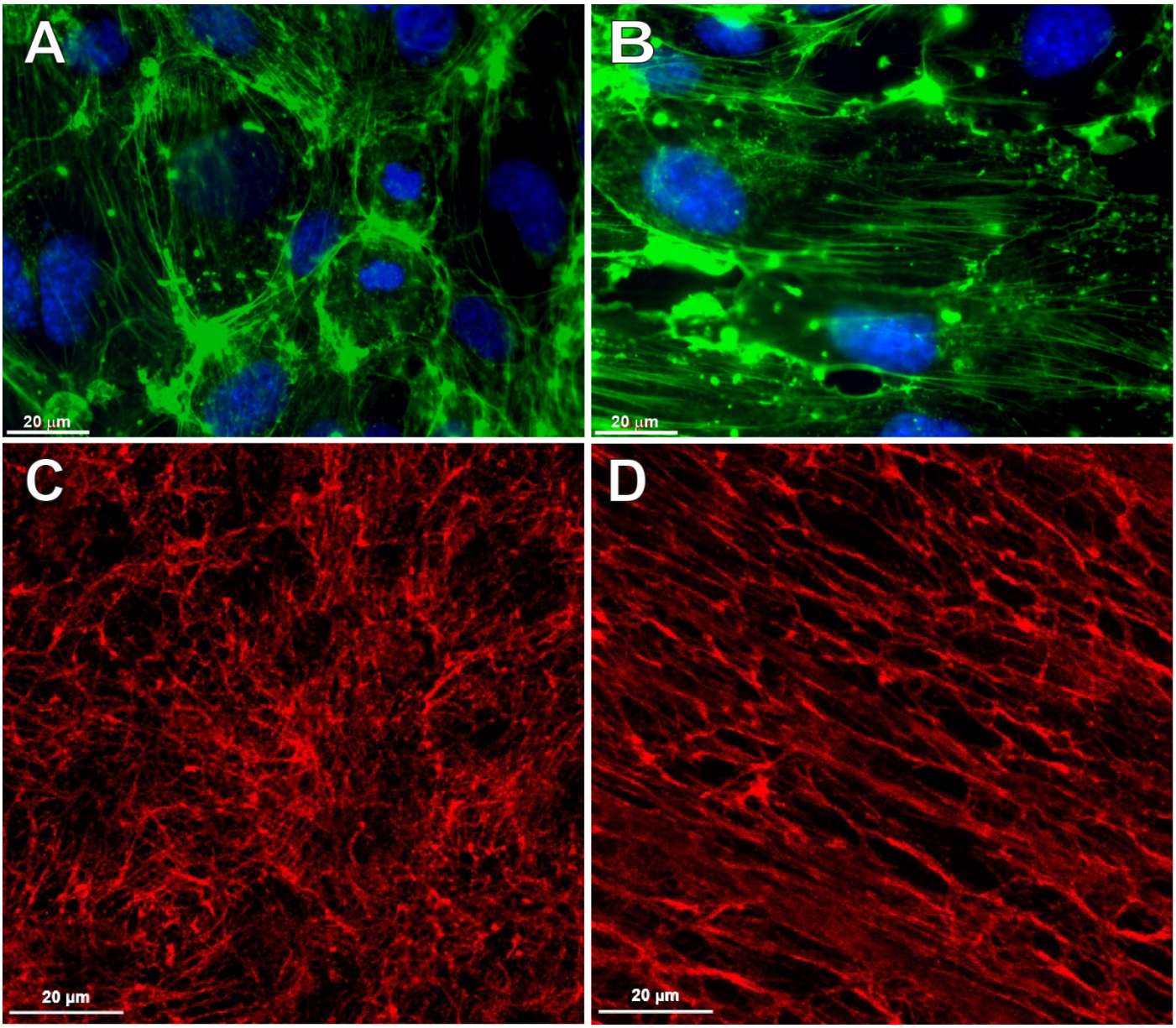

Figure 6. *Indirect immunofluorescent staining of HUVECs cultured for 7 days on **(A)** random and **(B)** aligned FBG-PLA nanofibers by phalloidin (green, actin) and Hoechst (blue, nuclei). Deposition of fibronectin secreted by HUVECs cultured for 7 days on **(C)** random and **(D)** aligned FBG–PLDLA nanofibers*

Table 1. Cell density at day 7 of culture on random and aligned nanofibres compared to control values (FBG-coated glass

	FBG-coated glass	FBG–PLA nanofibres	
		Random	Aligned
Average no. cells/square	100.25	88.5	89.25
SD	14.00	7.33	6.29

Data represent no. nuclei/microscopic field (magnification = × 20; n = 4).

pattern incells on aligned fibers, coinciding with the cell polarization (Figure 6B). Similarly, fibronectin (FN) secreted by cells after 7 days of incubation was mainly stochastically deposited around cells grown on random FBG–PLA fibers (Figure 6C). In contrast, FN matrix produced by cells grown on aligned fibers clearly assembled along the main fiber direction (Figure 6D). No significant difference in cell numbers was found for both random and aligned samples compared to controls after 7 days of culture (Table 1).

Nitric oxide secretion

To learn whether the NFs organization may affect the functional activity of HUVECs, we monitored the secretion of nitric oxide (NO) at two different time points. After 1 day of culture, no difference in NO secretion was found between random and aligned samples (Figure 7A); 2 days later, however, the cells cultured on random fibers secreted significantly higher amounts of NO than cells on aligned fibers (Figure 7B).

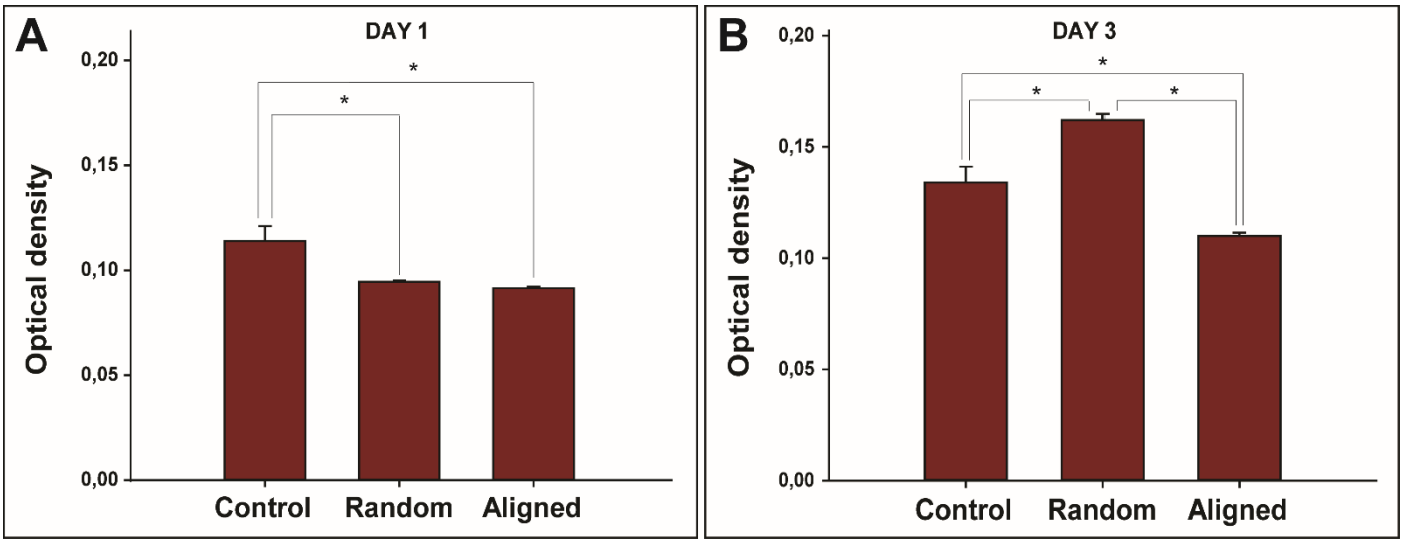

Figure 7. *Nitric oxide production of HUVECs cultured onto FBG-PLA nanofibers at day 1* ***(A)*** *and day 3* ***(B)*** *of incubation. Asterisk (*) indicates p<0.05*

Discussion

In a previous study (Gugutkov et al., 2013), we developed pure FBG nanofibers via electrospinning, a method that has been repeatedly used to create ultrathin fibers from a variety of matrix proteins (Wnek et al., 2003; Perumcherry et al., 2011). While pure FBG fibers were well recognized by endothelial cells, they had poor mechanical properties which hampers their application as scaffold materials in vascular tissue engineering. Therefore, we describe here a novel type of hybrid FBG–PLA nanofibers with strongly improved mechanical stability, but retaining the favorable cell-recognition properties of native FBG.

Utilizing established protocols (Wnek et al., 2003; He et al., 2011; Perumcherry et al., 2011), we obtained fibers with an average diameter of 300 nm that compared well with other FBG-based nanofibers (He et al., 2011). However, we observed that the diameters of aligned fibers are more heterogeneous than random fibers, presumably because of the turbulence forces caused from the rotating collector, with the result that small fibers are less orientated.

Three important aspects of our composite FBG–PLA fibers need to be clarified: (a) the influence of the electrospinning process on the protein structure; (b) the long-term stability of the electrospun fibers in a physiological environment; and (c) the improved biomechanical properties of these nanofibers. In this context, one has to consider that it is still not clear how FBG becomes insoluble during electrospinning. One possibility would be that FBG is cleaved to fibrin if traces of thrombin are present in commercially available FBG. However, we previously excluded that possibility by showing that FBG did not convert to fibrin during electrospinning (Gugutkov et al., 2013), as it did not display the typical electrophoretic band (between B′β’ and γ) present in fibrin and caused by fibrinopeptide loss from the polymer backbone (Mosesson, 2005). We thus hypothesize that electrospinning provides conditions where FBG molecules convert to an insoluble form by attractive van der Waals’ forces that overcome the electrostatic forces of repulsion. It should also be kept in mind that an insoluble FBG exists also in nature, as extrahepatic FBG can assemble into insoluble matrix fibrils in the presence of cells such as lung and mammary epithelial cells (Pereira et al., 2002; Rybarczyk et al., 2003). In that case, the cells are presumed to be involved in a process in which cryptic β-residues are exposed to form FBG fibrils (Rybarczyk et al., 2003). Although the relevance of such an assembly mechanism in the absence of cells is not clear, it may have consequences for the long-term stability of the nanofibers. We therefore used fluorescently labelled FBG (FITC–FBG) and traced the release of FITC from the fibers as they were exposed to physiological conditions.

Due to difficulties in measuring the initial amount of protein in the fibers (tightly packed FBG molecules cannot be completely extracted), we had to measure the relative loss of FITC–FBG into the medium, comparing with pure FBG nanofibers as a control. Both FITC–FBG–PLA and FITC–FBG nanofibers had similar release kinetics of FITC–FBG, indicating the entrapment stability of

FBG. Considering, as previously shown, that approximately 5% of the protein from pure FBG fibers dissolves within 1 week (Gugutkov et al., 2013), we concluded that the protein is stably incorporated within the polymer backbone and that the composite FBG–PLA fibers are sufficiently stable under physiological conditions.

Regarding the biomechanical properties, composite FBG–PLA nanofibers were significantly stiffer than pure FBG nanofibers, but much softer than pure PLA fibers when measured in the dry state. It should be emphasized, however, that pure FBG nanofibers possess extremely poor mechanical properties when immersed in wet conditions. Their elastic modulus decreases >1000 times (detailed by Baker et al. 2012), which makes their applicability in tissue engineering really questionable. For example, in our previous studies we could not introduce pure FBG fibers to the dorsal cell surface of HUVECs as the fibers broke immediately upon contact with the water surface. However, the elastic modulus of the new FBG– PLA fibers increased >100 times (Figure 2B), which in fact made possible the artificial wound settings described in this study (where we applied fibers over the cell layers through the medium). In our view, this is the main advantage of the FBG–PLA nanofibers – they combine the very good mechanical properties of PLA with the excellent biological properties of native FBG. In this context, although the technological aspects of producing artificial vessels are beyond the scope of this paper, we would like to emphasize that now we succeed in producing tubular structures using randomly deposited electrospun FBG–PLA NFs (over a rotating 2 mm metal drumstick), which was not possible with pure FBG NFs (see supporting information, Figure S1). Moreover, the surface of this scaffold is less thrombogenic, owing to lowered platelet aggregation at the surface of composite FBG–PLA NFs (whole blood test) in comparison with pure FBG NFs, thus acquiring surface properties similar to the relatively inert pure PLA fibers (see supporting information, Figure S2).

However, despite the promise of the composite fibrous scaffold, there is still a need to understand how cells respond to the spatial orientation of NFs, providing obviously ‘readable’ biological cues. Therefore, another issue we want to stress here is the morphological response of adhering endothelial cells to the nanofibers. We found clear differences in overall cell morphology, depending on the spatial organization of the fibers. On aligned fibers, the cells presented an extended morphology that strongly followed the orientation of the fibers, while on random ones they spread in multiple directions. It is well documented that, despite belonging to a common type, the cells display a variety of shapes, depending on the geometries of the adhesive environments on which they adapt their cytoskeletons (Théry et al., 2006). Indeed, the presence of highly extended actin stress fibers inserting into focal adhesions suggests that endothelial cells exert significant traction over the FBG–PLA fibers. Interestingly, the overall shape of HUVECs on random fibers resembles, to some extent, the stellate-like morphology characteristic of cells residing in 3D environments (Grinnell, 2003). This leads to the conviction that endothelial cells can ‘read’ the geometry of the underlining nanofibers

and, because they cannot enter between fibers, they perceive them rather as topography (i.e. 2.5D). It should be emphasized, however, that the appearance of well-established matrix contacts suggests that FBG–PLA nanofibers provide enough ligand density for the clustering of integrins, i.e. spaced in a < 60–70 nm distance, required for the assembly of focal complexes (Geiger et al. 2009). Collectively, this study provides morphological evidence that endothelial cells interact very well with the composite FBG–PLA fibers, which sets them among the prospective biomimetic scaffolds for vascular tissue engineering.

Beyond the events of initial morphological response, the time-lapse studies revealed that cell migration patterns also depended on the spatial orientation of the nanofibers. Understanding the factors that control cell migration is, in general, a key issue when designing implants for optimal integration with native tissue. In accordance with other studies (Sundararaghavan et al., 2013), we show here that HUVECs not only orientated themselves to aligned nanofibers but also migrated along them. The difference in cell migration on aligned fibers compared to randomly orientated fibers was particularly dramatic in the artificial wounds experiments, where aligned fibers were dorsally applied over the cells. In that case, the HUVECs migrated towards the empty regions of the wound, resulting in fast wound coverage. Conversely, when adhering to randomly deposited fibers, or when overlaid with them in the wound experiments, the cells were locally immobilized, most probably because of their anchorage with multiple projections. Nevertheless, while guided directional cell movement might be important for the recruitment of endothelial cells on scaffolds promoting angiogenesis, local immobilization of cells on randomly organized fibers could also be of interest, e.g. for the endothelization of blood-contacting devices, where the upregulation of the adhesive machinery is very important (de Mel et al., 2008). While tissue neovascularization and integration of many implants with the host circulation still remains a major barrier for the transplantation of engineered tissues – a field that has not yet identified an effective strategy (Lovett et al., 2009) – nanofibers that efficiently guide cell migration could be an important tool. Indeed, recent progress in this field suggests that allowing vascular cells to form orientated rudimentary vascular networks, either in vitro (prevascularization) or in vivo, might result in enhanced integration of grafted endothelial cells with the host vasculature (Kang and Bischoff, 2011; Baranski et al., 2013). Our studies contribute to the field by showing that an orientated nanofibrous scaffold can be used as a tool for the guided vascularization of implants. In addition, we show that the balance of adhesive and motile phenotypes influences the functionality of endothelial cells. In particular, we found that the orientation of the underlying nanofibers was clearly reflected in the organization of the confluent cell layers. Not only was the cellular actin cytoskeleton well aligned with the fiber direction, but the newly generated fibronectin matrix fibrils also followed its organization along the nanofiber direction. Those observations suggest that nanofibers orientation might be a key to regulated fibronectin matrix assembly, which may serve as a template for tailored ECM deposition. Interestingly, although

cells grew equally well on both type of nanofibers (Table 1), randomly orientated nanofibers provoked endothelial cells to produce significantly more NO, allowing the cells to better influence local vessel contractility and platelet activation (Förstermann and Münzel, 2006).

Conclusion

We report on successful electrospinning of novel composite FBG–PLA nanofibers that combine the good biomechanical properties of PLA with the excellent cell recognition properties of native FBG. Random nanofibers provoked a stellate-like morphology of endothelial cells, with multiple cytoplasmic projections, which made them relatively immobile. Conversely, an elongated cell shape combined with a significantly increased cell mobility and faster wound coverage were observed on aligned NFs. However, NO release assay showed that HUVECs possessed lower functionality on aligned NFs than on randomly deposited ones. Collectively, our studies show that randomly organized NFs may support the endothelization of blood-contacting devices, while aligned ones could provide a tool for the guided neovascularization of implants.

Acknowledgements

This study was supported by BIOSURFACES, Intramural program CIBER–BBN (Spain) and the European Commission (EC) through the FP7-People program Industry–Academia Partnerships and Pathways (IAPP) project 324386 FIBROGELNET and the EuroNanoMed project STRUCTGEL, respectively. The valuable support of Project No. MAT2012-38359-C03-03 HEALINSYNERGY, funded by the Spanish Ministry of Science and Innovation, is also acknowledged.

Supporting information on the internet

The following supporting information may be found in the online version of this article:

Figure S1. *Electrospun tubes produced from FBG–PLA nanofibers. Images were taken with a ZEISS SteREO Lumar V12 stereomicroscope in conventional light mode; magnifications = × 4 (top) and ×20 (bottom)*

Figure S2. *Adhesion and aggregation of platelets on FBG, FBG–PLA and PLA nanofibers upon incubation in fresh blood (whole blood test). The platelets are stained for actin (phalloidin, green) while fibrinogen is visualized by polyclonal anti-FBG antibody followed by secondary AlexaFluor 555 antibody (red)*

Video S1. *Time-laps record of HUVEC in ventral contact with aligned FBG/PLA nanofibers. Cell tracking in orange Video S2. Time-laps record of HUVEC in ventral contact with randomly deposited FBG/PLA nanofibers. Cell tracking in orange*

Video S3. *Dorsal response of HUVEC to aligned FBG/PLA nanofibers. Modified wound healing assay. Cell tracking in red Video S4. Dorsal response of HUVEC to randomly deposited FBG/PLA nanofibers. Modified wound healing assay. Cell tracking in red*

References

Arnold M, Cavalcanti-Adam A, Glass R, et al. 2004; Activation of integrin function by nanopatterned adhesive interfaces. Chem Phys Chem 3: 383–388.

Baji A, Mai YM, Wong SC, et al. 2010; Electrospinning polymer nanofibers: effects on oriented morphology, structures and tensile properties Compos Sci Technol 70: 703–718.

Baker S, Sigley J, Carlisle CR, et al. 2012; The mechanical properties of dry, electrospun fibrinogen fibers. Mater Sci Eng C Mater Biol Appl 1, 32: 215–221.

Baranski JD, Chaturvedi RR, Stevens KR, et al. 2013; Geometric control of vascular networks to enhance engineered tissue integration and function. Proc Natl Acad Sci U S A 110: 7586–7591.

Chiu JB, Luu YK, Fang D, et al. 2005; Electrospun nanofibrous scaffold for biomedical applications. J Biomed Nanotechnol 1: 115–123.

Cleary MA, Geiger E, Grady C, et al. 2012; Vascular tissue engineering: the next generation. Trends Mol Med 18: 394–404.

De Mel A, Jell G, Stevens MM, et al. 2008; Biofunctionalization of biomaterials for accelerated in situ endothelialization: a review. Biomacromolecules 9: 2969– 2979.

Dvir T, Timko BP, Kohane S, et al. 2010; Nanotechnological strategies for engineering complex tissues. Nat Nanotechnol 6: 13–22.

Edelman RE. 1999; Vascular tissue engineering: designer arteries. Circ Res 85: 1115– 1117.

Fang J, Wang X, Lin T. 2011; Functional applications of electrospun nanofibers. In Nanofibers – Production, Properties and Functional Applications, InTech – Open Access Publisher: Rijeka, Croatia, 287– 326.

Forner L, Salmerón-Sánchez M, Palomares M, et al. 2009; The use of atomic force microscopy in determining the stiffness and adhesion force of human dentin after exposure to bleaching agents. J Endod 35: 1384–1386.

Förstermann U, Münzel T. 2006; Endothelial nitric oxide synthase in vascular disease: from marvel to menace. Circulation 113: 1708–1714.

Fu X, Wang H. 2012; Spatial arrangement of polycaprolactone/collagen nanofiber scaffolds regulates the wound healing related behaviors of human adipose stromal cells. Tissue Eng Part A 18: 631–642.

Geiger B, Spatz JP, Bershadsky AD. 2009; Environmental sensing through focal adhesions. Nat Rev Mol Cell Biol 10: 21–33.

Grinnell F. 2003; Fibroblast biology in threedimensional collagen matrices. Trends Cell Biol 13: 264–269.

Guelcher SA, Goldstein AS. 2009; Effect of fiber diameter and alignment of electrospun polyurethane meshes on meshenchimal progenitor cells. Tissue Eng Part A 15: 2435–2445.

Gugutkov D, Gustavsson J, Ginebra MP, et al. 2013; Fibrinogen nanofibers for guiding endothelial cells' behavior. Biomater Sci 1: 1065–1073.

He Ch, Xi X, Zhang F, et al. 2011; Fabrication of fibrinogen/(PLLA–CL) hybrid nanofibrous scaffold for potential soft engineering application. J Biomed Mater Res A 97A: 339–347.

Kang KT, Bischoff J. 2011; Bioengineered human vascular networks transplanted into secondary mice reconnect with the host vasculature and re-establish perfusion. Blood 118: 6718–6721.

Kumar TRS, Krishnan LK. 2001; ECGF enmeshed with fibrin matrix enhances proliferation of EC in vitro. Biomaterials 22: 2769–2776.

Liu H, Ding X, Zhou G, et al. 2013; Electrospinning of nanofibers for tissue engineering applications. J Nanomater 2013: 11. Article ID 495708

Liu Y, Ji Y, Chosh K, et al. 2009; Effects of fiber orientation and diameter on the behavior of human dermal fibroblasts on electrospun PMMA scaffolds. J Biomed Mater Res A 90: 1092–2009.

Lovett M, Lee K, Edwards A, et al. 2009; Vascularization strategies for tissue engineering. Tissue Eng Part B Rev 15: 353–370.

Lutolf MP, Hubbell JA. 2005; Synthetic biomaterials as instructive extracellular microenvironments for morphogenesis in tissue engineering. Nat Biotechnol 23: 47–55.

Ma Z, Kotaki M, Yong T, et al. 2005; Surface engineering of electrospun polyethylene terephthalate nanofibers towards development of a new material for blood vessels engineering. Biomaterials 26: 2527– 2536.

Mosesson MW. 2005; Fibrinogen and fibrin structure and functions. J Thromb Haemost 3: 1894–1904.

Nisbet DR, Pattanawong S, Ritchie NE, et al. 2007; Interaction of embryonic cortical neurons on nanofibrous scaffolds for neuronal tissue engineering. J Neuron Eng 4: 35–41.

Pereira M, Rybarczyk BJ, Odrljin TM, et al. 2002; The incorporation of fibrinogen into extracellular matrix is dependent on active assembly of a fibronectin matrix. J Cell Sci 115: 609–617.

Perumcherry SR, Chennazahi KP, Nair SV, et al. 2011; A novel method for fabrication of fibrin-based electrospun nanofibrous scaffold for tissue-engineering application. Tissue Eng C 17: 1–10.

Rybarczyk BJ, Lawrence SO, SimpsonHaidaris PJ. 2003; Matrix–fibrinogen enhances wound closure by increasing both cell proliferation and migration. Blood 102: 4035.

Stevens MM, George JH. 2005; Exploring and engineering the cell surface interface. Science 310: 1135–1138.

Sundararaghavan HG, Saunders RL, Hammer DA, et al. 2013; Fiber alignment directs cell motility over chemotactic gradients. Biotechnol Bioeng 110: 1249– 1254.

Swartz DD, Russell JA, Andreadis ST. 2005; Engineering of fibrin-based functional and implantable small-diameter blood vessels. Am J Physiol Heart Circ Physiol 288: 1451–146

CONCLUSIONS

This thesis demonstrates that tailoring of the spatial organization of matrix proteins at cell-biomaterials interface can be used for guiding the cellular behavior - an issue that might have strong impact on the nowadays tissue engineering and regenerative medicine. Two systems were developed, both providing spacially organized cues to the adhering cells that mimick the fibrillar aspect of ECM: the first one is based on the phenomenon of **substratum-driven protein assembly** and the second one – on **electrospun nanofibers.**

More specifically, exploring the substratum-driven protein assembly the following scientific issues were successfully solved:

- Participation in the discovery of a new phenomenon – the substratum driven protein assembly that involves the adsorption behavior of at least two matrix proteins: fibronectin and fibrinogen.
- Detailed studies on the optimization of fibronectin and fibrinogen networks formation reveal an optimal substratum for its assembly: PEA – a polymer characterized with strong hydrophobicity and complete absence of –OH groups.
- The engineered protein networks were further biologically characterized utilizing endothelia cells and fibroblasts as cell models.
- Given that protein networks are well recognized by the cells, the conditions for the cellular interaction were optimized in both 2D and 3D systems, showing that they corroborate with the maximal fibronectin and fibrinogen networks assembly. Thus, the biological significance of the phenomenon and its applicability for nanoscale tissue engineering was unequivocally confirmed.

Concerning the development and use of the fibrinogen based nanofibers the following challenging tasks were successfully completed:

- A novel tailor-made device and corresponding technology for the production of nanofibers in random and aligned configuration was developed and optimized.
- Three novel types of nanofibers consisting of pure FBG, composite FBG/PLA and pure PEA, in both random and aligned configuration were successfully designed and produced
- The newly developed nanofibers were used to introduce positional cues to the adhering cells in either random or aligned geometry utilizing two cellular models - endothelial cells and fibroblast. The PEA nanofibers were used in the studies outlined above on the 3D aspect of FN and FBG networks.
- Studies on the initial cellular interaction with differently organized nanofibers were performed and the morphological and functional response of endothelial cells was evaluated in both 2D and 3D environments. It was found that random nanofibers tend to immobilize the calls and promote

their functionality (by means of NO secretion), while the aligned nanofibers support the directional cell migration and diminish NO secretion.

- The applicability of the fibrinogen-based nanofibers for vascular tissue engineering purposes was demonstrated, providing an important information that randomly organized fibers are more suitable for the endotelialization of putative implants, while random ones are rather applicable to direct their neovascularization. In addition, tubular structures from random nanofibers were produced as an attempt to engineer small diameter vascular grafts.

PERSPECTIVES

Collectively, this PhD thesis provides significant body of published research demonstrating succesful engineering of two systems for guiding the cellular behavior.

- The phenomenon of **substratum-driven protein assembly** is currently a topic for extensive research in the group of Prof Salmeron Sanches (University of Glasgow) with our partial cooperation within the project **MAT2012-38359-C03-03 (2012-2014) HELINSINERGY.** Furthermore, the substratum driven protein assembly has many potential applications, for example, for improving the biocompatibility of strongly hydrophobic materials and controlled release of bioactive molecules. It is also of fundamental interest for better understanding of proteins behavior on surfaces.

- The application of **electrospun nanofibers** that closely mimic the ECM organization comprises an independent work of the author of this thesis. The application of the developed **electrospun nanofibers** went far beyont the topic of the presented research. Fibrinogen based nanofibers were succesfully implicated in **two European projects** (see Chapter 5) dealing with differetntiation of mesenhymal stemm cells for **bone and cartilage tissue engineering purposes**. The personal research interests of the author are currently dedicated on the engineering of **small diameter vascular grafts** (see picture in Chapter 6) based on FBG/PLA nanofibers combined with living cells. In a more global plan, other tissue engineering applications are forseen, such as fabrication of wound healing mats, elaboration of protable electrospinning device for direct application of autologous fibrinogen nanofibers onto wounded skin, scaffolding for myoblast and myocardial differentiation of stem cells, controlled migration of cells in biological gradients, etc.

LIST OF FIGURES

| Chapter 1 | Introduction

| Chapter 2 | Fibronectin activity on substrates with controlled –OH density

| Chapter 3 | Biological activity of the substrate-induced fibronectin network: Insight into the third dimension through electrospun fibers

| Chapter 4 | Fibrinogen organization at the cell–material interface directs endothelial cell behavior

| Chapter 5 | Fibrinogen nanofibers for guiding endothelial cell behavior

| Chapter 6 | Electrospun fibrinogen–PLA nanofibers for vascular tissue engineering

LIST OF TABLES

Chapter 1 | Introduction

Chapter 2 | Fibronectin activity on substrates with controlled –OH density

Chapter 4 | Fibrinogen organization at the cell–material interface directs endothelial cell behavior

Chapter 6 | Electrospun fibrinogen–PLA nanofibers for vascular tissue engineering

ABBREVIATIONS

Abbreviation	Details
AC	Alternated current
ADAMs or **MDCs**	Adamalysin-related membrane proteinases
ADMIDAS	Adjacent to metal-ion dependent adhesion site
AFM	Atomic force microscopy
BM	Basement membrane
BMP	Bone morphogenetic protein
BSA	Bovine serum albumin
CAMs, ICAMs or **Ig-CAMs**	Cell adhesion molecules
CCD-25SK	Human dermal fibroblast cell line
Col IV	Collagen type IV
DMEM	Dulbecco's modified Eagle's medium
DMSO	Dimethyl sulfoxide
DNA	Deoxyribonucleic acid
DPPC	Dipalmitoyl phosphatidylcholine
EA	Ethyl acrylate
ECGS/H	Endothelial cell growth medium with Supplement Mix
ECM	Extracellular matrix
EDA	Extra domain A
EDB	Extra domain B
EDTA	Ethylenediaminetetraacetate
EGDMA	Ethylene glycol dimethacrylate
EGF	Epidermal growth factor
ESB	European Society for Biomaterials
ESI	Electronic supplementary information
EWC	Equilibrium water content
FAK	Focal adhesion kinase
FBG or FG	Fibrinogen
FBS	Fetal bovine serum
FDA	Fuorescein diacetate
FFT	Fast Fourier transformation

FITC	Fuorescein isotiocianate
FN	Fibronectin
FnBPs	Fibronectin-binding proteins
FpA and **FpB**	Fibrinopeptides A and B
FT-IR	Fourier transform infrared spectroscopy
GAG	Glycosaminoglycan
GFOGER or **Gly-Phe-Hyp-Gly-Glu-Arg**	Glycine-phenylalanine- hydroxyproline -glycine-glutamic acid-arginine
HA	Hyaluronic acid or Hydroxyapatite
HEA	Hydroxyl ethyl acrylate
HFIP	1-1-1,3-3-3 hexafluoroisopropanol
HUVEC	Human umbilical vein endothelial cells
IDAPS	Isoleucine-aspartic acid-alanine-proline-serine
ILK	Integrin-linked kinase
KGD or	Lysyl-glycyl-aspartic tripeptide
KLDAPT	Lysine-isoleucine-aspartic acid-alanine-proline-threonine
LDV or **Arg-Gly-Asp**	Leucyl-α-asparagyl-valin tripeptide
LIBS	Ligand-induced binding sites
LN	Laminin
LPA	Lipoprotein(a)
mAbs	Monoclonal antibodies
MAdCAM-1	Mucosal vascular addressin cell adhesion molecule 1
MAPK or **MAP**	Mitogen activated protein kinase
MIDAS	Metal-ion dependent adhesion site
MMPs	Matrix metalloproteinases
MSC	Mesenchymal stem cell
NFs	Nanofibers
NMR	Nuclear magnetic resonance
NO	Nitric oxide
PA	Peptide-amphiphiles
PAI-1	Plasminogen activator inhibitor-1
PBS	Phosphate buffered saline
PCL	Poly(caprolactone)
PDGF	Platelet-derived growth factor
PDMS	Poly(dimethylsiloxane)

PEA	Poly(ethylacrylate)
PEG	Poly(ethylene glycol)
PEO	Poly(ethylene oxide)
PGA	Poly(glycolic acid)
PHEA	Poly(ethylacrylate)
PKCs	Protein kinases C
PLA	Poly(lactic acid)
PLGA	Poly(DL-lactic-co-glycolic) acid or Poly(lactic- co -glycolic) acid
PLLA	Poly(L-lactic acid)
PMMA	Poly(methyl methacrylate)
PSI	Plexin-semaphorin-integrin domain
PVA	Poly(vinyl alcohol)
PVB	Poly(vinyl butyral)
RGD or Arg-Gly-Asp	Arginylglycylaspartic tripeptide
Rho-GTPases	Rho family of guanosine triphosphateases
SD	Standard deviation
SDS	Sodium dodecyl sulfate
SEM	Scanning Electron Microscopy
SyMBS	Synergistic metal ion binding site
TCP	Tri-calcium phosphate
TE	Tissue engineering
TGF-β	Transforming growth factor beta
THF	Tetrahydrofuran
TIMPs	Tissue inhibitors of metalloproteinases
t-PA	Tissue plasminogen activator
u-PA	Urokinase-type plasminogen activator
VCAM-1	Vascular cell adhesion protein 1
VN	Vitronectin
VWF	Von Willebrand factor
WCA	Water contact angle
XPS	X-ray photoelectron spectroscopy

PUBLICATIONS

Publications included in thesis

Gugutkov, D., González-García, C., Hernández, J.C.R., Altankov, G., Salmerón-Sánchez, M,
Biological activity of the substrate-induced fibronectin network: Insight into the third dimension through electrospun fibers
(2009) *Langmuir*, 25 (18), pp. 10893-10900.
Article
DOI: 10.1021/la9012203

Gugutkov, D., Altankov, G., Rodríguez Hernández, J.C., Monleón Pradas, M., Salmerón Sánchez,M.
Fibronectin activity on substrates with controlled - OH density
(2010) *Journal of Biomedical Materials Research - Part A*, 92 (1), pp. 322-331.
Article
DOI: 10.1002/jbm.a.32374

Gugutkov, D., González-García, C., Altankov, G., Salmerón-Sánchez, M.
Fibrinogen organization at the cell-material interface directs endothelial cell behavior
(2011) *Journal of Bioactive and Compatible Polymers*, 26 (4), pp. 375-387.
Article
DOI: 10.1177/0883911511409020

Gugutkov, D., Gustavsson, J., Ginebra, M.P., Altankov, G.
Fibrinogen nanofibers for guiding endothelial cell behavior
(2013) *Biomaterials Science*, 1 (10), pp. 1065-1073.
Article
DOI: 10.1039/c3bm60124b

Gugutkov, D., Gustavsson, J., Cantini, M., Salmeron-Sánchez, M., Altankov, G.
Electrospun fibrinogen-PLA nanofibres for vascular tissue engineering
(2016) *Journal of Tissue Engineering and Regenerative Medicine*, Article in Press.
Article in Press
DOI: 10.1002/term.2172

Publications not included in thesis

Keremidarska, M., Gugutkov, D., Altankov, G., Krasteva, N.

Impact of electrospun nanofibres orientation on mesenchymal stem cell adhesion and morphology

(2015) *Comptes Rendus de L'Academie Bulgare des Sciences*, 68 (10), pp. 1271-1276.

Article

Toromanov, G., Gugutkov, D., Gustavsson, J., Planell, J., Salmerón-Sánchez, M., Altankov, G.

Dynamic behavior of vitronectin at the cell-material interface

(2015) *ACS Biomaterials Science and Engineering, 1 (10), pp. 927-934.*

Article

DOI: 10.1021/acsbiomaterials.5b00147

Forget, J., Awaja, F., Gugutkov, D., Gustavsson, J., Gallego Ferrer, G., Coelho-Sampaio, T., Hochman-Mendez, C., Salmeron-Sánchez, M., Altankov, G.

Differentiation of human mesenchymal stem cells toward quality cartilage using fibrinogen-based nanofibers

(2016) *Macromolecular Bioscience*, pp. 1348-1359.

Article

DOI: 10.1002/mabi.201600080

Gugutkov, D, Awaja, F, Belemezova, K, Keremidarska, M, Krasteva, N, Kuyrkchiev, S, Gallego Ferrer, G, Seker, S, Elcin, AE, Elcin, YM and Altankov, G.

Osteogenic differentiation of mesenchymal stem cells using hybrid nanofibers with different configurations and dimensionality

(2017) *Journal of Biomedical Materials Research Part A*

Article

DOI: 10.1002/jbm.a.36065